MASSEY UNIVERSITY

PHD THESIS

Polysaccharide-DNA Strings for Single Molecular Polysaccharide Studies

---

Nimisha Mohandas

A thesis submitted in fulfillment of the requirements

for the degree of Doctor of Philosophy

in

Biophysics and Soft Matter

School of Natural Sciences

Massey University, Palmerston North,

New Zealand.

February 2022

Declaration of Authorship

I, Nimisha Mohandas, declare that this thesis titled, "Formation of Polysaccharide-DNA Strings for Single Molecular Polysaccharide Studies", and the work presented in it are my own. I confirm that:

- This work was done wholly or mainly while in candidature for a research degree at this University.
- Where any part of this thesis has previously been submitted for a degree of any other qualification at this University, or any other institution, this has been clearly stated.
- Where I have consulted the published work of others, this has been clearly referenced.
- Where I have quoted the work of others, the source has been mentioned. The other works in this thesis are solely my own work.
- I have acknowledged all main sources of help.
- Where the thesis is based on work done by myself jointly with others, I have clearly distinguished the work contributed by myself and the work contributed by others.

Signed: 

Date: 20/05/2022

Abstract

For several decades DNA has been the workhorse of single molecule experiments, owing to its large controllable size and simplicity of end group attachment. The use of DNA handles to study DNA-protein conjugates has also previously been employed to understand the behaviour of proteins at the single molecular level. In contrast, single molecule studies of polysaccharides are not widely known. This project attempts to develop a methodology in order to facilitate single molecule polysaccharide studies with optical tweezers (OT). Homogalacturonan (HG), a polysaccharide component extracted from pectin, a key component in plant cell walls, was chosen to be the subject of this study. The proposed strategy was to utilise DNA strands as "handles" with one end attached onto HG, and the other coupled to beads, to allow for stretching of HG, and other single molecule studies. In order to attach HG between different DNA handles, the chemistry present at the reducing and non-reducing ends of the polysaccharide which can be used to form bonds with end functionalised DNA strands was the point of focus. Ultimately the DNA-polysaccharide connection was mediated by streptavidin moieties linking biotin-functionalised ends.

Streptavidin is a tetrameric protein, renowned for its strong binding to biotin that has to led to multitudinous applications. By separating streptavidin species that have differing numbers of binding sites plugged, "linking hubs" with trivalent, divalent and monovalent functionality were obtained. Species identity, and the plugging process were studied with capillary electrophoresis, which in this case provides several advantages over traditional gels. Subsequently, divalent linkers were used to concatenate two biotin-terminated 5 kb pieces of double stranded DNA, and the resulting string stretched in an optical tweezers experiment, demonstrating the "plug-and-play" potential of the methodology for coupling and extending molecules for use in single molecule biophysical experiments.

Acknowledgements

First, I would like to express my thanks to my supervisors Bill and Geoff for their guidance and support throughout my PhD. It has been a memorable four years and I have learnt plenty and more from the both of you. This project would not have been possible without the help of some wonderful colleagues that I met in Massey, especially Lisa, Val, Nirosha, Allan, Pat and Yongdong. I would also like to thank the rest of my office mates Susav, Sashi, Ben and Josiah for a lively working atmosphere for the time I was here. My thanks also goes out to all those that I have met after joining Massey. Some of my closest friends that I met in New Zealand, Rusila, Vivian, Tina, Tae Rim and other amazing people I've met offline and online, it hasn't been an easy few years but thank you for being an incredible support system. Also, to my friends and family who I haven't been able to meet but have been sending me support and encouragement during the hard times, thank you so much for listening to all my thoughts, shall we say, and for believing in me and just being my side, more than anything.

I express my gratitude to Riddet Institute for funding my PhD and to Massey University for all the services and facilities which have aided me in carrying out this project, including the Mac-Diarmid institute for the additional 3 months funding to help ameliorate the issues caused by Covid-19.

Contents

List of Figures

List of Tables

List of Abbreviations

A	**A**denine
Ab	**A**nti**b**ody
Ag	**A**nti**g**en
AMO	**A**minooxy
B	**B**iotin
BGE	**B**ack**g**round **E**lectrolyte
bp	**b**ase **p**airs
BSA	**B**ovine **S**erum **A**lbumin
C	**C**yanine
CCD	**C**harge-**c**oupled **D**evices
CD	**C**ircular **D**ichroism
DNA	**D**eoxyribo **N**ucleic **A**cid
CCRC	**C**omplex **C**arbohydrate **R**esearch **C**entre
CE	**C**apillary **E**lectrophoresis
COSY	**Co**rrelation **S**pectroscop**y**
DBCO	**Di**benzo**c**yclo**o**ctynyl
DHA	3-**d**eoxy-D-lyxo-2-**h**eptulosaric **a**cid
DIG (D)	**dig**oxigenin
DM	**d**egree of **m**ethylesterification
DP	**d**egree of **p**olymerisation
ds	**d**ouble **s**tranded
ELISA	**E**nzyme **L**inked **I**mmuno**s**orbent **A**ssay
EOF	**E**lectro**o**smotic **F**low
EtBr	**E**thidium **B**romide
F	**F**orward
G	**G**uanine

GalpA	**G**alacturonic **A**cid
h	**h**ours
HG	**H**omo**g**alacturonan
HMBC	**H**eteronuclear **M**ultiple **B**ond **C**orrelation
HPAEC	**H**igh **P**erformance anion-**E**xchange **C**hromatography
HPLC	**H**igh **P**erformance **L**iquid **C**hromatography
HRP	**H**orse**r**adish **P**eroxidase
HSQC	**H**eteronuclear **S**ingle **Q**uantum **C**oherence
JIM7	antibody specific to high DM HG
KDO	3-deoxy-D-manno-2-octulosonic acid
MQ	**M**illi**q**ue
MWCO	**M**olecular **W**eight **C**ut-**O**ff
NA	**N**umerical **A**perture
Na-cit	Sodium (**Na**) **cit**rate
NHS	**N**-**h**ydroxysuccinimide
NMR	**N**uclear **M**agnetic **R**esonance
OT	**O**ptical **T**weezers
PAGE	**P**oly**a**crylamide **G**el **E**lectrophoresis
PBS	**P**hosphate-**B**uffered **S**aline
PC	**P**hoto**c**leavable
PCR	**P**olymerase **C**hain **R**eaction
PEG	**P**olyethylene **G**lycol
PG	**P**oly**g**alacturonase
PGA	**P**oly**g**alacturonic **A**cid
PL	**P**ectate/**P**ectin **L**yase
PME	**P**ectin **m**ethyl**e**sterase
PMG	**P**oly**m**ethyl**g**alacturonase
pri	**pri**mer
R	**R**everse
RG	**R**hamno**g**alacturonan
rt	**r**oom **t**emperature

s	**s**treptavidin
SDS	**S**odium **D**odecyl **S**ulfate
SLM	**S**patial **L**ight **M**odulator
Sod. Phos.	**Sod**ium **Phos**phate
ss	**s**ingle **s**tranded
T	**T**hymine
TAE	**T**ris-**a**cetate-**E**DTA
TMB	**T**ri**m**ethyl **b**enzidine
TBE	**T**ris-**b**orate-**E**DTA
TEAA	**T**ri**e**thyl **a**mmonium **a**cetate
TEG	**T**ri**e**thylene **G**lycol
TOCSY	**To**tal **C**orrelation **S**pectroscop**y**
TSB	**T**agment **S**top **B**uffer
UV	**U**ltra**v**iolet

List of Symbols

μ_{ep}	electrophoretic mobility	$m^2 V^{-1} s^{-1}$
L_{tot}	capillary length	m
L_{eff}	distance between injection and detection points in a capillary	m
V	applied voltage	V
t_{mig}	migration time of species	s
t_{EOF}	migration time of neutral species	s
F	force	N
k	optical trap stiffness	$N\,m^{-1}$
x	position	m
d	extension	m
r	radius	m
T	temperature	K
J	coupling constant	Hz
l	length	m

Chapter 1

Introduction

1.1 Introduction to Pectin

1.1.1 Pectin & the plant cell wall

The cell wall is an important constituent present in all plant species, responsible for various physicochemical properties of the plant [1]. Within a plant, it has been assumed that biosynthesis of pectin begins in the Golgi. Subsequently, Golgi vesicles deposit pectin outside the plasma membrane, in the cell wall, where it is incorporated and modified as needed during plant development [2]. Amongst the various plant polysaccharides, pectin is a family of heterogeneous polysaccharides that makes up to about 35%, by dry weight, of most plant cell walls. However, in Arabidopsis (*Arabidopsis thaliana*), this value is around 50% [3]. Pectin plays several important roles in plants including modulating cell growth and triggering defence mechanisms. In fruits and vegetables, the amount of pectin is crucial in determining the quality of the fruits as pectin is key in controlling the firmness of the cell walls [4–6]. Even after being discovered over two centuries ago, *in vivo* structure-function relationships of pectin are still a very active area of research [7].

As mentioned above, pectin is a complex carbohydrate made up of different polysaccharides. The composition of polysaccharides in pectin, as shown in Figure 1.1, includes homogalacturonan (HG), rhamnogalacturonan (RG) I and II, xylogalacturonan (XG) and apiogalacturonan (AG). Interestingly, the relative ratios of the various polysaccharides can vary in different parts within the same plant, at different stages of a plant life cycle and also from plant to plant. [8–10].

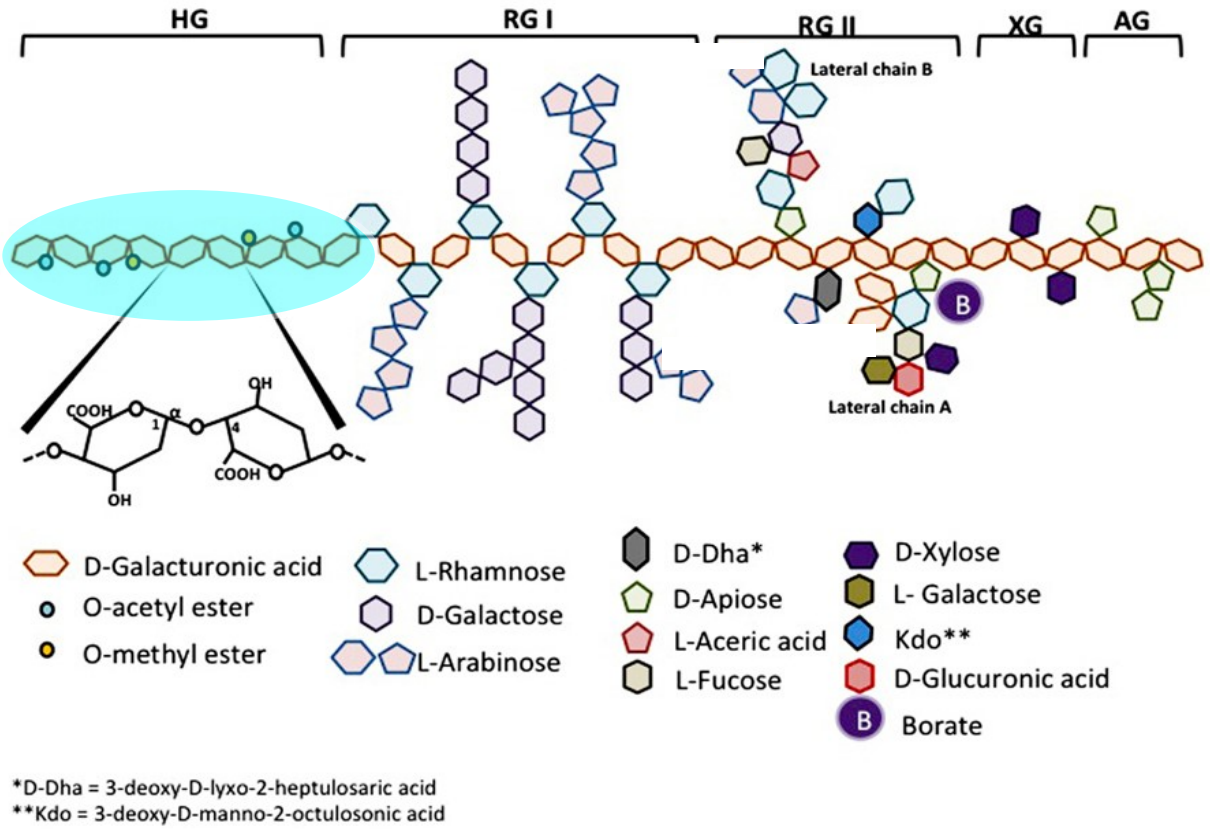

FIGURE 1.1: A diagram indicating the different polysaccharides along a pectin chain adapted from [10].

Homogalacturonan (HG)

Galacturonic acid, GalpA (where Gal denotes D-galactose, p denotes pyranose form and A denotes carboxylic acid at C6) residues are connected via α-(1,4)-glycosidic linkages between the units to form the linear backbone of the homogalacturonan (HG) chain. In plants, HG constitutes up to around 65% of pectin in a cell wall. HG chains, when extracted from commercial samples, are usually around 72 to 100 residues long. The carboxyl groups in the sugar residues of HG can be methylesterified. The degree and pattern of methylesterification of HG, and thus of pectin, influences its physical properties [11, 12].

Rhamnogalacturonan (RG)

There are two types of rhamnogalacturonan, RG: RG-I and RG-II. While HG is a linear polysaccharide, the backbones of RG-I and RG-II have several side chains, and these are referred to as the 'hairy' region in pectin. The number of side chains differs for different species, spatially and temporarily within the plant [13].

After HG, the next most abundant polysaccharide component in pectin is RG-I at around 20 to 35%, while the other polysaccharides (RG-II, XG and AG) make up the remaining 10% of the complex pectin molecule [14]. As seen from Figure 1.1, while HG is made up of GalpA residues only, the RG-I backbone is made up of repeated alternating rhamnose and GalpA residues. The GalpA residues in RG-I may be acetylated in the hydroxyl positions . For the side chains in RG-I, the rhamnose residues are substituted with side chains of galactose or arabinose units [15–18].

On the other hand, the backbone of RG-II comprises of α-(1,4)-GalpA units. However, unlike RG-I, several other sugar residues can be seen to be substituted on the GalpA residues as side chains such as apiose, aceric acid, 3-deoxy-*lyxo*-2-heptulosaric acid (DHA), and 3-deoxy-*manno*-2-octulosonic acid (KDO) as shown in Figure 1.2. Despite the high complexity of the structure, RG-II is a polysaccharide that is highly conserved in the plant cell wall [10].

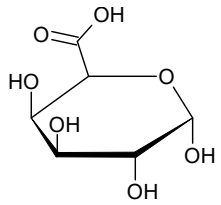

Galacturonic acid

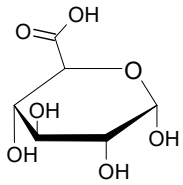

Glucuronic acid

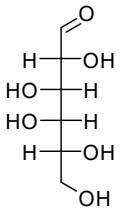

D-Galactose

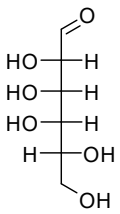

L-Galactose

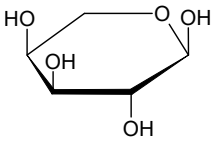

Arabinose

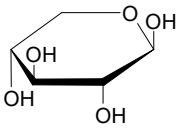

Xylose

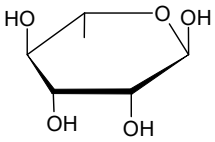

Rhamnose

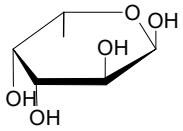

Fucose

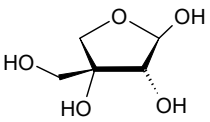

Apiose

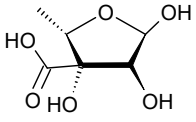

Aceric acid

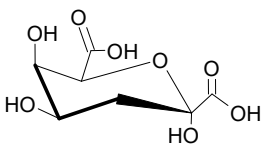

3-deoxy-*lyxo*-2-heptulosaric acid (DHA)

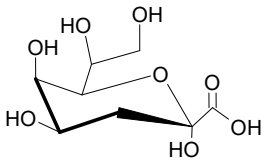

3-deoxy-*manno*-2-octulosonic acid (KDO)

FIGURE 1.2: The different sugars present in the side-chain of RG-II.

Extraction of Pectin:

Pectin is generally extracted by treating the source with dilute acids at a high temperature. It can be extracted from plants and also fruits, most commonly citrus and apples [19]. After treating the source with hot acid, the viscous pectin extract is separated from the solids. Pectin extracted from natural sources will be mostly methylesterified. The degree of methylesterification can be altered after extraction by enzymatic or chemical treatments as desired. This is explained further in section 1.2.1.

1.1.2 History of pectin

Although fruit jams and jellies have been around for centuries, the presence of pectin in fruits was not known till late in the 18^{th} century when Vaquelin discovered this water-soluble polysaccharide in fruit juice [20]. In 1825, pectin was discovered in plants, and isolated, by French chemist Henri Braconnot, who also discovered another polysaccharide, chitin. The constant occurrence of pectin in all plants led him to believe that pectin was an important constituent in the plant kingdom [21]. Over the next century, the isolation and significance of pectin in fruit was investigated in detail [22]. Eventually, the potential of pectin led to the patenting of pectin extraction and the commercial production of pectin started from the early 20^{th} century. Now, the use of pectin can also be seen outside the food industry, such as in the field of medicine and cosmetics [23, 24].

1.1.3 Properties of pectin

Pectin is, largely, a long chain of galacturonic acid residues some of which will exist in non-methyl esterified form. Hence, it is an anionic polysaccharide and, thereby, water soluble. When present at dilute concentrations, pectin solutions exhibit Newtonian flow where the viscous stress is linearly proportional to the strain rate of the solution. However, once the concentration of pectin increases, this behaviour deviates and the solution becomes non-Newtonian as expected for polymer solutions at concentrations well above overlap. These factors such as viscosity and solubility can affect the gelation properties of any subsequently formed gel. This gelation property of pectin is responsible for its function in plants and its use in industries [25, 26].

1.1.4 Applications of pectin

Pectin plays a significant role in the food industry as a hydrocolloid, mainly as a gelling agent and a stabiliser. Commercially, pectins are typically modified post-extraction to obtain different pectins with specific degrees of methylesterification (DM) in order to maximise their performance in particular functions.

As a gelling agent

Gels generally occur as a result of intermolecular interactions forming space-spanning three-dimensional networks. As mentioned, pectins are anionic polysaccharides and, hence, will tend to repel each other. However, intermolecular hydrogen bonding can occur between the carboxyl groups and hydroxyl groups present in pectin molecules. When the pH is approximately 7, repulsive forces dominate, preventing aggregation. There are two common ways in which the repulsive forces are reduced and interactions are enhanced, leading to the formation of two different types of gels; calcium gels and acid gels [27].

Pectins can gel easily with divalent salts, such as Ca^{2+}, due to the free charged groups, above the pKa of carboxyl groups, in their chain. In such calcium gels, the pectin chains are associated in a network by the electrostatic and ionic interactions between the positively charged ions and the negatively charged polysaccharides as shown in Figure 1.3. Gelation, however, can only occur if there is a minimum of ~8 to 16 free, and consecutive, carboxylate groups [27, 28]. As a result, this mechanism is more common for low methoxyl pectins owing to the abundance of consecutive anionic residues [29, 30].

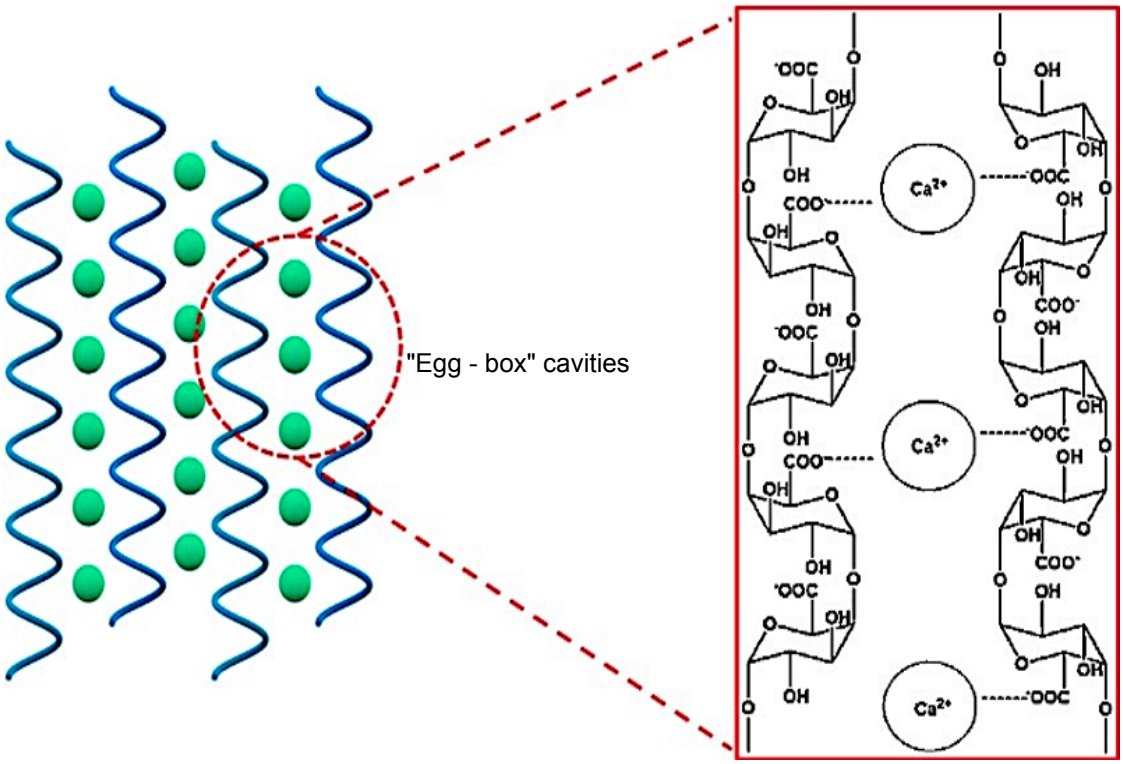

FIGURE 1.3: The proposed "egg-box" model indicating cross-links involved in the gelling of pectin with calcium ions [28].

On the other hand, acid gels are formed due to the lowering of repulsive forces between pectin chains when the carboxylate groups in the polysaccharide become protonated at an acidic pH. The protonated carboxylates experience less repulsion compared to their anionic polysaccharide and can associate to form a gel. Furthermore, hydrogen bonds are formed between the carboxylic acid groups and the hydroxyl groups [26]. This mechanism is more common for high methoxyl pectins, and is more pronounced at higher sugar concentrations [31, 32].

As a stabiliser

The stabilising properties of pectins are exploited in acidic dairy beverages. Pectins bind to the casein micelles preventing aggregation at a low pH range ~5.0 where κ-casein on the outside of the micelles collapses and ceases to be a steric barrier. This pH range is still high enough such that pectin maintains some of its charge and binds to the outside of the micelle acting as a replacement of κ-casein functionality (which exhibits the same functionality at pH 6.7) [33–35].

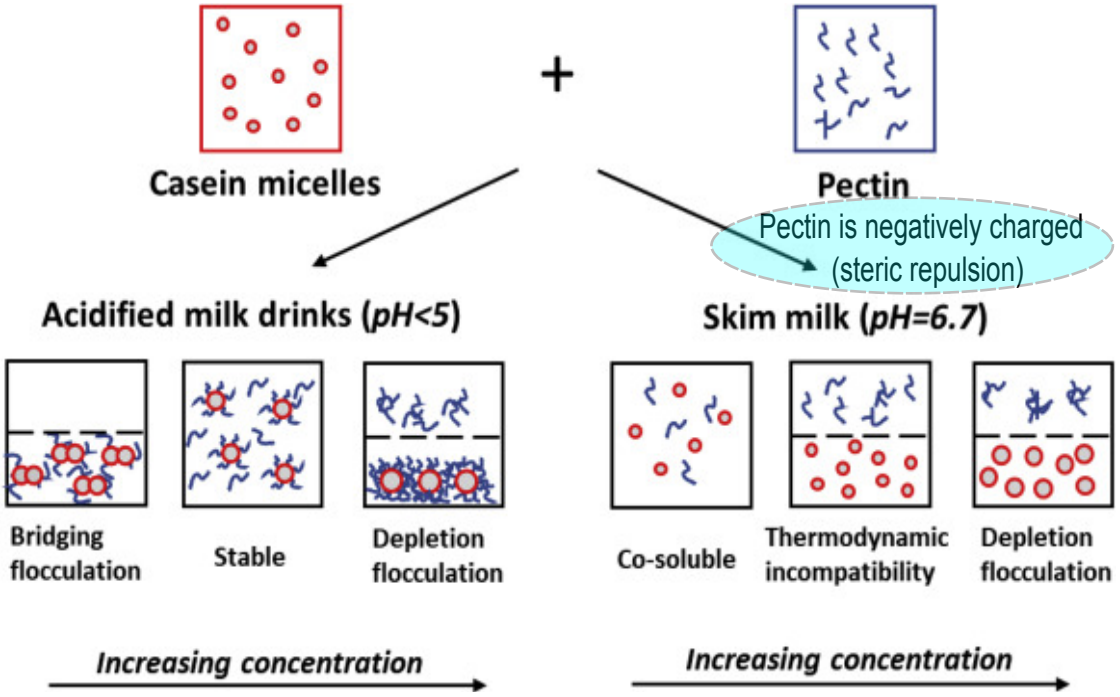

FIGURE 1.4: Interaction of pectin and casein micelles at different pH and different concentrations adapted from [36].

1.2 Modification of Pectin (HG)

Pectin has various functional groups along the chain, which provide potential sites for chemical modification. In addition, the terminal ends of pectin, the reducing and non-reducing end, can also be functionalised chemically. Modifications can be made along the chain or at terminal ends, as explained in the upcoming sections. **In this thesis, we are primarily concerned with the modification of homogalacturonan at the terminal ends to allow it to be more easily manipulated in state-of-the-art molecular biophysics experiments.**

1.2.1 Modification along the HG chain

As pectin is primarily made up of galacturonic acid residues (HG), the functional groups that can be present along the backbone are methyl esters, carboxylic acids and hydroxyls. The glycosidic linkages themselves also offer opportunity for modification. These functional groups, particularly the amount and pattern of methylesterification, can be modified enzymatically or chemically.

Enzymatic modification along the pectin chain

Several enzymes are involved in the modification of pectin within plants [37]. They can be classified broadly based on their mechanism of action:

- **Methylesterases**: perform the removal of methyl ester groups along the backbone.

  A prominent group of enzymes acting on HG are called pectin methyl esterases (PMEs). It was found that HG synthesised in the Golgi is highly methylesterified [38, 39]. PMEs essentially take part in the de-methyl esterification of the homogalacturonan units in the polysaccharide chain, which decreases the degree of methylesterification (DM). PMEs can be processive or non-processive. Processive PMEs remove methyl esters consecutively, forming blocks of anionic residues whereas non-processive PMEs remove methyl esters more randomly. The difference in distribution pattern of the methyl ester groups affects various physical properties within a plant cell wall and the behaviour of the polymer in commmercial applications [40, 41].

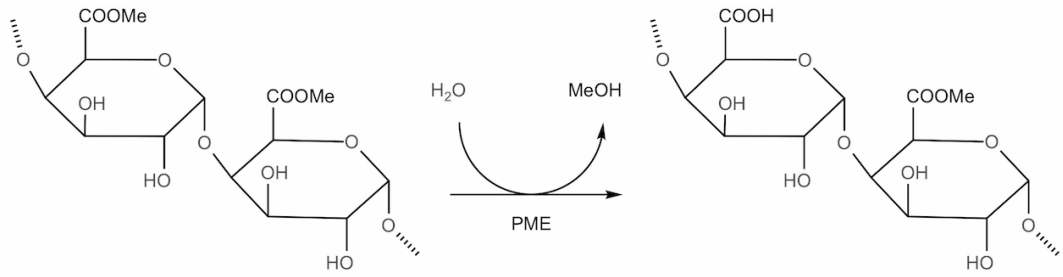

FIGURE 1.5: PME action on methylesterified residues.

  PMEs are not only present in plants but also in bacteria and fungi. While plant PMEs work in favour of the cell wall growth and many other physiologically relevant processes, bacterial and fungal PMEs work to weaken the cell wall and make the plant susceptible to infection and degradation. Most plant and bacterial PMEs are processive, whereas most fungal PMEs are non-processive [42–45]. This is, however, a simplification and while many bulk experiments have studied processsivity, single molecule experiments are yet to be studied.

- **Lyases**: perform fragmentation of the backbone.

  There are two types of lyases that can act on pectin. They are differentiated based on the position of where the fragmentation occurs. If the lyase cuts between two non-methylesterified residues, it is a pectate lyase and, if the lyase cuts between two methylesterified residues, it is a pectin lyase [46, 47]. Unlike pectin lyases, pectate lyases require calcium ions for activity

to acidify the C5α proton and aid lyase action. Two fragments are formed during lyase treatment. One of these fragments will have a terminal unsaturated residue generated by the β-elimination mechanism as shown in Figure 1.6 [48, 49]. Pectate disaccharide and trisaccharide lyases have found to generate the unsaturated oligosaccharides from the reducing end [50]. If the lyase acts at the terminal end, it is referred to as an exo lyase while a lyase that fragments within the HG backbone is referred to as an endo lyase [51, 52].

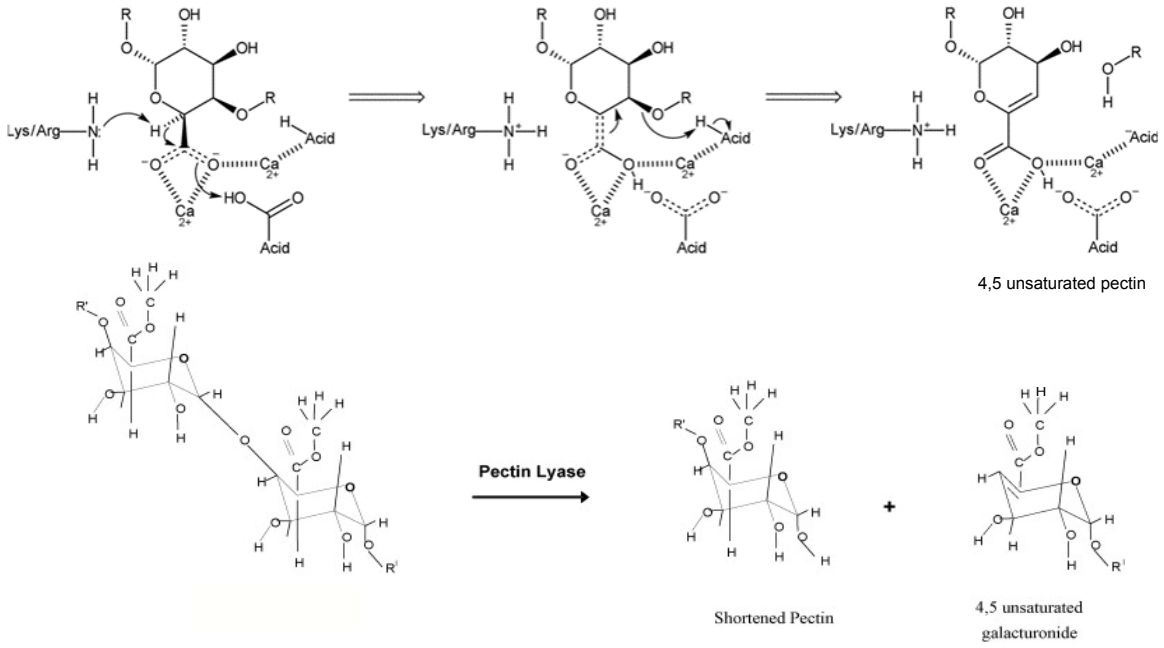

FIGURE 1.6: Pectate lyase mechanism (top) adapted from [48] and pectin lyase mechanism (bottom) adapted from [49].

- **Polygalacturonases**: perform fragmentation of the backbone.

  Polygalacturonases, PGs, also cleave the α-1,4-glycosidic bond but without generating an unsaturated residue. Hence, they are also known as pectin hydrolases.

  Polygalacturonases can be classified as endo- and exo-polygalacturonases based on where they cleave in a chain of galacturonic acid residues [53]. Endo-PGs act on random cleavage sites provided that there are more than four successive unmethylesterifid GalA residues [54, 55]. On the other hand, exo-PGs cleave at the de-methylesterified terminal ends of the HG chain. As polygalacturonases act between unmethylesterified residues, the pattern of methylesterification directly influence the chain cleavage. [56].

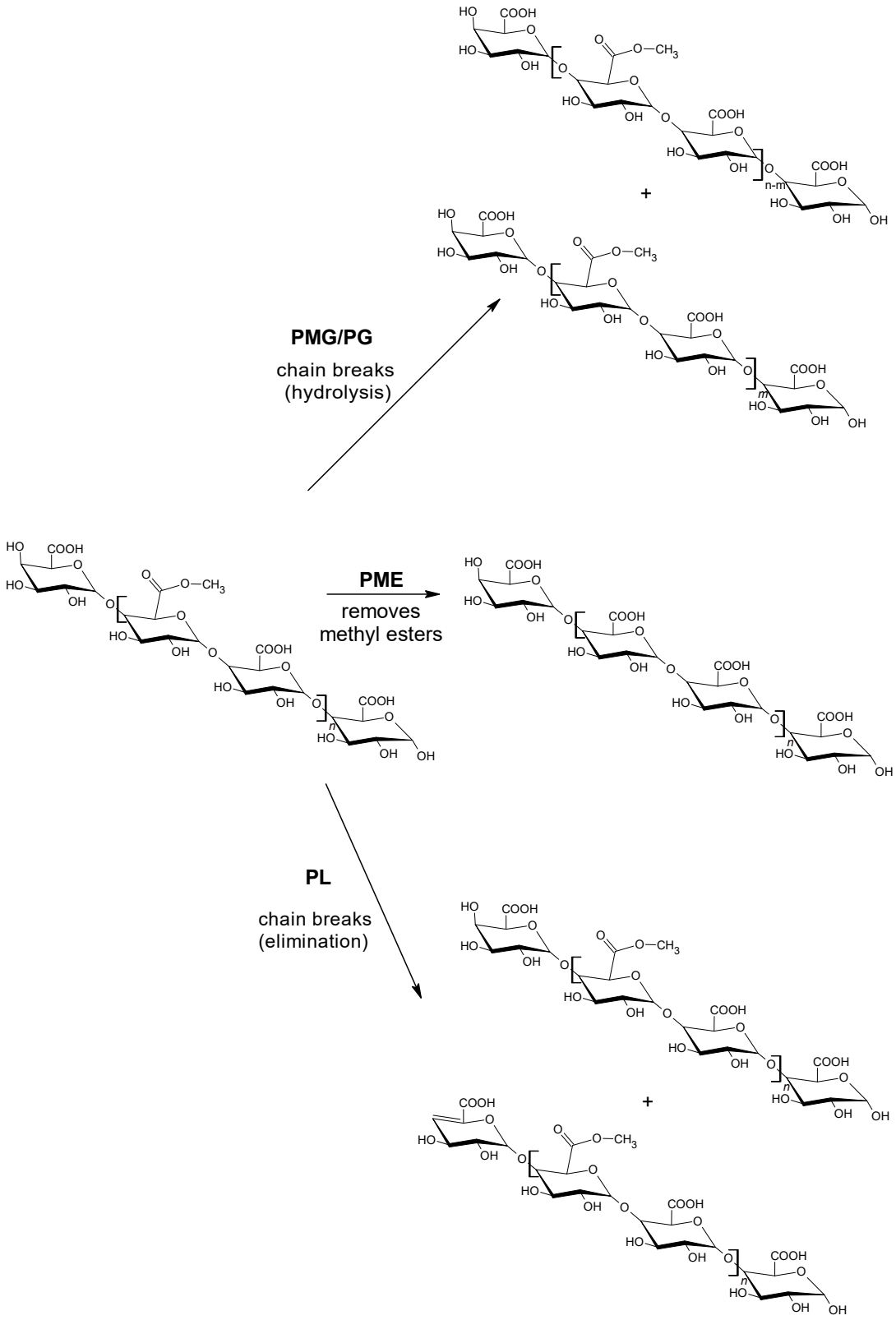

FIGURE 1.7: The different enzymes acting along a homogalacturonan chain: **PMG/PG**: polymethylgalacturonase/polygalacturonase, **PME**: pectin methyl esterase, **PL**: pectate/pectin lyase.

Chemical modification along the pectin chain

Due to the various functional groups present along the pectin chain, pectin can also be modified via various non-enzymatic mechanisms, such as substitution, chain elongation or depolymerisation [57].

Substitution Substitution reactions can be performed on the carboxyl and hydroxyl groups of the galacturonic acid residues.

- Alkylation: Alkyl groups can be introduced in pectin by methylesterification (at C-6 carboxyl groups) or methoxylation (at O-2 or O-3 hydroxyl groups).
- Amidation: Methylesterified residues can be treated by ammonia, hydroxylamine or amino acids, leading to formation of amidated pectins (primary or secondary).
- Thiolation: Thiols can be introduced into the pectin chain, generally, by linkers containing amide or ester bonds. Various reagents can be used to introduce the thiol groups such as cysteine or thioglycolic acid. Thiolated pectins can cross-link via disulfide bonds, and are stable materials for various applications in the pharmaceutical field.
- Oxidation: Pectin can be oxidised at the hydroxyl group at O-2 and O-3 using sodium periodate ($NaIO_4$) or potassium periodate (KIO_4). Treatment with periodate leads to cleavage of the bond and formation of fragments with aldehyde groups.

Depolymerisation Chemical depolymerisation of pectin is more commonly observed at alkaline pH, where the base can catalyse the β-elimination mechanism as shown in Figure 1.8. As the β-elimination mechanism is more efficient when electron-donating methylester groups are present in the pectin chain, high DM pectins degrade faster compared to low DM pectins when subjected to hot alkaline conditions. Along with depolymerisation, demethylesterification also occurs simultaneously in these conditions. However, the rate of demethylesterification is relatively slower than the rate of depolymerisation [58]. Interestingly, the dynamics between the relative rates of demethylesterification and depolymerisation can be varied by changing the pH and temperature [59, 60].

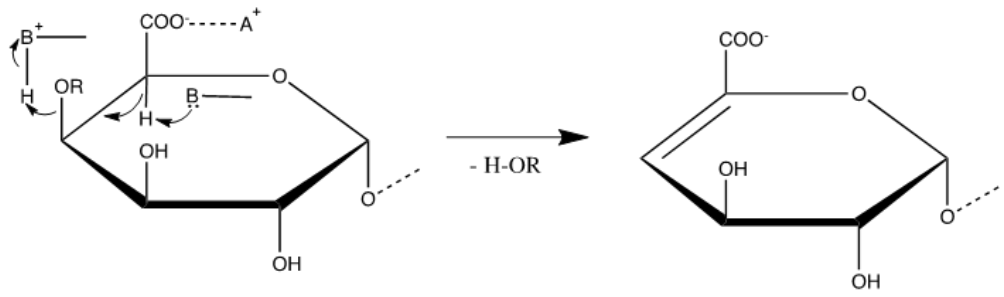

FIGURE 1.8: β-Elimination of galacturonic acid in a HG chain.

Depolymerisation of HG chains can also be carried out mechanically via methods such as ultrasonification, with varying results [61, 62]. Physical methods such as radiation and photochemical degradation are widely used in food and pharmaceutical industries while traditional methods such as grinding or dehydration are not commonly used [63, 64].

1.2.2 Modification of terminal ends of HG

Similar to most polysaccharides, HG also has a reducing end and a non-reducing end. While the reducing end has a characteristic aldehyde group present when the terminal sugar residue opens, the non-reducing end does not possess any unique functional group compared to the rest of the homogalacturonan chain making it a more challenging target for modification.

The reducing end of HG has an anomeric carbon which, in the open-chain form, has a free aldehyde group available for chemistry. As a carbonyl group, aldehydes can undergo nucleophilic addition. In this thesis, the fact that aldehyde groups can react with amine groups via reductive amination is considered. Alternatively, aldehyde groups can also react with aminooxy moieties forming a stable oxime linkage [65–67]. The functionalisation at the reducing end can, hence, be performed via reductive amination or oxime formation. For attachment to amines, the presence of a reducing agent, such as sodium cyanoborohydride, is necessary as the initial reaction to form an imine is reversible and reduction of the imine to the amine stabilises the linkage. However, this condition is not necessary for oxime formation and, hence, in this thesis, an aminooxy moiety for the functionalisation at the reducing end has been used.

Contrary to the reducing end, the non-reducing end of HG does not have a unique functional group available for chemical modification. One possibility investigated was introduction of a double bond to a terminal galacturonic acid residue by cleaving the α-1,4-glycosidic linkage between the galacturonic acid residues in the HG chain. Cleavage of these bonds and introduction of the unsaturated terminal residue can be carried out enzymatically or chemically. To produce

terminal ends, with the desired functional moiety, enzymatically, exo enzymes would be ideal so that the chain is not shortened by the introduction of the double bond, as they only cleave terminal linkages. Unfortunately, compared to endo lyases, fewer exo lyases are known. The first exo-pectin lyase was classified in 2014 by Danielle Biscaro Pedrolli and Eleonora Cano Carmona. Exo-pectin lyase was found to release unsaturated monogalacturonates from the reducing end of pectin [68]. Neither of these fragments are desired products, so exo lyases were not pursued here. Exo-polygalacturonases and exo-polymethylgalacturonases also exist; however, they do not generate new functional groups into the pectin chain [69].

In this thesis, the desired polysaccharide should have a double bond on the non-reducing end, ideally of the longest possible fragment for subsequent coupling; endo-pectate lyase or chemical β-elimination have both been investigated for their use in this thesis.

Once generated, an unsaturated terminal residue at the non-reducing end can be subjected to a variety of electrophilic addition reactions such as hydration, or photochemical reactions, such as the thiol-ene click reaction. For this thesis, a thiol-ene click is employed for further attachment purposes as shown in the figure below.

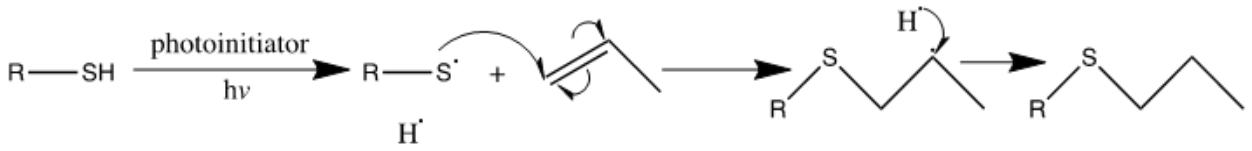

FIGURE 1.9: General mechanism of thiol-ene click reaction.

1.3 Streptavidin

1.3.1 Introduction

Streptavidin is a 66 kDa homologous tetrameric protein, with each monomer able to bind one biotin-displaying molecule [70]. Streptavidin from the bacterial protein *Streptomyces avidinii* has a strong ligand binding affinity (K_d = 10^{-15} M) for biotin [70, 71]. Streptavidin can also be considered as a dimer of a dimer of D2 (or 222) symmetry, where each monomer has an anti-parallel β-barrel tertiary structure with eight strands. A biotin-binding site is located at the end of each β-barrel. Four identical streptavidin monomers (i.e. four identical β-barrels) associate to give streptavidin's tetrameric quaternary structure [72, 73]. Hence, on incubation with biotin-binding species, a mixture of multi-valent species could be obtained. Being able to control the the number

of active valencies that the tetramer displays opens up potential pathways to further applications by allowing controlled linking hubs of known valency (1, 2, 3, or 4) to be created. As a result, although several coupling reactions (e.g. digoxigenin-anti-digoxigenin) could be pursued, streptavidin-biotin conjugation is chosen in this project owing to its utility and previous work demonstrationg the concatenation of long molecules. **Primarily, we are interested in divalent streptavidin for our thesis with a view to coupling biotin-terminated biopolymers.**

1.3.2 Streptavidin-biotin conjugation

Streptavidin-biotin features a widely known non-covalent attachment in biomolecule conjugation with a high binding affinity as mentioned above. The binding of biotin to streptavidin is found to be non-cooperative but also with every binding of biotin, the structural and thermodynamic stability of the protein increases [74–76]. As we are primarily interested in attaining divalent streptavidin for this thesis, preparation and isolation of divalent streptavidin were considered. Previous attempts in attaining streptavidin with different valencies for biotin binding have largely involved using genetic modification techniques to produce monomeric mutants that are not capable of biotin binding, but are still successfully incorporated into the tetramer [77, 78]. Furthermore, engineering of monomeric and dimeric streptavidin has also been successfully attempted on multiple occasions [79–82]. Other techniques that have sought to reduce the possible number of biotin-bearing molecules that can bind to modified tetramers have used preliminary incubations of streptavidin with biotin-terminated "plugging molecules". In this way, by controlling the stoichiometric ratios of components and the incubation time, partially filled monovalent, divalent, and trivalent streptavidin species can all be formed [83, 84]. In 2014, Xun Sun et al. performed an experiment where they incubated streptavidin protein with a biotin-labelled, 12 base pair, double-stranded DNA as the “auxiliary handle”. They then separated the different species using an anion-exchange chromatography column. After the incubation, the handles were conveniently cut off using the incorporated photocleavable (PC) 2-nitrobenzyl linker in one of the DNA strands, leaving “biotin-plugged” streptavidin of different valencies. The reaction has previously been monitored using native gel electrophoresis [83].

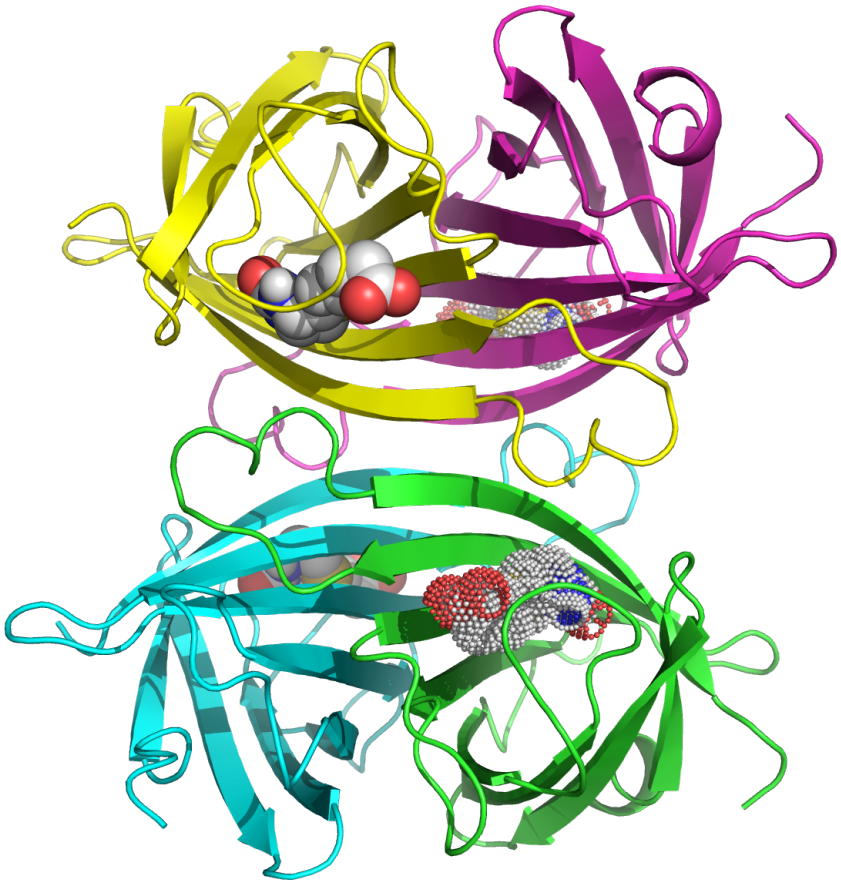

FIGURE 1.10: Structure of streptavidin-biotin conjugate species with the different valencies filled (Generated by PyMol) [85].

1.4 Overview of Single Molecule Studies

As the name suggests, single molecule studies are studies performed on individual molecules, rather than bulk ensembles. These studies can shed light on to several aspects that cannot be understood from bulk studies, and are especially advantageous in the study of biological mechanisms. Single molecule studies have continued to grow in popularity as technological capability improves and experimental platforms for their application become more available. While typically challenging compared to traditional bulk techniques, single molecule studies offer unprecedented access to the world of molecular biology, and incredible insights into the functioning of molecular machines in the noisy thermal bath in which they operate. However, the limited sensitivity of current scientific techniques hinders the application of these studies on biomolecules

in the smaller size range. Within biological molecules, single molecule studies are widely performed on DNA and protein molecules, while single molecule studies for polysaccharides are not well known. Indeed, the work in this thesis hopes to provide progress to develop protocols that can facilitate such studies. While a wide range of imaging techniques, such as atomic force microscopy, are used in the visualisation of single molecules, here, the target is to facilitate optical tweezer (OT) studies by understanding how to string polysaccharides of interest between OT-manipulatable beads.

1.4.1 Optical Tweezers (OT)

In single molecule studies, the importance of optical tweezers has increased over the years due to its superior force resolution compared to, for example, atomic force microscopy (AFM). Optical Tweezers (OT) have provided a key experimental tool for the pursuit of such studies, acknowledged recently by the award of a Nobel prize in 2018 to Arthur Ashkin for their application in biological systems. Optical tweezers, often called laser traps, can be considered as 'tweezers' formed by highly focused laser beams, typically, via a high numerical aperture objective. These laser beams will form a region where micron-sized particles can scatter the photons and from the resulting change in momentum, experience a force. This force traps the particles to the focus of the laser and can be used either to move particles by steering the beams, or by watching how particles are displaced from their equilibrium position, to measure tiny applied forces that originate for example from the stretching of molecules or the action of molecular motors. The measurement of forces can be deduced from how the particle moves within the tweezer set-up and shed light regarding the dynamics of biomolecules [86–88].

1.4.2 DNA stretching

Owing to the controllable and large size of DNA strands and to an array of molecular biology techniques available for manipulation of DNA strands, this biomolecule has become a standard in single molecule experiments. "Handles" that permit facile attachment to micro sized bead can be straightforwardly introduced into the termini of the chain and held in an optical tweezers set-up. Figure 1.11 shows an example of where DNA has been used as "handles" in an optical tweezers set-up [89]. DNA has been the molecule of choice in the development of single molecule studies. DNA stretching was first visualised with optical tweezers in 1992 [90]. In 1997, Michelle and team

studied the stretching of DNA molecules present in different buffer concentrations and compared the observations to elasticity theory. In the experiment, one end of the molecule was bound to a cover glass and the other end was attached to a bead. The trap was focused on the bead and stretching experiments were conducted [91].

After the discovery of this technique, numerous studies were later performed. An example is the visualisation of a 10kb DNA chain using fluorophores, attached to the backbone rather than intercalated with the bases, under an optical-tweezers set-up which was performed in our lab. While the initial study mentioned above had only one end trapped with a laser, in this study, both ends of the DNA were attached to beads, by non-covalent interactions, and positioned by optical traps. For attachment to beads, the ends of the DNA were functionalised by digoxigenin and biotin at each end, which could specifically attach to anti-digoxigenin and streptavidin beads, respectively [92].

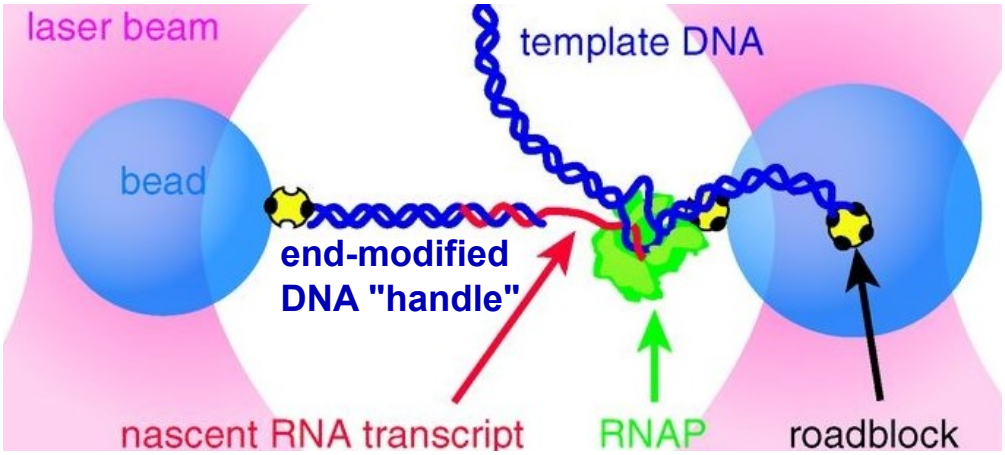

FIGURE 1.11: An example of an optical tweezers set-up where a DNA strand is attached to a bead and used as a handle adapted from [89].

As mentioned before, DNA has been the workhorse of single molecule experiments for several decades, especially those with OT. This is not only due to DNA's intrinsic biological relevance, but also owing to the facile control of its size and sequence, and the simplicity of attaching "handles" to the chain termini. The use of DNA to study DNA-protein conjugates has previously been employed to understand the behaviour of proteins at the single molecule level [93–97]. However, carrying out similar studies on other important biological macromolecules, such as polysaccharides, has somewhat languished behind. This is despite the clear need for such experiments in samples where, more often than not, heterogeneous sub-populations exhibit different properties that are masked in bulk studies. A generic strategy that enables the generation of a "plug-and-play" string

format and facilitates the study of shorter molecules with more challenging attachment chemistry, would represent significant progress towards helping to ameliorate this difficulty.

1.5 Statement of Objectives

This thesis aims to form "strings" where a single molecule of desired polysaccharide, in this case, HG, is attached in between two DNA "handles". Initial attempts that aimed to use direct chemical attachment of the polysaccharide to the DNA availed unsatisfactory results (shown in Appendix B). The idea was then slightly modified to use divalent streptavidin molecules as linkers in between the polysaccharide and DNA handles, as shown in Figure 1.12. It is to be noted that the set-up is not as rigid but could possibly be flexible. A step-by-step approach is followed:

1) Formation of divalent streptavidin (Chapter 3)

2) Modification of terminal ends of the polysaccharide (Chapter 4)

3) Assembly of the polysaccharide-DNA strings with divalent streptavidin linkers (Chapter 5).

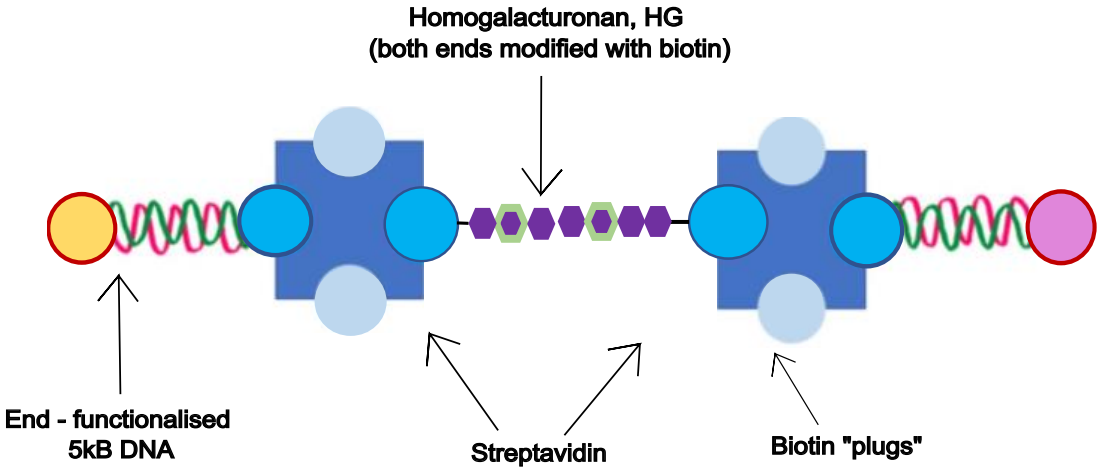

FIGURE 1.12: Illustration of the final "strings" set-up. (Pink and yellow circles represent different groups which can be used to attach to beads, e.g digoxigenin and dibenzocyclooctyne, DBCO groups.)

This set-up has several potential advantages but, most importantly, the polysaccharide of interest is not in direct contact with the laser field. Additionally, this set-up can also be generalised for any polysaccharide in which the two ends can be functionalised with biotin. In this thesis, the length of the polysaccharide is approximated to be at 25 nm which is much smaller compared to the total 1 µm length of the DNA. Hence, this set-up can be adapted to study short polysaccharides in the single molecular set-up, which is otherwise difficult.

Chapter 2

Experimental Methods

This chapter gives a brief overview into some of the experimental techniques that were employed in this project. A whole variety of techniques were employed in this study, the main ones being: Capillary Electrophoresis (CE), Enzyme Labelled ImmunoSorbent Assay (ELISA), Nuclear Magnetic Resonance (NMR), Polymerase Chain Reaction (PCR) and Polyacrylamide Gel Electrophoresis (PAGE). The following sections discuss the main principles of each of these techniques and how they are relevant in understanding the experimental results they convey. Further details regarding the experimental methods and material are given in each of the experimental chapters as relevant.

2.1 Capillary Electrophoresis (CE)

Electrophoresis is a separation technique based on how particles and molecules move with respect to their charge and size, in the presence of an electric field. Capillary electrophoresis (CE) is a widely used technique in the separation and analysis of charged molecules based on their electrophoretic or ionic mobility. The main advantage of the CE is that it only requires a small quantity of the sample (~30 µL) and is non-destructive. CE can also be coupled with other methods, such as mass spectrometry, to attain results with improved sensitivity [98].

The important constituents in the CE setup used here and illustrated in Figure 2.1 are:

- Capillary – A narrow (50 µm) bore, fused silica capillary is generally used.
- Electrodes – Platinum electrodes are used. Each electrode is dipped in to the background electrolyte (BGE) solution.
- Electrolyte – An ionic buffer (e.g. sodium phosphate buffer) is used where pH and ionic strength can be varied. Also known as the background electrolyte, BGE.

- High voltage supply – Variable from 5 to 30 kV.
- Sample injector.
- UV lamp and detector.

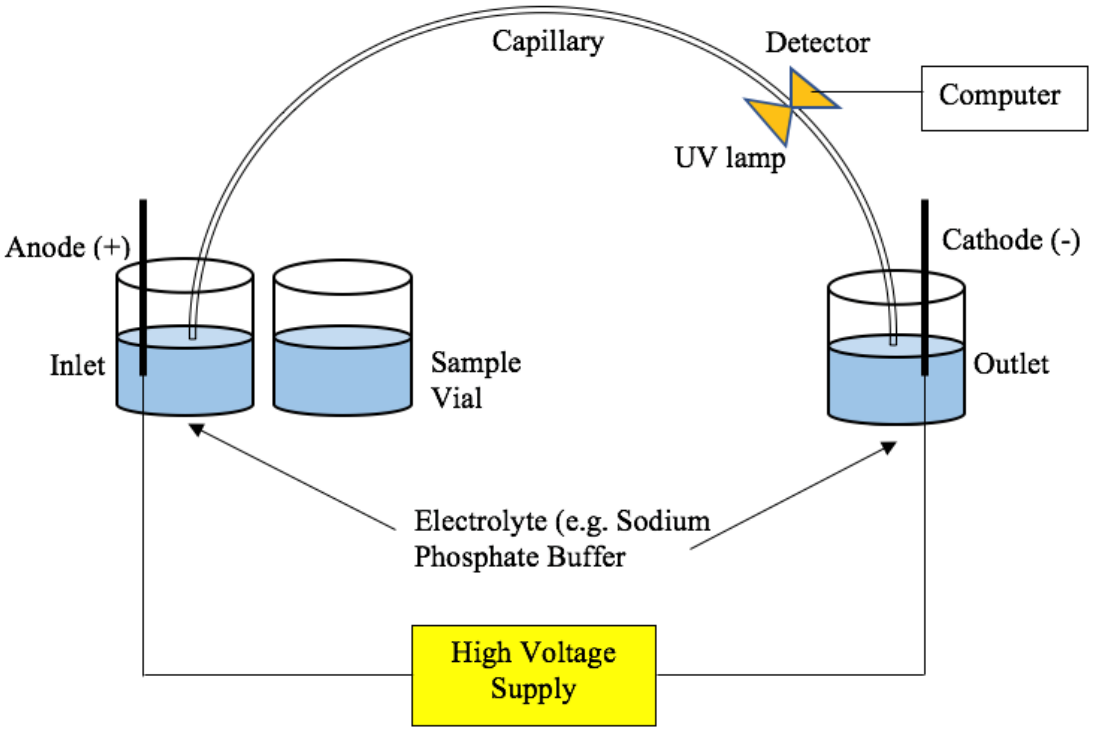

FIGURE 2.1: Schematic diagram showing the different components present in a CE set-up.

As the name suggests, the sample undergoes electrophoresis through a narrow capillary filled with BGE. On the application of a high voltage, analytes travel through the capillary at different velocities, depending on their size and charge, and the electroosmotic flow of the background electrolyte. Both the analyte molecules, and the ions in the buffer, move through a silica capillary (which conveniently has an electric double layer on its wall). The electric double layer illustrated in Figure 2.2 is formed due to the attraction between the negatively charged silanol groups, formed by conditioning the silica coated capillary with sodium hydroxide, and the cations in the buffer. When a potential is applied, the cations in the double layer move towards the negative electrode, dragging the fluid containing the analytes towards the cathode. As they move towards the cathode, the analyte molecules pass through a window in the capillary where their absorbances are determined using a UV lamp and a diode array detector, which is then expressed in the output, in the form of an electrophoregram [98–100].

Molecules migrate at a speed determined by a combination of the electroosmotive force (EOF) and their own mobility relative to that of the background electrolyte. Generally, in an electrophoregram, due to the polarity used and the direction of the electroosmotic flow, the positively charged molecules are eluted first, followed by the neutral molecules and finally, the anionic molecules which are swimming against the tide of the electroosmotic flow (EOF) [101]. For negatively charged species, molecules with low charge densities elute first followed by molecules of higher charge densities. In contrast to gel electrophoresis, the elution here is more dependent on the overall charge density of the molecule and the friction coefficient, rather than solely the molecular size or shape.

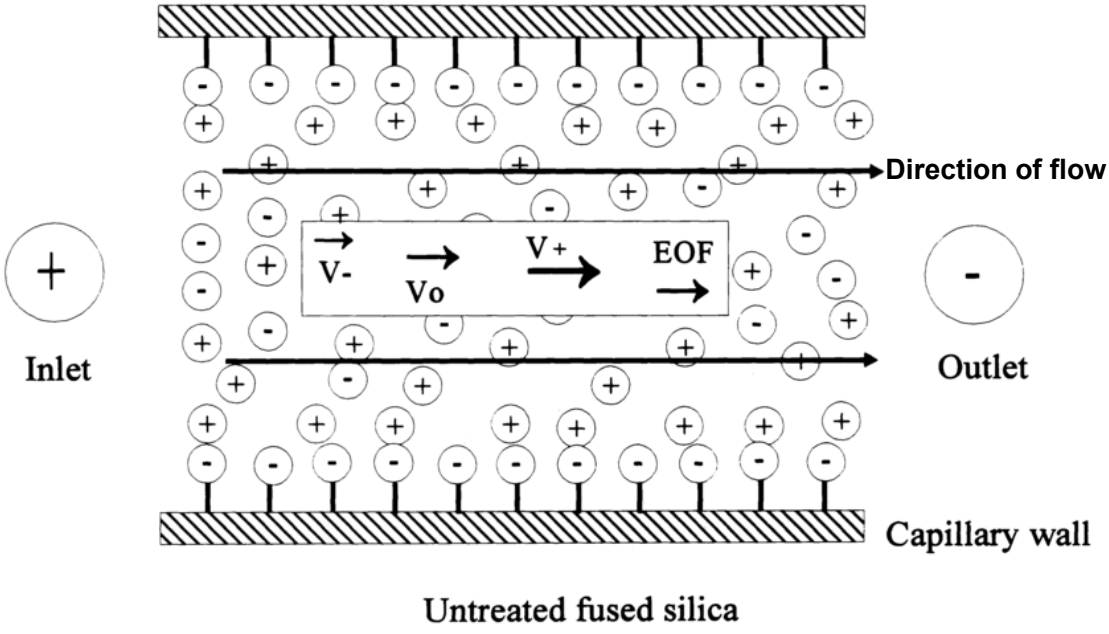

FIGURE 2.2: Schematic diagram showing the electrical double layer on the capillary wall (V-, V_0, V+ represent anionic, neutral and cationic species respectively) adapted from [102].

Analysing pectin using CE

As migration in CE is dependent on the electrophoretic mobility of the analyte, this technique can be highly useful for the analysis of pectin samples of varying degrees of methylesterification and polymerisation [103]. In the work reported in this thesis, the polysaccharide undergoes a change in its size or charge at every step of the reaction. The electrophoretic mobility can be calculated using the equation [104]:

$$\mu_{ep} = \frac{L_{tot} \cdot L_{eff}}{V} \cdot (\frac{1}{t_{mig}} - \frac{1}{t_{EOF}})$$

(2.1)

where,

μ_{ep} is electrophoretic mobility of species ($m^2\ V^{-1}s^{-1}$),

L_{tot} is total length of the capillary (m),

L_{eff} is distance between the point of injection and point of detection (m),

V is applied voltage (V)

t_{mig} is migration time of species (s) and

t_{EOF} is migration time of neutral species (electroosmotic flow) (s).

Furthermore, a new functional group, having a characteristic absorbance, is introduced in the homogalacturonan after each step. Hence, CE with UV detection can be used as an analytical tool to monitor the progress of the reactions [105].

2.2 Enzyme Labelled ImmunoSorbent Assay (ELISA)

Enzyme Labelled ImmunoSorbent Assay (ELISA) is a technique that utilises the specificity of antibodies and enzymes' ability to attach to a substrate in order to detect its presence. ELISA emerged in the early 1970s as a substitute for radioimmunoassays [106, 107]. ELISAs can be visualised colorimetrically, by the coloration developed on coupling an antibody with an appropriate enzyme capable of releasing a coloured product from a colourless substrate and research has been performed to improve this colorimetric sensitivity [108, 109]. The intensity of the colour allows for quantification of the reaction. ELISAs are commonly used for detection of proteins but can also be used for various other systems.

ELISAs can be divided into different types depending on how the procedures are modified. The different types of ELISAs are direct ELISA, indirect ELISA, sandwich ELISA and competitive ELISA are shown in Figure 2.3 [110]. Direct and indirect ELISAs differ based on whether the detection antibody is conjugated directly or indirectly with the enzyme used [111, 112]. Sandwich

ELISAs use a capture and detection antibody specific to the sample of interest, which can then be detected directly or indirectly [113]. As this technique uses two specific antibody pairs, sandwich ELISA has a much higher sensitivity compared to the other ELISAs [114]. In this thesis, sandwich ELISAs are used to detect if products of interest have been formed or not (specifically biotin and digoxigenin terminated species).

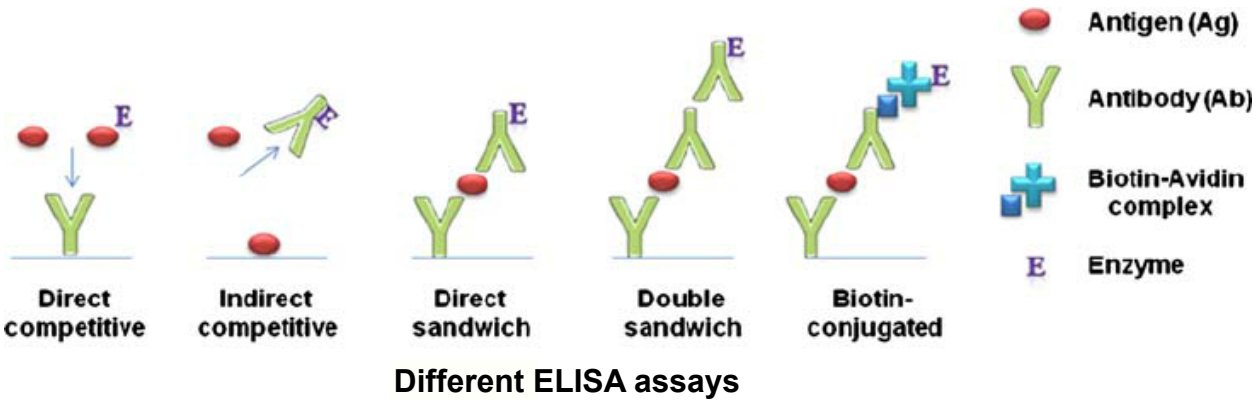

FIGURE 2.3: Schematic diagram showing different types of ELISA adapted from [115].

There are several steps to performing a sandwich ELISA test as shown in Figure 2.4. The first is to coat a surface of the well plate overnight with an antibody (capture antibody) that specifically binds to one end of the sample being sought. This forms the first layer on the ELISA plate. Before the next step, the excess antibodies are washed away, and the remaining non-specific binding sites of the plate are blocked with a blocking agent, such as BSA or milk protein. The plates are washed and the sample to be tested is then introduced. After incubation, the unbound samples are removed by washing and a specific enzyme-labelled antibody (detection antibody) is added for detection. The plates are washed again, and a colour developing substrate is added and the plate is then read. Before each addition step, it is crucial to remove all the excess species from the previous step. Hence, washing the plates several times before each step, is recommended [116, 117].

Detection using ELISA

In this project, the success or otherwise of the chemistries for modifying the reducing and non-reducing end of polysaccharides were tested using sandwich ELISA. At the reducing end, the goal was to attach biotin using a bifunctional polyethylene glycol linker, with an aminooxy group at one end and a biotin group at the other end. The attachment of the aminooxy group to

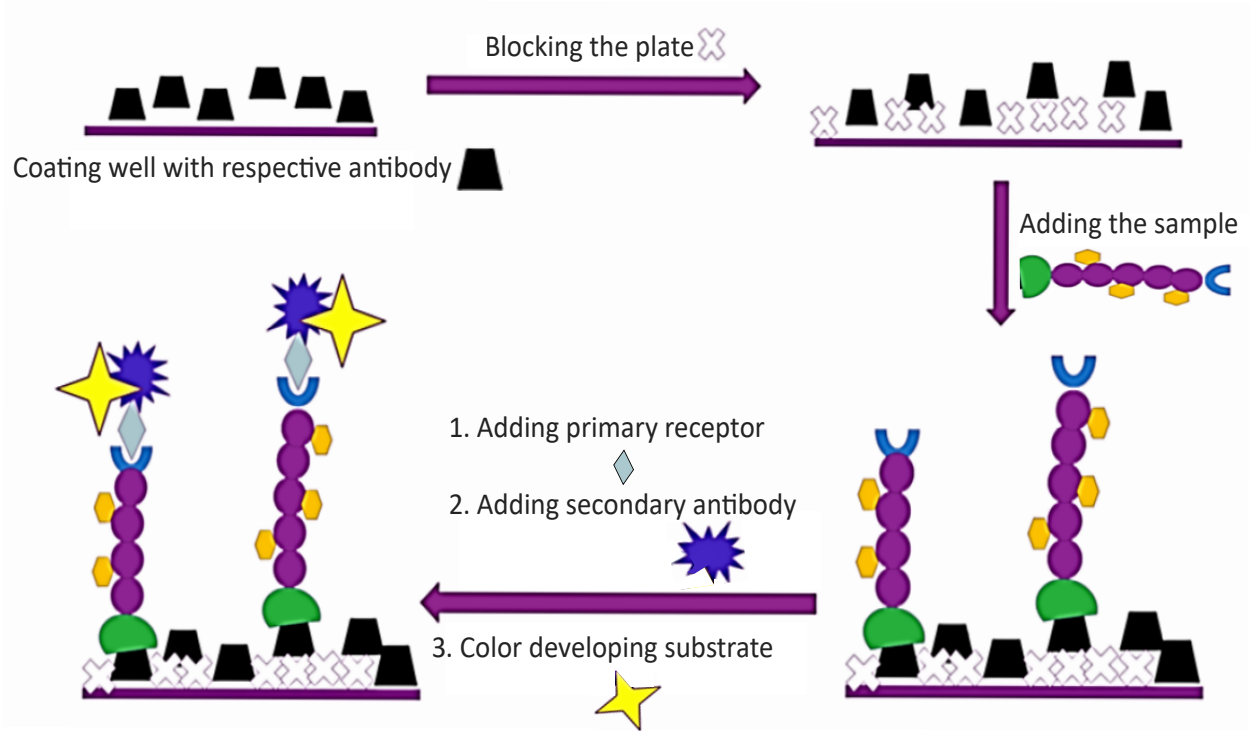

FIGURE 2.4: Steps involved in a sandwich ELISA.

the reducing end is tested using JIM7 (binds to highly methylesterified homogalacturonan epitopes) and streptavidin-HRP antibodies (binds to biotin epitopes). Ultimately, in this project, the polysaccharide of interest will be functionalised with biotin at both ends (to enable their linking to streptavidin). However, it is not possible to have suitable controls when you have the same epitope at both ends. Hence, for the purpose of detection, attachment of digoxigenin at the terminal non-reducing end was attempted. This attachment at the non-reducing end can then be detected in a sandwich ELISA using JIM7 and anti-digoxigenin (binds to digoxigenin antibodies). Moreover, to test if biotin and digoxigenin have been attached to the reducing end and non-reducing end respectively, streptavidin-HRP and anti-digoxigenin are used. 5 kb DNA end-functionalised with biotin and digoxigenin were used as positive controls (Figure 2.5). A positive result in ELISA would conclusively suggest that both ends have been functionalised with the desired moieties.

2.3 Nuclear Magnetic Resonance (NMR)

Amongst other things, such as imaging, and the study of dynamics, Nuclear Magnetic Resonance (NMR) is a spectroscopy technique that has been used widely for the structural determination of

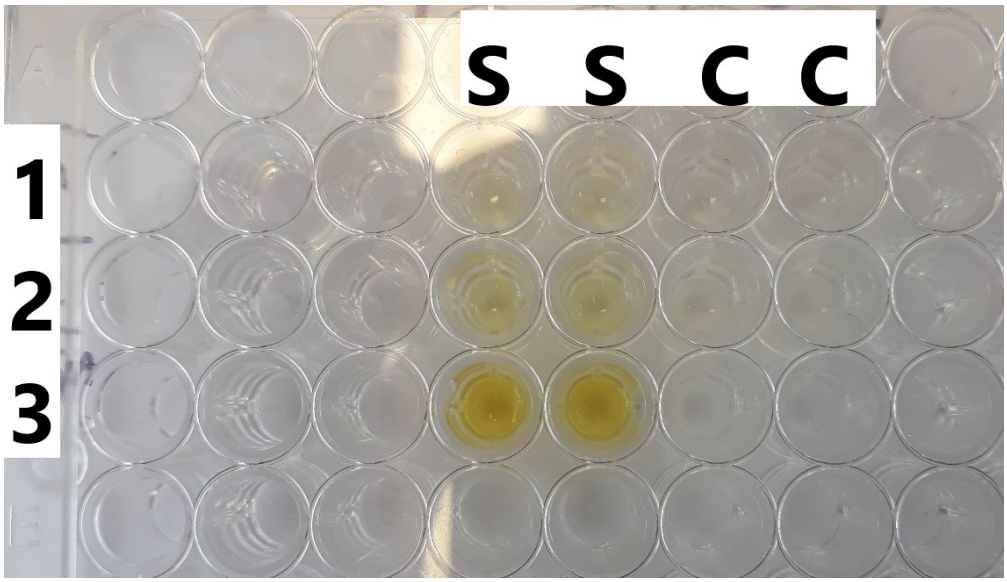

FIGURE 2.5: A figure showing different intensities of a positive result in an ELISA plate: **S** = sandwich, **C** = control, **1** = 50 ng/µL of biotin-DNA-dig, **2** = 75 ng/µL of biotin-DNA-dig, **3** = 300 ng/µL of biotin-DNA-dig.

unknown compounds for decades. There are different varieties of NMR techniques, ^{1}H NMR being the most common 1D spectroscopy (one axis only) and Correlation Spectroscopy (COSY), Heteronuclear Single Quantum Coherence Spectroscopy (HSQC) and Heteronuclear Multiple Bond Correlation Spectroscopy (HMBC) for 2D spectroscopy (two axes).

As the name suggests, NMR makes use of magnetic fields of different atoms which can interact with an applied external magnetic field. The applied field lifts the degeneracy of the nuclear spin levels, giving the permissible quantised angular momentum states different energies; providing a gap that can be probed via interactions with radio-frequency electromagnetic radiation of the same energy as the gap, the resonance condition. The energy difference between these nuclear spin states are not only different for different types of nuclei, but are also modified by the arrangement of surrounding electrons, and thus the NMR spectrum informs on local bonding and has become an indispensible structural tool for the chemist. Based on the local binding then, the positions of the so-called chemical shifts vary allowing detailed chemical information to be attained.

Some of the different NMR techniques employed in this project are briefly described below (The chemical structures used are selected as a means to explain how the different NMR analyses are performed and are not directly related to the project).

^{1}H NMR The most common 1D NMR technique used. Generally, deuterated solvents are used to obtain proton NMR spectra, so that the signals from the solvent can be ignored. If more than one

neighbouring proton is present in a molecule, the primary peak for a proton can split into different patterns as the magnetic fields of the different protons can interact. Observing such multiplicties allows the coupling constants to be calculated from how the peak has been split. The integration of proton peaks give us an idea of how many protons have the same chemical shift (Figure 2.6) [118].

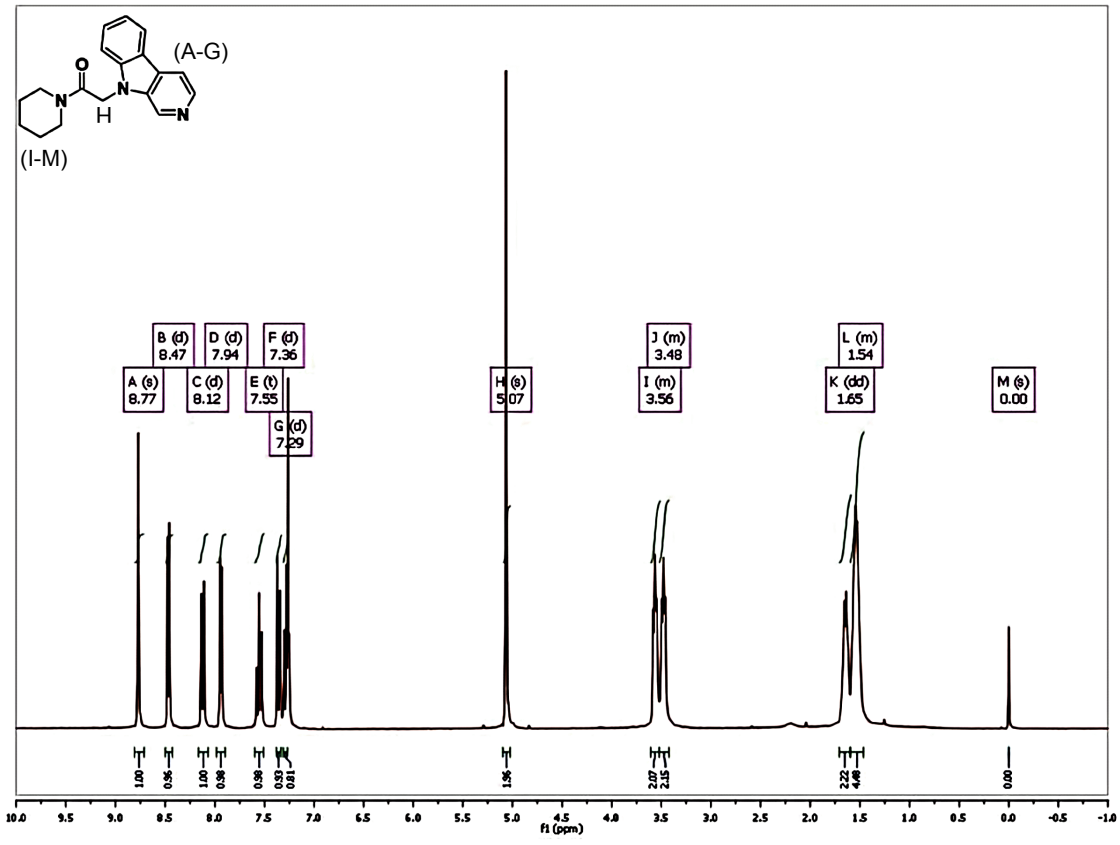

FIGURE 2.6: Example of a ^{1}H NMR spectrum adapted from [118].

COSY ^{1}H-^{1}H Correlation Spectroscopy (COSY) is a 2D NMR spectroscopy which reveals cross-peaks between protons that are a maximum of three bonds apart (Figure 2.7)[119].

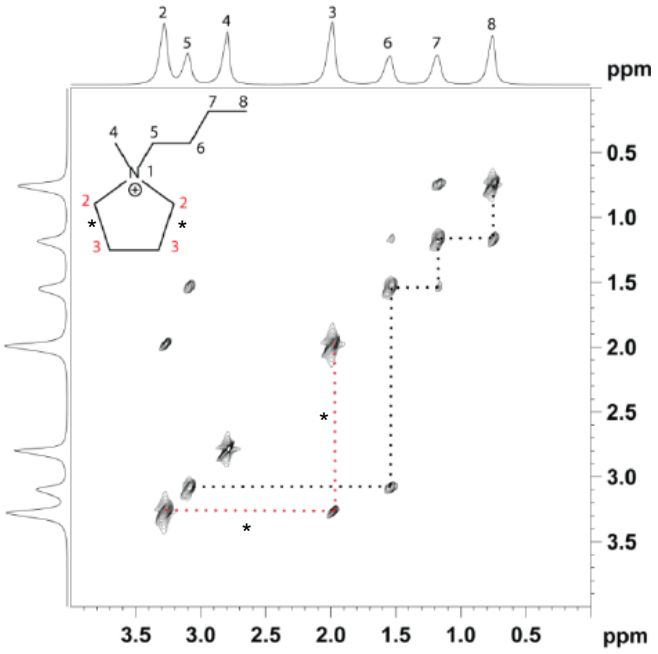

FIGURE 2.7: Example of a COSY spectrum showing how the different protons interact with each other (* indicates interactions between the protons attached at C-2 and C-3) adapted from [119].

HSQC ^{1}H-^{13}C Heteronuclear Single Quantum Coherence Spectroscopy (HSQC) is a 2D NMR spectroscopy that, in its most common incarnation, provides insight into how each proton peak is linked to a specific carbon atom (Figure 2.8) [120].

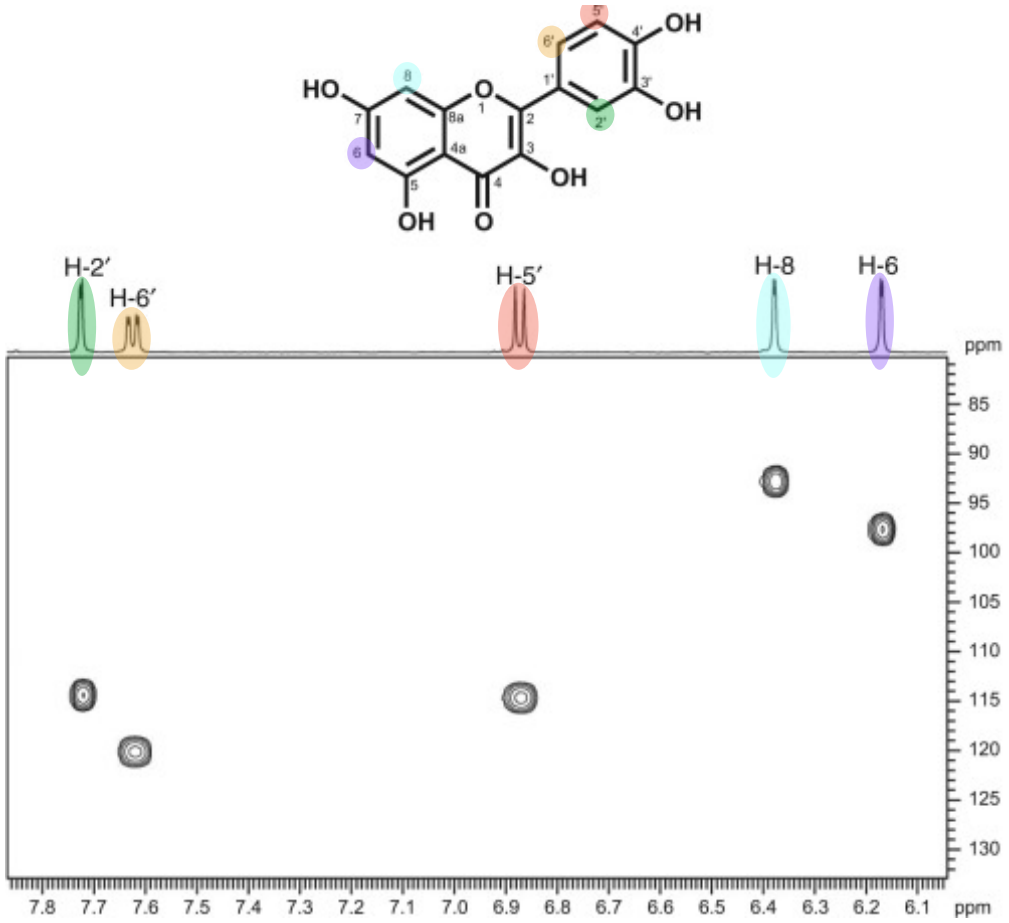

FIGURE 2.8: Example of a HSQC spectrum adapted from [120].

HMBC ^{1}H-^{13}C Heteronuclear Multiple Bond Correlation Spectroscopy (HMBC) is a 2D NMR spectroscopy which also probes how magnetically distinct protons and carbons are linked, but, unlike the HSQC, HMBC gives information on proton and carbon interactions that are multiple bonds apart (maximum three bonds apart) (Figure 2.9)[121].

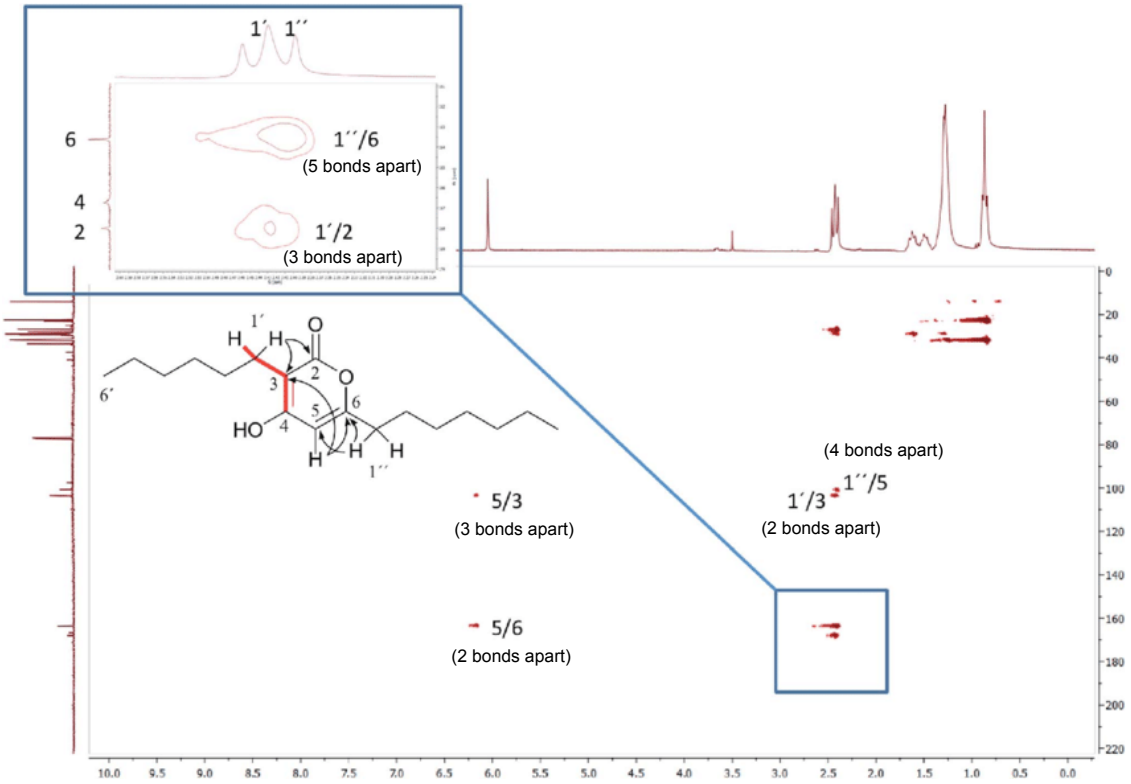

FIGURE 2.9: Example of an HMBC spectrum adapted from [121].

Monitoring using NMR

In this project, the desired modification of the terminal ends of polysaccharides was also performed on oligosaccharide fragments, so that NMR can more clearly reveal the changes generated. As a new functional group was introduced at every step of the reaction, the reactants and the products of each step were analysed using NMR. As a result, NMR has proven to be a very conclusive technique in determining whether the molecule of interest has been successfully functionalised or not. It is to be noted that, a relatively pure and high yield of product is needed for a good NMR analysis. Hence, for determining the successful functionalisation of the polysaccharide, HG, ELISA is preferred as the results are conclusive, despite having a low purity and yield.

2.4 Polymerase Chain Reaction (PCR)

Polymerase chain reaction, *PCR*, is an enzymatic procedure involving a repetitive cycle of steps, denaturation and annealing of DNA primers and extension, which can lead to the formation of controllable long double stranded DNA fragments. Primers are short, complementary single stranded DNA sequences from which a DNA strand is extended along a template DNA, by a

DNA polymerase. The complementary primers are referred to as forward and reverse primers based on the direction to which they attach on to the DNA strand that is synthesised [122].

A PCR reaction is carried out in a thermal cycler machine, which is able to vary the temperatures as required for each step. As shown in Figure 2.10, the mixture is first heated to a temperature above 90^{o}C to ensure denaturation. After the strands of the template DNA are separated in this step, the temperature is reduced to allow for the complementary primer sequence to bind or anneal. In the next step, the temperature is slightly increased and the DNA polymerase starts to bind the primers and extend a strand. Multiple repetitions of this cycle allows for replication of several DNA strands [122, 123].

1) Denaturation at 90^{o}C

2) Annealing at 54^{o}C

3) Extension at 72^{o}C

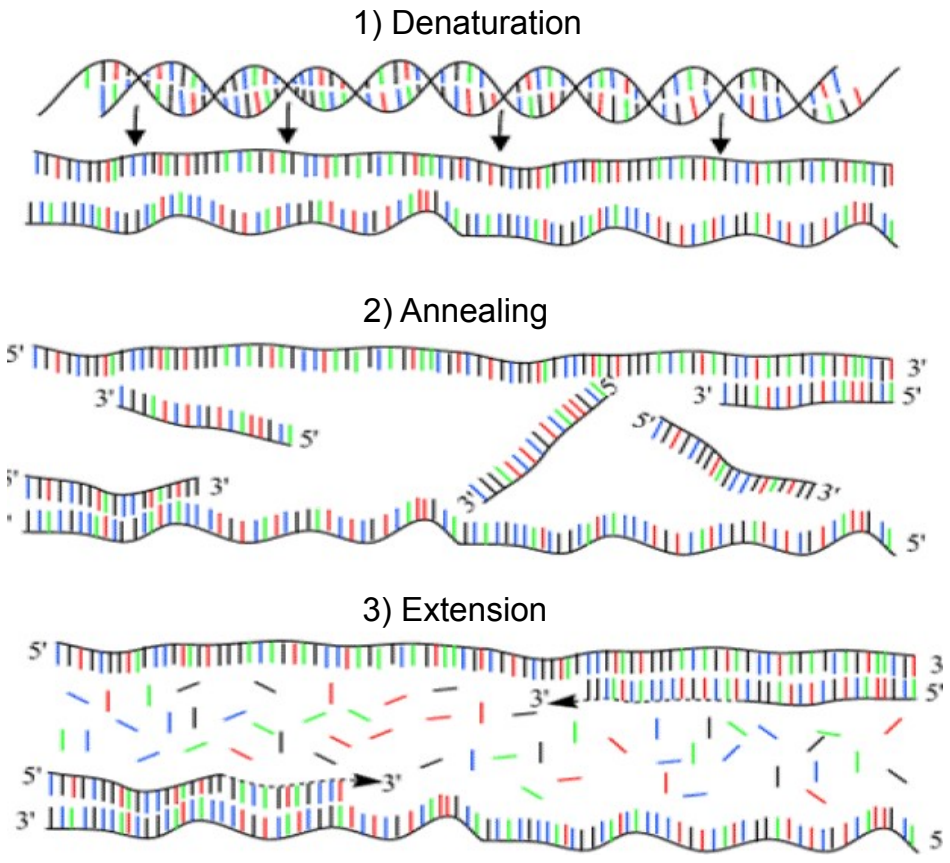

FIGURE 2.10: The basic steps involved in a PCR reaction. 3′ and 5′ labels indicate that the phosphate group is linked to either the 3^{rd} or 5^{th} carbon atom in the deoxyribose sugar adapted from [123].

The PCR product subsequently obtained can then be analysed by gel electrophoresis on an agarose gel. The products are run alongside a DNA ladder which indicates the standard sizes of different double-stranded DNA. Commonly used ladders have a range of 500 bp to 10 kB. The gel electrophoresis is run and the gel is stained for visualisation. A classic staining agent used is ethidium bromide, which stains by intercalating itself into a double-stranded DNA. The stained DNA bands can be clearly visualised, due to the intercalation of the staining agent, as a fluorescent band in the presence of UV light [123].

In order to synthesise DNA strands, functionalised at both ends, PCR is carried out using two different functionalised primers. Each DNA strand used in this study will have a biotin functional group on one end for conjugation with streptavidin, and a biotin, alkyne or digoxigenin at the other end for coupling to beads that can be manipulated using OT.

2.5 Polyacrylamide Gel Electrophoresis (PAGE)

As mentioned previously in section 2.1, electrophoresis is a separation technique depending on the size and charge of particles, and how they travel under an applied voltage. Unlike CE which is a free solution electrophoresis technique, PAGE makes use of a gel matrix in an attempt to resolve species based on the size and shape of the molecules and how they move through the pores, For a typical electrophoresis set-up, the separation of different components occurs in a support medium, which can be a gel or a membrane. In biochemistry, agarose and polyacrylamide are the most commonly used gel media. Polyacrylamide gel electrophoresis, also referred to as PAGE, has a much higher resolution in separating smaller molecules (lower than 500 bp). Sodium dodecyl sulfate polyacrylamide gel electrophoresis (SDS-PAGE) is most commonly used for proteins as SDS denatures the tertiary structure of proteins into linear structures to which the SDS can bind to uniformly [124]. In this thesis, non-denaturing PAGE gels (native PAGE gels), or SDS PAGE gels without boiling, are generally used with additional insight into net charge density and shape compared to denaturing SDS-PAGE gels. Highly charged molecules, with a smaller size and less friction through the pores, will migrate through gels faster.

Aqueous polyacrylamide is a viscous liquid polymer of acrylamide formed by free radical polymerisation. On addition of N,N'-methylenebisacrylamide, which acts as a cross-linker, to an

acrylamide solution, the long polyacrylamide chains connect together, as shown in Figure 2.11, to form a three-dimensional network, leading to gel formation [125].

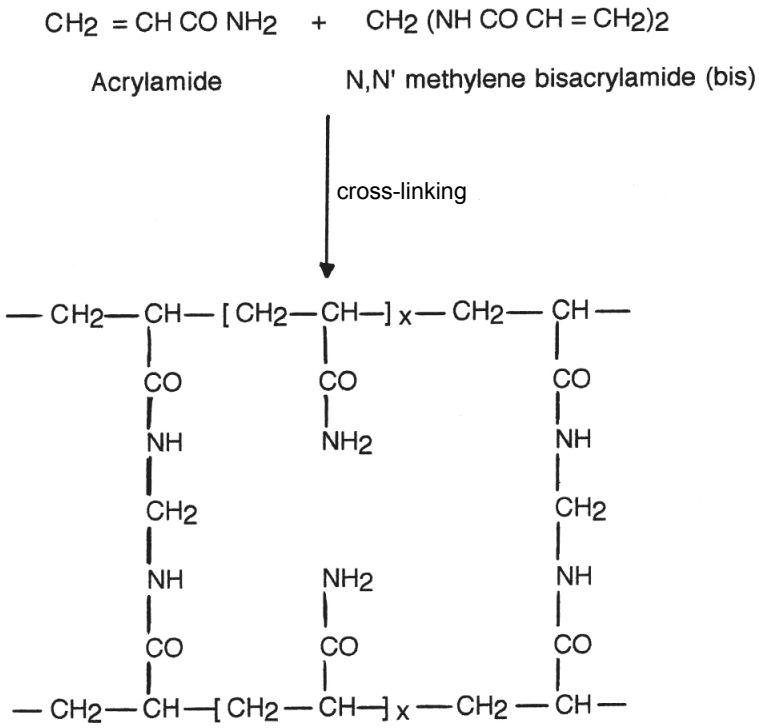

FIGURE 2.11: Formation of polyacrylamide adapted from [126].

While most gels have a horizontal set-up, PAGE gels are run in a vertical gel set-up, as shown in Figure 2.12, where the gel is placed between two glass plates, surrounded by a buffer solution, such that two electrodes are only connected to each other through the gel [127]. Hence, the voltage applied across the gel is controlled and consistent, further improving resolution. After a prescribed amount of time, the gel is visualised using staining agents. Ethidium bromide is widely used in the staining of PAGE gels for DNA and Coomassie Blue or Silver for proteins [127, 128]. In this project, PAGE is highly advantageous as both homogalacturonan and the primers can be visualised, separately, by using two different staining agents, stains-all, a carbocyanine dye, and ethidium bromide respectively. Although stains-all can be used for staining both the polysaccharide and the primer, ethidium bromide stains the primers only.

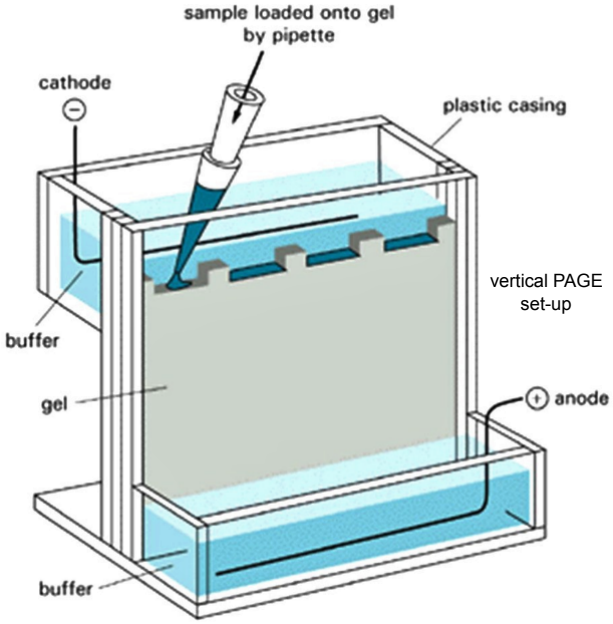

A

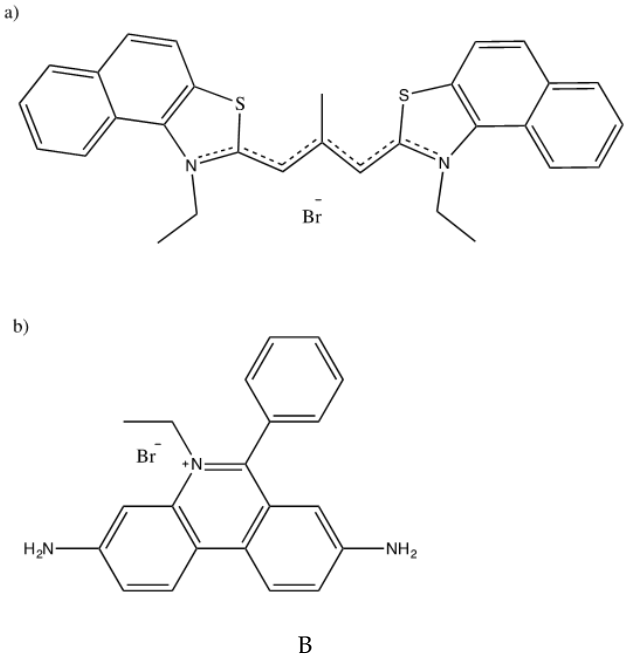

B

FIGURE 2.12: (A) The general vertical set-up of a PAGE gel adapted from [127]. (B) Structure of dyes used for staining PAGE gels: a) stains-all b) ethidium bromide.

Chapter 3

Divalent Streptavidin Linkers

DRC 16

MASSEY UNIVERSITY TE KUNENGA KI PŪREHUROA UNIVERSITY OF NEW ZEALAND | GRADUATE RESEARCH SCHOOL

STATEMENT OF CONTRIBUTION
DOCTORATE WITH PUBLICATIONS/MANUSCRIPTS

We, the candidate and the candidate's Primary Supervisor, certify that all co-authors have consented to their work being included in the thesis and they have accepted the candidate's contribution as indicated below in the *Statement of Originality*.

Name of candidate:	Nimisha Mohandas
Name/title of Primary Supervisor:	M.A.K. Williams
In which chapter is the manuscript /published work:	3

Please select one of the following three options:

(●) The manuscript/published work is published or in press

- Please provide the full reference of the Research Output:

IN PRESS Journal: ACS Omega; Title: "Progress towards plug-and-play polymer strings for optical tweezers experiments: Concatenation of DNA using Streptavidin-Linkers"
Author(s): Mohandas, Nimisha; Kent, Lisa; Raudsepp, Allan; Jameson, Geoffrey; Williams, Martin

( ) The manuscript is currently under review for publication – please indicate:

- The name of the journal:
- The percentage of the manuscript/published work that was contributed by the candidate: 75.00
- Describe the contribution that the candidate has made to the manuscript/published work:

Nimisha carried out the lion's share of the experimental work and contributed to the design, analysis and writing of the study.

( ) It is intended that the manuscript will be published, but it has not yet been submitted to a journal

Candidate's Signature:	
Date:	01-Feb-2022
Primary Supervisor's Signature:	ExpressVPN Client Digitally signed by ExpressVPN Client Date: 2022.02.02 13:34:26 +13'00'
Date:	2-Feb-2022

This form should appear at the end of each thesis chapter/section/appendix submitted as a manuscript/ publication or collected as an appendix at the end of the thesis.

GRS Version 5 – 13 December 2019
DRC 19/09/10

3.1 Introduction

Single molecule studies have continued to grow in popularity as technological capability improves and experimental platforms for their application become more available. While typically challenging compared to traditional bulk techniques, single molecule studies offer unprecedented access to the world of molecular biology and deep insights into the functioning of molecular machines in the noisy thermal bath in which they operate. Optical Tweezers (OT) have provided a key experimental tool for the pursuit of such studies, acknowledged recently by the award of a Nobel prize.

For several decades DNA has been the workhorse of single molecule experiments, especially those carried out with OT. This is not only due to DNA's intrinsic biological relevance, but also owing to the facile control of its size and sequence, and the simplicity of attaching "handles" to the chain termini. DNA-protein conjugates have also previously been employed to help understand the behaviour of proteins at the single molecule level [93–97]. However, similar studies on other important biological macromolecules, such as polysaccharides, have somewhat languished behind. This is despite the clear need for such experiments in samples where, more often than not, sub-populations of heterogeneous samples exhibit different properties that are masked in bulk studies. A generic strategy that enables the generation of a "plug-and-play" string format and facilitates the study of shorter molecules with more challenging attachment chemistry, would represent significant progress towards ameliorating this difficulty.

Streptavidin-biotin is one of the most widely known non-covalent binding pairs and can be used, among other things, to perform biomolecule conjugation. With a dissociation constant, K_d of $\sim$ 0.1-10 fM, streptavidin-biotin conjugation has found wide versatility in biotechnology, including in applications from biosensors to cell biology [129]. Streptavidin is a homotetrameric protein, with each monomer able to bind one biotin-displaying molecule [70]. The binding of biotin to streptavidin has been found to be non-cooperative but with every additional binding of biotin the structural and thermodynamic stability of the protein itself increases [74–76]. Being able to control the the number of active valencies that the tetramer displays opens up potential pathways to further applications by allowing hubs of known valency (1, 2, 3, or 4) to be formed. Previous attempts of this type have largely involved using genetic modification techniques to produce monomeric mutants that are not capable of biotin binding, but are still successfully incorporated into the tetramer [77, 78]. Furthermore, designed modifications of the binding properties

of monomeric and dimeric streptavidin have also been carried out [79–82]. Other methodologies that have sought to reduce the possible number of biotin-bearing molecules that can bind to tetramers have used preliminary incubations of streptavidin with biotin-terminated "plugging molecules". In this way, by controlling the stoichiometric ratios of components and the incubation time, partially filled monovalent, divalent, and trivalent streptavidin species can all be formed [83, 84].

A separation technique using anion-exchange chromatography for isolating different tetrameric "hubs" from streptavidin samples with different amounts of the potential binding sites blocked has previously been reported [83]. Specifically, after incubating streptavidin with 12 bp double-stranded DNA molecules carrying a biotin moiety at one end, species with different numbers of the binding sites filled were successfully separated using an anion-exchange chromatography column. By incorporating a photocleavable (PC) 2-nitrobenzyl linker between the 12 bp oligonucleotide and the biotin, it was then possible to remove the separation-facilitating DNA oligomers post-fraction-collection, leaving just the “biotin plugs”. This enabled the generation of a series of “pre-plugged” streptavidin species with certain sites passivated and others available for binding biotin-displaying species.

Herein we perform experiments of this type, but monitor the valency of the different species and the site-plugging process, using capillary electrophoresis (CE), in contrast to traditional gel chromatography. Based on our results, different valency species were resolved much more clearly in CE than in gels. Moreover, the *trans*-divalent streptavidin species collected here were incubated with $\sim$ 5 kb biotin-terminated DNA strands. Following the incubation concatenated $\sim$ 10 kb strings were detected using gel electrophoresis and, furthermore, were successfully stretched between beads in a traditional dual-trap dumbbell-style DNA-stretching experiment.

3.2 Materials and Methods

Streptavidin - DNA oligonucleotide binding. DNA oligonucleotides (Integrated DNA Technologies, Inc., Coralville, Iowa/Singapore) and streptavidin (PRO-283, ProSpec-Tany TechnoGene, Ltd., Rehovot, Israel) were purchased and used following the protocols described in detail in Sun et al. [83]. Briefly, a primer with a photocleavable biotin moiety attached via the 5′ end (biotin-PC-AGC-ACA-TCC-CCC) was annealed to its complement (GGG-GGA-TGT-GCT) in 10 mM sodium phosphate buffer, 50 mM NaCl pH 7.5 at 94 °C for 2 minutes and then cooled slowly, for a final

concentration of 450 µM double-stranded DNA. We combined this 12 bp DNA (40-160 µM final concentration) with streptavidin first dissolved in water (40 µM final concentration) overnight at room temperature in 100 mM sodium phosphate buffer pH 6.5. We tested various concentrations of 12 bp DNA with streptavidin to determine the optimal ratio for a maximum yield of streptavidin species with exactly two bound DNA oligomers. A ratio of 4:1 DNA to streptavidin (equivalently the total number of DNA oligos equal to the total number of binding sites on streptavidin) was used for sample preparation for running through the anion exchange column. Throughout, primer with photocleavable biotin was kept in the dark.

Anion Exchange Chromatography. To separate the streptavidin with different numbers of DNA oligos attached, we used a Uno Q column 5/50 (GE Life Sciences/Cytiva, Marlborough, Massachusetts) anion exchange column run in a NGC Quest 10 Plus Chromatography System (Bio-Rad Laboratories, Inc., Hercules, California). Following the protocol in Sun et al. [83], we used a linear salt gradient beginning with 100% Buffer A (20 mM Tris/HCl pH 8) and ending with 100% Buffer B (Buffer A with 1 M NaCl) over 400 mL at a rate of 2 mL/min.

Capillary Electrophoresis (CE). Experiments were carried out using an automated Agilent CE system (HP 3D), equipped with a diode array detector. Electrophoresis was carried out in a fused silica capillary of internal diameter of 50 µm and a total length of 48.5 cm (40 cm from inlet to detector), unless otherwise stated. The capillary incorporated an extended light-path detection window (150 µm) and was thermostatted at 25 °C. All new capillaries were conditioned by rinsing for 30 min with 1 M NaOH, 30 min with a 0.1 M NaOH solution, 15 min with water, and 30 min with Background Electrolyte (BGE). 50 mM sodium phosphate buffer at pH 7.0 was used as a CE background electrolyte (BGE) and filtered through 0.2 µm filters (Whatman) before use. Between runs, the capillary was washed for 2 min with 1 M NaOH, 2 min with 0.1 M NaOH, 1 min with water, and 2 min with BGE. Detection was carried out using UV absorbance typically at 192 nm or 260 nm with a bandwidth of 2 nm. Samples were loaded hydrodynamically (various injection times at 5000 Pa, typically giving injection volumes of the order of 10 nL) and typically electrophoresed across a potential difference of 25 kV. All experiments were carried out at normal polarity (inlet anodic) unless otherwise stated.

UV Irradiation. UV-induced cleavage of the 12 bp oligonucleotides from their biotin termini was performed using a multiband (254/366 nm) Mineralight UV lamp (Ultra-Violet Products,

Inc., San Gabriel, California). Samples in a quartz cuvette were subjected to UV irradiation for different times and the photocleavage monitored by Capillary Electrophoresis (CE).

DNA Gel Electrophoresis. To produce $\sim$ 5 kb DNA with biotin attached at one end, we performed PCR according to the manufacturer's recommendations (PCR Extender System, QuantaBio, Beverly, Massachusetts) using Lambda phage DNA as a template (New England Biolabs Inc., Ipswich, Massachusetts), a biotinylated primer and an unmodified primer (Forward 5'-BiotinTEG-CTGATGAGTTCGTGTCCGTACAACTGGCGTAATC-3', Reverse 5'-GTTTGTACTCCAGCGTCTC ATCTTTATGCGCC-3', Integrated DNA Technologies). This produced a single band in a conventional agarose gel electrophoresis experiment at the expected 5031 bp. The cleaned PCR product was combined with biotin-plugged divalent streptavidin, where the oligonucleotides of the two plugging molecules had been cleaved off with 5 minutes UV irradiation, and incubated overnight in 100 mM sodium phosphate buffer pH 6.5. Products of the incubation were visualised on a 0.5% agarose gel using staining with ethidium bromide.

Optical Tweezers (OT). DNA stretching experiments were carried out on an inverted microscope (Nikon Eclipse TE2000-U) equipped with Holographic Optical Tweezers (HOT) (Arryx, Chicago, USA). The set-up includes a fixed 5 W (1032 nm) infrared laser, a Spatial Light Modulator steered (SLM, Boulder NLS phase only) 2 W (1064 nm) infrared laser, and a high speed camera (Andor NEO). A high numerical aperture water immersion objective (Nikon plan apo, magnification = 60x, NA = 1.2) was used for focusing and trapping. The DNA studied here comprised of ~10 kb (10051 bp) pieces [130], ~5 kb (4682 bp) pieces, and ~10 kb assemblies of two of the 5 kb pieces concatenated with *trans*-divalent streptavidin. Each strand of the double-stranded duplex was terminated by either biotin or digoxigenin (pre-attached to the primers used in the PCR production process, 5'BiotinTEG or 5'DIGN, Integrated DNA Technologies) that bind to streptavidin- or anti-digoxigenin-coated beads, respectively, by physisorption. DNA was incubated in TSB (50 mM Tris, 150 mM NaCl, 1 mM EDTA, pH 7.6) with 1.26 µm diameter streptavidin-coated beads (SVP-10-5, Spherotech, Lake Forest, Illinois) for at least an hour and combined with 2.12 µm diameter anti-digoxigenin-coated beads (DIGP-20-2, Spherotech) in TSB in a well slide.

3.3 Results and Discussion

3.3.1 Observing streptavidin-dsDNA (12 bp) conjugates with CE

Streptavidin was mixed at varying stoichiometric ratios with 12 bp dsDNA oligomers (functionalized with biotin at one end via a photocleavable linker). Different ratios of dsDNA:tetravalent streptavidin (approximately 1:1 and 4:1) were incubated overnight, then analyzed by CE. The resulting electrophoregrams are shown in Figure 3.1A. By considering the different possible products of the incubation, i.e free streptavidin (N = 0), and streptavidin with one (N = 1), two (N = 2), three (N = 3) or four (N = 4) biotin-terminated DNA oligomers bound, and how the relative concentrations of these species would be expected to change as more DNA is added, the five peaks in the electrophoregram were preliminarily identified (see schematics in the figure). As shown in due course (Figure 3.6), there are three possible configurations (two *trans*-divalent and one *cis*-divalent) for the divalent product. Considering the evidence that the *cis*-divalent species is less stable due to steric hindrance [131], the *trans*-divalent products were expected to be dominant, with a minor quantity of *cis*-divalent streptavidin. Both possible *trans*-divalent species would be expected (i) to be populated similarly, as neither offers steric advantage, (ii) to be indistinguishable by electrophoretic techniques, and (iii) to stretch similarly in OT experiments. Statistically in plugging *trans* sites, both inter-dimer and intra-dimer *trans* arrangements are equally likely. The presence of distinct *trans* species, resulting from substantial tetrahedral distortion of the streptavidin homotetramer from the canonically depicted square-planar arrangement, does not appear to have been considered in prior work of tethering oligomers to streptavidin.

At the neutral pH of the CE separation, the streptavidin (pI = 5) is slightly negatively charged [132]. Under the CE conditions used, anionic species are dragged towards the cathode by the electroosmotic flow (EOF). The downward peak at around 3.5 minutes provides a neutral marker, (formed here by the refractive index change from injection plug solvent passing the detection window), and monitors the value of the EOF [104]. Peaks from positively charged species will migrate earlier than the EOF, and peaks from negatively charged species will be observed later. As the negative charge density of the complexes increases as an increased number of biotin-terminated nucleotides become bound, the migration time increases. Any unreacted DNA oligomers present elute considerably later owing to their high negative charge and small size and are not seen here. Based on the electrophoregrams (Figure 3.1A), a roughly 4:1 ratio of oligonucleotide species to streptavidin was adopted in order to produce an ideal distribution of multivalent species, and a

high yield of divalent species, for use in further trials.

The migration of species in the CE experiments was monitored using UV at several wavelengths including 192 nm, 260 nm, and 280 nm. DNA has a characteristic absorbance at 260 nm owing to their highly conjugated purine and pyrimidine bases, whereas proteins have a characteristic absorbance at 280 nm specific to the tryptophan and tyrosine moieties in proteins [133, 134]. Although using 260 nm and 280 nm is advantageous in monitoring DNA and proteins respectively, the maximum UV absorbance over the wavelengths monitored was found at 192 nm, reflecting the presence of the peptide bonds in the amino acids $\sim$ 205 - 220 nm [135, 136]. Hence, the absorbances at 192 nm were selected for rendering the electrophoregram figures (unless specified otherwise). The electrophoretic mobilities of the species observed in Figure 3.1A, were calculated according to:

$$\mu_{ep} = \frac{L_{tot} \cdot L_{eff}}{V} \cdot \left(\frac{1}{t_{mig}} - \frac{1}{t_{EOF}}\right) \tag{3.1}$$

where μ_{ep} is electrophoretic mobility of species, L_{tot} is total length of the capillary (0.485 m), L_{eff} is distance between the point of injection and point of detection (0.40 m), V is applied voltage (25 kV), t_{mig} is migration time of species and t_{EOF} is migration time of neutral species (electroosmotic flow) (3.35 min), and are shown in Table 3.1.

TABLE 3.1: Table showing the electrophoretic mobilities, μ_{ep}, of the various streptavidin:DNA conjugates shown in Figure 3.1A. Uncertainties are estimated at $\sim$5%.

Species (N)	t_{mig} (min)	μ_{ep} / 10^{-7} (m^2 V^{-1} s^{-1})
0	3.68	- 2.07
1	4.23	- 4.82
2	4.93	- 7.42
3	5.56	- 9.21
4	6.32	- 10.89

3.3.2 Fraction-collection of streptavidin-dsDNA (12 bp) conjugates of specific valency

While CE requires only tiny amounts of sample and resolves the differing species of interest well, in a relatively short time, its application as a preparative technique is limited. In order to collect specific partially-plugged species types, anion exchange chromatography was performed as

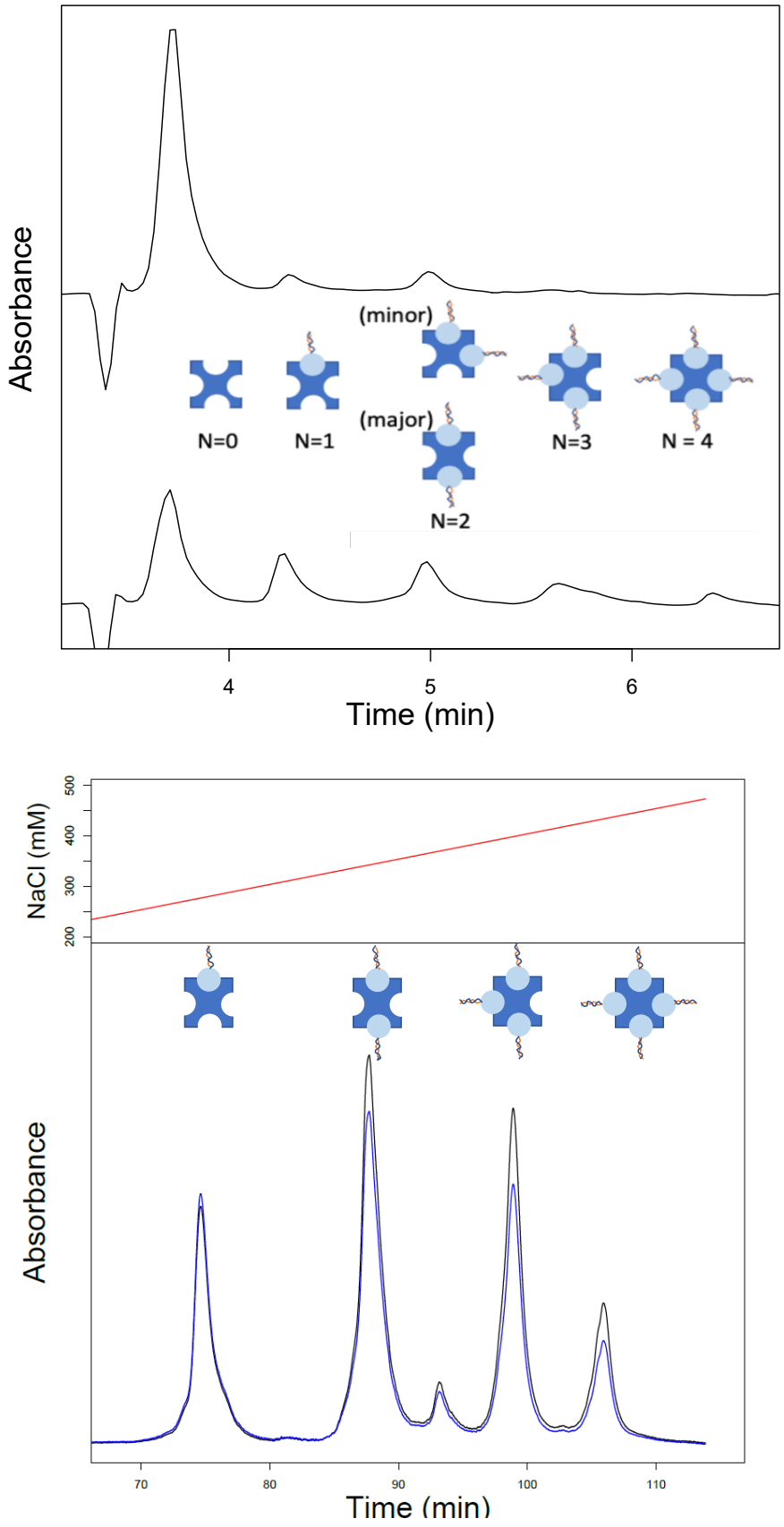

FIGURE 3.1: (A) Species formed when biotin-terminated 12 bp dsDNA was incubated with tetravalent streptavidin at different ratios (1:1 - top and 4:1 - bottom). Absorbance at 192 nm was recorded. (B) Separation of the different tetrameric species formed after overnight incubation of streptavidin with biotin-terminated 12 bp dsDNA, by anion-exchange chromatography, permitting fraction collection. The weakest band is tentatively assigned to a *cis*-divalent species. Absorbances at 260 nm (black) and 280 nm (blue) were recorded.

described in Materials and Methods. The resulting chromatogram following injection of the incubated sample is shown in Figure 3.1B.

This result compares well with that previously reported [83], and allowed known partially-plugged species types to be collected. As expected, there are two peaks observed for the divalent species, and following the original paper, the major peak is taken to be the *trans*-divalent species. The collected specific-valency streptavidin-DNA oligomer complexes were then run in CE experiments, in order to confirm the previous peak assignment shown in Figure 3.1A. A selection of these experiments is shown in Figure 3.2, which serves to highlight the utility of CE for the separation and monitoring of these species.

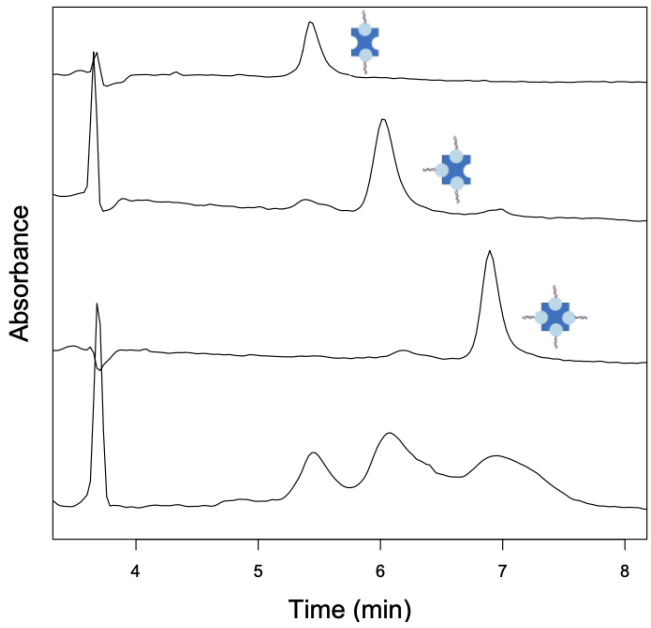

FIGURE 3.2: Electrophoregrams of the fraction-collected divalent (N = 2), monovalent (N = 3) and fully filled streptavidin (N = 4) fractions (obtained from the HPAEC column and labelled schematically), injected separately and co-injected (bottom) into the CE set-up.

When comparing Figures 3.1A and 3.2, it is worthwhile to mention a few points relevant to the interpretation of CE electrophoregrams. Firstly, it is not uncommon for the magnitude of the EOF to vary slightly, even between runs with nominally identical conditions, owing to its exquisite sensitivity to the zeta potential of the capillary walls that is difficult to regenerate exactly between successive runs [99, 100]. This means that the migration times of peaks representing species of interest (and thereby the observed resolution of different species) may be slightly different between runs. It should be noted, however, that the physical parameter distinguishing the electrophoretic transport of the analytes, the electrophoretic mobility, is of course unchanged, as can be confirmed

by its calculation which includes the migration time of the EOF. Secondly, depending on the relative composition (and thereby refractive index) of the sample and the BGE, the EOF-reporting peak can appear different in size and even negative or positive [101]. Here it is seen negative-going in Figure 3.1A, but positive-going in Figure 3.2, owing to the different solution conditions for the diluted fraction-collected samples.

3.3.3 Post-fraction-collection cleavage of dsDNA (12 bp) from streptavidin conjugates

Once the fractions were successfully collected, the oligonucleotide tails were cleaved off the separated species by UV irradiation to avoid any possible undesired interactions of subsequent molecules targeted for binding with those used in passivating the other sites. Figure 3.3A shows the products expected to be formed during the time-course of UV radiation exposure when starting with: the divalent species (i, top), the monovalent (ii, middle), and the fully-filled streptavidin conjugate (iii, bottom). On cleaving the linkage between the biotin and the DNA, this process leaves each streptavidin binding site, that was originally occupied by the 12 bp dsDNA oligomer, with only the biotin stub in the pocket. This essentially plugs the binding site so that it is not available for further interaction. The figure shows the possible mixture of species that would be expected to be found during the cleavage process, before its completion. For example, as the oligonucleotide is shaved off the divalent streptavidin species (Figure 3.3A(i, top)), a maximum of three species can be present (specifically: the original streptavidin carrying two biotin-12 bp dsDNA tails; streptavidin carrying one biotin-12 bp dsDNA tail and one biotin plug; and streptavidin carrying two biotin plugs). Similarly for monovalent streptavidin, a total of five possible products are expected (Figure 3.3A (ii, middle)) and for the initially fully-filled streptavidin, six (Figure 3.3A (iii, bottom)). All the species that could possibly be obtained upon UV irradiation are labelled as N*, where N is the number of 12 bp dsDNA oligomers still present in each species, and * denotes that UV was instrumental in the generation of the species.

Figure 3.3B shows the results from the corresponding experiment, using CE to monitor the species present and their relative concentrations after irradiating the sample for 60 s as described in Materials and Methods (electrophoregrams of starting and irradiated samples are shown as solid and dotted lines respectively). As alluded to earlier, the electrophoretic mobility of the species along with the electroosmotic flow determines the migration time in CE, depending primarily on the ratio of the charge to the hydrodynamic friction coefficient of the analytes. Once

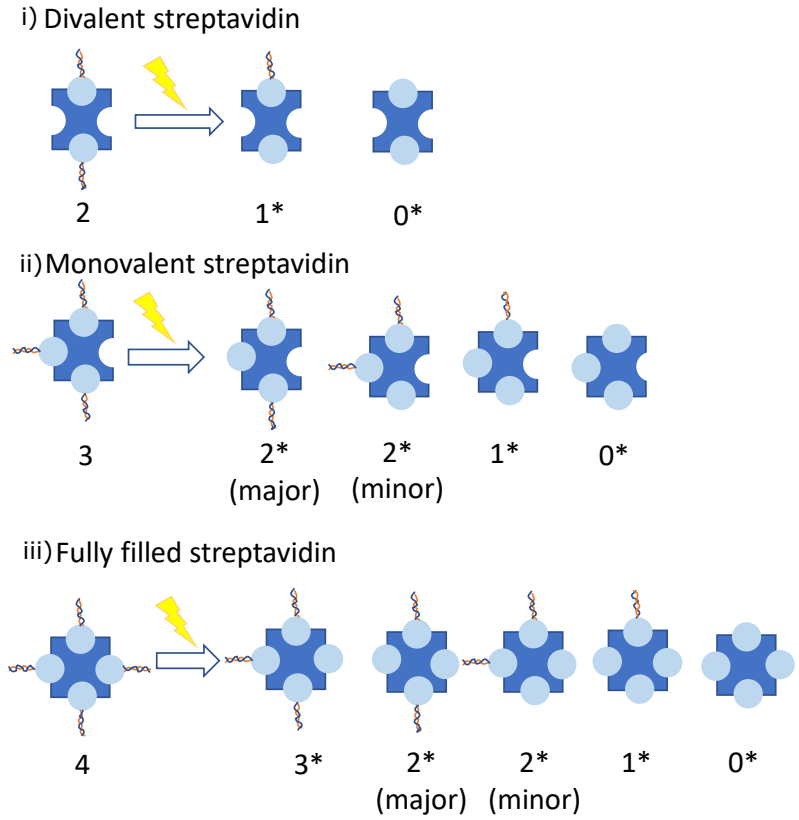

A

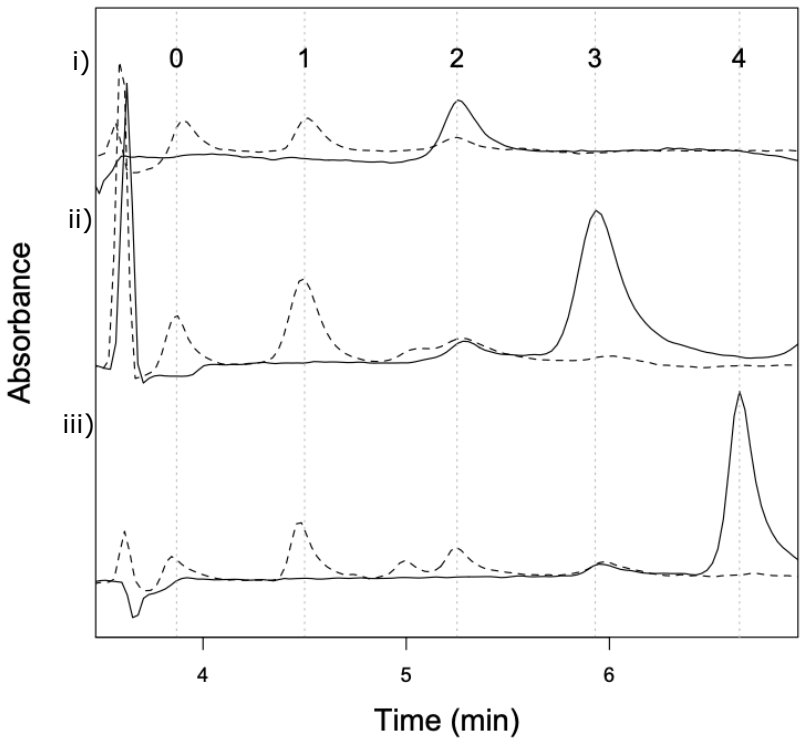

B

FIGURE 3.3: (A) Multiple species expected to be formed during UV irradiation of the different starting streptavidin-12 bp dsDNA conjugates. (B) Electrophoregrams monitoring the species present after 60 s UV irradiation of different starting streptavidin-12 bp dsDNA conjugates (solid line represents the electrophoregram of reactants before UV irradiation, dotted line represents the electrophoregrams of products after UV irradiation). The smaller peak adjacent to the N = 2 peak is assigned to be the *cis*-divalent species.

the 12 bp dsDNA is removed, the streptavidin binding site it once occupied, now simply contains a neutral biotin-stub, that is not expected to significantly affect the electrophoretic transport behavior of the complex in which it resides. Hence, when cleavage of all the oligonucleotides is complete, all the streptavidin conjugates, no matter how many plugged sites they contain, would be expected to migrate past the detection window at the same time, with a mobility comparable to pure streptavidin (position 0). Similarly, species that at some point during the cleavage process only possess one nucleotide tail (and any number of biotin plugs in other sites) would be expected to have the same electrophoretic mobility as the starting trivalent streptavidin (position 1) species, and so on and so forth. The experimental results shown in Figure 3.3B indeed follow the expected progression mapped out in Figure 3.3A, confirming the generation and correct identification of the starting species, as well as the UV-induced removal of the oligonucleotides. It is worth noting that the irradiation of fully filled and monovalent streptavidin yields an additional peak intermediate between those designated 1 and 2. Based on the position of the peak, it seems likely that this is a *cis*-divalent streptavidin species, which could not be distinguished on a traditional gel.

3.3.4 Time-course of removal of dsDNA (12 bp) from streptavidin conjugates

Figure 3.3B still shows a variety of different streptavidin-biotin-dsDNA conjugates present in samples after 60 s of UV irradiation, indicating that this reaction time was insufficient to cleave all the oligonucleotides from the conjugates. Differing UV exposure times were subsequently applied in order to find the time required to remove all oligonucleotide tails and thereby generate the sought-after streptavidin species with known numbers of biotin-plugged or available biotin-binding sites. The oligonucleotide removal is illustrated further in Figure 3.4A for the HPAEC-collected monovalent streptavidin species (the tetramer with three biotin-dsDNA oligomers initially bound). The complex was subjected to UV for a total of 30 mins and the progress of the photocleavage of the DNA tails was monitored by taking 30 µL aliquots of the sample at different time intervals and running the sample in the CE. Figure 3.4A clearly shows how the peaks move to lower charge density as time progresses and the 12 bp nucleotide tails are removed, with the expected progression through the intermediate species. After 5 minutes, the majority of the oligonucleotides have been cleaved, and the streptavidin itself (now containing three "passivating" biotin plugs) still remains intact (as inferred from the similarity of the peak shape to that obtained with unadulterated streptavidin). Furthermore, the protein seems relatively stable even after 10 mins of UV. Some

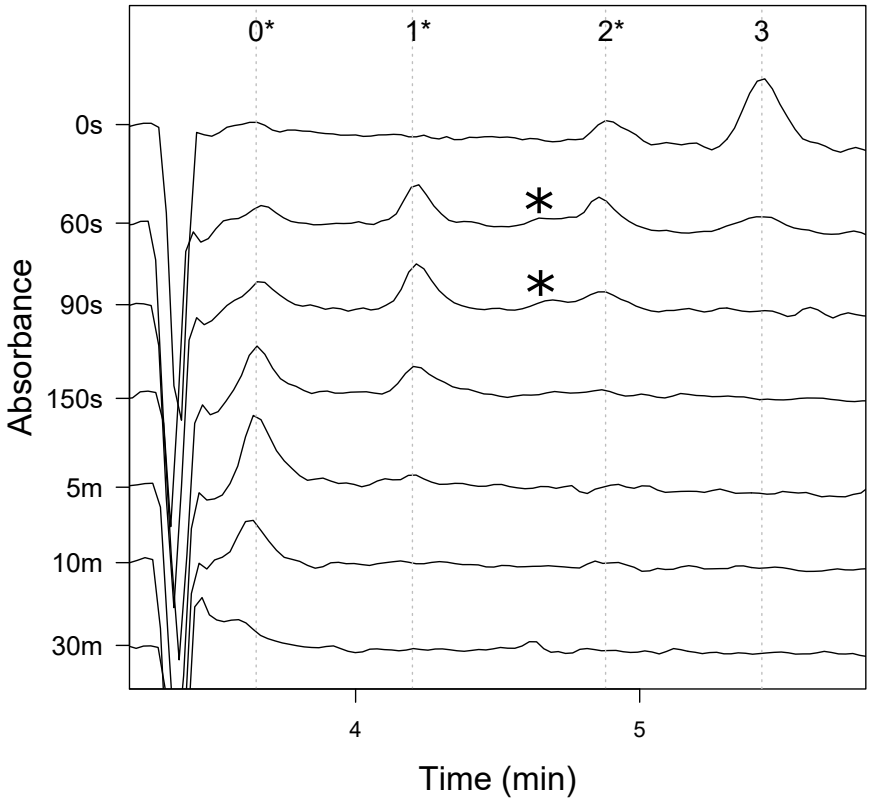

A

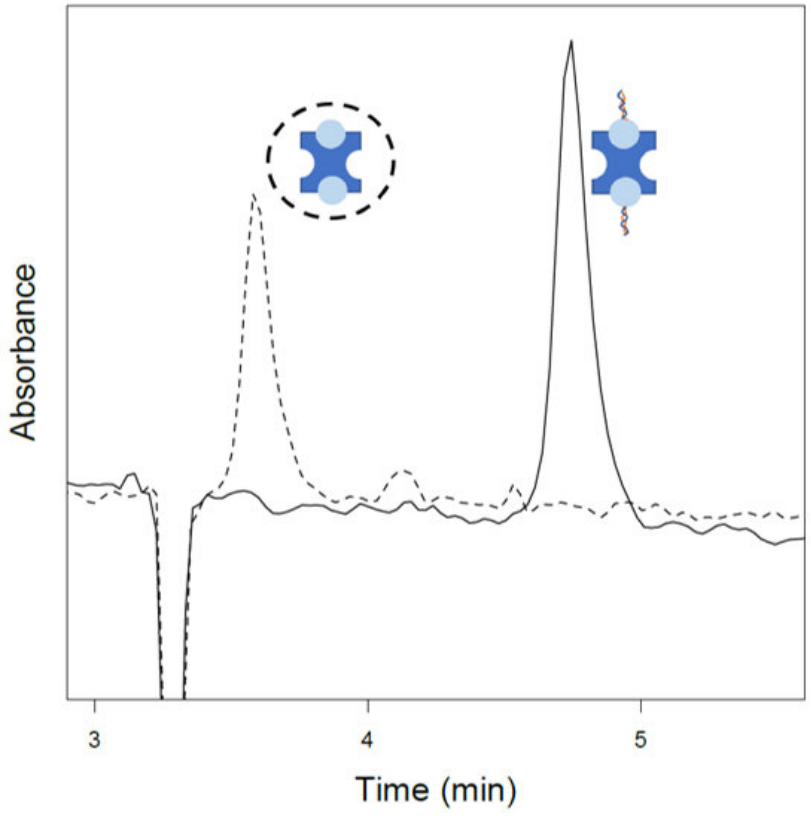

B

FIGURE 3.4: Electrophoregrams monitoring the species present (A) with different times of UV irradiation of monovalent streptavidin-dsDNA (12 bp) (N = 3) conjugates (peak marked by * indicates presence of *cis*-divalent species) and (B) after 5 minutes UV irradiation of divalent streptavidin-dsDNA (12 bp) (N = 2) conjugates, while dotted electropherogram is the control with no UV exposure.

modification of the protein itself is, however, evident at 30 mins, as changes in the peak shape attest to. An interesting feature is seen $\sim$ 4.6 mins in the electrophoregrams recorded after 60 s and 90 s UV irradiation. A peak manifests as a slight shoulder towards the 2* peak and is presumed to be the *cis*-equivalent of the double tail. This peak is only visible during a short time-frame in the process of cleaving the tails, and is not clearly observed in the formation of the different valencies, confirming that *cis*-configuration is much more unstable than any of the other configurations as previously suggested [137].

As the primary interest here is producing divalent streptavidin species that can be used as linking molecules, the fraction-collected *trans*-divalent streptavidin (N = 2) sample was subsequently exposed to UV irradiation for 5 mins. Figure 3.4B shows the pre-and post-irradiation electrophoregrams, again confirming that under these conditions the oligonucleotides are removed, leaving simple biotin stubs plugging two sites, and with the protein intact.

3.3.5 Using divalent streptavidin as a linker

The results of the CE experiments performed on incubations of streptavidin with 12 bp dsDNA, and on the fraction-collected samples and their subsequent UV-generated species, provide confidence that specific divalent streptavidin species can be generated in large amounts and investigated for their potential as a linker molecule as described below.

Investigating the yield of concatenated 10 kb DNA.

Initial tests of this linking functionality were carried out by incubating the *trans*-divalent streptavidin species with biotin-terminated DNA that could be visualized straightforwardly using a standard agarose gel, as described in the Experimental Section. For this purpose, $\sim$ 5 kb DNA that would, upon successful concatenation, effectively result in the formation of an $\sim$ 10 kb DNA strand was selected. Figure 3.5 does indeed show the presence of an $\sim$ 10 kb band post-incubation. The visualised band is relatively faint, however, suggesting that the yield of the concatenated species was lower than might be expected ($\sim$12 %) for the $\sim$ 2:1 ratio of streptavidin:DNA used in this experiment. To investigate the hypothesis that the first of the $\sim$ 5 kb DNA strands binding to the streptavidin obscures the remaining binding sites, the sequential filling of the streptavidin sites with biotin-terminated DNA oligomers of different lengths was investigated. While with

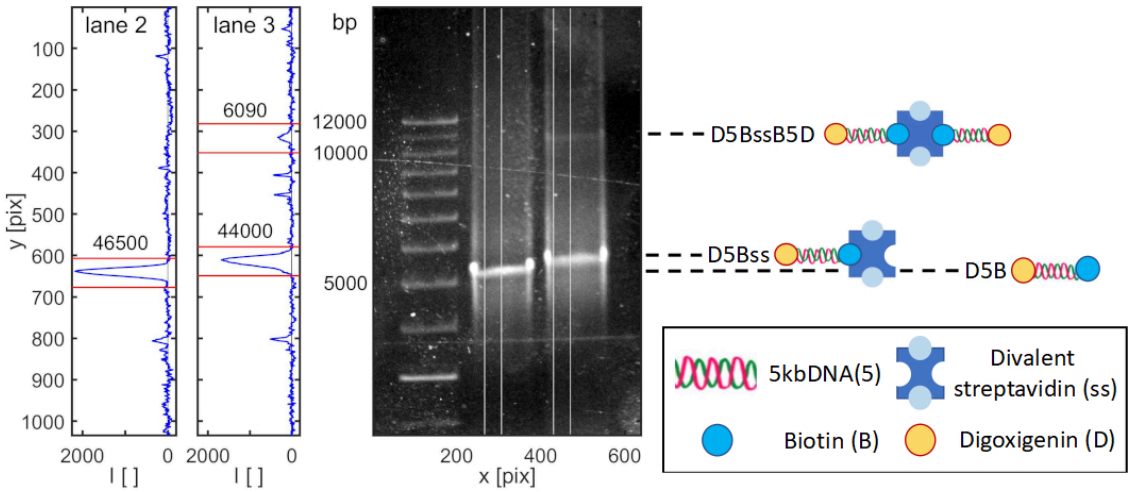

FIGURE 3.5: Gel electrophoresis experiment showing a standard size ladder (Invitrogen 1kb+ DNA Ladder) in lane 1, the 5 kb biotin-terminated DNA in lane 2 and the results of an incubation of the divalent streptavidin with the 5 kb biotin-terminated DNA in lane 3. Background corrected integrated intensity profiles for lanes 2 and 3, between the pairs of vertical white lines indicated on the image of the gel, are shown to the left. Integrated intensities along these profiles, between the red lines indicated, are reported in the figure. Schematics of the species observed are also shown on the right (not drawn to scale).

cis-divalent streptavidin attachment of one DNA molecule has previously been shown to sterically and electrostatically hinder the binding of another moiety [137], it seems less likely with the *trans*-divalent streptavidin used here.

The distance between the two biotin binding faces of a streptavidin tetramer is ~ 2.0 nm [131] (Figure 3.6). Two different lengths of biotin-terminated DNA oligomer (12 bases (~ 4.0 nm) and 28 bases (~ 9.5 nm)) were used to investigate the role that steric and electrostatic effects might play in the consecutive binding of biotin-terminated DNA into potential valencies (Data Not Shown). It was found that when tetravalent streptavidin was incubated with 12 bp biotin-terminated DNA, the DNA oligomers seamlessly filled the open valencies until nearly all the sites in the streptavidin conjugate species were completely filled. However, substantially more valencies remained unfilled when the same experiment was repeated with 28 bp DNA oligomers. This observation does suggest that, as the length of the molecules targeted to be coupled increases, steric and/or electrostatic effects will limit the yield of the concatenated species derived [137]. It is worth noting that despite the low yield, two large (micron-sized) DNA pieces can be successfully concatenated in this way in sufficient quantities to undertake single-molecule stretching experiments, for example by optical tweezers.

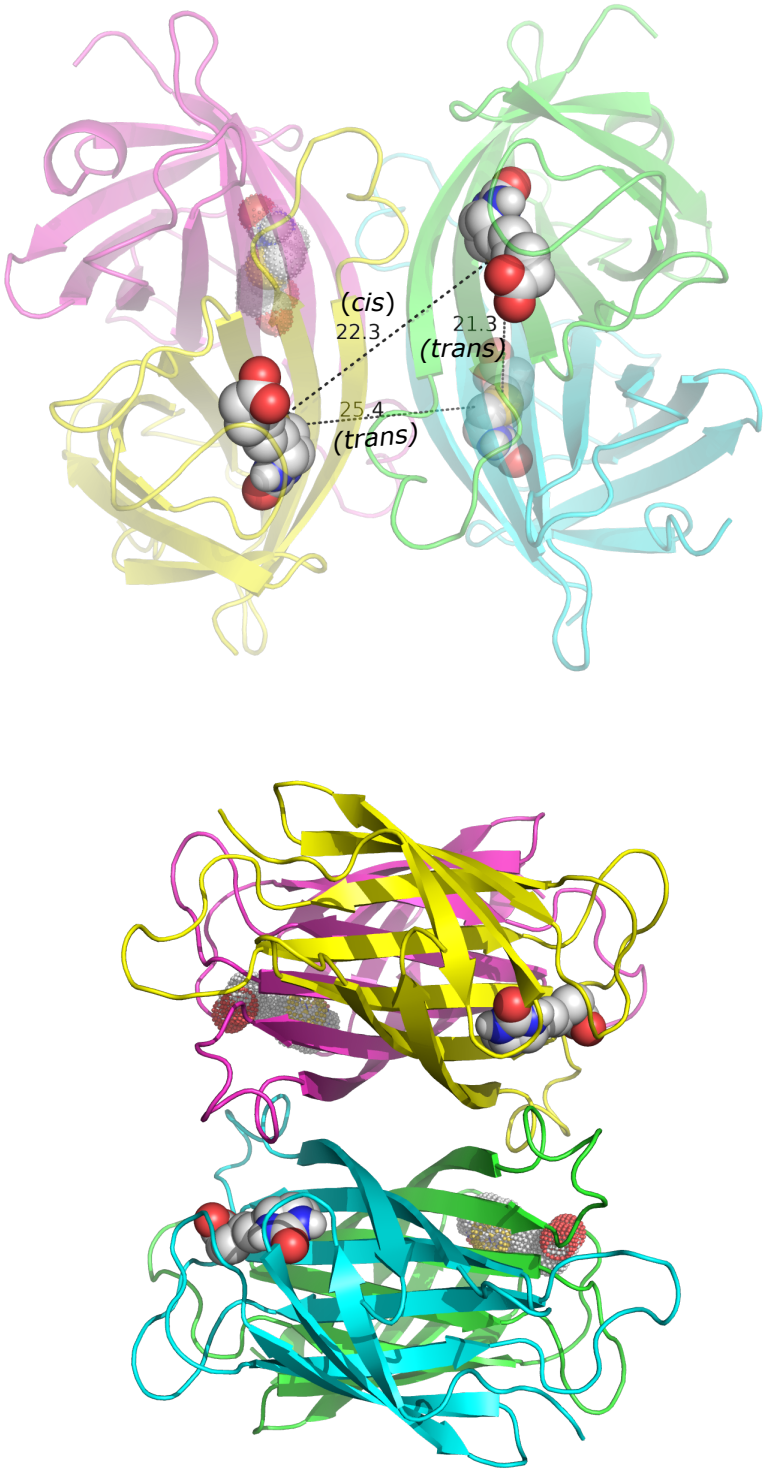

FIGURE 3.6: Completely filled biotin-streptavdin conjugate with the biotin S...S distances between the *cis* and possible *trans* sites marked as 22.3 Å, and 21.3 Å and 25.4 Å respectively. Solid spheres indicate biotin "plugs" while the dotted renderings of the biotin indicate the potential, currently-vacant biotin-binding sites.

Stretching streptavidin-linked strings in a dual-trap Optical Tweezers Set-up.

DNA concatenation via the divalent streptavidin linker (ss) was additionally verified by stretching the formed DNA string using optical tweezers. The set-up for the experiment is illustrated in Figure 3.7A and 3.7B. Initially, standard samples, nominally 5 kb or 10 kb DNA, terminated by either biotin (B) or digoxigenin (D) at the termini, are bound to streptavidin- (S) or antidigoxigenin- (A) coated beads, which are optically trapped in the tweezers. This bound DNA can be stretched by separating the beads (Figure 3.7A). By tracking the position of the beads, as shown in 3.7B, a force $F = k(x_b - x_{b0})$ can be determined, where k is the optical trap stiffness, with extension $d = x_s - x_b - r_s - r_b$, and r_s and r_b, are the radii of the beads, and the subscripts s and b relate to the small(er) and big(ger) of the beads respectively.

Four samples were examined: 1) A-D-10kb-B-S (reference DNA) (Figure 3.7C); 2) A-D-5kb-B-S (Figure 3.7D); 3) A-D-10kb-D-A (Figure 3.7E); and 4) A-D-5kb-B-ss-B-5kb-D-A (concatenated DNA)(Figure 3.7F). Sample 1 is a standard DNA stretch with the two DNA strands terminated by biotin at one end and digoxigenin at the other; where one streptavidin-coated and one anti-digoxigenin coated bead are utilized in the experiment. Sample 2 is a standard 5 kb stretch of the same nature as 1. Sample 3 is similar to 1, but has both bead-facing ends terminated with digoxigenin, as a prelude to sample 4 in which the biotin-displaying ends of both chains are free to couple to the divalent streptavidin linker. Typical single-duplex force-extension curves for the four samples are shown in Figure 3.7 (C-F) repectively. These force-extension curves were fitted to the wormlike chain model (WLC):

$$F = \frac{k_B T}{l_p}[\frac{1}{4}(1 - \frac{d}{l_c}^{-2}) + \frac{d}{l_c} - \frac{1}{4}] \tag{3.2}$$

to determine the chain's persistence length, l_p, (the length over which the chain might be considered straight) and the contour length, l_c, (the end-to-end length along the chain). The statistics of the fitted parameters are shown in Table 3.2. Note: a single trap stiffness k was assumed for all measurements - this value was chosen so that the mean l_p-value for the D-10kb-B measurements matched that previously found for this reference sample [92, 138].

Based on these statistics: 1) All DNA tested has the same l_p. 2) The ratio of the extracted contour lengths of the 5 kb and 10 kb dsDNA samples, l_c(D-5kb-B) / l_c(D-10kb-B) = 0.46 (0.438-0.490) is consistent with the known ratio of their base pairs 4682/10051 = 0.466. 3) The ratio of the extracted contour lengths of two 10 kb dsDNA samples, with different termini, l_c(D-10kb-D) / l_c

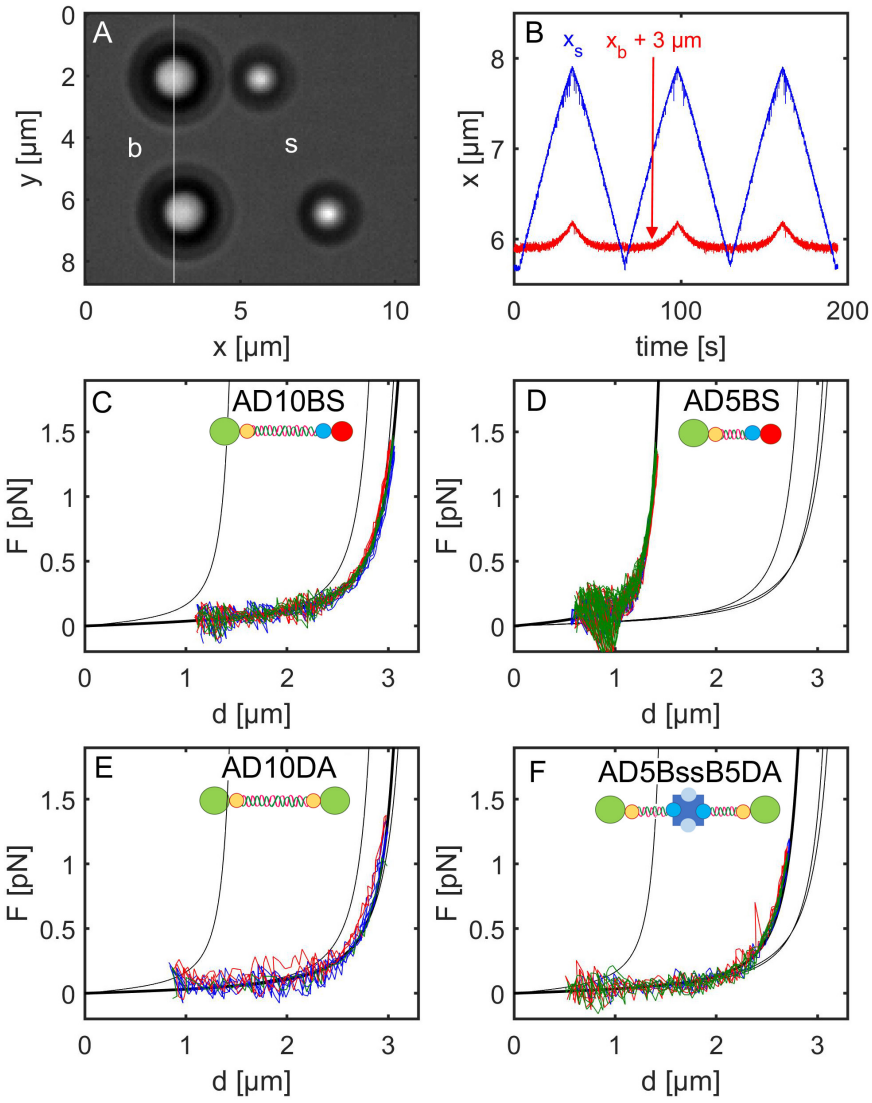

FIGURE 3.7: Optical Tweezers Experiments: Stretching control and concatenated DNA. (A) Micrograph of the set-up showing a big (b) and small (s) bead tethering DNA, their separation using OT and the consequential movement of the left hand bead in response to moving the right hand one of the pair. (B) Displacements of the beads as they are made to approach and retract from each other. (C-F) Derived force-extension curves for the four samples described in the text are illustrated in the respective panes.

(D-10kb-B) = 0.98 (0.943-1.01) is consistent with the known ratio of their base pairs 10051/10051 = 1.00. 4) The ratio of the extracted contour lengths of the string resulting from the incubation of 5 kb DNA with *trans*-divalent streptavidin, and the 5 kb DNA, l_c(D-5kb-B-ss-B-5kb-D)/l_c(D-5kb-B) = 1.93 (1.81-2.07) is consistent with the expected ratio of base pairs, 9364/4682 = 2.00, if concatenation occurs (the slight difference observed is due to the difference in the total number

TABLE 3.2: OT Experimental results for the samples described in the text and illustrated in Figure 3.7 (C-F). Individual stretches were independently fitted to the WLC model, and means and standard deviations of the fitted l_p and l_c for each DNA sample calculated.

Sample	Stretches	Mean l_p [nm]	Mean l_c [µm]	bp
A-D-10kb-B-S	28	59 ($\pm$ 10)	3.425 ($\pm$ 0.047)	10051
A-D-5kb-B-S	9	54 ($\pm$ 9.8)	1.588 ($\pm$ 0.066)	4682
A-D-10kb-D-A	23	72 ($\pm$ 12)	3.342 ($\pm$ 0.066)	10051
A-D-5kb-B-ss-B-5kb-D-A	13	75 ($\pm$ 12)	3.069 ($\pm$ 0.075)	9364

of base pairs between two 5 kB DNA strands vs one 10 kB DNA strand). *This observation confirms that the concatenated structure with the intervening biotin-streptavidin bridge (D-5kb-B-ss-B-5kb-D) was formed, and is robust enough to run intact in an agarose gel and to be held in an OT experiment*.

3.4 Conclusion

CE provides a rapid methodology for studying the results of incubating streptavidin with biotin-terminated DNA oligomers, requiring minimal amounts of sample and consumables. Using HPAEC to collect fractions, and UV to remove separation-facilitating DNA oligomers, specific divalent streptavidin species can be generated and have the potential to be used as linker molecules to create "plug-and-play" strings for single-molecule experiments. This divalent streptavidin, when incubated with $\sim$ 5 kb biotin-terminated DNA, produces a $\sim$ 10 kb concatenated species which can be observed on an agarose gel. Furthermore, in optical tweezers experiments, the ratio of the extracted contour lengths of the string resulting from the incubation of $\sim$ 5 kb DNA with divalent streptavidin, and the $\sim$ 5 kb DNA, l_c(D-5kb-B-ss-B-5kb-D)/l_c(D-5kb-B) = 1.93 (1.81-2.07), is consistent with the known ratio of base pairs, 9364/4682 = 2.00, which is to be expected if concatenation occurs. *This observation confirms that the concatenated structure D-5kb-B-ss-B-5kb-D was formed*. Moreover, the force-extension curve of the concatenated string was experimentally indistinguishable from that which would be expected from a single DNA chain of the same length, showing that, at least at these forces, the tightly bound divalent streptavidin linker does not modify the stretching behaviour significantly. It is hoped that as an extension to this work, by using two streptavidin linkers, any biotin-terminated polymer might be inserted between two sections of DNA of substantial length in order to facilitate single-molecule experiments on molecules that are currently difficult to address by other means.

Chapter 4

Modifying Polysaccharide Ends for Single Molecule Studies

DRC 16

MASSEY UNIVERSITY TE KUNENGA KI PŪREHUROA UNIVERSITY OF NEW ZEALAND | GRADUATE RESEARCH SCHOOL

STATEMENT OF CONTRIBUTION
DOCTORATE WITH PUBLICATIONS/MANUSCRIPTS

We, the candidate and the candidate's Primary Supervisor, certify that all co-authors have consented to their work being included in the thesis and they have accepted the candidate's contribution as indicated below in the *Statement of Originality*.

Name of candidate:	Nimisha Mohandas
Name/title of Primary Supervisor:	M.A.K. Williams
In which chapter is the manuscript /published work:	4

Please select one of the following three options:

○ The manuscript/published work is published or in press

- Please provide the full reference of the Research Output:

○ The manuscript is currently under review for publication – please indicate:

- The name of the journal:
- The percentage of the manuscript/published work that was contributed by the candidate:
- Describe the contribution that the candidate has made to the manuscript/published work:

◉ It is intended that the manuscript will be published, but it has not yet been submitted to a journal

Candidate's Signature:	
Date:	01-Feb-2022
Primary Supervisor's Signature:	ExpressVPN Client Digitally signed by ExpressVPN Client Date: 2022.02.02 13:36:57 +13'00'
Date:	2-Feb-2022

This form should appear at the end of each thesis chapter/section/appendix submitted as a manuscript/ publication or collected as an appendix at the end of the thesis.

GRS Version 5 – 13 December 2019
DRC 19/09/10

4.1 Introduction

Polysaccharides

Polysaccharides are biopolymers that exist in all living species, in different sizes, shapes and forms, and are utilised both in energy-storage and in key structural roles. Their fine structures are usually complex and typically comprise multiple saccharide elements and assembly motifs. In addition to their clear biological relevance, polysaccharides have also found increasing applications in various technological fields from pharmacy and medicine, to food and the environment [139–141]. Despite this growing interest, several fundamental aspects of polysaccharides such as understanding their detailed structure-function relationships remain a challenge.

Pectin

Amongst the various plant polysaccharides, pectin is a family of heterogeneous galacturonic-acid-containing polysaccharides that make upto about 35% dry weight of most plant cell walls and around 50% in Arabidopsis (*Arabidopsis thaliana*) [3]. Pectin plays many important roles in plant physiology including modulating cell growth and triggering defence mechanisms. In fruits and vegetables, the pectin composition is crucial in determining the firmness of cell walls and, ultimately, fruit quality [4–6]. Homogalacturonan (HG) constitutes around 65% of the pectin in the cell wall. HG chains, when extracted from commercial samples, have been found to be around 100 galacturonic acid residues long [142–144]. The linear backbone of the homogalacturonan (HG) chain consists of galacturonic acid, or GalpA residues (where Gal denotes D-galactose, p the pyranose form, and A the carboxylic acid group at C6), connected together via α-(1,4)-glycosidic linkages. The carboxyl groups in the sugar residues of HG can be methylesterified, with the degree and pattern of methylesterification influencing pectin's physical properties [11, 12]. Even two centuries after its identification, the detailed natures of *in vivo* and *in vitro* pectin structure-function relationships are still an active area of research [7]. While samples presented for studies are typically characterised by averages of fine structure descriptors, no two chains will possess the identical fine structure. Indeed, it is the capability of enzymatic processing to locally manipulate the polymeric fine structure and thereby manifest different functionalities that gives pectin its seemingly endless utility.

Towards Single-molecule Experiments for Polysaccharides

In cases where the individual biopolymer molecules within a bulk sample exhibit variations in fine structure, single-molecule studies uniquely offer the promise of revealing deep structure-function relationships. However, single-molecule studies of polysaccharides are complicated by the difficulty of studying molecules that are typically shorter than the routinely studied DNA, have more complex end-group chemistry, and lack the analogous tools of molecular biology. Promisingly though, divalent streptavidin linkers have recently been shown to be capable of concatenating two pieces of biotin-terminated DNA, producing robust composite strings that can be used in single-molecule experiments [145]. Such linkers could then be used to insert polysaccharides of interest into DNA strings, providing access to a plug-and-play single-molecule format, as long as a biotin moiety can be attached at both ends of the polysaccharide chain. Herein, homogalacturonans (HG) (the major components of the pectic polymers found in land plants), and oligomers thereof, are used as exemplars to investigate the chemistry involved in the introduction of the required biotin-handles.

Approach to the Modification of HG Termini

Basic Strategy

Similar to most polysaccharides, the HG molecule has so-called "reducing" and "non-reducing" ends. While the reducing end has a characteristic aldehyde group displayed by the ring-opening of the hemiacetal at anomeric position 1, the non-reducing end does not possess an easily addressable functional group, making it a more challenging target for modification [146]. The free aldehyde group at the reducing end of HG is available for chemical reactions. As a carbonyl group, aldehydes can undergo nucleophilic addition. Aldehyde groups can react with amine groups, or with aminooxy moieties to form a stable oxime linkage [65–67]. The functionalisation at the reducing end could then be performed via reductive amination or by oxime formation. For attachment to amines, the presence of a reducing agent, such as sodium cyanoborohydride, is necessary to reduce initially formed imines to amines and stabilise the formed linkage [147], whereas this is unnecessary for oxime formation. Hence, despite the considerable precedent for reducing end coupling using reductive amination with amines in the presence of reducing agents, here the use of aminooxy coupling for the functionalisation of HG with biotin has been investigated.

In contrast to the reducing end, the non-reducing end of HG does not have a unique and reactive functional group available for chemical modification. Therefore, before biotin coupling strategies can be investigated for this end of the molecule, an initial transformation is required in order to produce a functional non-reducing end-specific handle to which biotin could ultimately be attached. In this regard, introducing a double bond into the ring of the non-reducing end terminal galacturonic acid residue by a preliminary cleavage of the α-1,4-glycosidic linkage between the galacturonic acid residues in the HG chain using β-elimination is explored. While the initial controlled cleavage leaves the chains undesirably shorter, this can be limited somewhat so that the occurrence of chain scission is sparse, and one of the resulting daughter chains now carries an unsaturated terminal residue, that can be specifically targeted. Such a pre-treatment can be carried out enzymatically or chemically. Herein, both endo-pectate lyase and chemically induced β-elimination have been investigated [60, 148]. Once generated, unsaturated terminal residues at the non-reducing end can be subjected to a variety of electrophilic addition reactions. In particular, a photochemical thiol-ene click reaction has been investigated here, with a coupling molecule inserting a sulfur-bearing moiety into the ring and displaying an amine-bearing end for final coupling to biotin.

Reducing Terminus

As mentioned earlier, the reducing end can easily be modified due to the hemiacetal terminal reducing sugar transiently opening in solution to expose an aldehyde moiety.

Aminooxy-aldehyde conjugation can be carried out under mild aqueous conditions and results in the formation of a stable oxime linkage. Furthermore, oxime linkages have been shown to be more stable than hydrazone linkages, and, hence, are investigated as a convenient option for biotin-functionalisation at the reducing end [149]. The reaction scheme exploited is shown in Figure 4.1.

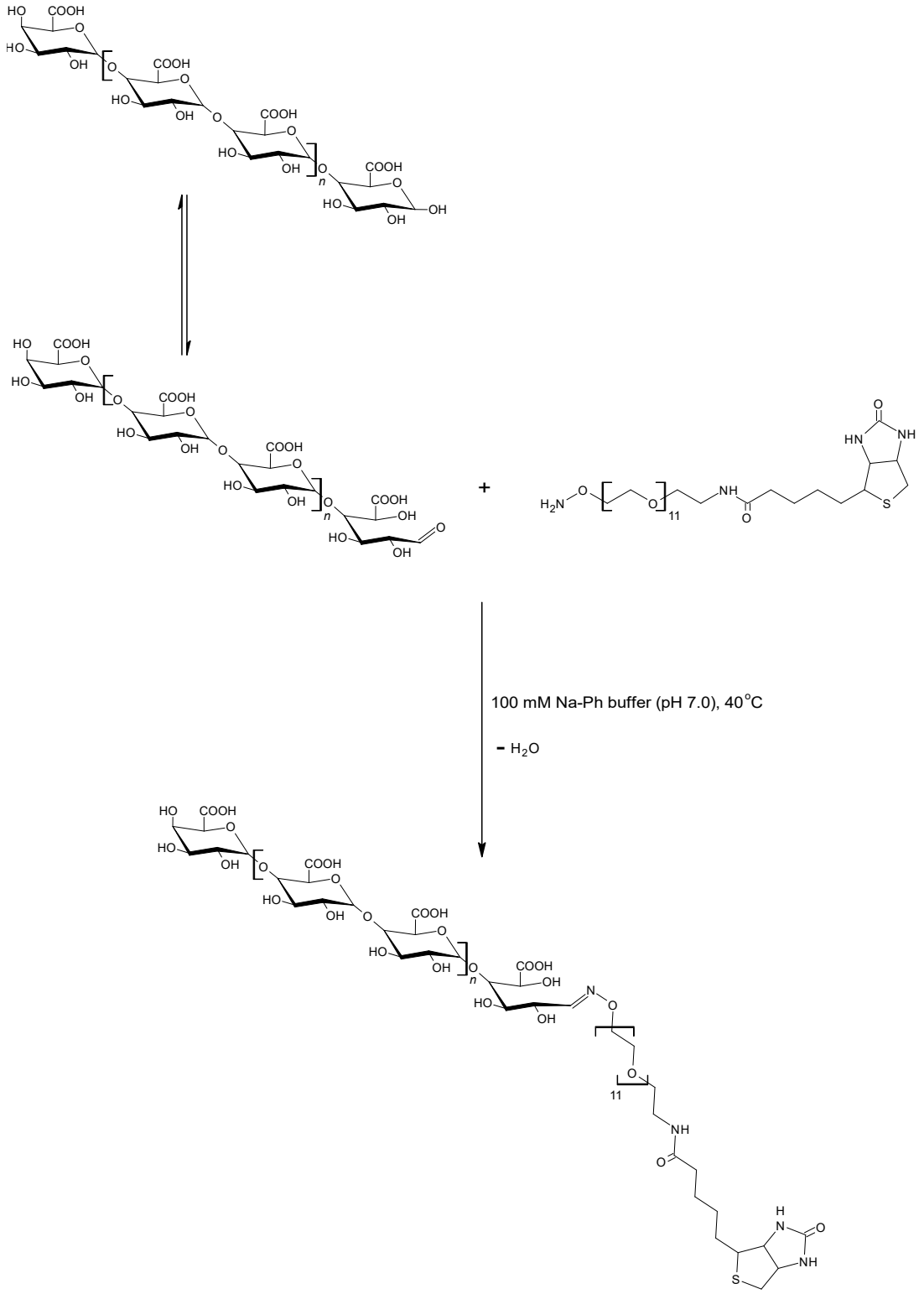

FIGURE 4.1: Reaction conditions for the chemical modification of tetragalacturonic acid at the reducing terminus with aminooxy-$(PEG)_{12}$-biotin, resulting in the addition of a biotin handle. These reaction conditions have been optimised from literature [66].

Non-Reducing Terminus

For modification at the non-reducing end, three steps are required to be performed to complete the suggested biotin functionalisation. Namely:

Step 1: The desired polysaccharide of study (here HG) should be carefully treated (here using a pectate lyase or a chemically catalysed β-elimination reaction) to produce (slightly shorter) molecules that bear a double bond in the sugar ring at the non-reducing end. It is worth noting that pectate lyase action is favourable for HG with a low degree of methylesterification [49, 50, 150, 151], while chemical elimination works most efficiently for highly methylesterified substrates. This is due to the fact that the presence of electron donating methylester groups can facilitate β-elimination [58–60].

Step 2: Once generated, the unsaturated terminal residue at the non-reducing end can be subject to a variety of electrophilic addition reactions. To prepare a biotin bearing molecule that can be attached to the terminal sugar residue in this manner, a biotin-N-hydroxysuccinimide ester was pre-linked to a thiol-containing moiety, as shown in Figure 4.2 [152, 153].

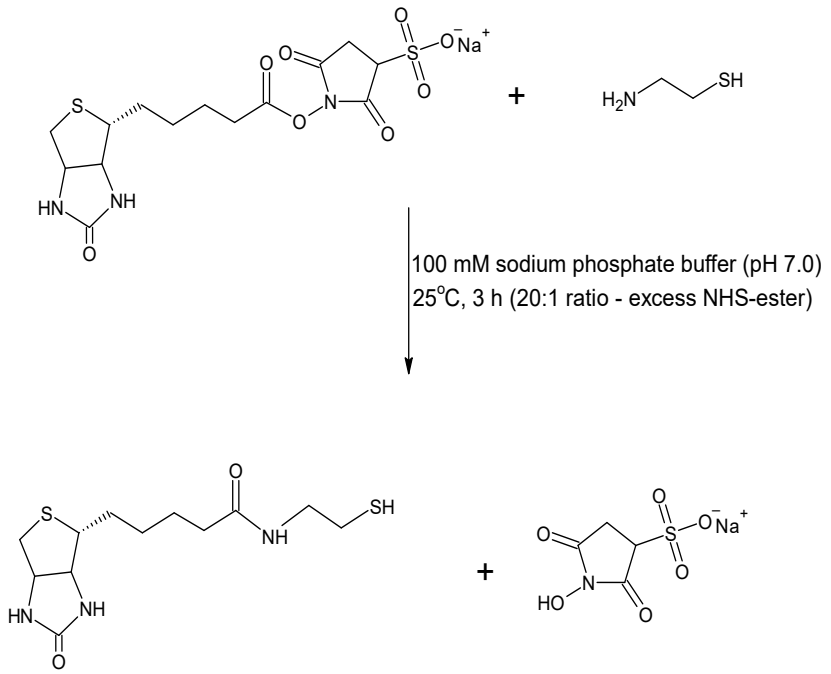

FIGURE 4.2: Reaction conditions for the preparation of a biotin-terminated handle using sulfo-NHS-biotin and cysteamine, for attachment to the unsaturated terminal sugar at the non-reducing end. These reaction conditions have been optimised from literature [154].

Step 3: Finally, the biotin-bearing thiol-terminated molecule produced in step 2 can be reacted with the unsaturated terminal HG residue at the non-reducing end, produced in step 1, via a photochemically catalysed thiol-ene click reaction as shown in Figure 4.3 [155, 156].

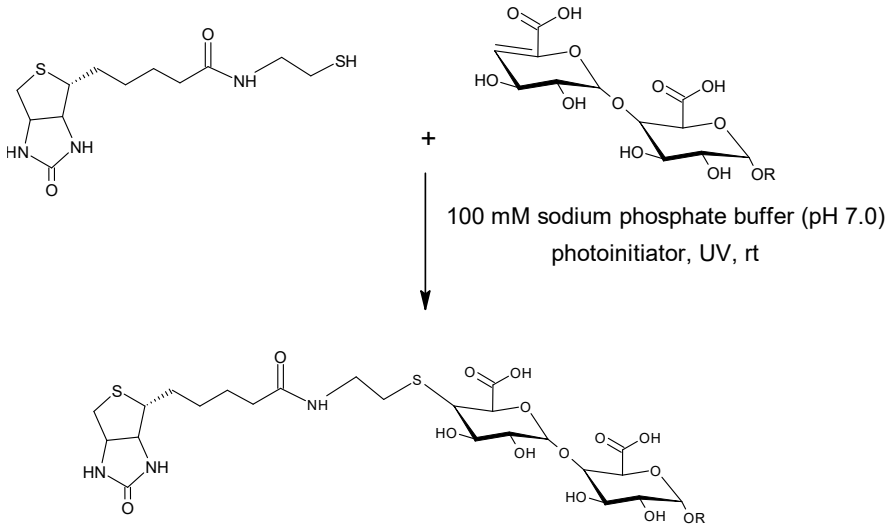

FIGURE 4.3: Reaction conditions for the thiol-ene click reaction performed at the non-reducing end of the unsaturated oligomer with thiol-terminated biotin species. Reducing end of the oligomer is protected by aminooxy species (R) to prevent unwanted side coupling reactions of the thiol linker to the reducing end aldehyde moiety. These reaction conditions have been optimised from literature [157].

Reactions were carried out with homemade HGs with controllable degrees of methylesterifcation, with commercially available tetragalacturonic acid, and with small, homemade, unsaturated oligomers. The species of low degree of polymerisation (DP) were particularly useful in confirming the chemistry occurring at the termini of HGs using NMR.

4.2 Materials and Methods

Materials

Tetragalacturonic acid (DP4) (Elicityl, France), polygalacturonic acid sodium salt (PGA) (Merck/Sigma Aldrich, New Zealand), pectate lyase *Aspergillus* sp. (Megazyme - Food Tech Solutions Ltd., New Zealand), cysteamine (Sigma-Aldrich, New Zealand), alkoxyamine/aminooxy-$(PEG)_{12}$-biotin (Thermo Fisher Scientific, New Zealand), NHS-digoxigenin ester (Sigma-Aldrich, New Zealand), sulfo-NHS-biotin (Sapphire Bioscience, Australia), and 2-hydroxy-4'-(2-hydroxyethoxy)-2-methylpropiophenone (Irgacure 2959) (Sigma Aldrich, New Zealand) were purchased and used without

further purification.

Homogalacturonan (HG) having a molecular weight of around 20 kDa was produced by extracting short polygalacturonic acid sections from pectin using mild acid hydrolysis, followed by methylesterification using methyl iodide (MeI) to a high degree of methylesterifcation, and finally controlled by removal of methylesters, as described previously in literature [158–160].

An Eppendorf Thermomixer (Biolab Scientific, New Zealand) and multiband (254/366 nm) Mineralight UV lamp (Ultra-Violet Products, Inc., San Gabriel, California), were also employed in sample preparation and manipulation. Samples were dialysed using SnakeSkin™ Dialysis Tubing, 3.5 kDa MWCO (Thermo Fisher Scientific, New Zealand) against MQ water.

For ELISA, capture and detection antibodies (JIM7 and streptavidin-HRP) were obtained from the Paul Knoxx Cell Wall group (University of Leeds, United Kingdom). Anti-digoxigenin-AP Fab fragments (Sigma-Aldrich, New Zealand) were diluted 1000x before use. Hydrogen peroxide (Thermo Fisher, New Zealand), sodium acetate (Sigma Aldrich, New Zealand), trimethylbenzidine, TMB (Sigma Aldrich, New Zealand) and 10X PBS, pH 7.4 (Thermo Fisher, New Zealand) were also purchased and used without further purification. ELISA walls were blocked with store bought milk powder (Pams, 3.8% fat content) made up to 5% solution in 1X PBS.

Purification of unsaturated oligosaccharide mixture was attempted using an anion-exchange HPLC at 35 ^{o}C in a Thermo Scientific Ultimate 3000 machine using an Amberlite exchange column (7 x 75 mm, 10 µm) (TSKgel SuperQ-5PW) (Agilent, USA) in a gradient of 1 M sodium acetate (pH 4.5) (0 $\rightarrow$ 5% for 4 mins, 5 $\rightarrow$ 55% for next 50 mins, 55 $\rightarrow$ 100% for final 14 mins, 0.8 mL/min) in MilliQ water.

Experimental Procedures

Biotin functionalisation at the reducing end

In the first experiments to test the proposed reducing-end chemistry, tetragalacturonic acid (DP4) was used as the saccharide-containing substrate, obtained commercially, as noted in the Materials

section. Latterly, the same reactions were carried out with HGs, obtained as described in Materials.

Aminooxy-$(PEG)_{12}$-biotin was used for functionalisation; the aldehyde group at the reducing end of HG reacting with the aminooxy group to form a stable oxime linkage by adapting and modifying protocols explored in literature [161, 162]. First, 1 mg of polysaccharide/oligosaccharide was dissolved in 100 µL 100 mM sodium phosphate buffer pH 7.0. Aminooxy-$(PEG)_{12}$-biotin (2 µL of 100 µM) was added in excess into the reaction mixture. The reaction was left shaking at about 1250 rpm on an Eppendorf shaker-hotplate at 40 ^{o}C for 3 days (for the oligosaccharide) and 7 days (for HG). Subsequently, the product was precipitated with 80% ethanol. The final solution was centrifuged at 14800 rpm for 30 s and the supernatant removed. The precipitate was rinsed twice with 50% ethanol, dried and then analysed by Capillary Electrophoresis (CE), Nuclear Magnetic Resonance (NMR) spectroscopy and/or Enzyme-Linked ImmunoSorbent Assay (ELISA).

Biotin functionalisation at the non-reducing end

Double-bond-containing terminal sugar residues at the non-reducing end were first generated. Unsaturated oligosaccharide substrates were obtained by performing the enzymatic degradation of polygalacturonic acid (PGA) using pectate lyase. In the case of homogalacturonan, the chemically catalysed β-elimination of a highly methylesterified homogalacturonan (DM93) substrate was preferred.

A: Protocol for the generation of unsaturated sugar residues at the non-reducing end: (a) *Oligosaccharides*. The procedure was adapted from previous experiments in literature [163, 164]. PGA (1 mg) was dissolved in 100 µL of 100 mM Tris buffer (pH 8.0) in an Eppendorf tube. 4 µL of pectate lyase was added and left for 1 week at 50 ^{o}C, shaking at 1250 rpm. Enzyme activity was quenched by placing the reaction mixture in a boiling water bath for 3 mins. Oligomers (including the unsaturated target molecules) were precipitated using 80% EtOH. The precipitate was rinsed twice with 50% ethanol, and dried and this sample was analysed using CE and NMR. (b) *HG*. The chemical elimination protocol to generate unsaturated HG was adapted from previous protocols in literature [165, 166]. HG (DM93) of 1% w/v was made up in 100 mM Na-citrate buffer (pH 6.0) and left at 90 ^{o}C for 45 minutes. The reaction was quenched by placing the reaction vessel in ice. After precipitation with 80% EtOH, the precipitate was rinsed twice with 50% ethanol, dried, re-dissolved in 200 µL 100 mM sodium phosphate buffer (pH 6.5) and run in the CE.

B: Conjugation of cysteamine and biotin-displaying NHS ester: Cysteamine and pre-dissolved as-purchased sulfo-NHS biotin ester were dissolved in a 1:20 ratio in 100 mM sodium phosphate buffer (pH 7.0) at room temperature for 2 hours. The product was run in the CE and analysed by NMR.

C: Assembly of the products from A and B: Unsaturated saccharide substrates from (A) and the biotin displaying thiol-terminated linker molecule from (B) were dissolved in a 1:1 ratio in 100 mM sodium phosphate buffer (pH 7.0). Photoinitiator Irgacure2959 (0.1% w/v) was added and the mixture was subjected to UV irradiation (wavelength = 254 - 366 nm) in a quartz cuvette (15 mins for oligosaccharide and 45 mins for HG). It should be noted that, as elaborated on in the Results and Discussion, the reducing-end aldehyde first needs to be protected before this step is undertaken. This is most efficiently achieved using the reducing end functionalisation described above. After potential linking, the samples were dialysed for 24 h against MilliQ water using a 300 Da cut-off membrane. The final sample was also precipitated with 80% EtOH, after dialysis, for further purification. The precipitate was rinsed twice with 50% ethanol, dried, re-dissolved in 100 mM sodium phosphate buffer (pH 7.0). The products were examined in CE and analysed by NMR for oligos, and by ELISA for HG.

Methods

Capillary Electrophoresis (CE)

Experiments were carried out using an automated Agilent CE system (HP 3D), equipped with a diode array detector. Electrophoresis was carried out in a fused silica capillary with an internal diameter of 50 µm and a total length of 48.5 cm (40 cm from inlet to detector), unless otherwise stated. The capillary incorporated an extended light-path detection window (150 µm) and was thermostatted at 25 °C. All new capillaries were conditioned by rinsing for 30 min with 1 M NaOH, 30 min with a 0.1 M NaOH solution, 15 min with water, and 30 min with background electrolyte (BGE). Sodium phosphate buffer (50 mM at pH 7.0) was used as a CE background electrolyte (BGE) and filtered through 0.2 µm filters (Whatman) before use. Between runs, the capillary was washed for 2 min with 1 M NaOH, 2 min with 0.1 M NaOH, 1 min with water, and 1 min with BGE. Detection was carried out using UV absorbance typically at 192 nm (and 235 nm where specified), with a bandwidth of 2 nm. Samples were loaded hydrodynamically (various injection times at

5000 Pa, typically giving injection volumes of the order of 10 nL) and typically electrophoresed across a potential difference of 25 kV. All experiments were carried out at normal polarity (inlet anodic) unless otherwise stated.

Nuclear Magnetic Resonance (NMR)

Spectra of samples in either D_2O or 95% H_2O/D_2O were recorded at 25 ^oC using a cryoprobe-equipped 700 MHz Bruker Avance NMR spectrometer (Bruker Biospin, Rhinestetten, Germany). Experiments typically consisted of 1D ^1H, 2D COSY and ^{13}C-^1H HSQC, HSQC-TOCSY and HMBC spectra, recorded using Bruker's standard parameter sets. Data were processed with Topspin (Bruker Biospin, Rhinestetten, Germany).

Enzyme Linked Immunosorbent Assay (ELISA)

A general sandwich ELISA protocol as shown in Figure 4.4 was adapted [113, 167] in order to detect the simultaneous presence of the groups forming the termini handles for the treated HG molecules. In all the following ELISAs, two sandwich wells and two controls were set-up for each sample. In the control wells, the capture antibody is not introduced. First, the sandwich wells only were incubated overnight, in the fridge, with 100 µL of their respective capture antibody. The plates were then washed 5 times under tap water and dried. The sandwich and control wells are treated with the blocking buffer of 5% w/v milk in 1X PBS, for 2 hours, at room temperature. The plates were then washed 5 times under tap water and dried. Next, 100 µL of the sample (dissolved in the blocking buffer) was added to the sandwich and control wells and left at room temperature for an hour. The plates were then washed 5 times under tap water and dried. 100 µL of the respective detection antibody is added to the wells, next, and left at room temperature for an hour. The plates were then washed 7 times under tap water and dried. For the final step, 100 µL of the reveal solution was added and the plates were observed for a maximum of 15 minutes to see if any colour developed. For a 1 mL reveal solution, the composition is 0.9 mL H_2O, 0.1 mL 1 M sodium acetate (pH 6.0), 10 µL TMB and 1 µL of 6% hydrogen peroxide (added last). The development of colour is quenched by adding 100 µL of 2.5 M H_2SO_4. The plates were then read, at a wavelength of 450 nm, using a plate reader.

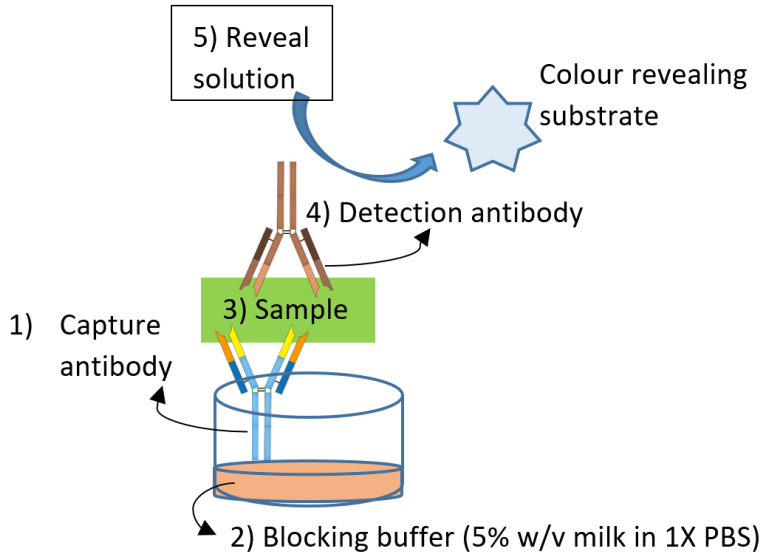

FIGURE 4.4: Schematic of the steps involved in a sandwich ELISA that has been employed in this project.

At the reducing end of the HG molecule, the goal is to attach a bifunctional polyethylene glycol linker that has an aminooxy group at one end that links to the terminal sugar and a biotin group at the other end. The success of this reaction can be tested by using the JIM7 antibody (that binds to highly methylesterified homogalacturonan epitopes) and additionally a streptavidin-HRP antibody (that binds to biotin epitopes) [168, 169]. Where both epitopes were present on the same molecule, this assay will report a positive colormetric result. For biotin-HG samples, the capture and detection antibodies used were JIM7 (1:10 in 5% milk) and strep-HRP (1:500 in 5% milk) respectively.

Ultimately, the polysaccharide of interest will be functionalised with biotin at both ends (to enable their binding to streptavidin linking hubs). However, it is not possible to have suitable controls if the same epitope exists at both ends. Hence, for the purpose of detection using this methodology, digoxigenin (using the NHS-digoxigenin ester rather than the sulfo-NHS-biotin ester) can be used and displayed at the terminal non-reducing end as a substitute. The final chemistry-validating construct in this case, with biotin at one end and digoxigenin at the other, can be tested for using streptavidin and digoxigenin antibodies in the sandwich ELISA assay. Positive controls are available in the form of a DNA construct with the same termini (in that case introduced through the primers used in PCR). For digoxigenin-HG-biotin samples, the capture and detection antibodies used are anti-dig (1.5 µL in 1.5 mL 1X PBS) and strep-HRP (1:500 in 5% milk), respectively.

4.3 Results and Discussion

4.3.1 Oligogalacturonides

Reducing end functionalisation

Figure 4.5 shows the electrophoregrams obtained by CE after the injection of the reactants (tetragalacturonic acid (DP4) only (A, Top) and immediately after the addition of aminooxy-biotin (A and B, Middle)) and subsequently the mixture after 3 days (A, B and C, Bottom), clearly showing the formation of a new peak (C) of intermediate mobility. As a function of time, this new peak increases in size while those of the reactant peaks decrease in concert (data not shown), suggesting that indeed this new peak corresponds to biotin-functionalised tetragalacturonic acid as expected. It can be seen in Figure 4.5 (Top) that the initial sample of tetragalacturonic acid contains a small fraction of pentagalacturonic acid (DP5) and consequently, the second smaller product peak in C is assigned to DP5 attached to aminooxy-biotin. Additionally, as expected, the product peaks are observed have a higher absorbance than the initial oligogalacturonic acids owing to the high absorbance of the introduced aminooxy-biotin, that has now been attached to the oligogalacturonic acid species.

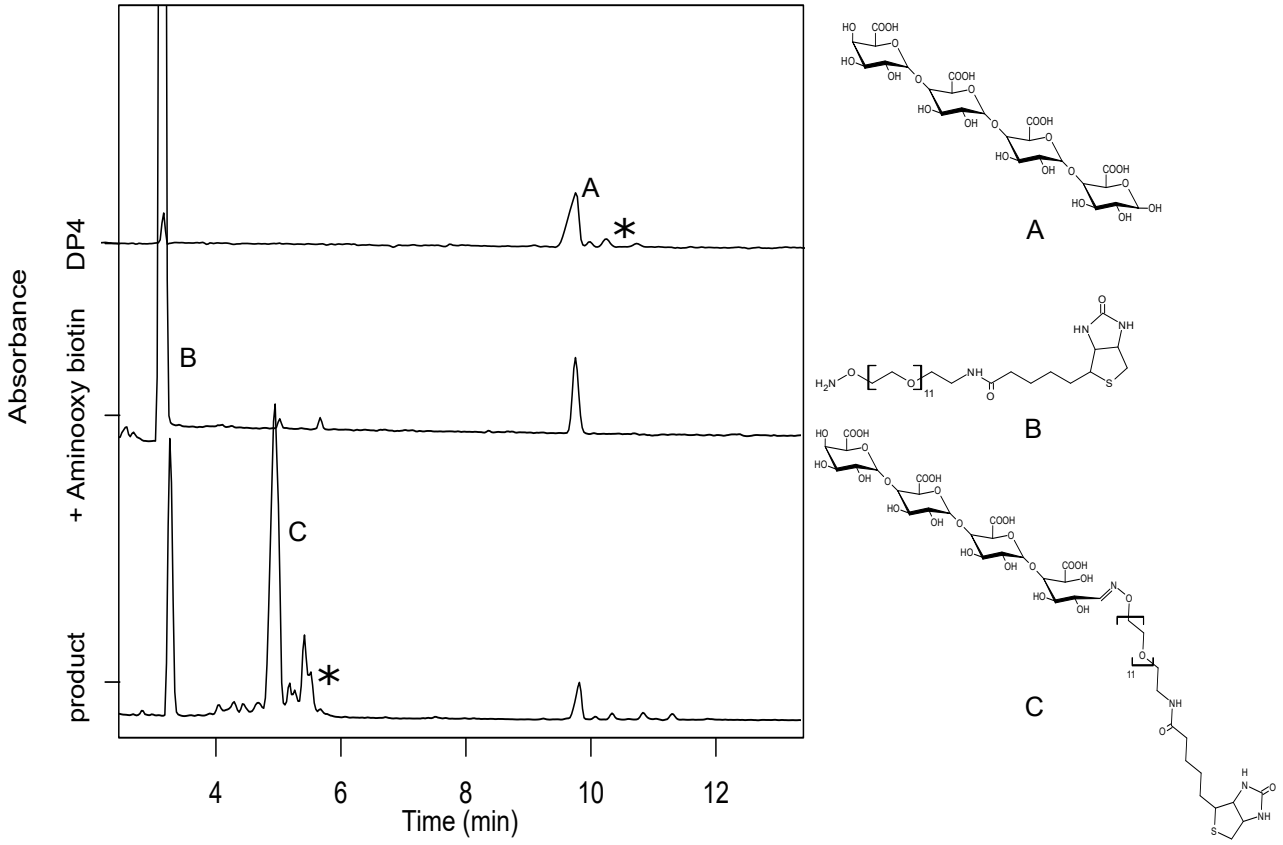

FIGURE 4.5: Monitoring the progress of the reaction of tetragalacturonic acid (DP4) (A) with aminooxy-$(PEG)_{12}$-biotin (B) using CE. The formation of the product can clearly be seen as a new peak (C) after 3 days (* indicates contamination due to presence of pentagalacturonic acid - DP5).

Under the CE conditions used, anionic species are dragged towards the cathode by the electroosmotic flow (EOF). The peak at around 3.5 minutes in the DP4 sample provides a neutral marker (formed here by the refractive index change from injection plug solvent passing the detection window), and monitors the value of the EOF [104]. Peaks from positively charged species will migrate earlier than the EOF, and peaks from negatively charged species will be observed later. With the BGE at pH 7, as described in the methods section, the DP4 species is fully charged (the pKa of GalpA is around 3.5) and comes out at around ten minutes under the conditions used here. Adding the aminooxy-$(PEG)_{12}$-biotin immediately yields an additional large peak at the EOF, corrresponding, as expected to a neutral molecule with high absorbance.

The proposed chemical structure of the product was supported by NMR (Figure 4.6). In particular, by comparing the ^{1}H spectra of the product and reactants, a new major and minor doublet at 7.59 ppm (J = 5.4 Hz) and 7.62 ppm (J = 5.70 Hz) respectively was observed. These signals correlated to ^{13}C signals at 150.53 and 153.14 ppm in the HSQC spectrum (not shown), chemical

shifts consistent with syn and anti oxime linkages between the reactants. The ^{1}H and ^{13}C chemical shifts mentioned are also consistent with oxime chemical shifts that have been observed in literature [170, 171]. A COSY correlation (not shown) between the putative oxime doublet at 7.59 ppm at a signal at 4.58 ppm (the simulated value was at 4.57 ppm: MestReNova 14. 1, MestreLab Research S.L., Santiago de Compostela, Spain) is consistent with the connectivity between the oxime and H-1 and H-2 of the former reducing end ring I (now ring-opened), of the tetragalacturonic acid moiety of the product, (D). The integral of these peaks, normalized to the integral of the 4 biotin protons at ~1.6 ppm suggests the reaction has gone to ~40% completion after 3 hours.

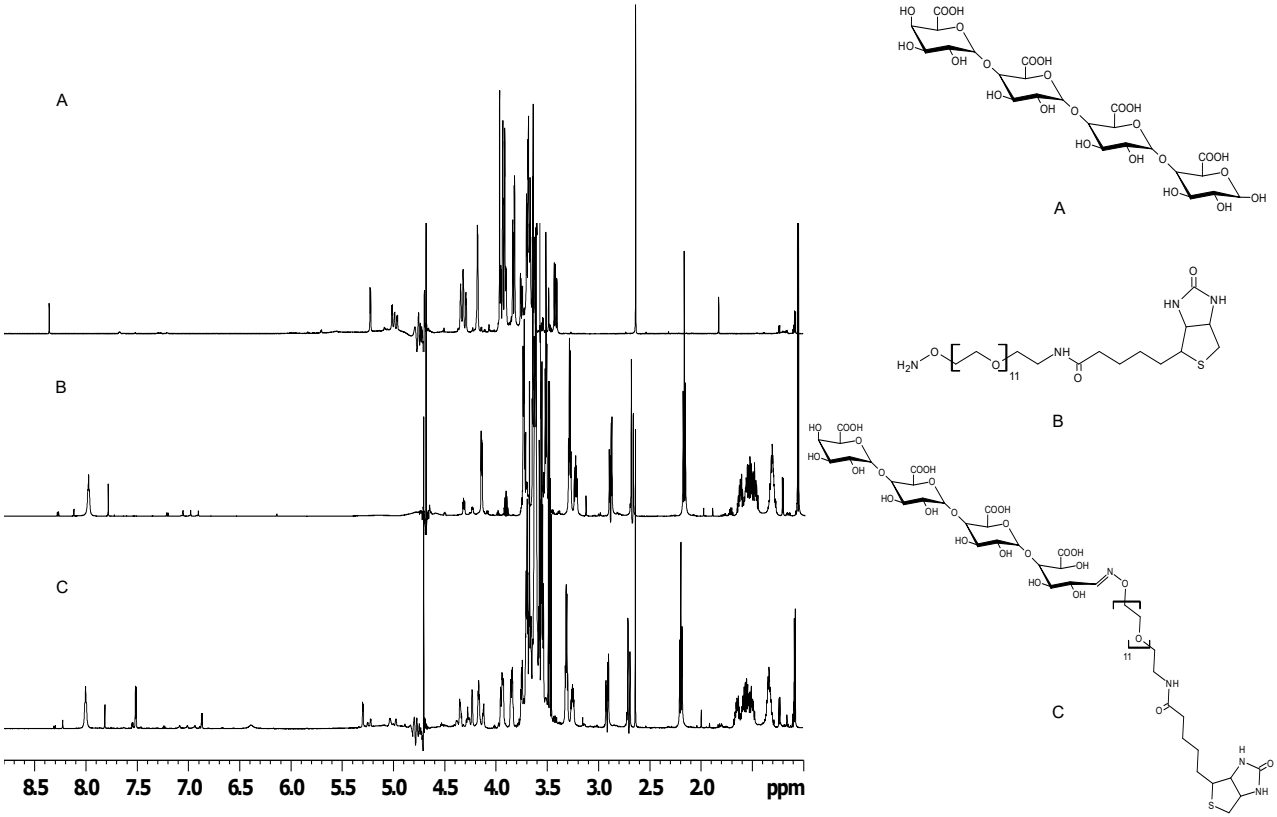

FIGURE 4.6: ^{1}H NMR spectra of the reactants: tetragalacturonic acid (A) and aminooxy-$(PEG)_{12}$-biotin (B), and the resulting product, reducing end biotinylated tetragalacturonic acid (C). The major doublet, consistent with oxime formation can be seen at 7.59 ppm in C.

Non-reducing end functionalisation

As described in the Introduction, and in the Materials and Methods, adding a biotin (or digoxigenin) handle to the non-reducing end of the saccharide substrates requires successful completion of a number of steps.

Step 1: Firstly, substrates with a double bond present in the non-reducing-end terminal-sugar residue were generated. CE results showed that a pectate lyase treatment of polygalacturonic acid (PGA) could be used to generate unsaturated oligogalacturonide species, as expected from the mode of action of these enzymes. Using the initially-trialled digest time-frame resulted in the formation of multiple (a minimum of two) different DP oligogalacturonic fragments. Before performing NMR on these products, attempts were made to isolate just one unsaturated oligogalacturonide.

Figure 4.7A shows that by using an ion-exchange HPLC, individual species could be separated, in this case, a dimer (see Figure 4.8). However, the effort and time involved was substantial, leading us to pursue a second approach. Here, the pectate lyase digestion was simply carried out for a longer period (increasing the 3 days at 40 ^{o}C to 1 week at 50 ^{o}C, with extra enzyme added after 3 days). Figure 4.7B shows CE results confirming that the more prolonged enzyme digestion generated predominately one unsaturated oligogalacturonide species and this method was subsequently used to generate the unsaturated species for use in the further steps. It should be noted that the presence of the double bond is reflected by the substantial UV absorbance at 235 nm, and that the chemical nature of this base species was confirmed using NMR.

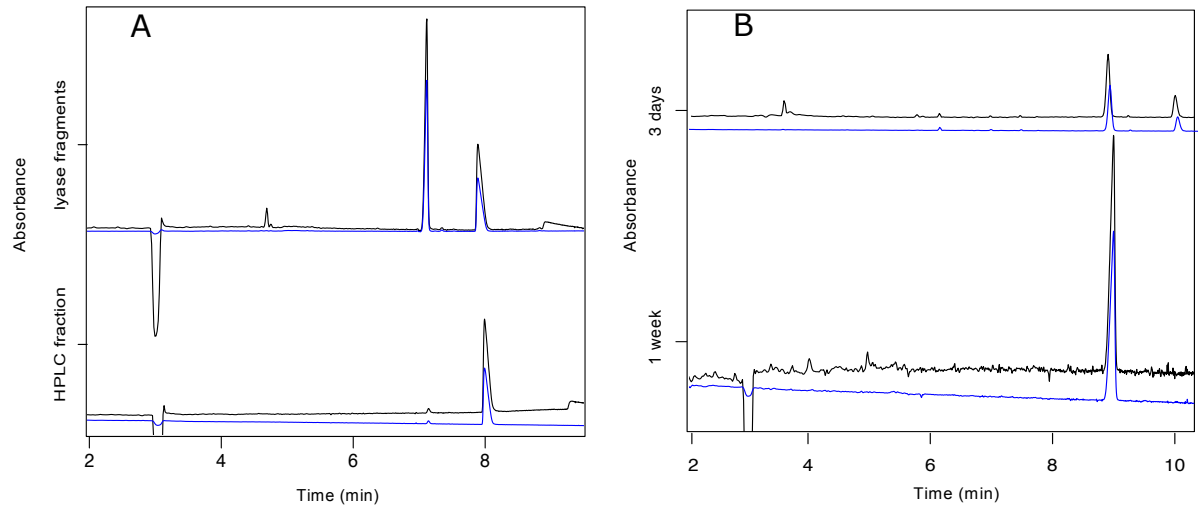

FIGURE 4.7: (A) Electrophoregrams of lyase fragments run before and after HPLC treatment. (B) Pectate lyase treatment on polygalacturonic acid for 3 days and 1 week at 50^{o}C. (Black: Absorbance at 192 nm, Blue: Absorbance at 235 nm).

The 2D spectra in Figure 4.8 show the unsaturated product, which appears to be a digalacturonic acid. The black spectrum is the ^{1}H-^{13}C HSQC (which correlates the H's to the ^{13}C to which

they are directly attached). The blue spectrum is an HSQC-TOCSY which contains additional signals for H in the same spin system as the C-H correlation (in this case, in each uronic acid ring). The red spectrum is the HMBC which correlates H to C 2,3,4 bonds away.

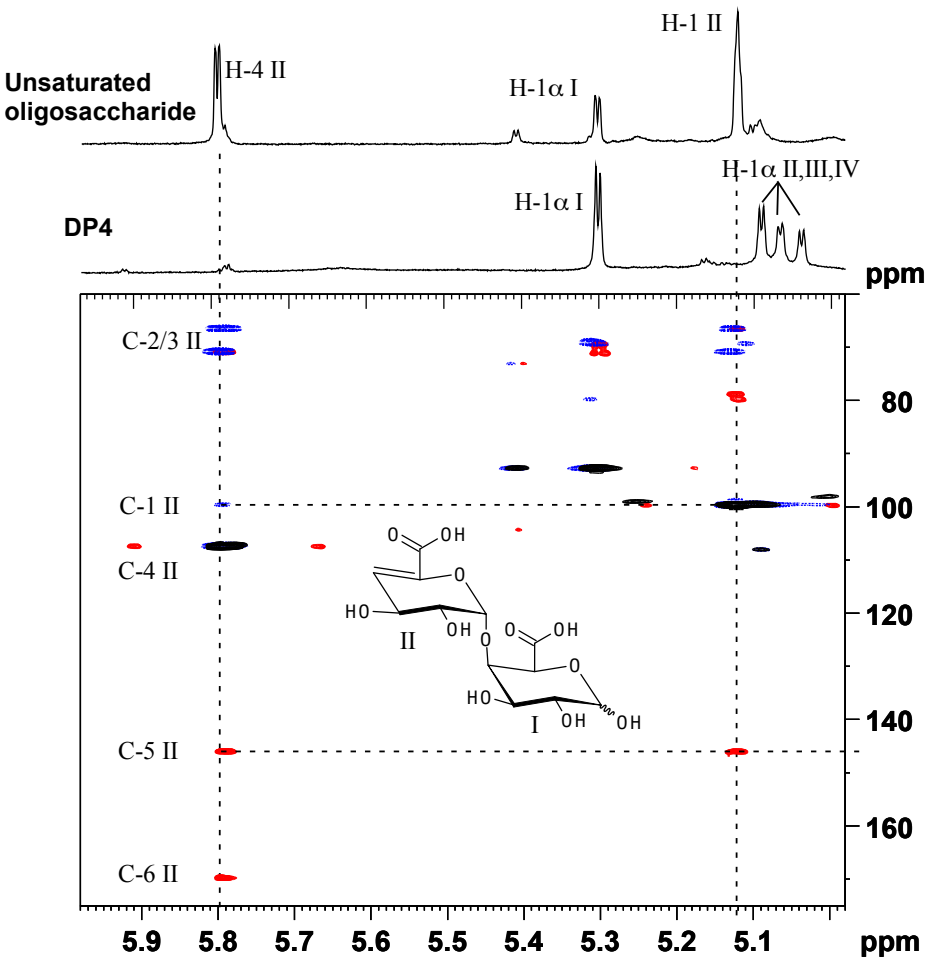

FIGURE 4.8: 2D HSQC (black), HSQC-TOCSY (blue) and HMBC (red) NMR spectra (^{13}C vs ^{1}H) of the unsaturated product obtained after extended lyase treatment. The 1H spectrum of the tetragalacturonic acid reactant and the unsaturated product are shown above the 2D spectra. The red spectrum is the HMBC which correlates H to C 2,3,4 bonds away.

There is a ^{1}H signal at 5.79 ppm in the lyase digest of PGA which is attributed to the unsaturated H-4 of ring II of the digalacturonic acid product. The C-4 II ^{13}C shift is 107.3 ppm (from the HSQC). H-4 II shows a correlation in the HMBC to the quaternary C-5 II at 145.8 ppm, which is in the expected chemical shift range for an olefinic carbon, with an attached carboxyl group. It also shows a correlation to the C-6 II carboxyl at 169.3 ppm. There is a signal at 5.12 ppm which is

likely to be H-1 II, since it is correlated to the signal assigned to H-4 II in the HSQC-TOCSY. Note the attenuation of the H-1α I-IV signals in the tetragalacturonic acid is due to the suppression of the nearby water signal (4.7 ppm).

Step 2: The next step proposed was to add a cysteamine linker that was pre-functionalised with a biotin handle to the unsaturated group. However, to prevent the unwanted coupling of the cysteamine amine group to the aldehyde reducing ends of these molecules, the reducing end was first protected, by introducing the reducing end handle as described in section 4.2 (Experimental Procedures) as the next step of the non-reducing end functionalisation. Unwanted attachment of the cysteamine linker to the reducing end aldehyde moiety instead of the alkene moiety when both are available could easily be detected by NMR (data not shown). Figure 4.9 presents electrophoregrams taken during this reducing-end protection-step. These are analogous to the results shown in Figure 4.5, but for the unsaturated disaccharide generated in step 1, rather than the saturated DP4 substrate. Specifically, Figure 4.9 shows the electrophoregrams obtained by CE after the injection of the reactants (unsaturated digalacturonide (D) only (top), aminooxy-$(PEG)_{12}$-biotin (B), middle)) and subsequently the mixture, containing (E) after 3 days (bottom), clearly showing the formation of a new peak (E) of intermediate mobility.

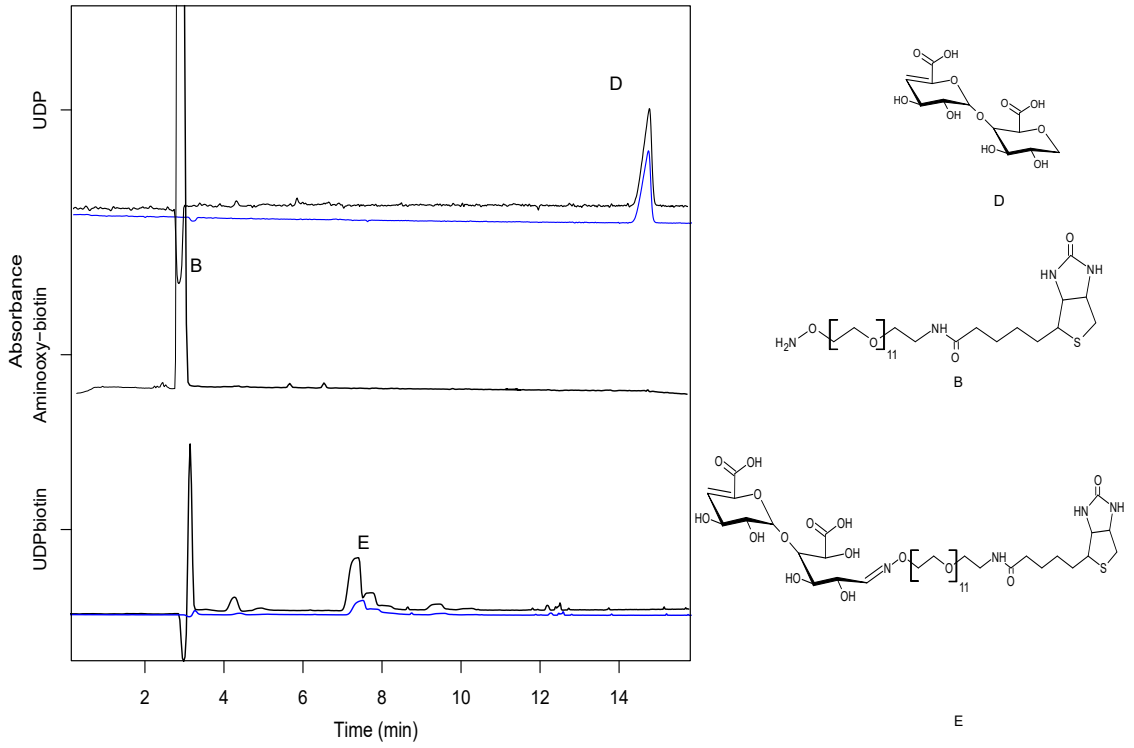

FIGURE 4.9: Electrophoregrams of unsaturated oligogalacturonic acid (UDP) (D) and aminooxy-$(PEG)_{12}$-biotin (B) before incubation, and the resulting product (E), reducing end biotinylated unsaturated oligogalacturonic acid, after incubation.

The ^1H spectra of reactants and product are shown in Figure 4.10. The peak at 7.633 ppm (doublet, J = 5.09 Hz) is analogous to the major and minor doublets formed on reaction of aminooxy-$(PEG)_{12}$-biotin with tetragalacturonic (Figure 4.6) and is evidence of the new oxime linkage in the product. It is to be noted that due to the resolution from Figure 4.10, although the peak appears to be more of a single peak, it is a doublet peak. Furthermore, the absence of a companion doublet indicates the product is predominantly either *syn* or *anti*. The integral of the peak assigned to the oxime linkage, normalized to the integral of the four biotin protons' signals at ~1.6 ppm) suggests the reaction has gone to ~20% completion.

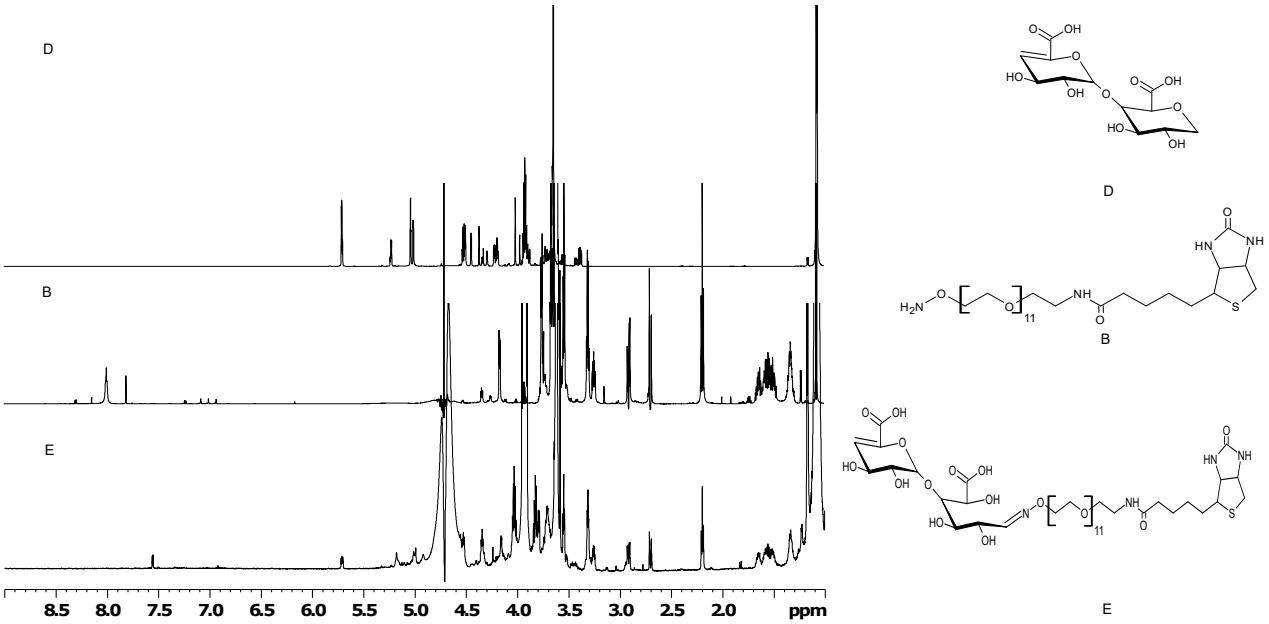

FIGURE 4.10: ^{1}H NMR spectra of the reactants: unsaturated digalacturonic acid (D) and aminooxy-$(PEG)_{12}$-biotin (B) and the resulting product with the biotinylated reducing end of the unsaturated galacturonic acid (E). The peak at 7.633 ppm is evidence of the new oxime linkage in the product.

Step 3: With the double bond present in the ring (Step 1), and the reducing end already functionalised with biotin (Step 2), a cysteamine linker was pre-functionalised with a biotin handle via attachment to the amine terminus. Figure 4.11 shows electrophoregrams that follow the generation of this biotin-handle containing molecule that is terminated with a thiol moiety (ready for coupling into the sugar ring in the final step).

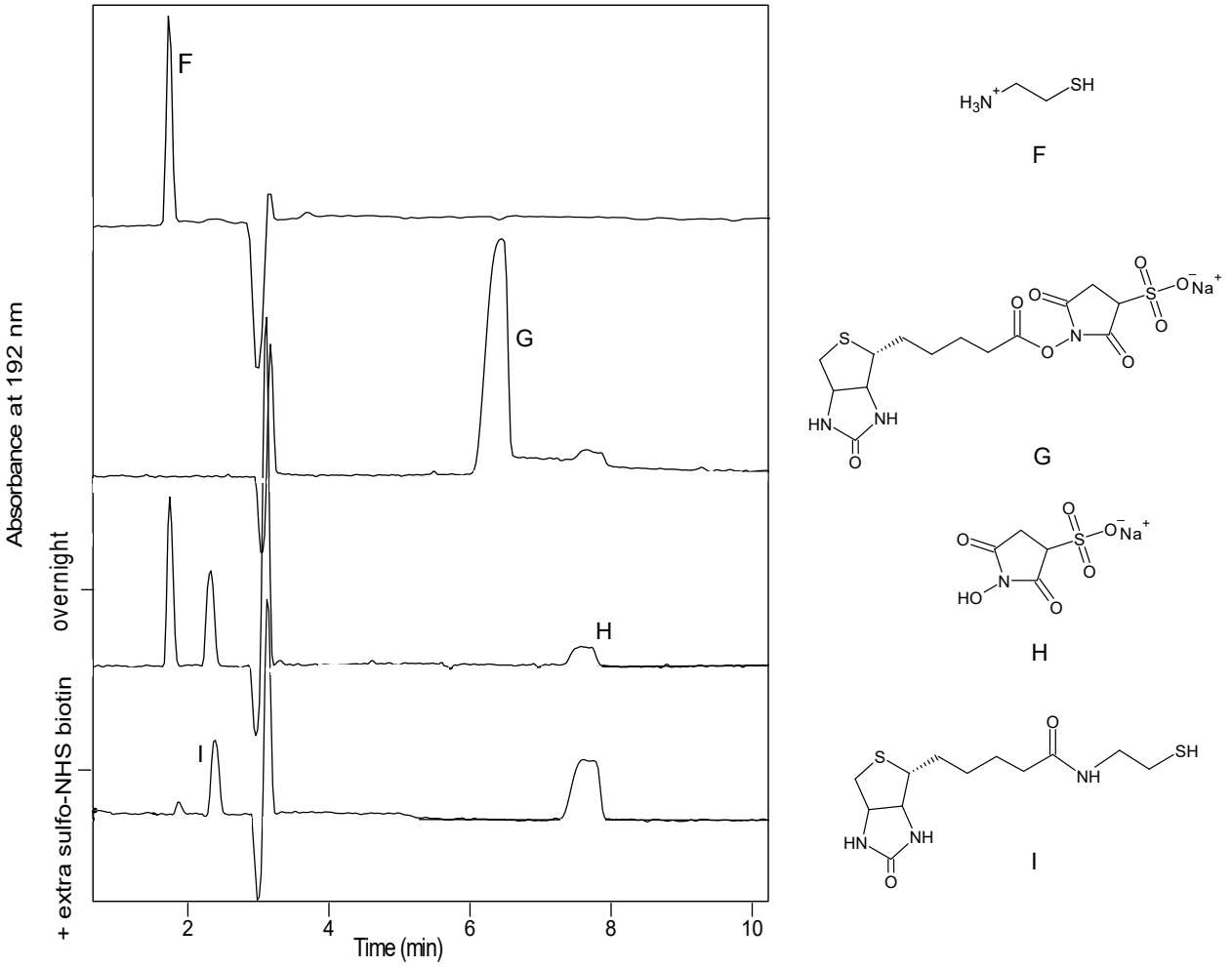

FIGURE 4.11: Electrophoregrams of the reactants for preparation of the biotinylated linker: cysteamine (F) and sulfo-NHS-biotin (G), and the products obtained overnight: sulfo-NHS-ester (H) and the biotinylated cysteamine (I). Extra sulfo-NHS-biotin is added to maximise the yield of biotinylated cysteamine.

From Figure 4.11, cysteamine (F) can be seen to elute as a positively charged species (to the left of the EOF in the polarity in which the CE is run). When sulfo-NHS-biotin as purchased is run in the CE, two negatively charged peaks can be seen (G plus small amount of H). These two peaks are most likely the desired sulfo-NHS-biotin molecule (the major peak, G) and sulfo-NHS-ester (the small but detectable peak, H), a side product from sulfo-NHS-biotin hydrolysis. On incubation of cysteamine with sulfo-NHS-biotin, we observe a new product peak (I), and in concert, the expected by-product, sulfo-NHS-ester (H). (There is a higher peak of side product (H) than expected due to the continuous hydrolysis of the sulfo-NHS-biotin reactant as the coupling reaction progresses). The structure of the product including, crucially, the new amide linkage formed were confirmed using NMR (Figures 4.12 and 4.13).

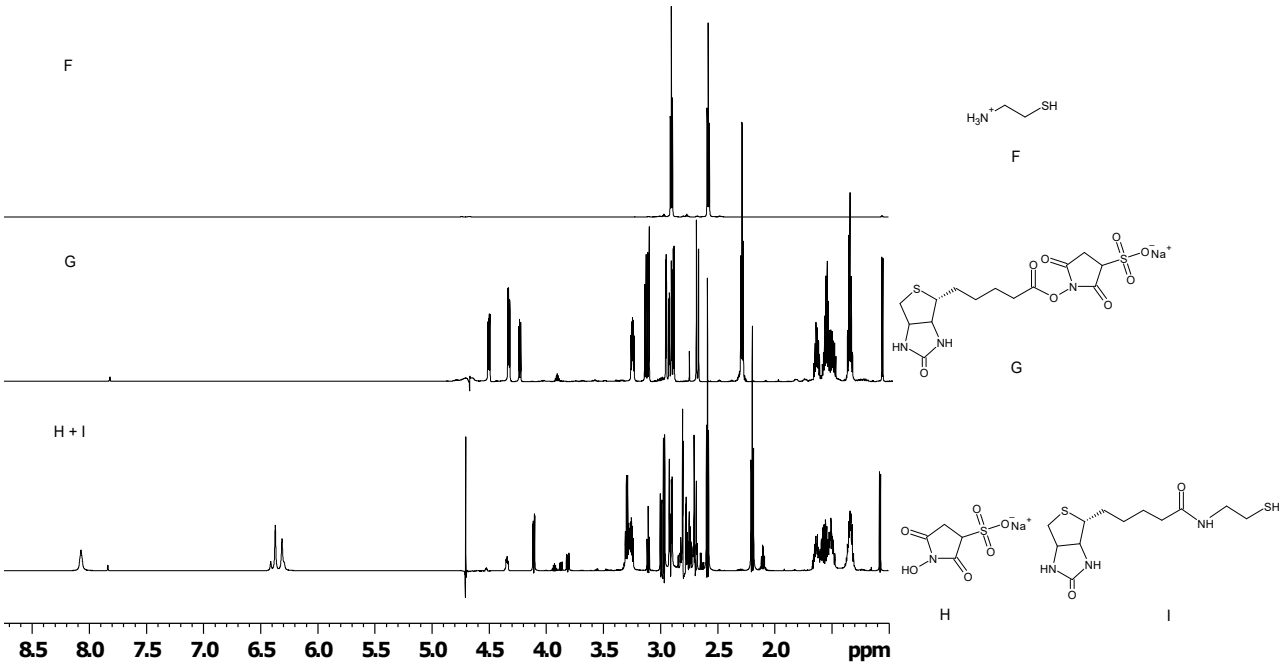

FIGURE 4.12: ^{1}H NMR spectra of the reactants: cysteamine (F) and sulfo-NHS-biotin (G) and the products; sulfo-NHS-ester (H) and the biotinylated cysteamine (I). The new broadened triplet at 8.15 ppm in the spectrum of H + I is consistent with the amide linkage.

Figure 4.13 shows the HSQC, HSQC-TOCSY and HMBC spectra of the biotinylated linker. In the HSQC (black) a quartet at 3.369 ppm and a triplet at 2.665 ppm correspond to H-14 and H-15, as labelled in the structure. Both of these show correlations in the HSQC-TOCSY (blue) via signals assigned to C-14 and C-15 to the broadened triplet amide proton (H-13) at 8.152 ppm. The amide linkage is confirmed by the correlations of both H-14 and H-15 with C-1, shown in the HMBC (red) i.e. long range coupling is observed across the amide linkage. The identity of C-1 is supported by the HMBC correlation to H-2 in the biotin moiety's pentamide side chain at 2.272 (triplet) and also H-3 at 1.640 ppm.

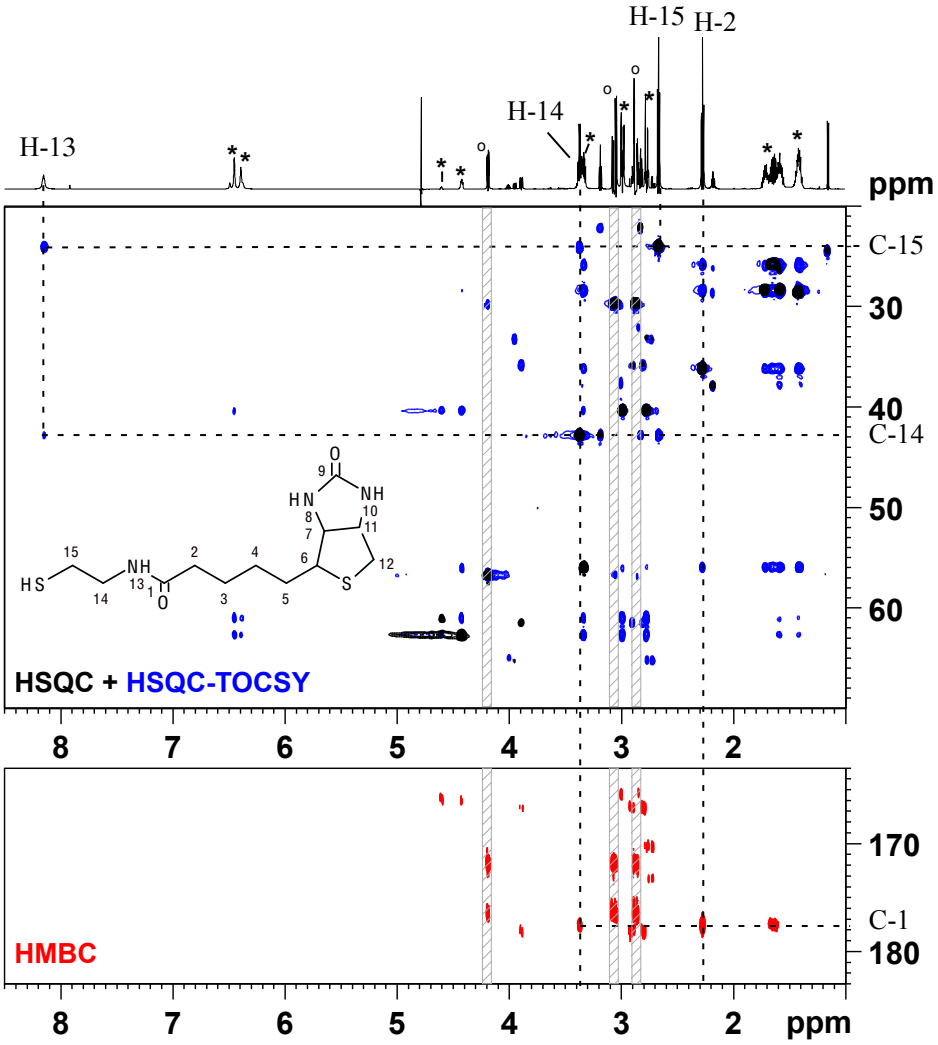

FIGURE 4.13: 2D spectra of the biotinylated linker: HSQC (black), HSQC-TOCSY (blue) and HMBC (red). H-2 and peaks marked with "*" belong to the product's biotin moiety (signals close to the residual water signal at 4.7 ppm have been partially suppressed); H-13, 14 and 15 belong to the cysteamine moiety. Peaks marked with "^{o}" are from the sulfo-NHS-ester (major) impurity. Their 2D correlations are marked with hatched rectangles and can be ignored. Other unassigned peaks are minor impurities.

Step 4: Having prepared the disaccharide with a double bond in the non-reducing-end (E) and a pre-attached handle at the reducing end (I), the final step was to form a bond between these two species. The reaction of the thiol group of the biotin handle and the unsaturated terminal sugar ring was photo-catalysed with the addition of a photoinitiator Irgacure2959 and subsequent exposure to UV irradiation, as described in Materials and Methods. Figure 4.14 shows the the electrophoregrams obtained as the reaction is carried out. It can be seen that the 235 nm absorbance

predominant in the initial unsaturated oligomer is absent in the product, as would be expected as the alkene protons become alkane upon coupling. Unfortunately, any distinguishing signals in the NMR spectra of the product were overwhelmed by the presence of substantial amounts of starting materials. However, the functionalisation at both ends was still attempted for longer saccharide pieces of HG and tested using ELISA, for which impurities do not affect the presence of a final positive result.

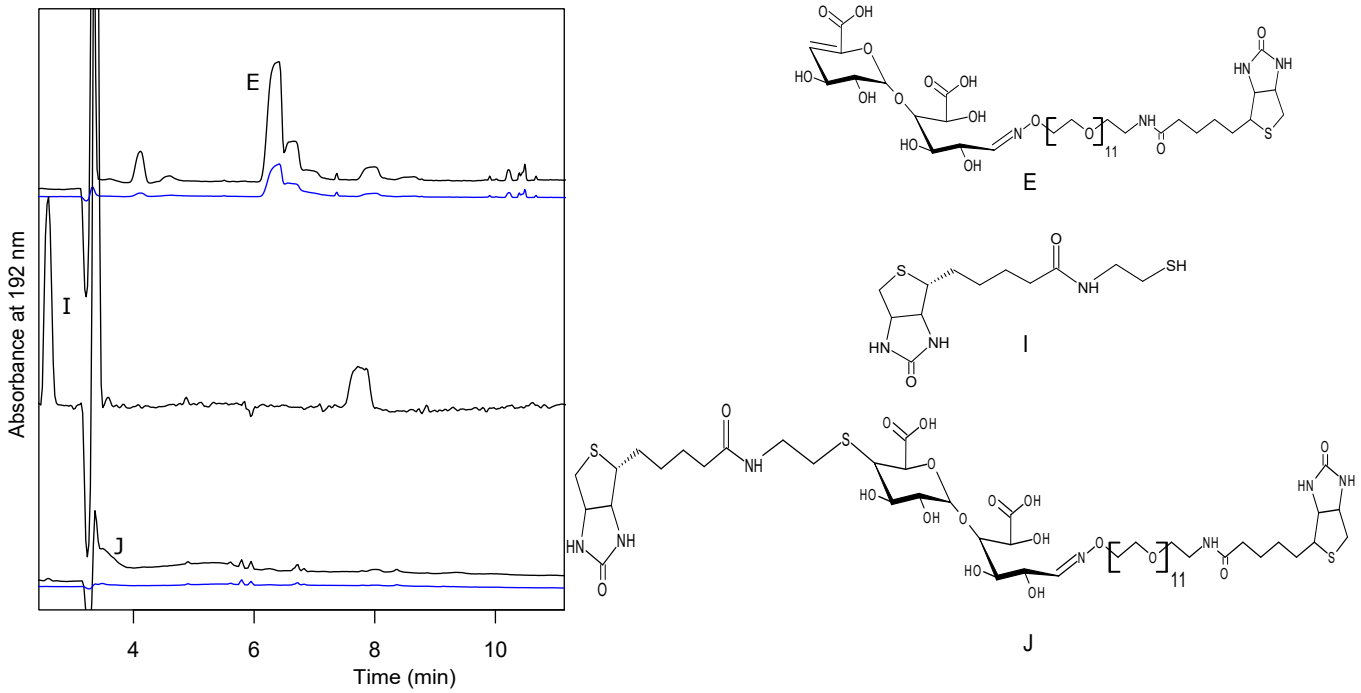

FIGURE 4.14: Electrophoregrams of the reactants; reducing end biotinylated unsaturated oligogalacturonic acid (E) and biotinylated cysteamine (I) before UV treatment, and the purified product with biotinylated reducing and non-reducing ends (J), after 15 mins UV exposure with a photoinitiator.

4.3.2 Homogalacturonan (HG)

Having confirmed a chemical route for modifying oligosaccharides, specifically oligogalacturonides, by attaching biotin handles covalently to both ends, the general strategy was then applied to a considerably longer saccharide chain in the form of HG. An increase in length results in an electrophoretic migration time becoming independent of the degree of polymerisation (DP). Additionally, given the extra complexity of the product and likely peak broadening, due to its high molecular weight, CE and NMR were considered to be less than ideal techniques for confirming the generation of the dual-handled substrate. However, an additional technique capable for determining whether the terminal ends of a polymeric molecule bear the desired functional

groups, so-called Sandwich ELISA, is ideal in this situation [167]. While ELISA cannot be performed on small oligosaccharides and is not able to detect if both ends have been functionalised with the same group, a control double-stranded DNA substrate (in which biotin and digoxigenin have been introduced into the DNA substrate by PCR using modified primers) is available as a positive control molecule, demonstrating how the successful functionalisation of the ends can be confirmed (Figure 2.5). Hence, the protocol described in Step 3 above was modified by using NHS-digoxigenin instead of sulfo-NHS-biotin at the non-reducing end. Steps involved in the attachment of digoxigenin species to biotin functionalised unsaturated homogalacturonan is shown in Figure 4.15. If the protocols demonstrated for oligogalacturonides can be successfully transferred to HG then a biotin-HG-digoxigenin molecule should be able to be generated and observed by sandwich ELISA.

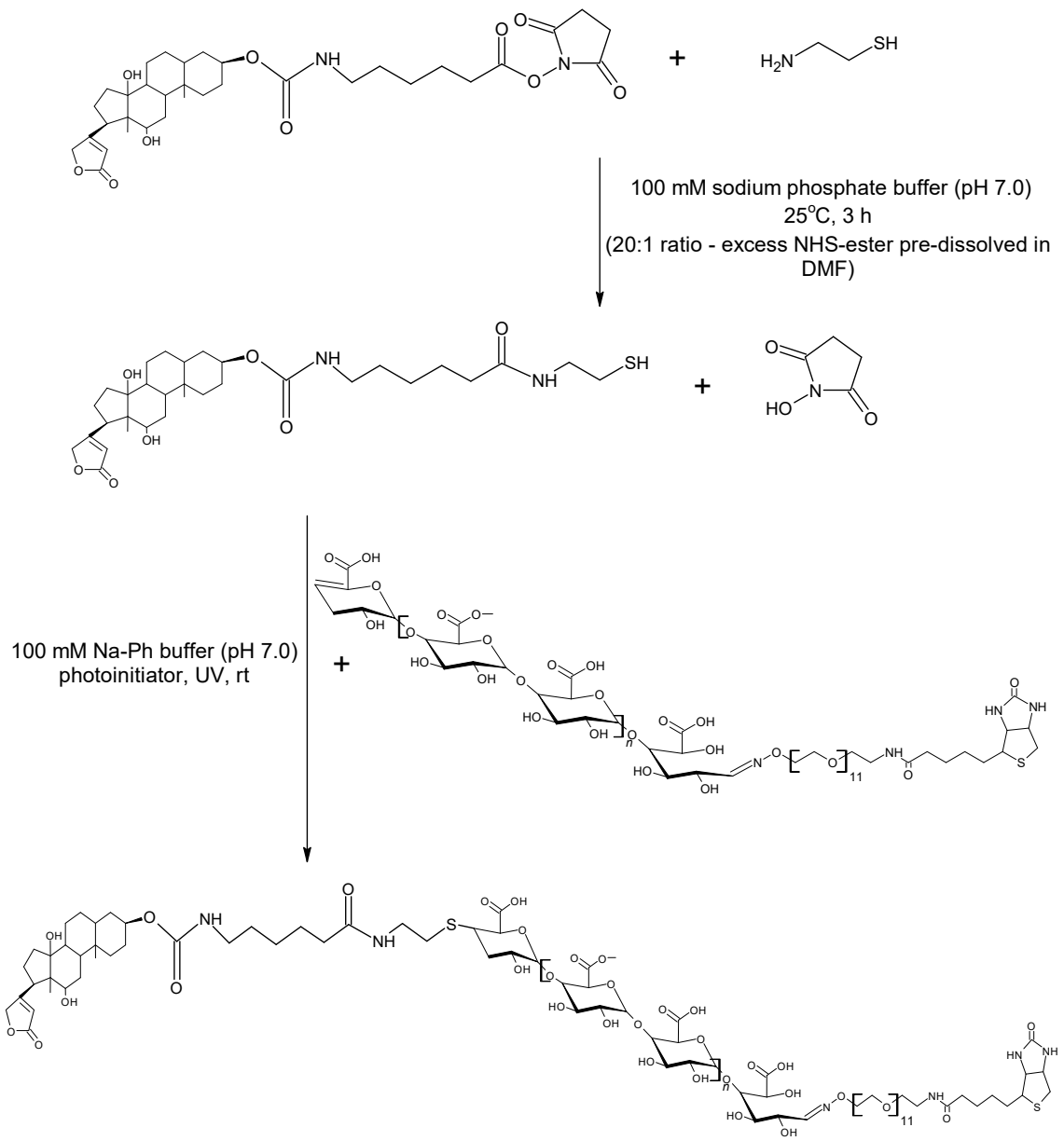

FIGURE 4.15: Reaction conditions for the formation of digoxigenin-thiol species from NHS-digoxigenin ester and cysteamine, followed by thiol-ene click reaction to attach the generated species to reducing end biotinylated unsaturated homogalacturonan.

Reducing end functionalisation of HG

ELISA was performed on HG samples that were subject to aminooxy-aldehyde conjugation with a functionalised biotin handle, as described in Materials and Methods (and shown above to be successful for tetragalacturonic acid), for two different incubation times (3 days and 7 days). Figure 4.16 shows that positive results were attained in both cases, indicating that molecules with one pectic end (bound by pectin-recognizing antibodies) and the other end terminated with biotin (bound by streptavidin) were present. As expected the signal was higher for the sample that had

been subjected to the longer incubation time of 7 days, showing this reaction is reasonably slow under the conditions used (unfunctionalised HG was used as a control).

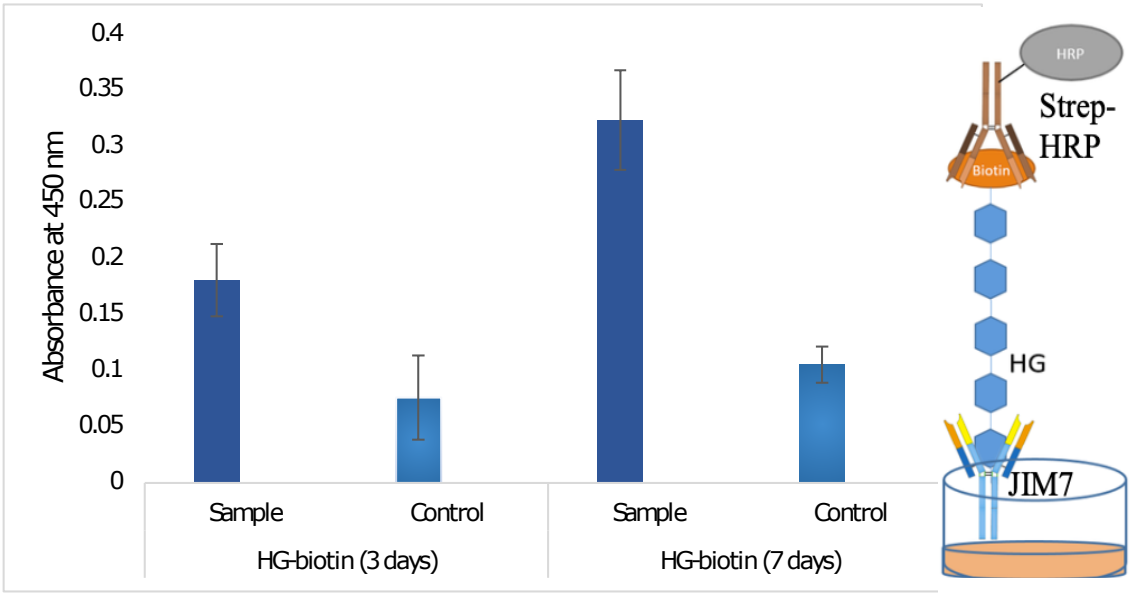

FIGURE 4.16: Absorbance at 450 nm recorded of the ELISA signals detected for reducing-end biotinylated HG and their controls (3-day incubation vs 7-day incubation). Here, JIM7 and streptavidin-HRP have been used as the capture and detection antibody respectively.

Non-reducing end functionalisation of HG

HG samples were subjected to chemical β-elimination before being functionalised by biotin and digoxigenin at the reducing end and non-reducing end, respectively, as described in Section 4.2. (Experminental Procedures, A (b)). ELISA was also performed on 100 ng/µL 5 kB DNA (synthesised by PCR) with biotin and digoxigenin termini as a positive control. Here, the ends were detected using streptavidin-HRP and anti-digoxigenin respectively (unfunctionalised HG and HG with only one ends functionalised were used as controls). Figure 4.17 clearly shows that positive results were observed in both cases. Based on these results, it can be seen that attachment of HG to biotin or digoxigenin, at the respective end, or at both ends, was successful, albeit at low yields. This entire protocol has been repeated 10-20 times and is found to be reproducible.

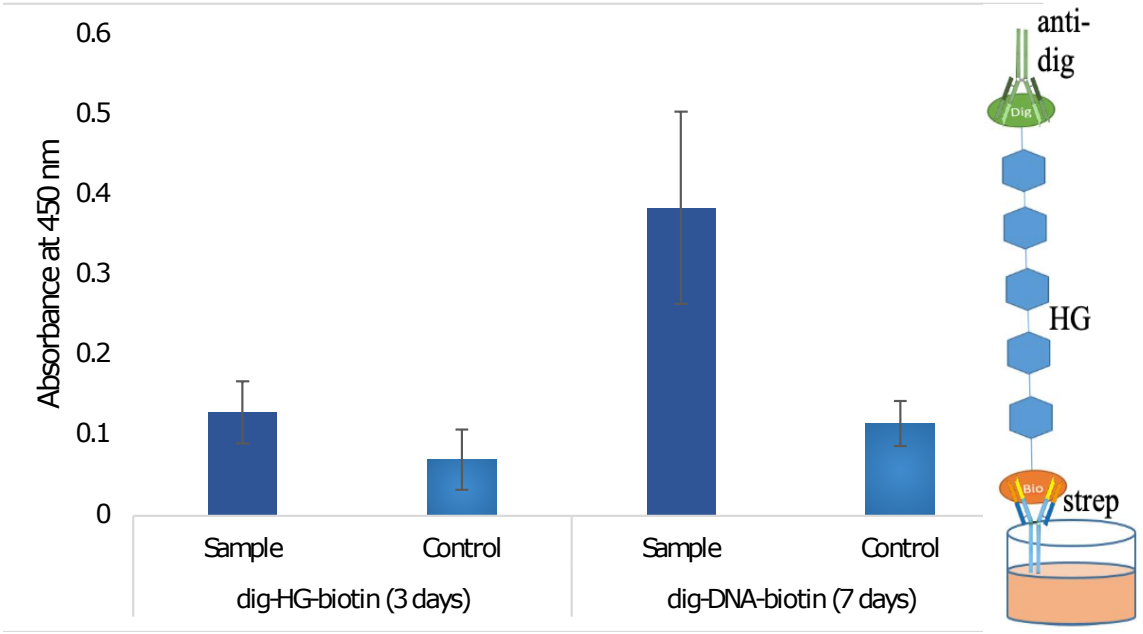

FIGURE 4.17: Absorbance at 450 nm recorded of the ELISA signals for digoxigenin-HG-biotin vs digoxigenin-DNA-biotin their controls. Here, streptavidin-HRP and anti-digoxigenin have been used as the capture and detection antibody respectively.

4.4 Conclusion

A generic approach has been described for placing biotin moieties (or other handles such as digoxigenin) at both ends of polysaccharide substrates. NMR and CE have been used to confirm the successful attachment chemistry for the respective reducing and non-reducing ends of oligosaccharides and ELISA has been used to confirm the successful attachment chemistry for both ends. Compared to coupling at the reducing end, the functionalisation at the non-reducing end proved to be challenging with low yields. Although this proved to be a challenge in attaining the final NMR for the oligosaccharides, it is not a major setback for future single molecule experiments. If needed, optimisation of the final step can be explored in further work by varying conditions such as temperature, pH, amongst other conditions, to repeat the final NMR on the doubly functionalised oligosaccharide. It is the hope that such methodologies will be used to produce plug-and-play polysaccharide inserts for incorporation into composite polymer strings using streptavidin linking hubs.

Chapter 5

Assembly of Polysaccharide-Streptavidin-DNA strings

5.1 Introduction

Once the components, bifunctional streptavidin linkers (described in Chapter 3) and biotin-terminated HG (described in Chapter 4), were prepared, the next step was to try and piece them together for string formation. Before moving onto using bifunctionalised homogalacturonan with DNA to form long HG-containing strings (Figure 5.1), the connection between oligosaccharide and/or polysaccharide components and tetravalent streptavidin was examined. Experiments studying the binding of the biotin-terminated saccharide substrates to streptavidin with pre-bound oligomers were also performed in certain cases. Binding of the reducing and non-reducing end functionalised oligosaccharides and polysaccharide were all tested separately before attempting formation of the full "construct" with bifunctional inserts.

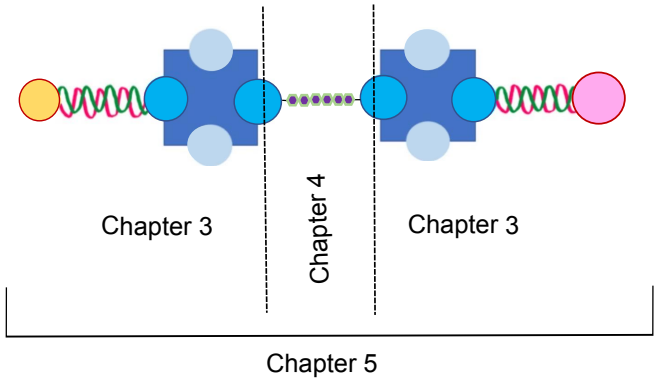

FIGURE 5.1: Brief illustration of the experimental chapters so far.

5.2 Materials and Methods

Oligosaccharides and polysaccharides were functionalised with biotin as described in Chapter 4. For simplification, schematics are used in this chapter to indicate the different moieties. The table of schematics and the molecular diagrams of the different oligosaccharide and polysaccharide species used in this chapter are given in Figures 5.2, 5.3 and 5.4, respectively. Each of these substrates was incubated with tetrameric streptavidin (1:10 dilution from stock (~4 µM final concentration after dilution), at different ratios (specified in each section), and the compositions of the solutions, in terms of partially filled streptavidin linkers, were monitored using CE and SDS PAGE gel. In most experiments, standard CE conditions (as described in Section 2.1) were applied. In certain runs, the electroosmotic flow, EOF, was manipulated so that the migration times of species lengthened substantially in an attempt to improve resolution. To lengthen the EOF here, a reduced voltage of 10 kV was applied and a 100 mM sodium phosphate buffer (pH 7.0) was used as the background electrolyte. Another option (not attempted here) would be to vary the temperature as temperature can affect the viscosity of the background electrolyte and, hence, the migration time [104]. Similar to chapter 3, it is to be noted here that all the electrophoregrams were monitored at 192 nm due to the highest absorbance of the species of interest being at this wavelength.

Schematic	Name
	Biotin (B)
	Unknown biotinylated valencies (i.e could be 1-, 2-, 3- or fully filled)
	tetravalent streptavidin
	galacturonic acid residue
	methylesterified galacturonic acid residue
	primer (single stranded - ss)

FIGURE 5.2: Table showing the different schematics used in Chapter 5. Gradation circles are used to indicate all the possible multiple valencies for ease to represent drawing out the different valency structures.

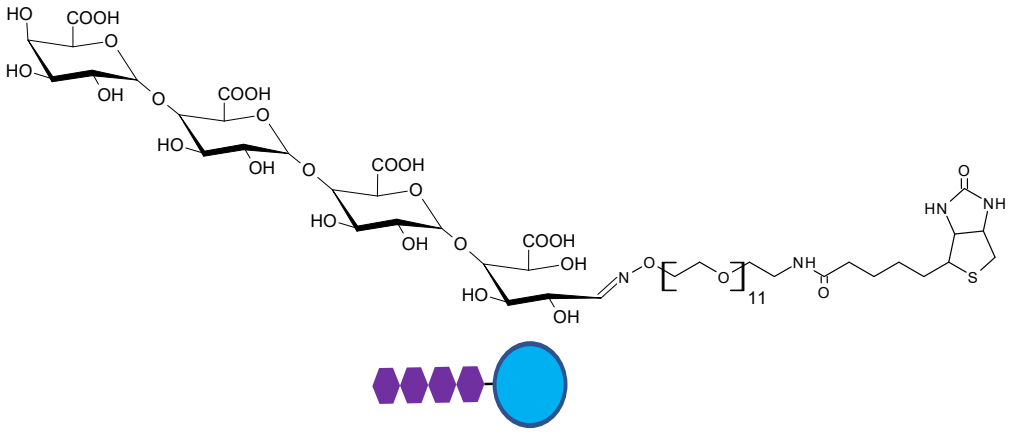

Reducing end biotinylated
tetragalcturonic acid (DP4B)

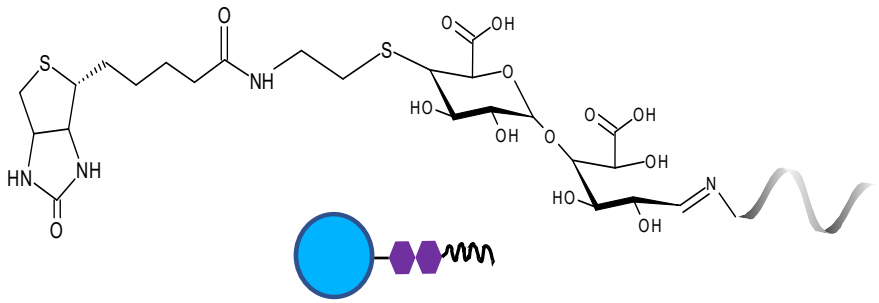

Non - reducing end biotinylated digalacturonic acid
(reducing end protected with 32 bases primer) (BUDPpri)

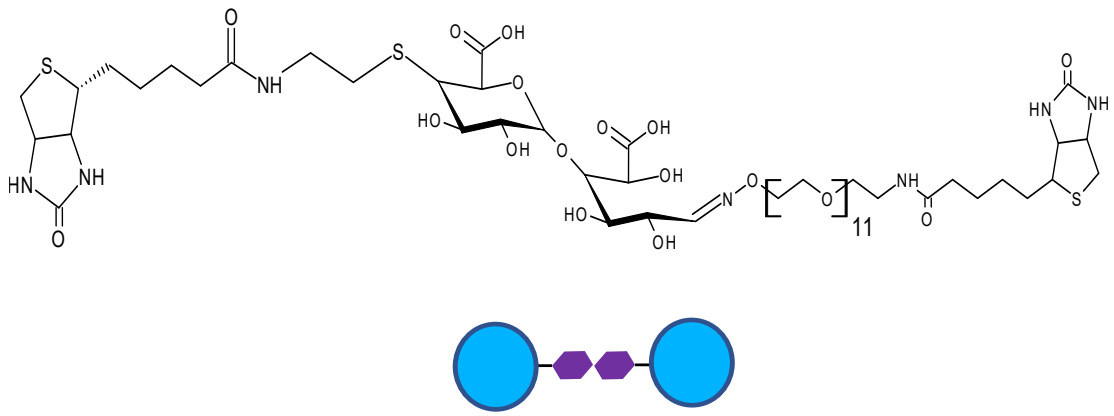

Both ends biotinylated
digalcturonic acid (BUDPB)

FIGURE 5.3: Different oligogalacturonide species modified at reducing end (DP4B), biotinylated non-reducing end protected with primer on the reducing end (BUDP-pri) and doubly functionalised oligogalacturonide (BUDPB).

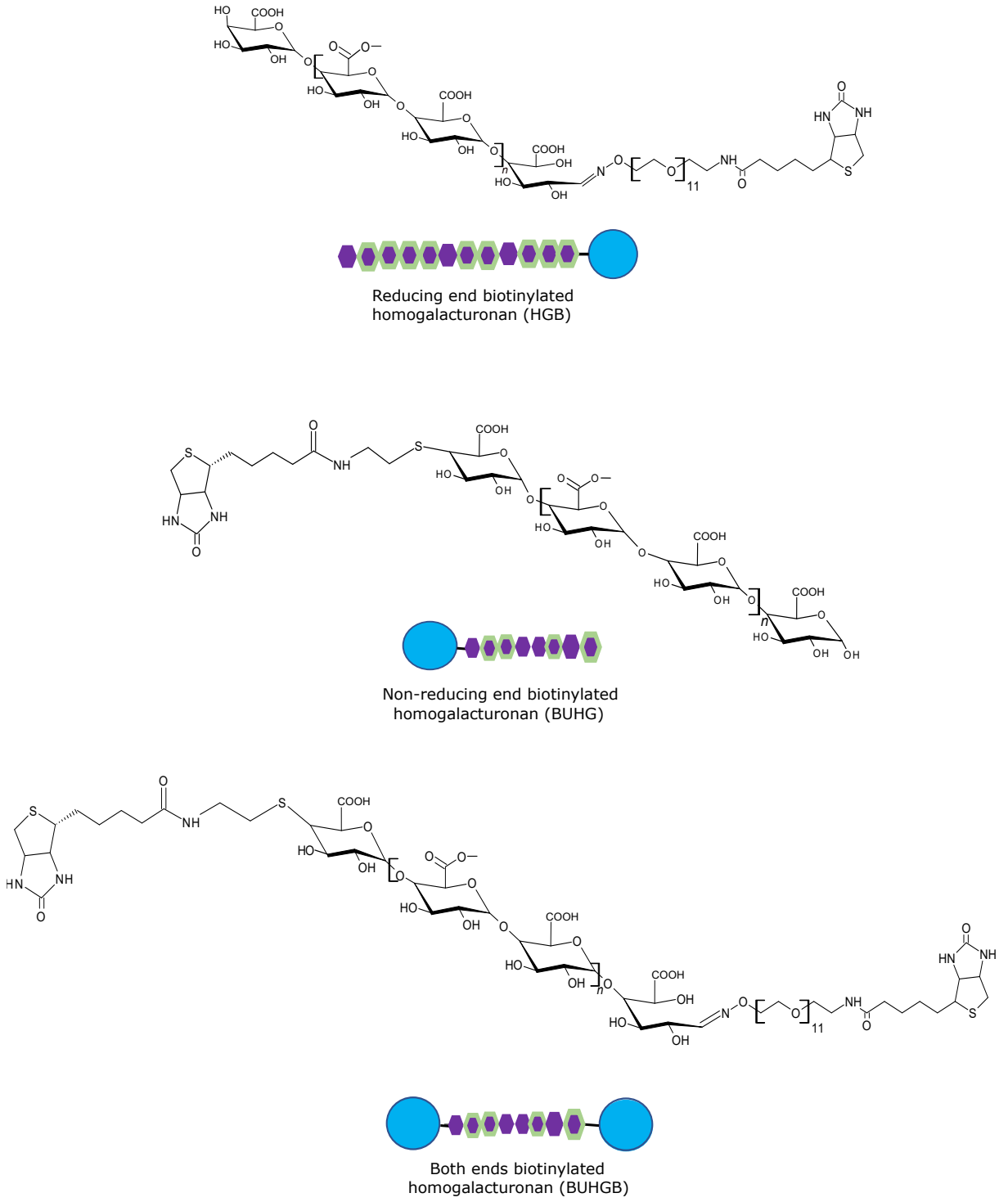

FIGURE 5.4: Different homogalacturonan species modified at reducing end (HGB), biotinylated non-reducing end (BUHG) and doubly functionalised homogalacturonan (BUHGB).

The quantities and reagents used for the SDS PAGE gel are listed in Table 5.1. All these reagents (excluding the ladder) are combined and left overnight at room temperature before loading on a standard 12% separating SDS PAGE gel with a 4% stacking gel. Additionally, the samples are

not boiled here to prevent the tetravalent streptavidin protein from breaking into monomers (Figure 5.5). The gel is run at 200 V with standard 1X Tris-Glycine SDS running buffer, stained with Coomassie blue for ~45 mins and destained with water. From the gel, unboiled samples of streptavidin contain 3 different bands at ~37kDA (faint), ~60kDa (dominant) and a ~100kDa (visible only at higher concentrations) presumably corresponding streptavidin dimer, streptavidin tetramer and dimer of a truncated tetravalent streptavidin protein, respectively [172]. For concentrations of streptavidin used in the following incubation experiments here, tetravalent streptavidin is the most dominant band and, hence, presence of the other two bands are not of significance.

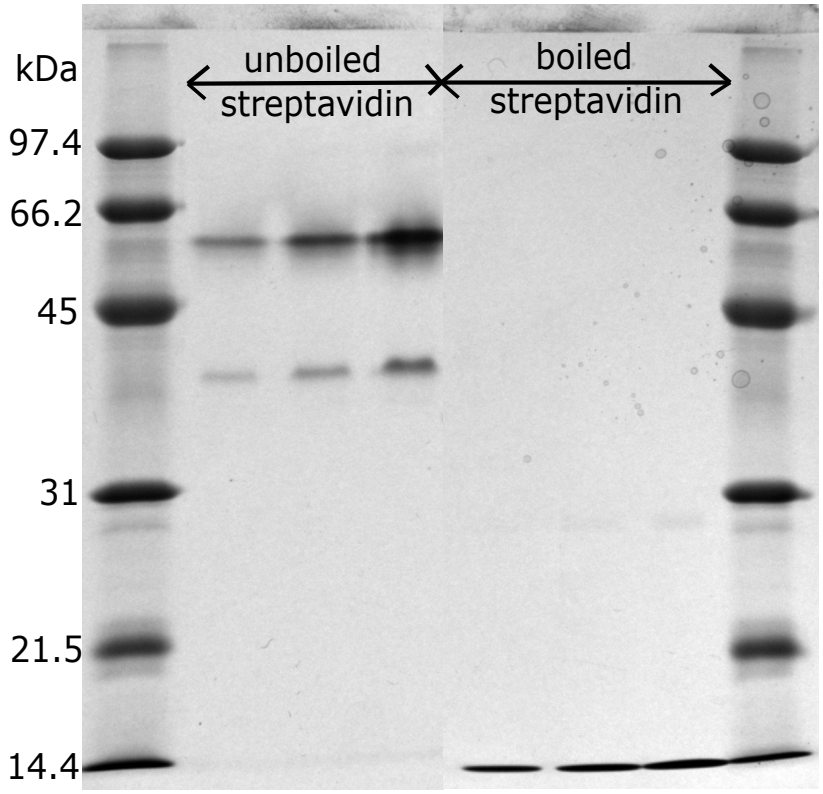

FIGURE 5.5: Streptavidin run at different concentrations in an SDS PAGE gel without boiling (lanes 2, 3 and 4) and after ~5 mins boiling (lanes 5, 6 and 7). Unboiled SDS PAGE gels are used hereforth in this chapter.

TABLE 5.1: List of reagents and quantities used for SDS PAGE gels in Chapter 5.

Reagent	Volume (µL)
Sodium phosphate buffer (pH 6.5, final concentration 0.25 M)	4
Streptavidin (1:10 diluted)	4
Oligosaccharide/polysaccharide	As specified
Ladder (PrecisionPlus Dual Xtra Prestained Protein Standard)	5

5.3 Results and Discussion

5.3.1 Oligogalacturonides

For the following experiments, the three different oligosaccharide species (as shown in Figure 5.3) used are reducing-end functionalised tetragalaturonic acid (DP4B), non-reducing end functionalised digalacturonic acid with primer-protected reducing end (BUDPpri) and digalacturonic acid functionalised at both ends (BUDPB) (all functionalised with biotin). These species were incubated with multivalent streptavidin species and the changes observed are monitored.

Reducing End As an initial experiment, streptavidin was added stepwise (3 µL first, followed by an additional 3 µL) to an excess of tetragalacturonic acid functionalised with biotin at the reducing end (DP4B). As observed in Figure 5.6, three new peaks are formed on addition of streptavidin. According to the ratios, these peaks are presumably streptavidin filled with 2, 3 and 4 units of the functionalised oligosaccharide. Compared to the valency pattern observed from streptavidin-12 bp primer incubation (Figure 3.1A), the peaks here are much closer together, reflecting the smaller difference in electrophoretic mobility of the streptavidin with different numbers of oligosaccharide bound compared to the differences seen for the different primer-incubated streptavidin valencies, owing to the differences in the sizes and molecular charge of the binding moiety. Additionally, there is not much decrease seen in the size of the peaks of the oligosaccharide as the molar quantities of oligosaccharide (~1 mM) are much more than those of streptavidin (~4 µM) added. In order to obtain further support for this interpretation, the experiment was repeated but with step-wise addition of the functionalised oligosaccharide to an excess of streptavidin instead.

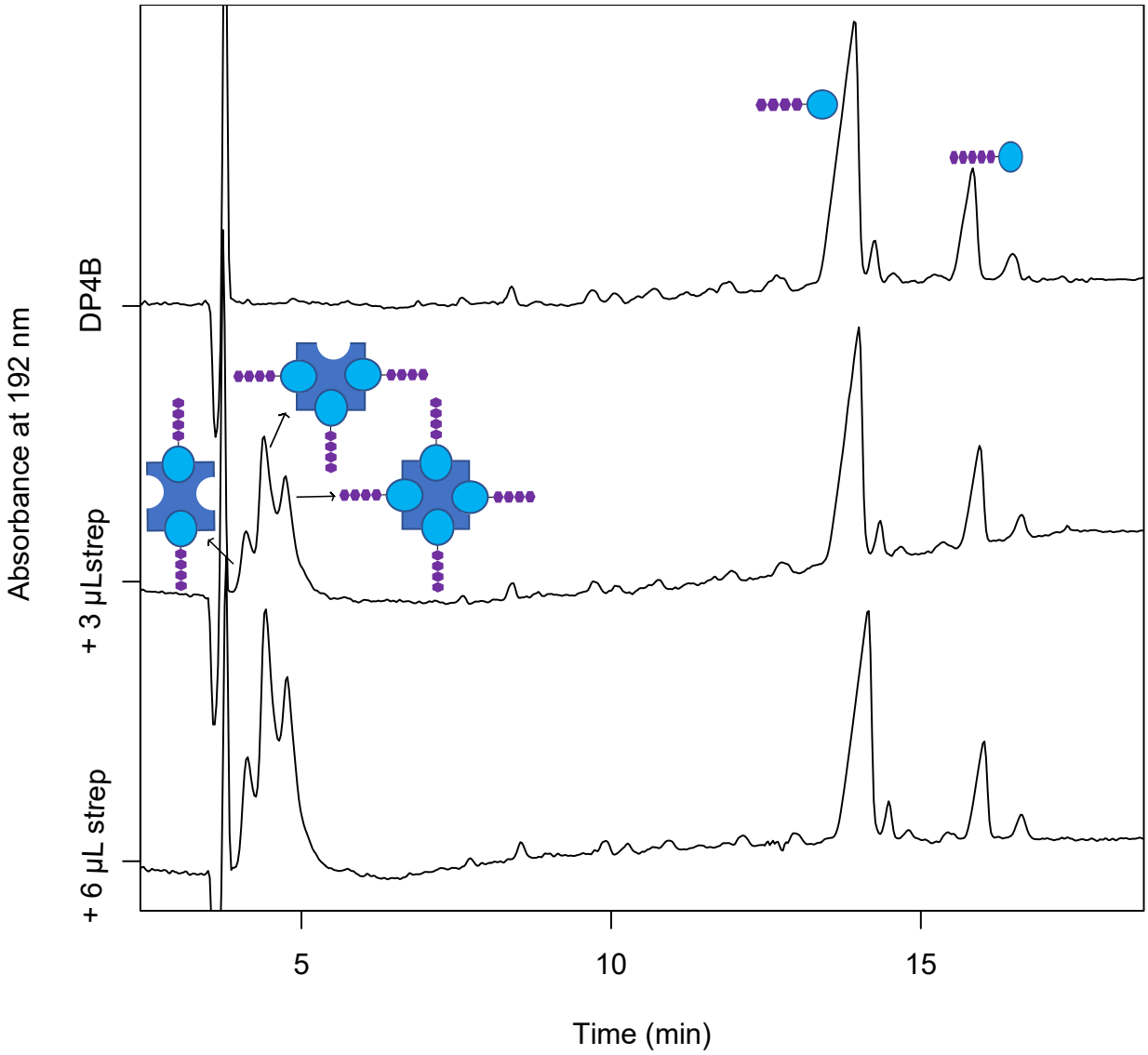

FIGURE 5.6: Electrophoregram of excess reducing end biotinylated tetragalacturonic acid (DP4B) (contaminated with pentagalacturonic acid) incubated with tetravalent streptavidin (strep). Three new peaks, presumably 2-filled, 3-filled and 4-filled streptavidin are observed. (Refer to Figure 5.2 for schematics).

In the next experiment, changes were monitored from an initial 4 µM streptavidin following a stepwise addition of the functionalised oligosaccharide (1:100 dilution). From the previous electrophoregram shown in Figure 5.6, it was assumed that the initial peaks were the different valencies of streptavidin. In order to investigate this further, the CE was run at decreased voltage and increased molarity of background electrolyte so that the EOF was at ~10 mins (or later). This allowed for the peaks to be more clearly baseline resolved. (A shift in the position of the EOF can be seen in the final electrophoregram, most likely owing to the changes in the concentration of the BGE and the sample after 3 days, and the sticking of molecules to the capillary walls, resulting in a changed zeta potential).

In Figure 5.7, changes are seen after 3 µL of functionalised oligosaccharide is added to streptavidin. Further changes are not observed after an hour or overnight, which indicates that the reaction occurs within 5 minutes (similar to what is observed during a streptavidin-DNA incubation). On increasing the concentration of the oligosaccharide, the initial streptavidin peak decreases in size and there is a gradual rise in three other peaks adjacent to each other. The pattern of the the peaks is similar to what is observed during a streptavidin-primer incubation (Figure 3.1A). On the other hand, it could also be that streptavidin with just one valency filled with the oligosaccharide has a similar electrophoretic mobility compared to streptavidin itself, and 2, 3 and 4 filled streptavidin are observed, as assumed in Figure 5.6.

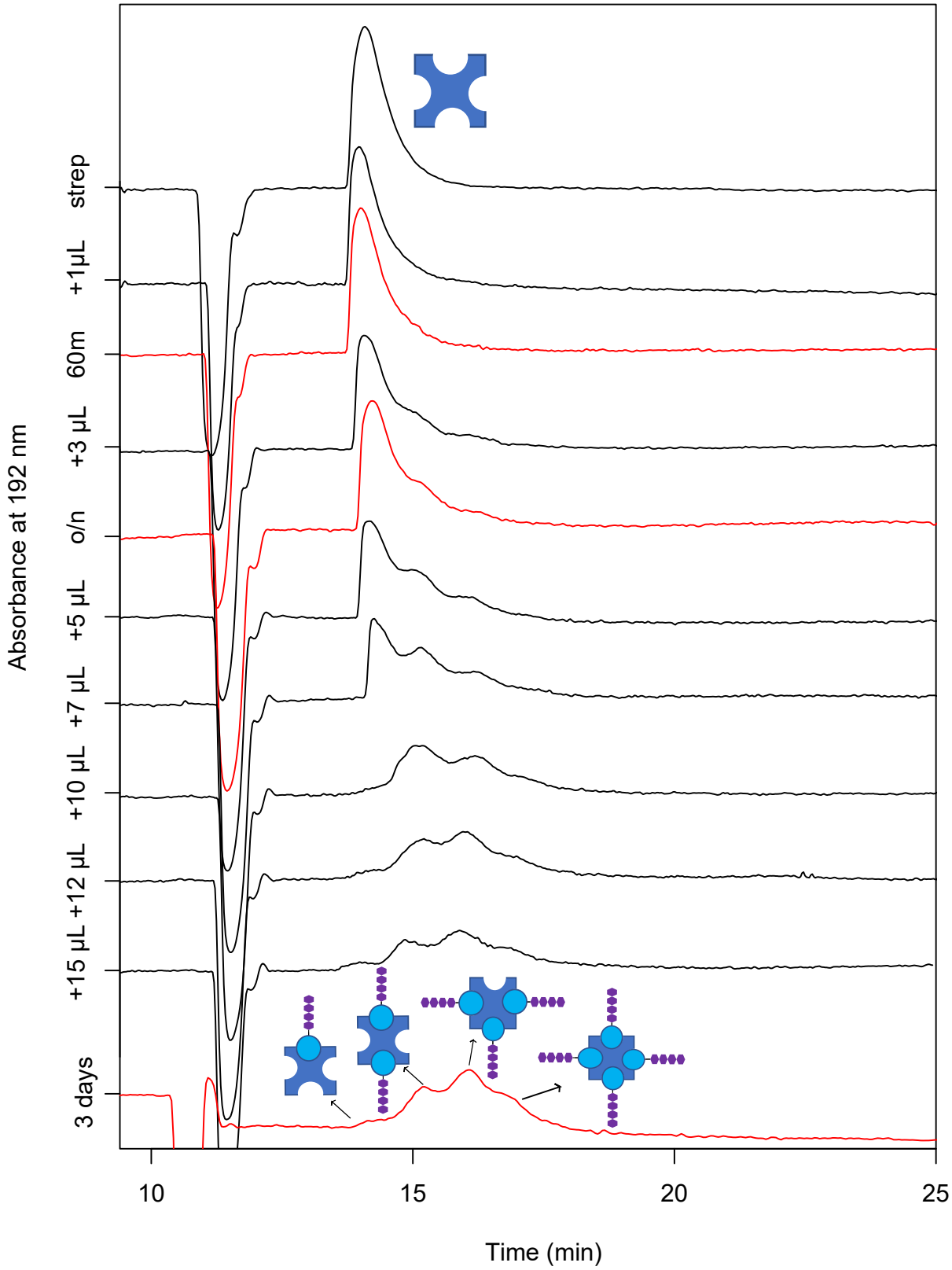

FIGURE 5.7: Electrophoregrams showing stepwise addition of reducing end functionalised tetragalacturonic acid, DP4B (1:100 dilution) to excess tetravalent streptavidin (strep). Initial streptavidin peak decreases in size and multi-valent streptavidin species can be observed. (Refer to Figure 5.2 for schematics).

The streptavidin-DP4 (negative control) and streptavidin-DP4B samples were also run in a gel as shown in Figure 5.8A. Complementary to Figure 5.7, multiple bands are observed when streptavidin is incubated with biotinylated tetragalacturonic acid. This pattern has been observed previously when streptavidin was incubated with biotinylated DNA oligomers as shown in Figure 5.8B. Observations of bands above and below the initial streptavidin band indicate that size is not the only factor affecting how the species runs through the gel, but also the charge and the overall hydrodynamic friction of the different species. *In either case, both the CE and PAGE gel observations, it can be confirmed that functionalisation of the reducing end of the oligosaccharide and the binding of this biotinylated species to streptavidin have been successful.*

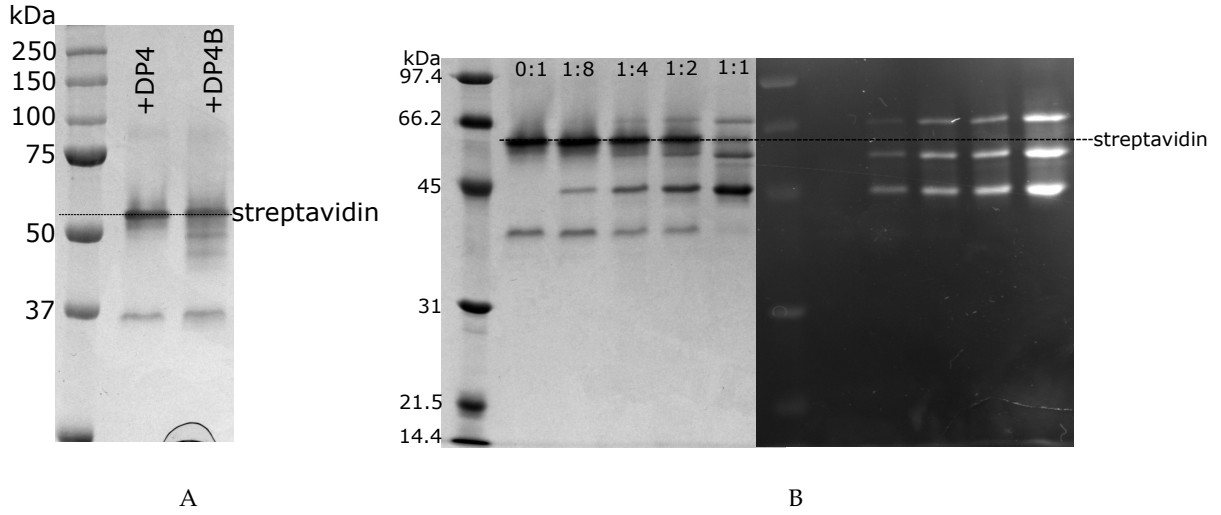

FIGURE 5.8: (A) SDS PAGE gel showing runs with streptavidin-DP4 (negative control) and streptavidin-DP4AB. (B) SDS PAGE gels at various ratios of 28 base biotinylated primer:streptavidin incubation, stained with Coomassie (left) or Ethidium Bromide (right).

For the next experiment, streptavidin was first incubated with 28 bases single-stranded DNA oligomers to first generate partially filled streptavidin species as shown in Figure 5.9 (top). The sample was then, divided in half, with non-functionalised tetragalacturonic acid (negative control - middle) added to one half, and reducing end biotinylated tetragalacturonic acid (bottom) to the other. As seen from the electrophoregrams above, no significant changes were seen for the negative control. However, when a biotin-terminated tetragalacturonic acid (DP4B) was added, changes are observed particularly in the first two peaks. For the previously tetravalent streptavidin peak, the re-creation of the split peak is observed similar to that seen in Figure 5.6, indicating multiple valencies of oligosaccharide substrate attached species. As expected, a number of additional mixed species can be formed as shown in Figure 5.9. The electrophoretic mobility of these

change by only a small amount due to the small size and neutrality of the attached functionalised oligosaccharide. *From this and the previous experiment, we can conclude that, we can easily bind biotin-functionalised tetragalacturonic acid to streptavidin, even when some of the sites are initially filled with other species*. This would be facilitated further with the plugged streptavidin (tails cleaved off).

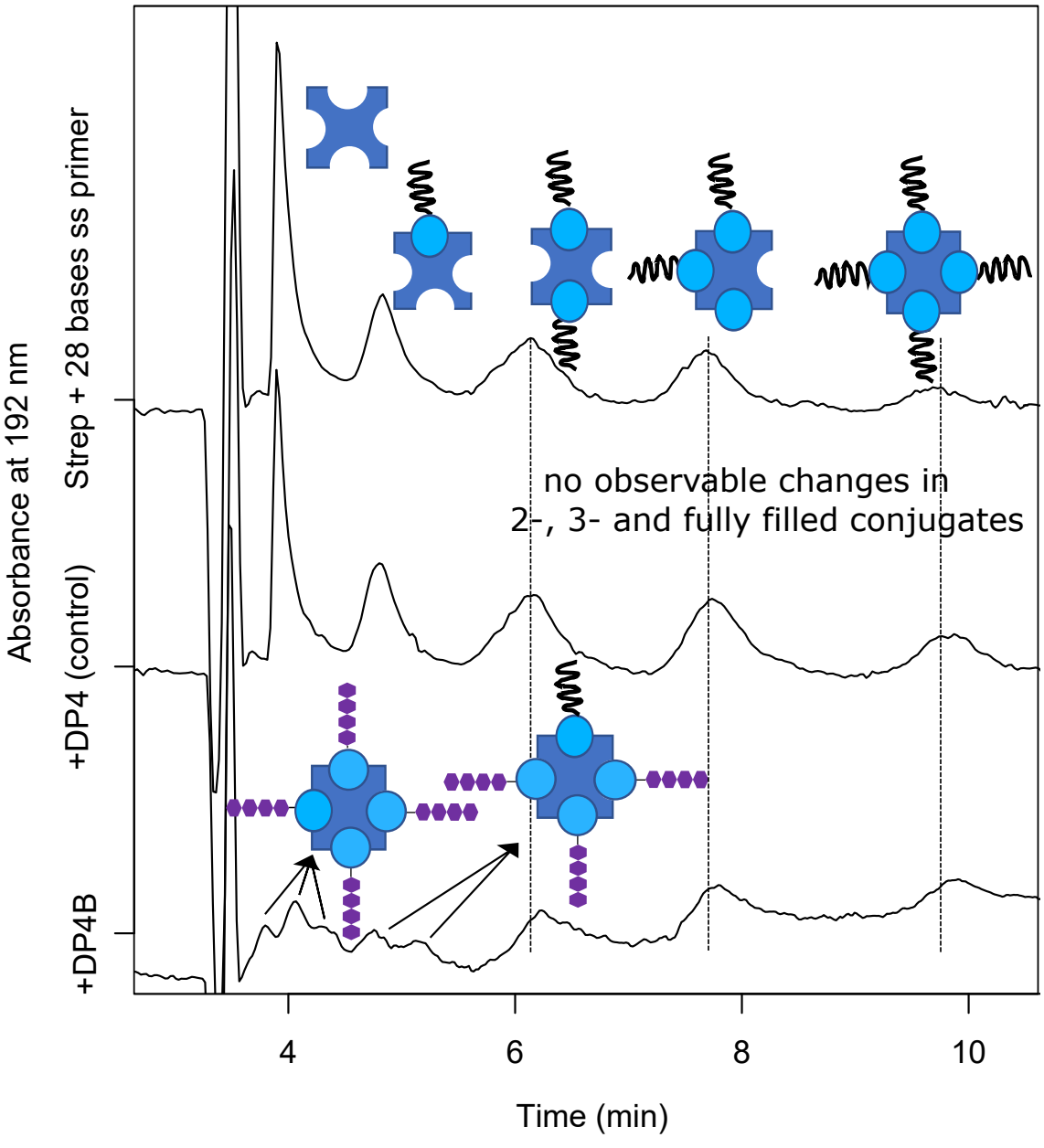

FIGURE 5.9: Electrophoregrams showing a mixture of multivalent streptavidin-primer species incubated with unfunctionalised and functionalised tetragalacturonic acid (DP4 and DP4B respectively). Gradation circles indicate multiple valency of the functionalised oligosaccharide. (Refer to Figure 5.2 for schematics).

Non-reducing end In order to observe the differences of having biotin at the non-reducing end of the oligosaccharide only (digalacturonic acid, here, as confirmed by NMR in Chapter 4), an alternative step was included in the synthesis after the lyase treatment to protect the reducing end. In Chapter 4, the reducing end was protected by conjugation to aminooxy-biotin before the non-reducing chemistry was carried out but here, so as to focus on the biotin at the non-reducing end only, the reducing end was protected with a 32-base DNA oligomer.

The aminooxy primer allows to see how the biotinylated non-reducing end alone interacts with the tetravalent protein. Otherwise, at the non-reducing end, biotinylation was performed as described in Materials and Methods of Chapter 4 (Section 4.2). However, it should be noted that although the presence of the primer is expected to provide an extra charge contribution that can influence how the final incubated species elutes in the CE, it is possible that after a certain size limit, the resulting species would have a similar size-to-charge ratio and elute at similar positions.

For this set of CE experiments, the EOF was adjusted (~6 min) where a better separation was observed during the reducing end test. As seen from Figure 5.10, on incubation, it does appear that the peak has shifted towards the right (more negative) as expected if the biotin at the non-reducing end of the construct has been bound. The incubated sample was co-injected with streptavidin (1:1) to check whether unreacted streptavidin can be differentiated from the peak resulting after incubation. If both the samples were unreacted streptavidin, then an increase in peak size would be observed. From Figure 5.10, rather than observing an obvious increase from the original peak size, an apparent "shoulder" of the oligosaccharide-bound streptavidin species is more prominently seen. This suggests that the peak resulting from the incubation is indeed streptavdin that has been bound to a negatively charged biotinylated species. Interestingly, the presence of 32 bases at the reducing end did not give as much of a change to the electrophoretic mobility as expected. Hence, it is more likely that all valencies with attached DNA, i.e a DNA 32mer and its multiples (64mer, 96mer and 128mer DNA bases in total) are eluting out in a similar time frame as their long average charge density is the same. Note that the unsaturated oligosaccharide molecule is only two residues long, as confirmed in Chapter 4, giving only subtle peak shifts.

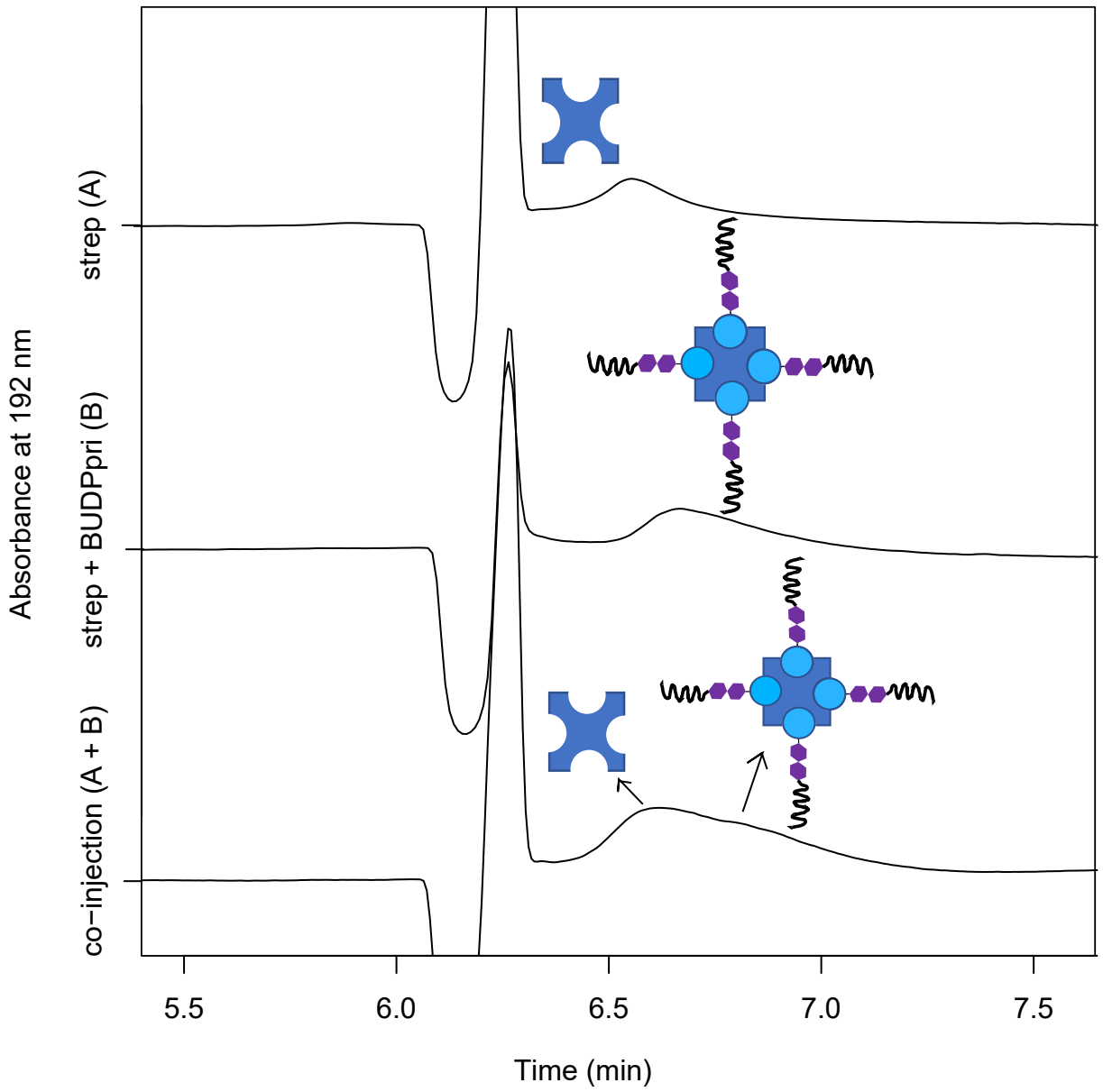

FIGURE 5.10: Electrophoregrams showing incubation of tetravalent streptavidin with biotinylated unsaturated digalacturonic acid with primer at the reducing end (BUDPpri). Resultant species was then co-injected with tetravalent streptavidin. Gradation circles indicate multiple valency of the functionalised oligosaccharide. (Refer to Figure 5.2 for schematics).

Similar to the reducing end, the non-reducing end biotinylated oligosaccharide was incubated with streptavidin and run in a SDS PAGE gel (Figure 5.11). A band pattern was indeed observed, moving above the original streptavidin band here, as in the gel modality the cause of mobility is quite different from the CE. For these gels, the migration of the species depends on charge and how easily it can migrate through the gel. Hence, it is likely that the substantiallly increased construct length from the aminooxy primer used to protect the reducing end has caused the streptavidin

valencies to move slower than tetravalent streptavidin. In order to confirm this, the sample was treated with DNAse (an enzyme used to degrade DNA). From Figure 5.11, a shift in pattern is observed after DNAse treatment. Firstly, the initial streptavidin band has completely disappeared and has seemingly shifted towards the higher end of the streptavidin-BUDPpri band pattern. This suggests that losing the DNA bases has most likely removed the steric hindrance that the 32 base primer posed, and facilitated filling of the valencies resulting in a more prominent uppermost band, i.e streptavidin fully filled with non-reducing end biotinylated disaccharide with a few primer bases on the non-reducing end. The experiment was repeated once more in lanes 5 and 6, and the same changes are observed. *This confirms that the oligosaccharide biotinylated at the non-reducing end can be successfully attached to streptavidin.*

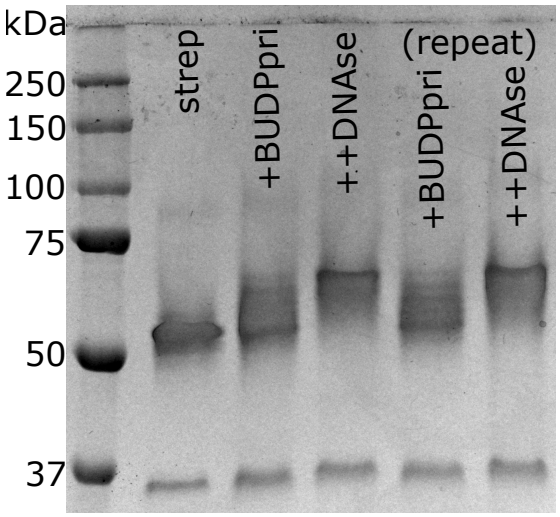

FIGURE 5.11: SDS PAGE gel run with streptavidin (strep) alone, streptavidin incubated non-reducing end biotinylated oligosaccharide, functionalised with primer on the reducing end (BUDPpri), and the resulting species treated with DNAse. DNAse treatment has facilitated formation of fully-filled streptavidin. (Refer to Figure 5.2 for schematics).

Both ends The oligosaccharide was functionalised as described in Materials and Methods in Chapter 4 (Section 4.2).

For this experiment, streptavidin was incubated with doubly functionalised oligosaccharide (BUDPB) and solely reducing end functionalised unsaturated oligosaccharide (UDPB), as a control. As observed from Figure 5.12, the peak elutes earlier for streptavidin incubated with doubly functionalised saccharide compared to reducing end functionalised unsaturated oligosaccharide. This peak shift towards the neutral is expected due to the additional biotin moieties in

the doubly functionalised species. For doubly functionalised saccharide, there is a possibility for cross-linkings for which changes may not be observed if the electrophoretic mobility remains unchanged. It is to be noted that preferential binding between reducing end or non-reducing end biotinylated ends would not be observed due to the spacer molecules from the biotin moiety to the sugar chain. From Figure 5.12, it seems like the streptavidin has completely reacted and shifted to a more broader peak. The control looks similar to what was observed from the reducing end-tetravalent streptavidin incubation as seen in Figure 5.7.

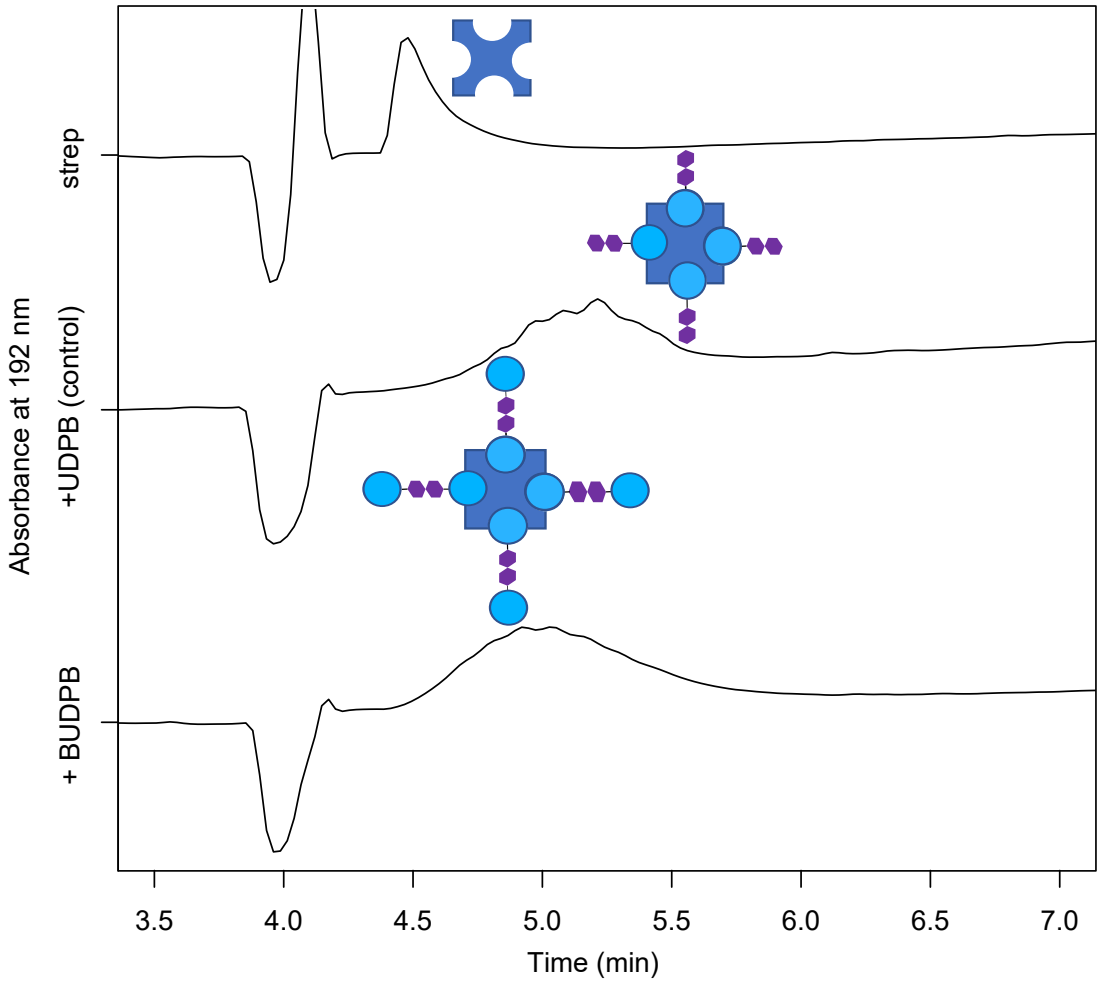

FIGURE 5.12: Electrophoregrams monitoring the changes as tetravalent streptavidin (strep) is incubated with reducing end functionalised unsaturated oligosaccharide (UDPB) and doubly functionalised disaccharide (BUDPB), separately. Gradation circles indicate multiple valency of the doubly functionalised oligosaccharide. (Refer to Figure 5.2 for schematics).

Streptavidin was incubated with increasing concentrations of doubly functionalised oligosaccharide: 2 µL and 4 µL of 1:100 dilution, followed by 1 µL, 2 µL and 4 µL of 1:10 dilution of stock

sample, and run on a SDS gel (Figure 5.13). A clear downward smearing pattern of the streptavidin band is observed in the final lane, with the highest concentration of the oligosaccharide sample. This confirms that the oligosaccharide has bound to the streptavidin. Contrary to the band patterns obtained in Figures 5.6 and 5.9 for reducing end and non-reducing end only functionalised samples respectively, slight smearing around the initial streptavidin band is observed. This suggests that the oligosaccharide is of a very small size (disaccharide). Furthermore, considering that bands at higher molecular weight, such as at ~120 kDa for an oligosaccharide attached to two streptavidin, are not observed, this also indicates that the oligosaccharide is very small, as a disaccharide. Considering the depth of the streptavidin pockets, it will only be possible to have streptavidin attached to each end of the oligosaccharide if the oligosaccharide is a tetramer or longer. As the oligosaccharide is a dimer, this observation shows that even on functionalisation with biotin at both ends, the final species is not long enough to bind to two molecules of streptavidin, at each of their ends. *This confirms that small oligosaccharide species have been created with both ends displaying biotin, and that these species can be bound to streptavidin linkers.*

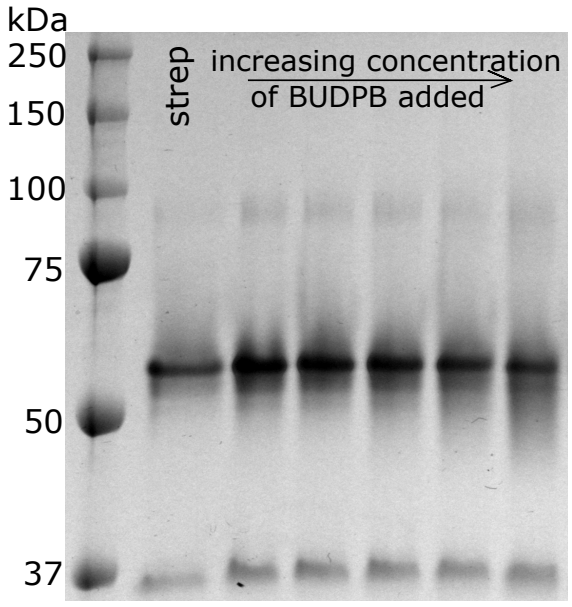

FIGURE 5.13: Streptavidin and streptavidin incubated with an increasing concentration of doubly functionalised oligosaccharide (BUDPB) run on a SDS PAGE gel. Smearing is most evident at the highest saccharide concentration added (Lane 7). Furthermore, although the gel does show loading issues, the streptavidin band shows a decrease in intensity.

5.3.2 Homogalacturonan (HG)

The focus is now shifted to investigating the binding of HG biotinylated at the reducing end only, non-reducing end only, and both ends, in the same way as carried out for the oligosaccharide. A major difference observed here, compared to the experiments with the oligosaccharides, is the character of the assemblies and thus the shape of the final peaks. In the previous CE experiments with oligosaccharide binding, the peaks of the final conjugates resembled the initial streptavidin peak shape. In this case, with a considerably longer saccharide section (on average ~50 residues to a maximum ~100 residues, molecular weight, MW~10kDa) the peaks of the composite species are much broader and resemble the HG peak more. This is not unexpected because in this case the bigger species involved is the HG and so changes in the mobility would primarily be observed as perturbations on the HG migration behaviour, whereas in the previous cases, streptavidin was the bigger moiety with its mobility perturbed by the bound oligomers. Additionally, the product peaks are also broader compared to the peaks observed from the oligosaccharide experiments due to the distribution of the degrees of methylesterification of the HG.

For the following experiments, the three different homogalacturonan species (as shown in Figure 5.4) used are reducing-end functionalised homogalacturonan (HGB), non-reducing end functionalised homogalacturonan (BUHG) and homogalacturonan functionalised at both ends (BUHGB) (all functionalised with biotin). These species were incubated with multivalent streptavidin species and the changes obseved are monitored.

Reducing End In this experiment, streptavidin was added to 1% HG that has been functionalised with biotin at the reducing end (as described in Chapter 4). For the negative control, streptavidin was incubated with unfunctionalised 1% HG (Figure 5.14A). As can be seen from Figure 5.14A, the size of the streptavidin and HG peaks in the negative control are unchanged for 3 days, while there is a difference in the position where the streptavidin elutes. However, this has been observed in almost every control where the streptavidin has been incubated with another species and could either be due to the sensitivity of the migration time to the change in background electrolyte concentration after 3 days due to evaporation, or the presence of HG in the mixture affects the overall ionic strength of the final species. In contrast, following the incubation of streptavidin with biotin-functionalised polysaccharide, the initial streptavidin peak can be seen to have decreased in size and there is now a new peak with a shape similar to HG that elutes between unreacted streptavidin and functionalised HG. This is evidence that HG has been successfully

functionalised with biotin and can be bound to streptavidin. The remaining presence of a small peak at the position of streptavidin is most likely due to leftover aminooxy-biotin species that did not get incorporated in the sugar conjugation, and was not removed during dialysis. As this molecule is small, it easily fills all the streptavidin sites, blocking the valencies without changing the electrophoretic mobility and, hence, elutes at the position as tetravalent streptavidin.

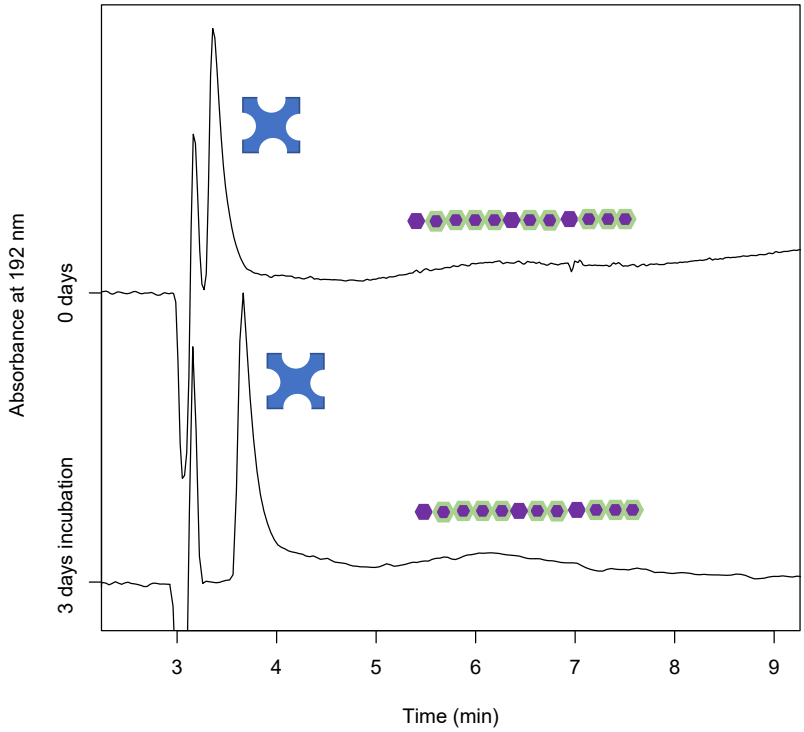

A

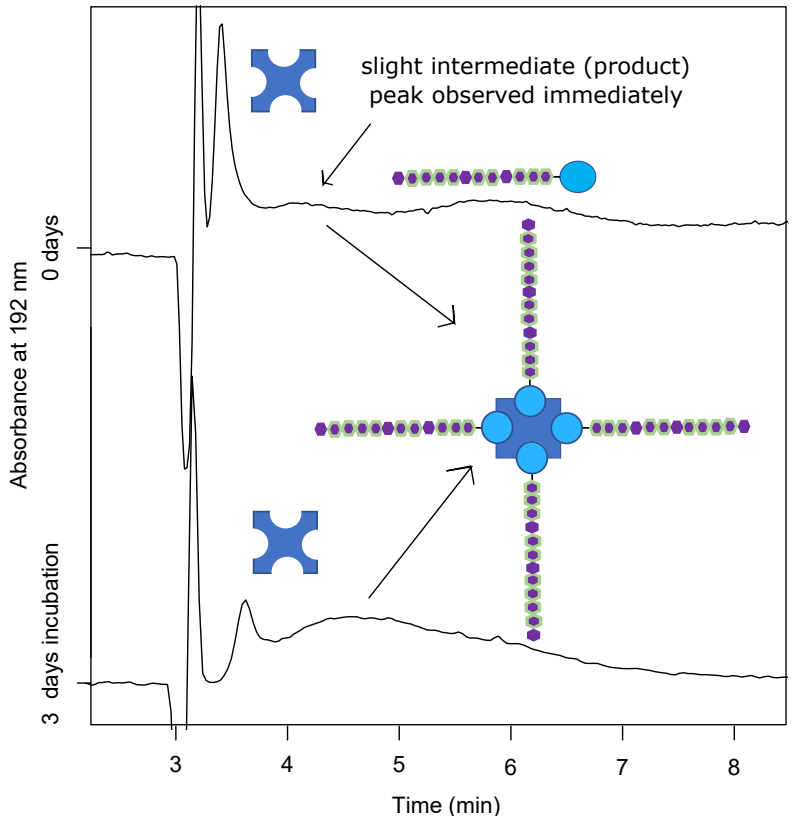

B

FIGURE 5.14: (A) Electrophoregrams of streptavidin (strep) incubated with unfunctionalised homogalacturonan (HG), initially and after a 3-day incubation (negative control). (B) Electrophoregrams of reducing end biotinylated homogalacturonan (HGB), initially and after a 3-day incubation. An intermediate peak at ~5 mins is observed. (Refer to Figure 5.2 for schematics).

An additional experiment performed was to treat the sample after incubation with 0.1% orange pectin methyl esterase (PME) as seen in Figure 5.15. As expected, PME removal of the methyl groups of HG increases the negative charge density of HG and results in the lengthening of the polysaccharide migration time. Furthermore, as the PME action is processive, this results in a much wider distribution of the degrees of methylesterification to be generated, causing the peak to broaden and eventually disappear into the baseline [173]. As a side note, the disappearance of the peak due to potential adsorption or noncovalent binding between homogalacturonan and streptavidin is eliminated as a possibility from the negative control as shown in Figure 5.14A and binding is only possible between the polysaccharide and streptavidin via biotin moieties. Furthermore, in the neutral pH conditions that the CE is run in, the polysaccharides are negatively charged preventing aggregation. *This confirms that the product peak observed upon incubation indeed contains HG conjugated to streptavidin.*

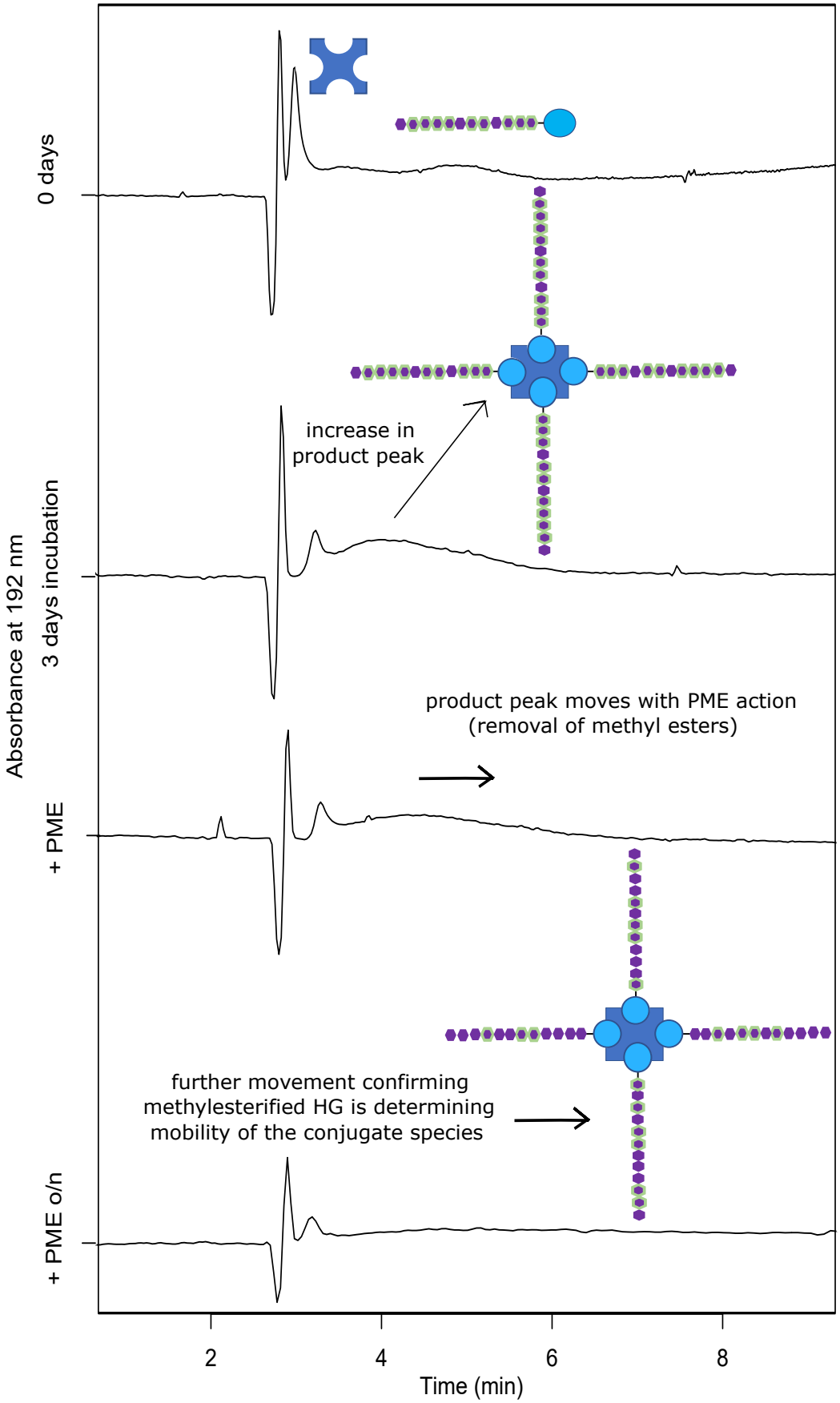

FIGURE 5.15: Electrophoregrams showing immediate and overnight pectin methyl esterase (PME) action on streptavidin-HGB species. The arrows indicate the direction of which the peak shifts as the products gets demethylesterified. (Refer to Figure 5.2 for schematics).

Non-reducing end In contrast to the reducing end experiments, the non-reducing end functionalised HG species are more heterogeneous, i.e varied degrees of methylesterification (DM) and differing (smaller) degrees of polymerisation (DP), due to the initial cleavage step that was required to introduce the double bond used for functionalisation. These factors are expected to somewhat affect the electrophoretic mobility of the product peaks.

Similar to incubation with the oligosaccharide shown in Figure 5.10, Figure 5.16 shows a slight shift compared to the original streptavidin peak towards the more negative side (right) after incubation. On co-injection, a shoulder aligning with initial tetravalent streptavidin was seen, confirming that a separate species has been generated, assigned to streptavidin bound to biotinylated species.

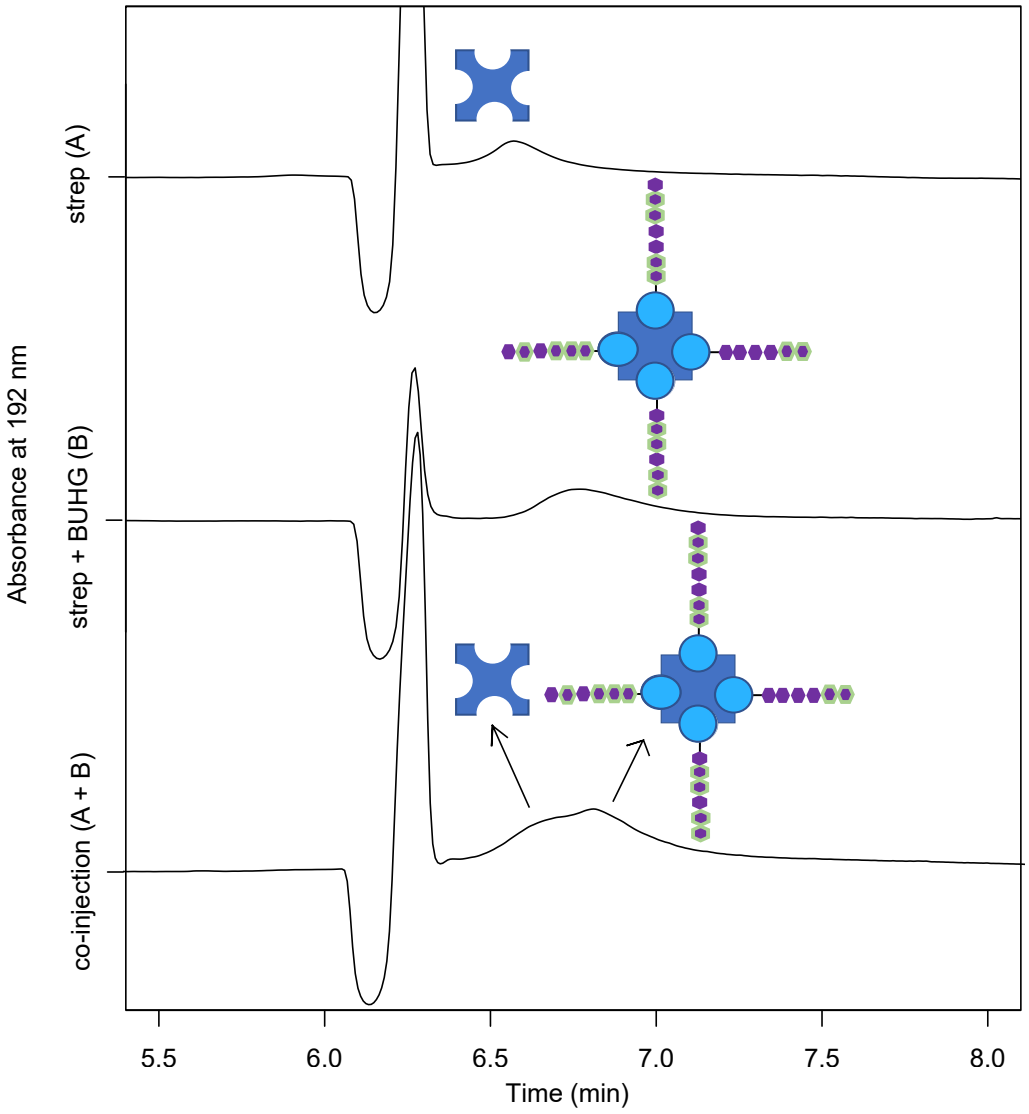

FIGURE 5.16: Electrophoregram of tetravalent streptavidin (strep) incubated with biotinylated of unsaturated homogalacturonan (BUHG). Resultant species is also coinjected with tetravalent streptavidin. (Refer to Figure 5.2 for schematics).

In the next experiment, the same multivalent streptavidin-DNA conjugates generated from the streptavidin-primer mixture as used in Figure 5.12, was incubated with non-reducing end biotinylated polysaccharide. As expected, Figure 5.17 (middle) shows that a mobility shift and a change in concentration is observed, mainly in the region of the first two peaks (tetravalent and trivalent streptavidin). This is because the HG species with biotin-functionalised non-reducing ends can bind relatively easily into the emptiest streptavidin species. Excess biotinylated primer was then added to this mixture. Interestingly, the pattern obtained in Figure 5.17 (bottom) suggests that there are still available valencies for the primer to bind to, yielding a typical streptavidin-primer pattern. However, this pattern does not line up with the original streptavidin-primer pattern nor with the streptavidin-primer-oligo pattern. It seems more like that the initial tetravalent and trivalent peaks have shifted considerably towards the right. The observation indicates that the primer has attached to streptavidin-primer-HG species where HG has likely not filled all the available valencies, but just one or two (i.e the filling of streptavidin pockets are dependant on both size and charge). This is also consistent with the steric issues that have been observed previously in Chapter 3, with longer DNA strands. Compared to the oligosaccharides, longer pieces of HG are bound slowly to the streptavidin over time, and can lead to the steric blocking of the other available streptavidin sites, with an efficiency depending on the size of the prospective binding partner. Hence, it is crucial to have the DNA tails cleaved off when making the final construct, to facilitate binding of biotinylated HG to divalent streptavidin. *This confirms that the non-reducing end of the HG moieties has been biotinylated and that these species can bind to streptavidin linkers.*

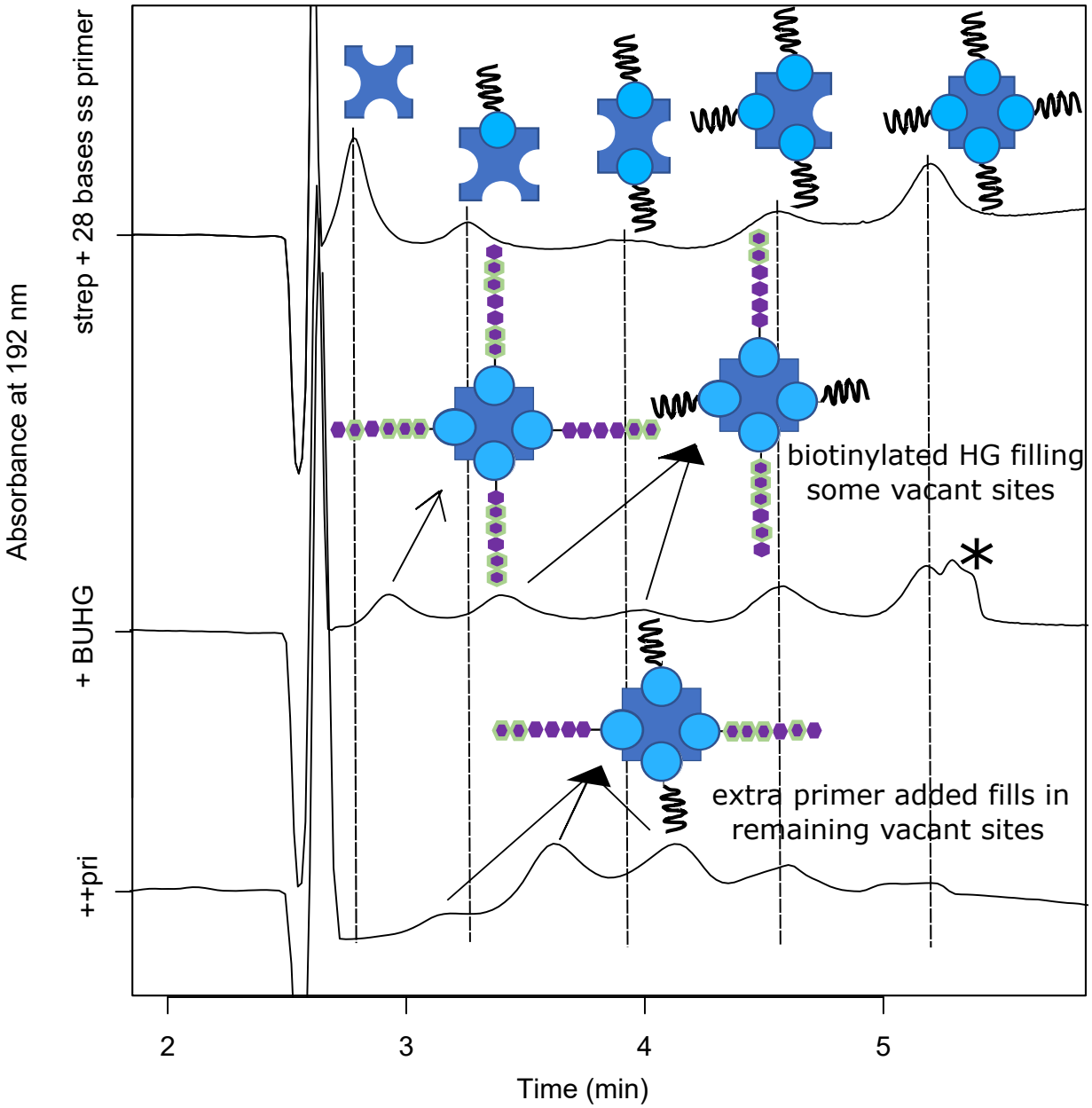

FIGURE 5.17: Electrophoregrams showing a strep-primer incubation mixture, before and after incubation with biotinylated unsaturated homogalacturonan (BUHG). Extra primer is added to the resulting species. * indicates presence of impurity in the BUHG sample. Gradation circles indicate a mixture of multiple valency of the functionalised oligosaccharide and biotinylated primer. (Refer to Figure 5.2 for schematics).

Both ends For the following incubations, 1% HG, reducing end functionalised unsaturated HG (BUHG) and doubly functionalised HG (BUHGB) were used. To remove the leftover reactants and purify the samples as much as possible, they were all dialysed overnight, using a 3500 MWCO membrane against Milli-Q water, before incubation. Since CE is primarily governed by the pH and ionic strength of the background electrolyte buffer, dialysis of the analyte is not expected to

have a significant affect the mobility of the different species.

Figure 5.18 shows the CE runs for tetravalent streptavidin (strep), doubly biotinylated HG (BUHGB), tetravalent streptavidin incubated with 1% HG, and doubly biotinylated HG incubated in a 1:1 (v/v) ratio. It can be seen that the peak for the doubly functionalised HG has slightly shifted towards neutral on incubation with streptavidin, and is also intermediate of both starting materials (tetravalent streptavidin and doubly functionalised HG). The final peak also has a higher absorbance than the original product peak, owing to the strong absorbance of streptavidin at 192 nm.

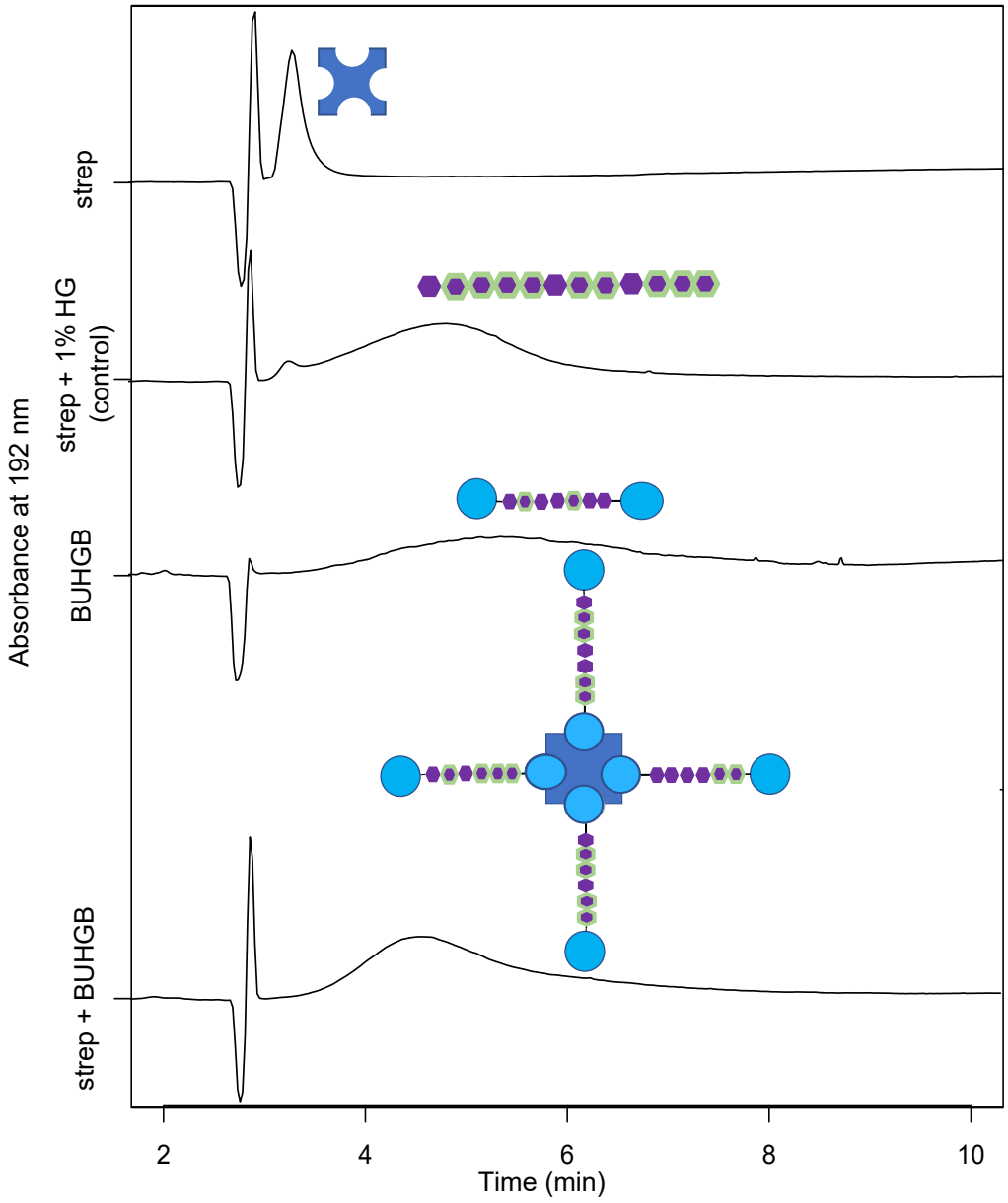

FIGURE 5.18: Electrophoregram showing tetravalent streptavidin (strep) incubated with unfunctionalised (1% HG), and doubly biotinylated HG (BUHGB). An intermediate peak is observed closer to ~4 mins. (Refer to Figure 5.2 for schematics).

A single SDS PAGE gel (Figure 5.19) was used to monitor changes in streptavidin on incubation with unfunctionalised HG, reducing end biotinylated HG (HGB) and doubly biotinylated HG (BUHGB) at $1/100^{th}$ and $1/10^{th}$ dilution. Different concentrations of the saccharide were attempted because from previous streptavidin-primer gels, there was an optimum ratio of reactants that would result in the highest yield (prominent band). This gel is stained with Coomassie, so HG only can be visualized where it is linked to streptavidin. From an earlier work, using stains-all has shown that HG runs as a long smear, due to the diversity of its length and charge consistent with streptavidin band is observed for reducing end functionalised HG and doubly functionalised HG. A smearing pattern is indicative of streptavidin being attached to HG with various degrees of polymerisation and methylesterification.The higher smear pattern for the doubly functionalised HG compared to reducing end only functionalised HG is indicative that the *functionalisation has been successful at both ends of the polysaccharide. This also confirms that doubly functionalised HG can be linked to tetravalent streptavidin.*

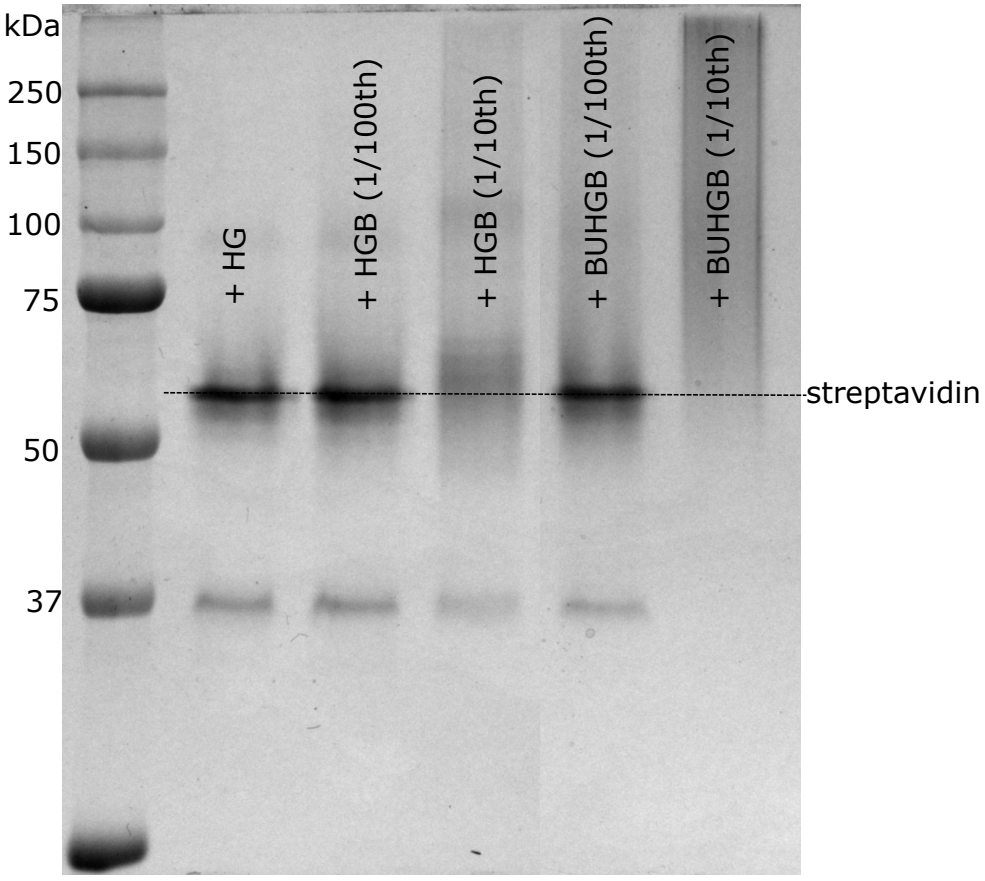

FIGURE 5.19: Streptavidin incubated with unfunctionalised HG, reducing end biotinylated HG (HGB) and doubly biotinylated HG (BUHGB) at $1/100^{th}$ and $1/10^{th}$ dilution, and run in a SDS PAGE gel.

5.4 Strategy for Stretching with Optical Tweezers (OT)

Once it was confirmed that the doubly functionalised polysaccharide could be attached to streptavidin-primer species, the next step was to try and bind the doubly functionalised polysaccharide in between the divalent streptavidin linkers with a 5 kB DNA handle attached onto one valency.

A suggested protocol for the final assembly is shown in Figure 5.20 and outlined as follows:

- Generation of 5 kB DNA by PCR with biotin and digoxigenin ends, and with biotin and DBCO ends.
- Incubation of divalent streptavidin with a limiting quantity of the different 5 kB DNA strands, separately, to avoid presence of leftover DNA and limit the formation of unwanted DNA strings.
- Removal of any excess streptavidin with DNA purification spin column. **The resulting sample should only contain 5 kB DNA strings bound to divalent streptavidin, terminated with either a digoxigenin or DBCO moiety.**
- Run the samples on a gel and/or CE to check for purity.
- Sequentially incubate limiting quantities of doubly functionalised homogalacturonan, with both streptavidin bound 5 kB DNA strings to minimize formation of species with identical ends, i.e both digoxigenin or both DBCO ends.
- Run the incubated sample on a gel. If ~10 kB bands are observed, stretching can be attempted with anti-digoxigenin and azide functionalised beads (which bind to digoxigenin and DBCO ends respectively) in an optical tweezers set-up.

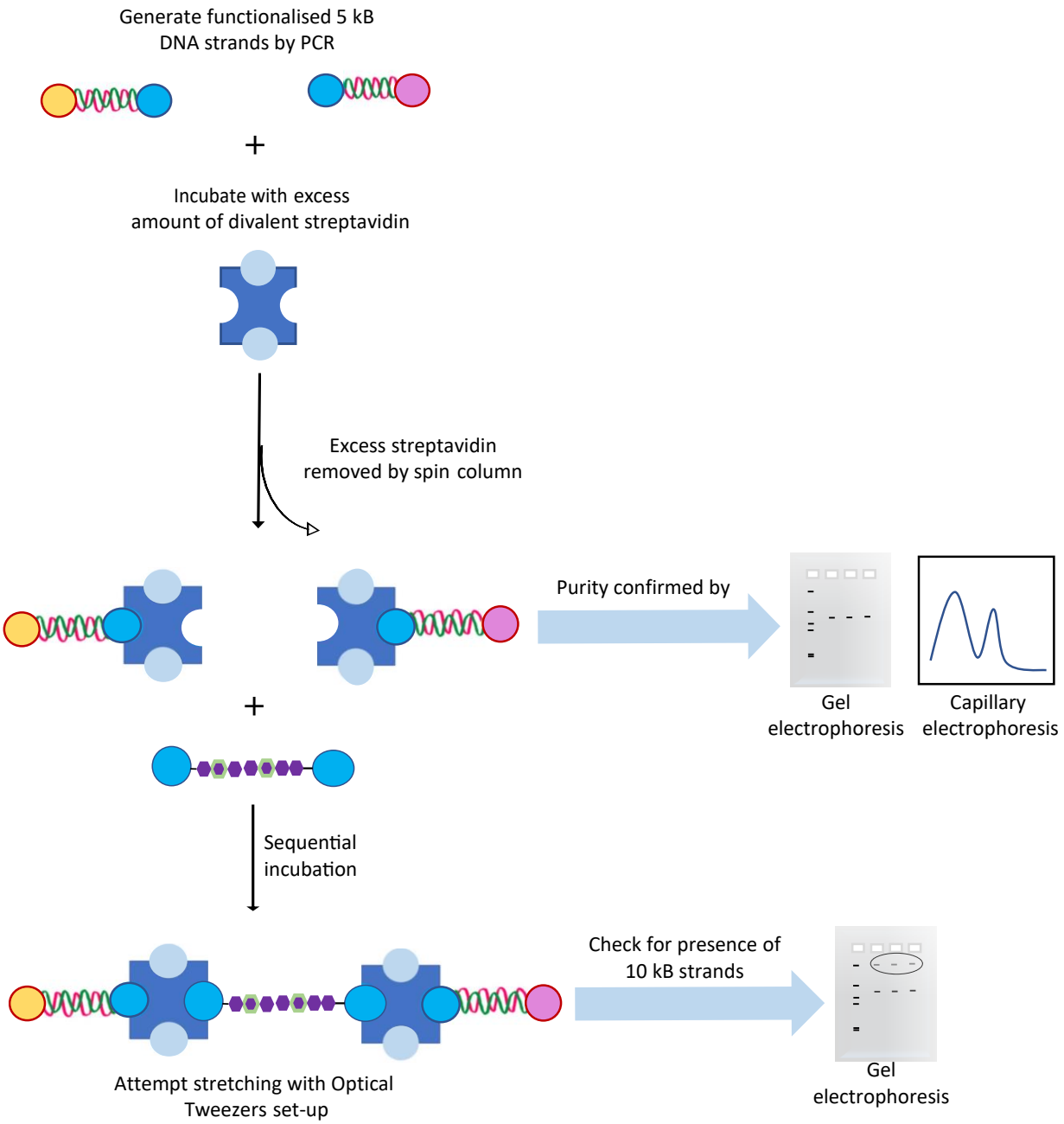

FIGURE 5.20: Illustration of the suggested final protocol for an attempt in stretching polysaccharide-DNA strings (Pink and yellow circles represent different groups which can be used to attach to beads, e.g digoxigenin and dibenzocyclooctyne, DBCO groups).

5.5 Conclusion

In this chapter, the different modified oligosaccharide and polysaccharide samples prepared from Chapter 4 were incubated with tetravalent streptavidin and streptavidin-primer mixture, and

were analysed using CE and SDS PAGE gels. Here, all experiments were performed with tetravalent streptavidin instead of divalent streptavidin experiments as a preliminary test to get a better idea on how biotinylated saccharide species interacts with streptavidin with the multiple valencies. Additional experiments can be performed for further confirmation, e.g circular dichroism, however due to insufficient yield and time-limitations, these were not performed (further discussed in Chapter 6). *Based on the observations in all cases, it can be said that the functionalised polysaccharide can be bound to streptavidin protein and primer-bound streptavidin with available valencies.*

Chapter 6

Conclusions and Future Work

6.1 Scope of Thesis

In cases where the individual biopolymers that comprise bulk samples exhibit variation in fine structure, single molecule studies uniquely offer the promise of revealing deep structure-function relationships that are masked in studies reporting only on the statistical average properties of a large heterogeneous ensemble of molecules rather than an individual molecule. Polysaccharides are typically studied in samples of this kind and, as such, their study could benefit immeasurably from the application of single molecule techniques. However as mentioned in Chapter 1, single molecule studies of polysaccharides have not yet been exploited to their full capability due to various limiting factors, such as the small size of most polysaccharides compared with DNA, and their more complex end-group chemistry. This project aimed to develop a strategy that would facilitate these single molecule studies in an optical tweezers set-up. The most fruitful approach proved to be the usage of divalent streptavidin as linkers between single polysaccharide chains functionalised with biotin at both terminal ends and a biotin end-functionalisd DNA "handles". Having DNA as handles are advantageous because they give a separation that can be visualised, and also keep the molecule of interest away from direct exposure of the laser beams. In order to achieve this, the project was divided into three main steps: 1) Formation of divalent streptavidin (Chapter 3), 2) preparation of doubly functionalised polysaccharide, homogalacturonan (Chapter 4), and finally, 3) attempts at multi-species string formation (Chapter 5). The analyses of the samples were carried out primarily using capillary electrophoresis (CE), gel electrophoresis, ELISA and NMR spectroscopy (detailed in Chapter 2).

6.2 Summary

Chapter 1 provided an introduction to the main aspects of this thesis: pectin and its modification, streptavidin-biotin conjugation and a brief note on single molecule studies. The chapter ends with a brief statement of objectives which outlines the project.

Before moving on to the experimental chapters, Chapter 2 briefly outlined the methods used in the project. The chapter mainly covers aspects of Capillary Electrophoresis (CE), Enzyme Labelled ImmunoSorbent Assay (ELISA), Nuclear Magnetic Resonance (NMR), Polymerase Chain Reaction (PCR) and Polyacrylamide Gel Electrophoresis (PAGE).

For the first experimental chapter, Chapter 3 dealt with the formation of divalent streptavidin linkers. Based on conclusive evidence from the CE and DNA stretching experiments, it was confirmed that divalent streptavidin linkers could be synthesised, purified and used for further applications.

In Chapter 4, the chemical conjugations of the reducing and non-reducing ends of both oligogalacturonides and homogalacturonan (HG) were attempted with biotin handles. Based on evidence from NMR and ELISA, it can be confirmed that HG can be biotinylated at both the terminal ends.

Once it was clear that these two main components could be prepared, Chapter 5 details the attempts made to form polysaccharide-DNA strings with divalent streptavidin linkers. Here, the preliminary experiments involved incubating tetravalent streptavidin or the multivalent streptavidin-primer mixture with the modified saccharide samples synthesised in Chapter 4. The changes were monitored using CE and SDS polyacrylamide gel electrophoresis.

Due to time restrictions, stretching of these concatenated strings was not thoroughly investigated; however we have established that it is possible to use divalent streptavidin as linkers to bind polysaccharide inserts and DNA strings "handles" to be studied using optical tweezers, provided that the polysaccharide of interest has biotin functionalised ends.

6.3 Future Work

Although limited by time in this project, the potential of the proposed methodology has been demonstrated. Further experiments could be carried out to purify and improve the yield of the final doubly biotinylated oligogalacturonide species by varying conditions such as temperature,

pH and other experimental conditions. Once purification of the final species is achieved, NMR analysis can be attempted to get a clear proof of coupling for the final product. Alternatively, other experiments such as Circular Dichroism (CD) could also be beneficial for studying changes in streptavidin through the conjugation process. In terms of polysaccharide-DNA strings, other single molecular spectroscopy techniques (e.g Raman spectroscopy) would also be useful in providing insight into polysaccharide-DNA formation.

On successful string formation, this would open a multitude of research possibilities. Although at low forces below the overstretching transition at 65 pN would not expect to show a different DNA stretch profile with or without "inserts" like divalent streptavidin or polysaccharide, however, the application of optical tweezers as a method to hold the polysaccharide of interest still poses high potential for further studies. For example, the visualisation of how various pectin methylesterases act on a highly methylesterified pectin. This could be done by fluorescently labelling the PMEs of interest and watching as they "walk" along the chain. Other possible studies including stretching/dynamic measurements of various polysaccharides which were previously not possible due to their size limitations. Such studies could of course be extended to examine the interaction of other individual polysaccharides with antibodies, enzymes or other relevant systems. On further optimisation, these studies can provide deeper insight into the mechanism of how polysaccharides function in nature with focus on their structure-function relationship which could potentially lead to diverse industrial applications.

Appendix A

Extra Protocol details

A.1 Materials used in this project

- HG: Prepared by Nirosha
- Primers: All primers were ordered from Integrated DNA Technologies
- Endo-pectate lyase: from *Aspergillus niger*, ordered from Megazyme
- Thiol-PEG-azide linker: from BiochemPG
- Cysteamine: Sigma-Aldrich
- NHS-Dig ester: from Sigma-Aldrich
- Antibodies used in ELISA: JIM7, rat-HRP and strep-HRP were obtained from Paul Knox's lab from University of Leeds. Anti-digoxygenin-AP-Fab fragments were ordered from Roche diagnostics.
- 10X PBS Recipe: For 1 L 10X PBS (10 mM phosphate, 137 mM NaCl) at pH 6.8, we add 80 g NaCl, 2 g KCl, 14.4 g Na_2HPO_4 and 2.4 g KH_2PO_4.

A.2 Instruments used in this project

- ELISA plates: 96-well plate from Thermo Scientific
- Plate reader: PowerWave XS (BioTek)
- UV lamp: Mineralight lamp (Model UVGL-58)
- CE: Agilent

- Shaker: Thermomixer (Biolab)
- Incubator: Thermocycler (Actoristierter Thermocycler)
- PCR: Machine X-LAB new

A.3 PCR

Program named **LAM5m65l** was used for every PCR experiment.

TABLE A.1: PCR cycle.

Temperature (°C)	T ime (min)	
95	3:00	
95	0:15	
*	0:15	30 cycles
72	2:00	
72	5:00	
15	hold	

The specific quantities of reagents used for each PCR detailed in Appendix A are as follows:

i) Primer-HG construct with all 4 modified primers involved in the PCR mix

TABLE A.2: The list of reagents involved in each PCR tube, their quantities and the PCR method used for primer-HG construct with all 4 modified primers.

No. of tubes: 9 (Vol./tube: 25 µL)				
Reagents	**Conc. stock**	**Final conc.**	**Vol./tube (µL)**	**Vol. in mix (µL)**
MQ H_2O			14.5	145
50 mM $MgCl_2$	15 mM	3.00	5	-
Buffer 5X		1X	5	50
dNTPs (inc. in buffer)	5 mM	1.00	5	-
F Pri	10 µM	0.40	1	-
R Pri	10 µM	0.40	1	-
Taq	5 U/µL	0.10	0.5	5
template (lambda)	5 ng/µL	0.20	1	10
		TOTAL	**21**	**210**

Tube (#)	Water (µL)	F_BIO (µL)	R_AMO (µL)	F_DBCO (µL)	R_DIG (µL)	Construct (µL)
1	2	1	1			
2	2			1	1	
3		1	1	1	1	
4	2	1			1	
5	1	1			1	1
6	2				1	1
7	2	1				1
8	1	1	1	1		
9	1		1	1	1	

ii) Primer-HG construct with 3 modified primers involved in the PCR mix

TABLE A.3: The list of reagents involved in each PCR tube, their quantities, and the PCR method used for primer-HG construct with 3 modified primers.

No. of tubes: 4 (Vol./tube: 25 µL)				
Reagents	**Conc. stock**	**Final conc.**	**Vol./tube (µL)**	**Vol. in mix (µL)**
MQ H_2O			14.5	145
50 mM $MgCl_2$	15 mM	3.00	5	-
Buffer 5X		1X	5	25
dNTPs (inc. in buffer)	5 mM	1.00	5	-
F Pri	10 µM	0.40	1	-
R Pri	10 µM	0.40	1	-
Taq	5 U/µL	0.10	0.5	2.5
template (lambda)	5 ng/µL	0.20	1	5
		TOTAL	**21**	**105**

Tube (#)	Water (µL)	F_BIO (µL)	R_AMO (µL)	F_DBCO (µL)	R_DIG (µL)	Construct (µL)
1	1	1	1	1		
2		1	1	1		1
3	2	1				1
4		1				3

iii) Primer-HG construct or HG only with 3 modified primers involved in the PCR mix

TABLE A.4: The list of reagents involved in each PCR tube, their quantities, and the PCR method used for primer-HG construct with 3 modified primers (additional controls).

No. of tubes: 5 (Vol./tube: 25 µL)				
Reagents	**Conc. stock**	**Final conc.**	**Vol./tube (µL)**	**Vol. in mix (µL)**
MQ H_2O			14.5	72.5
50 mM $MgCl_2$	15 mM	3.00	5	-
Buffer 5X		1X	5	25
dNTPs (inc. in buffer)	5 mM	1.00	5	-
F Pri	10 µM	0.40	1	-
R Pri	10 µM	0.40	1	-
Taq	5 U/µL	0.10	0.5	2.5
template (lambda)	5 ng/µL	0.20	1	5
		TOTAL	**21**	**105**

Tube (#)	Water (µL)	F_BIO (µL)	R_AMO (µL)	F_DBCO (µL)	R_DIG (µL)	100 mM Sod. Phos. buffer (µL)	1% HG (µL)	Construct (µL)
1	1	1	1	1				
2		1	1	1				1
3	0.9	1	1	1				0.1
4		1	1	1		1		
5		1	1	1			1	

iv) Primer-HG half-construct (attachment only at reducing end) with the 2 modified primers, relevant to the reducing end, involved in the PCR mix

TABLE A.5: The list of reagents involved in each PCR tube, their quantities and the PCR method used for primer-HG half-construct with 2 modified primers.

No. of tubes: 5 (Vol./tube: 25 µL)				
Reagents	**Conc. stock**	**Final conc.**	**Vol./tube (µL)**	**Vol. in mix (µL)**
MQ H_2O			14.5	93
50 mM $MgCl_2$	15 mM	3.00	5	-
Buffer 5X		1X	5	30
dNTPs (inc. in buffer)	5 mM	1.00	5	-
F Pri	10 µM	0.40	1	6
R Pri	10 µM	0.40	1	-
Taq	5 U/µL	0.10	0.5	3
template (lambda)	5 ng/µL	0.20	1	6
		TOTAL	**23**	**132**

Tube (#)	Water (µL)	F_BIO (µL)	R_AMO (µL)	Construct (µL)
1	1	1	1	0
2		1	1	1
3		1	1	1 ($1/10^{th}$ diluted)
4	1	1		1
5	1	1		1 ($1/10^{th}$ diluted)

The specific quantities of reagents used for each PCR detailed in Appendix are as follows:

A) To form 5 kB DNA strand with an aminooxy group and a biotin group on each end

TABLE A.6: The list of reagents involved in each PCR tube for AMO-5 kB DNA-BIO, and their quantities.

No. of tubes: 5 (Vol./tube: 25 µL)				
Reagents	**Conc. stock**	**Final conc.**	**Vol./tube (µL)**	**Vol. in mix (µL)**
MQ H_2O			16.5	99
50 mM $MgCl_2$	15 mM	3.00	5	-
Buffer 5X		1X	5	30
dNTPs (inc. in buffer)	5 mM	1.00	5	-
F Pri	10 µM	0.40	1	separate
R Pri	10 µM	0.40	1	separate
Taq	5 U/µL	0.10	0.5	3
template (lambda)	5 ng/µL	0.20	1	separate
		TOTAL	**23**	**132**

Tube (#)	*Temp (°C)	Contents	Primers
1	65	lambda	F_BIO, R_AMO
2	65	lambda	F_BIO, R_AMO
3	65	lambda	F_BIO, R_AMO
4	65	lambda	λ5FA, λ10R
5	65	water	F_BIO, R_AMO

B) To form 5 kB DNA strand with a strained alkyne (dibenzocyclooctynyl group, DBCO) group and a digoxygenin group on each end

TABLE A.7: The list of reagents involved in each PCR tube for DBCO-5kB DNA-DIG, and their quantities.

No. of tubes: 7 (Vol./tube: 25 µL)				
Reagents	**Conc. stock**	**Final conc.**	**Vol./tube (µL)**	**Vol. in mix (µL)**
MQ H_2O			16.5	132
50 mM $MgCl_2$	15 mM	3.00	5	-
Buffer 5X		1X	5	40
dNTPs (inc. in buffer)	5 mM	1.00	5	-
F Pri	10 µM	0.40	1	separate
R Pri	10 µM	0.40	1	separate
Taq	5 U/µL	0.10	0.5	4
template (lambda)	5 ng/µL	0.20	1	separate
		TOTAL	**25**	**176**

Tube (#)	Contents	Primers
1	lambda	F_DBCO, R_DIG
2	lambda	F_DBCO, R_DIG
3	lambda	F_DBCO, R_DIG
4	lambda	λ5FA, λ10R
5	water	F_DBCO, R_DIG

Appendix B

Preliminary Experiments

Initially, the project aimed to form polysaccharide-DNA strings by attempting direct attachment of homogalacturonan strands using covalent bonds to modified DNA strands, without streptavidin linkers. This involved modifying the terminal ends of DNA by PCR of end-functionalised primers. The experiments carried out for direct attachment are detailed in this appendix. Upon concluding that direct covalent conjugation was unsuccessful, the project was modified to use streptavidin as linkers to form polysaccharide-DNA strings (covered in this thesis).

B.1 Methods

In this study, a polysaccharide strand is aimed to be attached between micron-sized beads for optical tweezers experiments. Homogalacturonan was chosen as the polysaccharide of interest as it is the main component in pectin, and pectic enzymes act along the homogalacturonan strand. On successful attachment of the polysaccharide between beads, via DNA handles, the interaction between homogalacturonan and pectic enzymes can be studied using optical tweezers. In order to attach a polysaccharide between beads, the ends of the polysaccharide need to possess 'sticky' groups such as biotin and digoxigenin. The biotinylated end can then stick to streptavidin-coated beads, while the digoxigenin end can bind to anti-digoxigenin beads via strong non-covalent interactions. This project takes different approaches to functionalise both the ends of homogalacturonan. They are further explained in the following sections. An overview of the reactions involved in this project is outlined in Figure B.1.

All the materials and instruments used for the following reactions are listed in Appendix A.

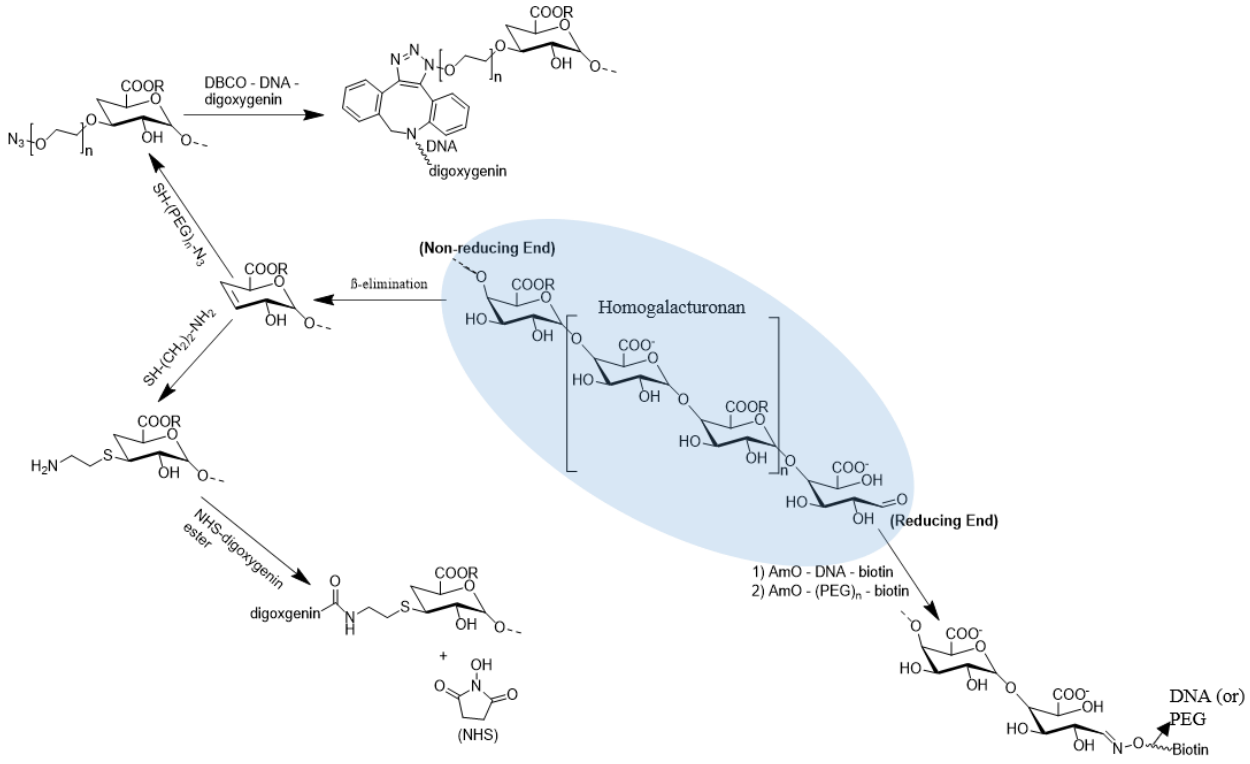

FIGURE B.1: A brief overview of the different steps taken in this project.

B.1.1 Attaching "sticky" ends to HG

The first approach taken to attach homogalacturonan to beads involves direct attachment of the reducing and non-reducing ends of the polysaccharide to "sticky" biotin and digoxigenin (which can bind to streptavidin and anti-digoxigenin coated beads respectively. This method is a good strategy when long polysaccharides are to be studied. However, as the homogalacturonan used is short (around 100 residues), this method will yield a very short polysaccharide attached to beads, which cannot be studied in optical tweezers. With the possibility of using enzymes to grow HG chains, this strategy is still being investigated. Functionalisation of the end groups of HG was monitored using ELISA and the general protocol is outlined below,

The following protocols are adapted from the protocol published by Valerie Cornuault [167]. Figure B.2 shows the basic steps involved in a typical sandwich ELISA set-up. The specific antibodies used in each case are mentioned in their respective sections.

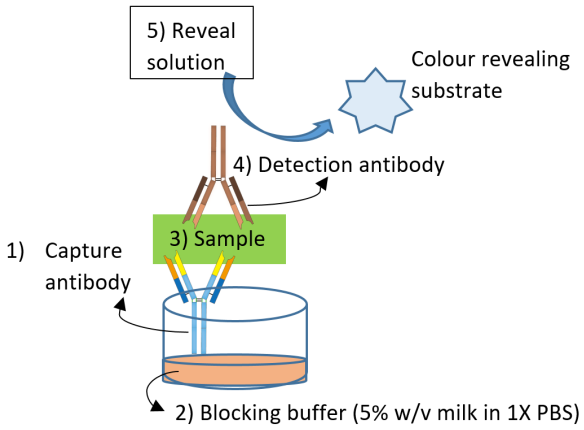

FIGURE B.2: A schematic diagram showing the general steps taken in a sandwich ELISA set up.

In all the following ELISAs, two sandwich wells and two controls are set-up for each sample. In the control wells, the capture antibody is not introduced. First, the sandwich wells only are incubated overnight, in the fridge, with 100 µL of their respective capture antibody overnight. The plates are then washed 5 times under tap water and dried. The sandwich and control wells are blocked with the blocking buffer of 5% w/v milk in 1X PBS, for 2 hours, at room temperature. The plates are then washed 5 times under tap water and dried. Next, 100 µL of the sample (dissolved in the blocking buffer) is added to the sandwich and control wells and left at room temperature for an hour. The plates are then washed 5 times under tap water and dried. 100 µL of the respective detection antibody is added to the wells, next, and left at room temperature for an hour. The plates are then washed 7 times under tap water and dried. For the final step, 100 µL of the reveal solution is added and the plates are observed for a maximum of 15 minutes to see any colour developed. For a 1 mL reveal solution, the composition is as follows:

0.9 mL H_2O + 0.1 mL 1 M sodium acetate + 10 µL TB + 1 µL of 6% hydrogen peroxide (added last).

The development of colour is quenched by adding 100 µL of 2.5 M H_2SO_4. The plates are then read, at a wavelength of 450 nm, using a plate reader.

Functionalisation at the reducing end only

At the reducing end, aminooxy-$(PEG)_{12}$-biotin is used. The aldehyde group at the reducing end of HG reacts with the aminooxy group to form a stable oxime linkage as follows:

Protocol:

1 mg of HG is dissolved in 100 µL 100 mM sodium phosphate buffer pH 6.5 in two separate Eppendorf tubes. 2 µL of aminooxy-$(PEG)_{12}$-biotin is added into the reaction mixture. The reaction is left on the stirrer at 25 °C for 3 days (A) & 1 week (B) at 1250 rpm. The product is precipitated with 50% isopropanol and left in the freezer overnight. The mixture is centrifuged at 14800 rpm for 10 minutes and the supernatant is removed. The precipitate is rinsed with 50% ethanol, twice, and lyophilised. It is then analysed by ELISA.

ELISA protocol for the functionalised reducing end:

The wells are designated as follows for ease:

TABLE B.1: The setting of samples on an ELISA plate (reducing end) (S are the sandwich wells and C are the control wells).

Sample	S	S	C	C
Biotin-HG (3 days)	A1	A2	A3	A4
Biotin-HG (1 week)	B1	B2	B3	B4

For biotin-HG samples, the capture and detection antibodies used are as follows:

- Capture antibody: JIM7 (1:10 in 5% milk)
- Detection antibody: strep-HRP (1:500 in 5% milk)

Functionalisation at the non-reducing end only

Protocol:

For enzymatic production of unsaturated non-reducing end, two sets of 1 mg of HG are dissolved in 100 µL of 100 mM Tris buffer pH 7.0 (Set A) and 100 µL of 100 mM Tris buffer pH 8.0.0 (Set B) in an Eppendorf tube. 4 µL of pectate lyase (final activity at 3 U/mL) is added to sets A & B each and left overnight. Enzyme activity is quenched by heating the reaction mixtures for 3 mins in a boiling water bath.

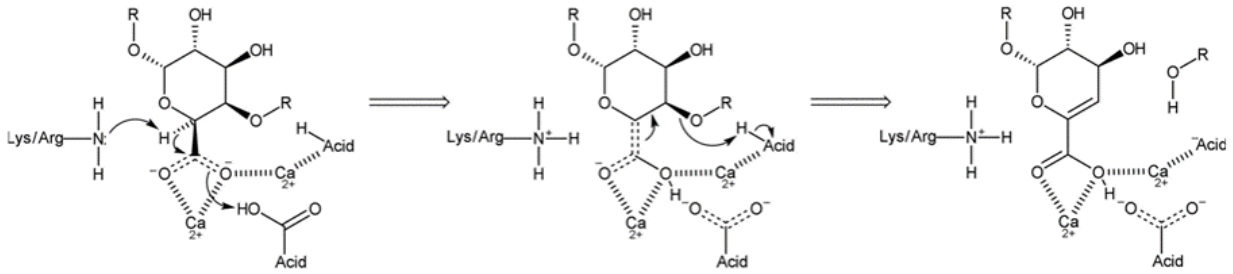

FIGURE B.3: Mechanism for pectate lyase action.[48]

For chemical production of unsaturated non-reducing end, two sets of 1 mg of HG are dissolved in 100 µL 100 mM sodium citrate buffer pH 6.0 in an Eppendorf tube (Consider them as Set C & Set D). Sets C & D are placed in an oil bath, at 90 °C. Set C is removed after 30 mins while set D is removed after 45 mins of β-elimination as shown in Figure B.3. The reaction is quenched by placing the tubes in ice for 15 to 30 mins. All the products (Sets A-D) are precipitated and lyophilised. The sets of chopped HG are re-dissolved in 200 µL 100 mM sodium phosphate buffer pH 6.5, separately. To each set, 1 mg of Irgacure 2959 and 1 mg of cysteamine are added. Once the reactants have dissolved, the mixture is subjected to 2 hours of UV treatment (wavelength = 254 - 366 nm) in a quartz cuvette. After 2 hours, the samples are precipitated and lyophilised. The two sets of HG, with linker attached, are re-dissolved in 100 µL 100 mM sodium phosphate buffer pH 6.0, separately. 2.5 µL of 50 µM NHS-digoxigenin ester is added to each set, and the reaction is left for 1 week. The products are precipitated as before and then analysed in ELISA.

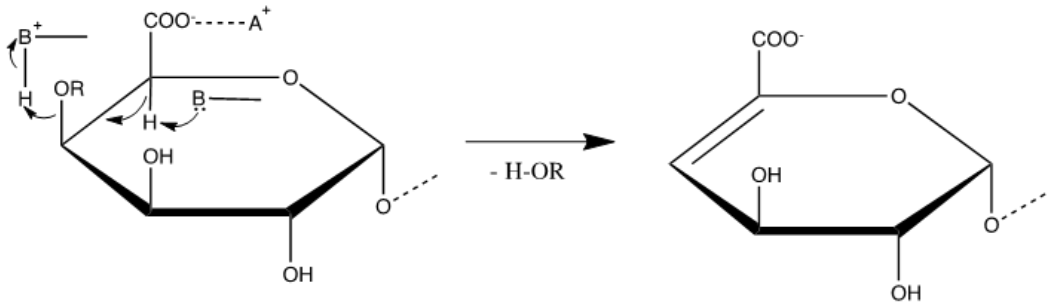

FIGURE B.4: Mechanism for β-elimination, leaving an unsaturated uronic acid residue at the non-reducing end.

ELISA protocol for the functionalised non-reducing end:

The wells are designated as follows for ease:

TABLE B.2: The setting of samples on an ELISA plate (non-reducing end). The conditions in brackets are those used to generate the double bonds that were then attached to the digoxigenin, via a linker. (S are the sandwich wells and C are the control wells).

Sample	S	S	C	C
HG-Dig (Enzymatic elimination: Tris buffer-pH 7.0)	A1	A2	A3	A4
HG-Dig (Enzymatic elimination: Tris buffer-pH 8.0)	B1	B2	B3	B4
HG-Dig (Chemical elimination: Na-cit. buffer, 30 mins)	C1	C2	C3	C4
HG-Dig (Chemical elimination: Na-cit. buffer, 45 mins)	D1	D2	D3	D4

For HG-digoxigenin samples, the capture and detection antibodies used are as follows:

- Capture antibody: anti-dig (1.5 µL in 1.5 mL 1X PBS)
- Detection antibody: JIM7 (1:10 in 5% milk), Rat-HRP (1:1000 in 5% milk)

Sequential functionalisation at the non-reducing and reducing ends

Protocol:

For the non-reducing end, sodium citrate buffer is used for chemical chopping followed by conjugation to digoxigenin. Once the conjugation at the non-reducing end is complete, 2 µL of aminooxy-$(PEG)_{11}$-biotin is added into the reaction mixture in 100 mM sodium phosphate buffer. The reaction is left on the stirrer at 25 °C for 1 week at 1250 rpm. The product is precipitated with 50% isopropanol and left in the freezer overnight. The mixture is centrifuged at 14800 rpm for 10 minutes and the supernatant is removed. The precipitate is rinsed with 50% ethanol, twice, and dried. It is then analysed in ELISA.

ELISA protocol for the functionalised reducing and non-reducing ends:

The wells are designated as follows for ease:

TABLE B.3: The setting of samples on an ELISA plate (reducing and non-reducing ends). The conditions in brackets are those used to generate the double bonds that were then attached to the digoxigenin, via a linker (S are the sandwich wells and C are the control wells).

Sample	S	S	C	C
Dig-HG-biotin (Chemical β-elimination: Na-cit. buffer, 30 mins)	A1	A2	A3	A4
Dig-HG-biotin (Chemical β-elimination: Na-cit. buffer, 30 mins	B1	B2	B3	B4

For biotin-HG-digoxigenin samples, the capture and detection antibodies used are as follows:

- Capture antibody: anti-dig (1.5 µL in 1.5 mL 1X PBS)
- Detection antibody: strep-HRP (1:500 in 5% milk)

B.1.2 Attaching HG in between two functionalised DNA primers

Before attempting to attach the HG between double-stranded DNA fragments, we tried to attach a strand of HG between two functionalised DNA primers. The primers used are 32 bp DNA primers with a functional group, either dibenzocyclooctyne (DBCO) or aminooxy (AMO), attached at the 5′ end of the primer. The protocols for attachment at the reducing and/or non-reducing ends are outlined below. The products obtained were analysed using CE, PCR and/or PAGE.

Protocol for attaching primer at the reducing end only:

For PAGE, two different sample sets of 0.2% and 1% (w/v) HG, each (4 sets in total), are prepared by dissolving HG in 100 µL 100 mM sodium phosphate buffer (pH 6.5). 10 µL of 100 µM aminooxy-modified DNA primer (final concentration: 10 µM) is added into a 0.2% HG and 1% HG solution. In addition, as a negative control, 10 µL of 100 µM λ5RB DNA primer, unmodified DNA reverse primer (final concentration: 10 µM) is added into a 0.2% HG and 1% HG solution. The reaction is left on the stirrer at 25 °C for 1 week 1250 rpm. The product, or "half-construct", was monitored on a PAGE gel.

Protocol for attaching the primer at the non-reducing end only:

For production of the unsaturated non-reducing end, the 45 minute chemical chopping with sodium citrate buffer is employed. The chemically chopped HG is re-dissolved in 200 µL 100 mM sodium phosphate buffer (pH 6.5) to which 1 mg of Irgacure 2959 is added. Once the reactants have dissolved, the mixture is subjected to 2 hours of UV treatment (wavelength = 254 - 366 nm) in a quartz cuvette. After 2 hours, the sample is precipitated and lyophilised as before. The cleaned precipitate is re-dissolved in 100 µL 100 mM sodium phosphate buffer and 1 mg of NHS-digoxigenin ester (final concentration is 10 µM) and the reaction is left for 3 days. 10 µL of 100 µM λ5FA DNA primer, unmodified DNA forward primer (final concentration is 10 µM) is added to sets B & D, and the reaction is left for 3 days. The product, or "half-construct", was monitored on a PAGE gel.

Protocol for sequentially attaching primers to the non-reducing and reducing ends:

For production of the unsaturated non-reducing end, the 45 minute chemical chopping with sodium citrate buffer is employed. The cleaned precipitate obtained after chemical β-elimination is re-dissolved in 100 µL 100 mM TEAA (pH 7.2). 10 µL of 100 µM (dibenzocyclooctyne) DBCO modified DNA primer (final concentration is 10 µL) is added to and the reaction is left for 3 days. The resulting product is precipitated with 50% isopropanol and left in the freezer overnight. The mixture is centrifuged at 14800 rpm for 10 minutes and the supernatant is removed. The precipitate (HG with primer attached at its non-reducing end) is rinsed with 50% ethanol, twice, and dried. After rinsing and drying, the precipitate is re-dissolved in 100 µL 100 mM sodium phosphate buffer (pH 6.5). 10 µL of 100 µM aminooxy modified DNA primer (final concentration is 10 µM) is added into the reaction mixture. The reaction was left on the stirrer at 25 °C for 1 week 1250 rpm. The product is precipitated and lyophilised. The product or 'construct' obtained was analysed using PCR and/or PAGE by Lisa Kent while the reaction was monitored throughout using CE.

- CE:

  CE was used in an attempt to monitor the progress of the reaction. The CE method used is detailed in Appendix B.

- PCR:

  We investigated the possibility of using PCR to extend the primer ends of the "construct" to attain a polysaccharide attached in between two strands of DNA.

  General PCR protocol:

  To produce double-stranded DNA fragments, the reagents are taken in required quantities into PCR tubes. The detailed reagents and quantities involved in each PCR are specified in tables and listed in appendix A. The PCR tubes are placed into the PCR machine, and Lam5m65l program is chosen as the program run in the PCR machine (detailed in Appendix A). After completion of PCR, 3 µL from each tube is run in a 0.5% agarose gel and 1X TAE (Tris-acetate-EDTA) running buffer, with a 10 kb+ ladder, at 70 mV, approximately. The gel is then stained with ethidium bromide for 30-60 mins, de-stained and imaged using Bio-Rad software.

  To form 5 kb DNA strand with a HG construct (primers attached to both ends of HG), different reagent mixtures were tried as shown below:

  i) Primer-HG construct with all 4 modified primers involved in the PCR mix

  The different primers used in the PCR mix are forward biotin primer (F_BIO), reverse aminooxy primer (R_AMO), forward DBCO primer (F_DBCO) and reverse digoxigenin primer (R_DIG).

  ii) Primer-HG construct with 3 modified primers involved in the PCR mix

  The different primers used in the PCR mix are forward biotin primer (F_BIO), reverse aminooxy primer (R_AMO) and forward DBCO primer (F_DBCO) only.

  iii) Primer-HG construct or 1% HG only with 3 modified primers involved in the PCR mix

  The different primers used in the PCR mix are forward biotin primer (F_BIO), reverse aminooxy primer (R_AMO) and forward DBCO primer (F_DBCO) only.

  iv) Primer-HG half-construct (attachment only at reducing end) with the 2 modified primers, relevant to the reducing end, involved in the PCR mix

The different primers used in the PCR mix are forward biotin primer (F_BIO) and reverse aminooxy primer (R_AMO) only.

- PAGE

  PAGE was used in addition to CE in attempt to monitor the reactions. For analysis using PAGE, the reaction was performed using different 0.2% HG, 0.5% HG and 1% HG. Here, the different half-constructs (AMO primer or DBCO primer attached to one end of HG, reducing or non-reducing end, respectively) and the construct (AMO primer and DBCO primer attached to reducing and non-reducing ends of HG, respectively) were tested using a PAGE gel.

  PAGE protocol:

  4 µL of the product is run on a 20% PAGE gel with 1X TBE (Tris-borate-EDTA) as the running buffer. (For each product, two 20% gels are run simultaneously) at 100 mV until the run is complete, as indicated by the loading dye. After the run is completed, one of the gels is stained with ethidium bromide for 30-60 mins, de-stained and imaged using Bio-Rad software. The other gel is then stained using stains-all for 10- 20 mins, de-stained under light and imaged using Bio-Rad software.

B.1.3 Attempts to attach HG in between two functionalised DNA strands

In the previous section, we investigated the attempts to attach the HG between primers, and to see if PCR could then be used to extend the primer ends of the "construct" formed. In this section, we attempt to attach HG to long double stranded DNA with desired functional groups required for conjugation to HG.

The desired functionalised DNA strands were obtained by PCR (Protocol followed by Lisa Kent).

PCR protocol:

To produce the double-stranded DNA fragments with functionalised ends, the reagents are taken in required quantities into PCR tubes. The detailed quantities of reagents used are specified in tables listed in Appendix A. The PCR protocol employed is detailed in section X. On successful band observations, the PCR products are combined and precipitated using 5:1 v/v ratio of 3 M

sodium acetate (pH 5.2) and 1:1 v/v ratio of 100% isopropanol, and left in the freezer overnight. The mixture is centrifuged at maximum speed for 30 minutes and the supernatant is removed carefully. The pellet is, then, washed with 500 µL to 1 mL 70% ethanol, twice, removing the supernatant each time. The resulting pellet is air-dried, to remove any excess ethanol, and re-suspended in 30 µL water. The concentration of the resulting DNA is then measured using a nanodrop.

A) To form 5 kb DNA strand with an aminooxy group and a biotin group on each end (AMO-5 kb DNA-BIO)

The different primers used in the PCR mix are forward biotin primer (F_BIO) and reverse aminooxy primer (R_AMO) only.

B) To form 5 kb DNA strand with a strained alkyne (dibenzocyclooctynyl group, DBCO) group and a digoxigenin group on each end (DBCO-5 kb DNA-DIG)

The different primers used in the PCR mix are forward DBCO primer (F_DBCO) and reverse digoxigenin primer (R_DIG) only.

The reducing end and non-reducing end of HG were, separately, attached to AMO-5 kb DNA-biotin strand and DBCO-5 kb DNA-digoxigenin strand, respectively.

Protocol for attaching AMO-5 kb DNA-BIO at the reducing end only:

1 mg of HG is dissolved in 100 µL 100 mM sodium phosphate buffer (pH 6.5). 10 µL of ~1000 ng/µL AMO-DNA-BIO 5 kb strand (final concentration is ~100 ng/µL) is added into the reaction mixture. The reaction was left on the stirrer at 25 °C for 1 week at 1250 rpm. The final product obtained was analysed using ELISA and restriction digestion.

Protocol for attaching DBCO-5 kb DNA-DIG at the non-reducing end only:

1 mg of HG is dissolved in 100 µL 100 mM sodium citrate buffer (pH 6.0) in an Eppendorf tube. It is placed in an oil bath, at 90 °C, for 45 mins. The reaction is quenched by placing the tubes in ice for 15 to 30 mins. The product is precipitated and lyophilised. The chemically chopped HG is re-dissolved in 200 µL 100 mM sodium phosphate buffer (pH 6.5). 1 mg of Irgacure 2959 and 1 mg of thiol-PEG-azide are added. Once the reactants have dissolved, the mixture is subjected to 2

hours of UV treatment (wavelength = 254 - 366 nm) in a quartz cuvette. After 2 hours, the samples are precipitated and lyophilised as mentioned before. The cleaned precipitate is re-dissolved in 100 µL 100 mM TEAA (pH 7.2). 10 µL of ~1000 ng/µL DBCO-5 kb DNA- dig (final concentration is ~100 ng/µL) is added to and the reaction is left for 3 days. The mixture is then dialysed for a week, against 1 L MQ H_2O, and the water is changed regularly. The final product obtained was analysed using ELISA and restriction digestion.

- ELISA

  To test whether this strategy to attach functionalised 5 kb DNA strands to HG was successful, we employed ELISA, which can detect polysaccharides attached to biotin and/or digoxigenin. Refer to Section B.1 for ELISA protocols at each end.

- Restriction Digest

A restriction digest was employed to check the success of this strategy of assembling HG-DNA conjugates. Reagents for digestion at the reducing and non-reducing ends are taken into separate tubes as shown in Tables B.4 and B.5. For the reducing end, a double restriction digest is performed using MscI and PvuI enzymes as shown in table A.13 and for the non-reducing end, restriction digest is performed using EcoRV as shown in table A.14. The tubes are incubated at 37 °C for ~ 3 hours to overnight. The entire volume (10 µL) from each tube is then loaded onto a 2% agarose gel, with a 5 µL 10 kb+ ladder. The gel is run at 70-90 mV for an hour, or until run is completed. After the run, the gel is then stained with ethidium bromide for 30-60 mins, de-stained and imaged using Bio-Rad software.

TABLE B.4: The list of reagents involved in each PCR tube, and their quantities for the restriction digestion of the DNA conjugated to the reducing end of HG.

Sample	NEB surecut buffer "4" (µL)	Water (µL)	Sample (~150 ng/µL)	MscI (µL)	PvuI (µL)
5 kb DNA-biotin (-ve control)	1	6.5	2.5	0.1	0
	1	6.5	2.5	0	0.1
	1	6.5	2.5	0.1	0.1
5 kb DNA-biotin+HG (-ve control)	1	6.5	2.5	0.1	0
	1	6.5	2.5	0	0.1
	1	6.5	2.5	0.1	0.1
AMO-5 kb DNA-biotin + HG	1	6.5	2.5	0.1	0
	1	6.5	2.5	0	0.1
	1	6.5	2.5	0.01	0.01

TABLE B.5: The list of reagents involved in each PCR tube, and their quantities for the restriction digestion of the DNA conjugated to the non-reducing end of HG.

Sample	Invitrogen reaction buffer (µL)	Water (µL)	Sample (~150 ng/µL)	EcoRV (µL)
5 kb DNA-DIG + HG (-ve control)	1	6.5	2.5	0.1
DBCO-5 kb DNA-DIG + HG	1	6.5	2.5	0.1

B.2 Results and Discussion

B.2.1 Attaching HG to sticky ends

The attachment of HG to sticky biotin and digoxigenin at the reducing and non-reducing ends, respectively, was monitored using ELISA. The signals were recorded and plotted (Figure B.5).

a) Attachment at the reducing end

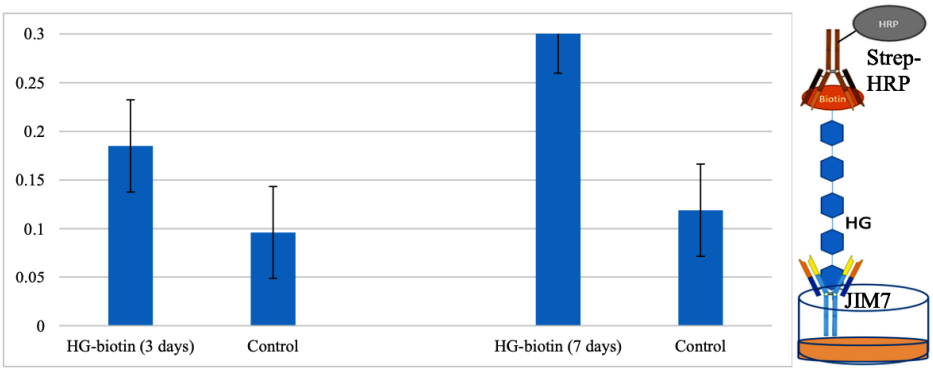

FIGURE B.5: The comparison of the ELISA signal intensities of conjugation at the reducing end, after 3 days and 1 week, and their corresponding controls, are plotted.

According to the results for the reducing end, positive results can be seen after 3 days but the yield is seen to improve after a week, as indicated by the higher intensity. This suggests that the aldehyde moiety at the reducing end of HG has successfully reacted with the aminooxy moiety in aminooxy-$(PEG)_{12}$-biotin.

b) Attachment at the non-reducing end

i) Using pectate lyase enzymatic β-elimination in Tris buffer to generate the double bond

For the non-reducing end, pH 7.0 and 8, were used for the lyase treatment of HG for the generation of a double bond at the terminal sugar residue of the chain. The double bond is, then, subjected to photochemical thiol-ene click, followed by conjugation to NHS-dig ester. Although the optimum pH suggested for lyase treatment is pH 8.0, a lower pH is also tested as we aim to achieve "minimum" fragmentation to generate an unsaturated fragment with maximum length. However, the ELISA results, from Figure B.6, indicate that the attachment of digoxigenin to HG was done successfully on fragments generated at pH 7.0 only. As double bonds are generated at both pH conditions, this could suggest that the unsaturated fragments generated by lyase treatment at pH 8.0 were not easily detected by the JIM7 antibody. As JIM7 antibodies attaches to high

DM residues easily and as de-methylesterification is faster at a higher pH, there is a possibility that the unsaturated fragments generated at pH 8.0 has lost a lot of methyl ester groups.

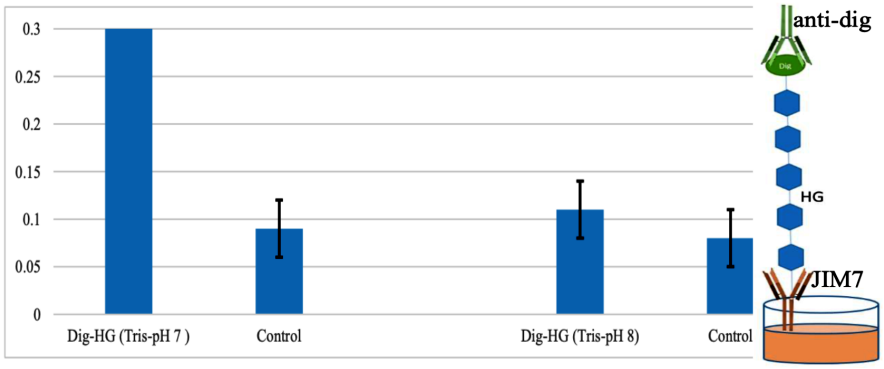

FIGURE B.6: The comparison of the ELISA signal intensities of enzymatic β-elimination with endo-pectate lyase at pH 7.0 and pH 8.0, are plotted.

ii) Using chemical β-elimination in sodium citrate buffer to generate the double bond

Compared to the enzymatic β-elimination, the signal intensities, for samples that were treated chemically for 30 minutes elimination and 45 minutes elimination, were similar. From Figure B.7, it can be noted that both the controls had a much higher signal than expected, probably due to less efficient blocking; however, the difference in intensities between the samples and controls were observable.

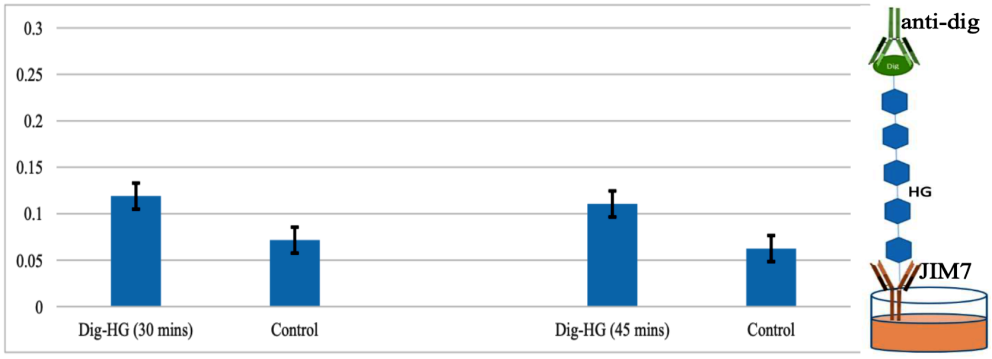

FIGURE B.7: The comparison of the ELISA signal intensities of chemical β-elimination with sodium citrate buffer, for 30 mins and 45 mins, are plotted.

c) Sequential attachment at the non-reducing and reducing end

Since the lyase treatment and chemical elimination yielded positive results, the method which generated a double bond at the non-reducing end of a longer HG fragment was chosen for the attachment of HG to digoxigenin. This was determined by CE, as detailed in the next section. From the CE, it was seen that chemical treatment of HG resulted in the presence of double bond at the non-reducing end of the longer HG fragment, when compared to lyase treatment. Hence, this method was used for double bond generation at the non-reducing end.

As shown in Figure B.8, the results indicate that a 45 minute chemical elimination gives a stronger ELISA signal on comparison to the 30 minute chemical elimination. This might be due to the difference in chain length attained by a longer chemical elimination. A 45 minute chemical elimination would result in a smaller chain and this could imply that the reaction at the reducing and/or non-reducing end occurs faster on smaller HG fragments. This is also supported by the strong signal obtained for the attachment of digoxigenin to lyase treated HG from Figure B.6, on which the double bond is present on a much smaller HG fragment.

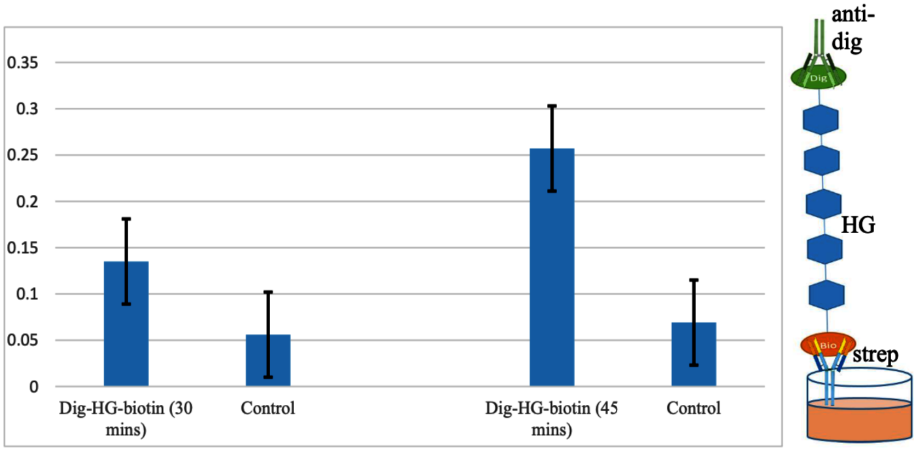

FIGURE B.8: The comparison of the ELISA signal intensities of HG samples, conjugated at the reducing and non-reducing end to biotin and digoxigenin, respectively, are plotted.

Based on the ELISA results, it can be seen that attachment of HG to biotin or digoxigenin, at the respective end, or both ends, was successful. Following the method used for HG, most polysaccharides can also be functionalised at their terminal ends and attached to sticky ends in a similar manner. However, for single molecule studies the polysaccharide has to be sufficiently long. In optical tweezers, if the beads are too close to each other, they can stick together and the molecule of interest would also be in the direct exposure to the light beam. Studies on the

polysaccharide cannot, thus, be performed. As this is not the case with HG, we aim to attach HG between two DNA strands instead.

B.2.2 Attaching HG in between two functionalised DNA primers

Introducing a double bond at the non-reducing end of HG

In all the reaction protocols outlined, the chemistry at the non-reducing end of HG is performed first. Alternatively, if the reducing end was conjugated first, we risk destabilising the oxime bond formed at this end, during the thiol-ene click conducted for conjugation of the non-reducing end to the linker. This requires the non-reducing end of HG to be functionalised first and, hence, the two chain-scissoring methods were monitored in CE and the better method was used primarily for double bond formation, throughout the project. CE was used to monitor the reaction, as double bonds have a characteristic UV absorbance at 235 nm.

A) Enzymatic β-elimination of HG

Homogalacturonan was enzymatically fragmented by treatment with pectate lyase in a 100 mM Tris buffer at pH 7.0. The reaction was monitored after 2 h, 4 h, 8 h and an overnight lyase treatment. For the enzymatic elimination, a new fragment with a 235 nm absorption is seen after 2 hours. This peak increases in intensity as the reaction time increases. However, this peak comes out much later than the original HG peak, suggesting that it the unsaturated fragment is much smaller. Furthermore, the absorption at 235 nm corresponding to the original HG peak does not vary during the lyase treatment. After an overnight treatment, it can be seen that the original HG peak has disappeared mostly and different fragments with 235 nm absorptions are seen, indicating that the polysaccharide has been completely chopped up into fragments. Interestingly, although pectate lyases are expected to act randomly along the fragment, the spectra indicates that, an unsaturated peak of a specific size is primarily formed. The interaction between pectate lyase and HG is yet to be addressed in detail.

B) Chemical β-elimination of HG

Homogalacturonan was chemically fragmented by subjecting it to a high temperature of 90 °C, in a 100 mM sodium citrate buffer at pH 6.0. The reaction was monitored every hour, for 3 hours, and after 24 hours. In contrast to lyase treatment, chemical elimination results in increase

of the 235 nm absorption at the original HG peak. The increase is observed even after 1 h treatment. However, the broadness of the peak suggests that unsaturated HG fragments of different sizes (~25 to 50) are formed, from an initial length of ~100 residues. As the reaction progresses, the fragments become slightly more distinct, and are also observed to be shifting away from the neutral peak. This shifting will, most probably, be due to the simultaneous de-methylesterification along with the β-elimination of homogalacturonan.

When comparing both the methods described above, it was decided that chemical elimination was the better option for functionalising HG at the non-reducing end as it gives a longer piece of unsaturated fragment, and in a shorter time frame. This is evident when comparing the different electrophoregrams obtained from the enzymatic and chemical β-eliminations at different time intervals, as shown in Figure B.9.

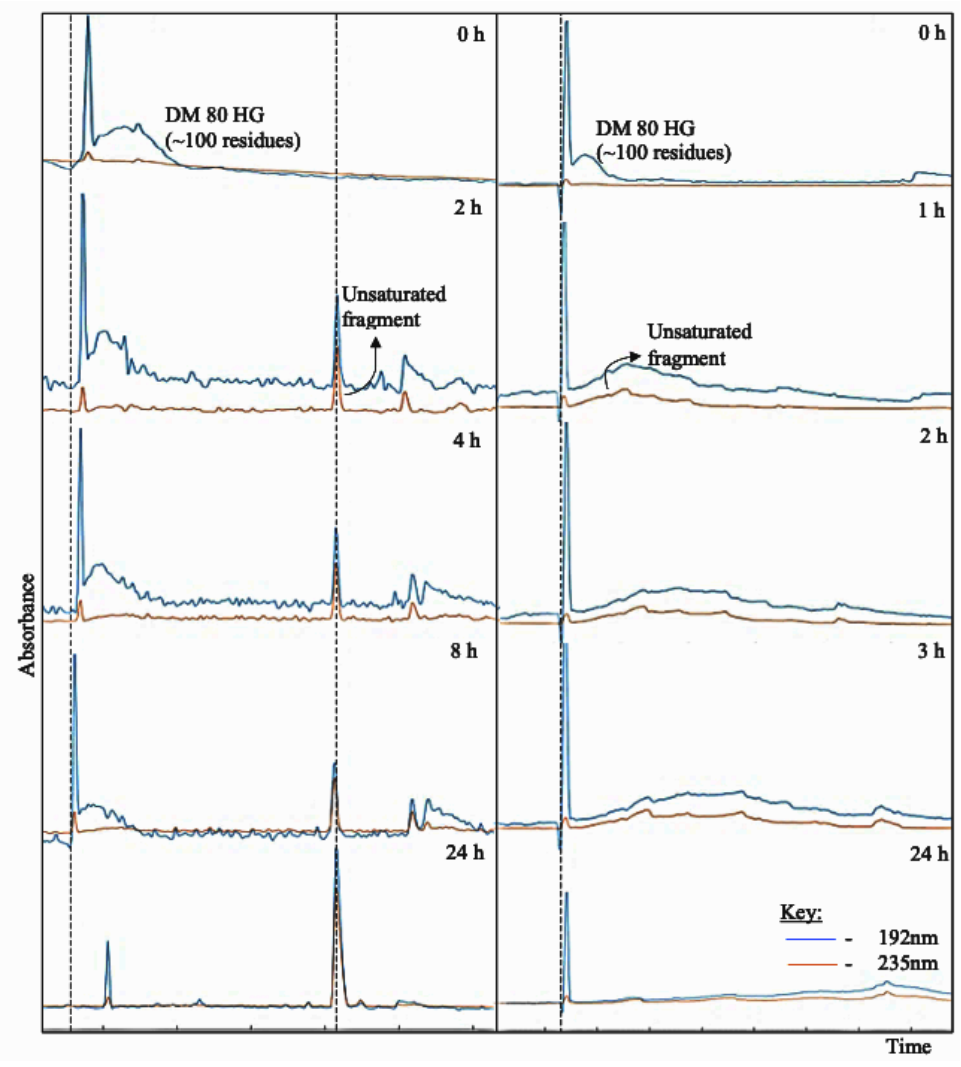

FIGURE B.9: Comparison of the electrophoregrams obtained from (A) enzymatic β-elimination and (B) chemical β-elimination at different time intervals.

Introducing primers sequentially at the terminal ends of HG

In this section, we are monitoring the reaction of attaching the aminooxy primer (AMO) and dibenzocyclooctynyl primer (DBCO) to the reducing and unsaturated non-reducing end of HG, respectively. As mentioned before, the reaction is monitored using CE because at each step, there is a presence of a functional group with a characteristic UV absorbance. The UV absorbances involved are listed below:

- ~200 nm: aminooxy/oxime (N containing compounds)
- 235 nm: unsaturated (double bonds)
- 250 nm: azide
- 260 nm: primer
- 280 nm: triazole ring

Components:

The electrophoregrams and their corresponding UV spectra for the main components are shown in Figures B.10, B.11 and B.12.

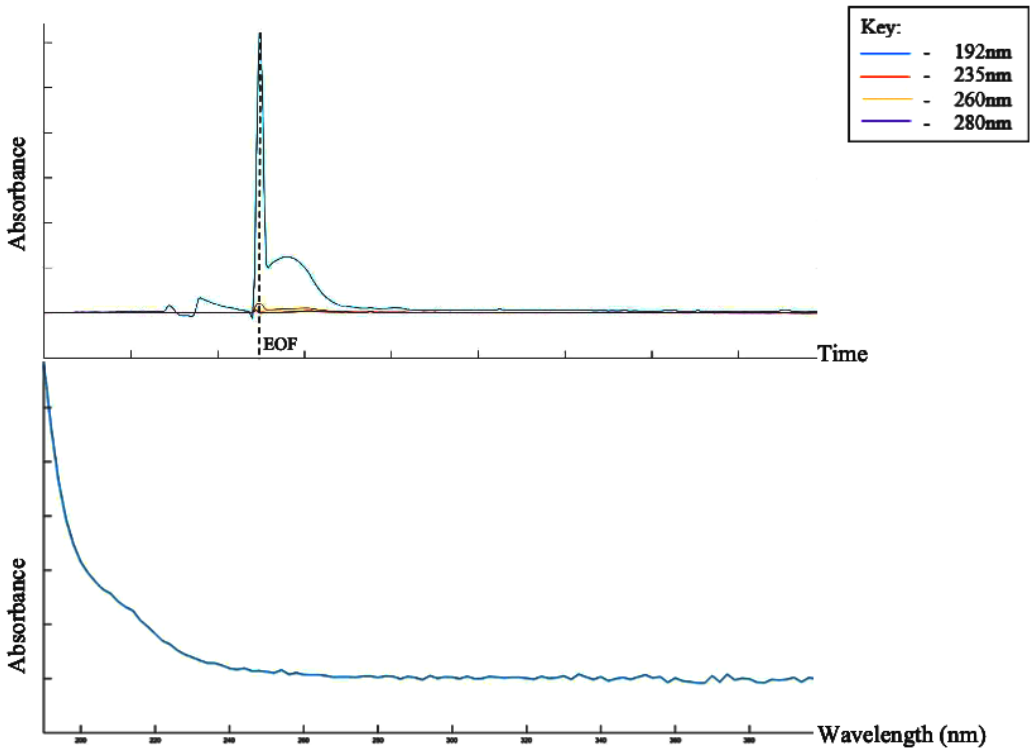

FIGURE B.10: CE spectra (top) and corresponding UV spectrum (bottom) of chemically chopped 1% HG.

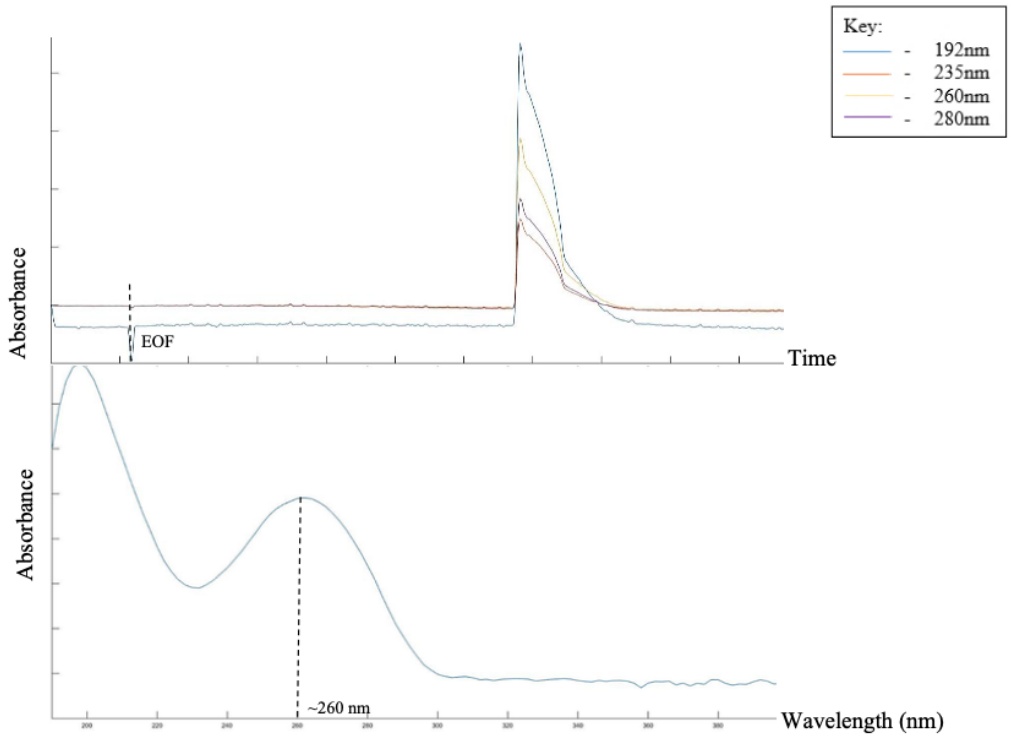

FIGURE B.11: CE spectra (top) and corresponding UV spectrum (bottom) of 20 µM aminooxy primer.

FIGURE B.12: CE spectra (top) and corresponding UV spectrum (bottom) of 20 µM DBCO primer.

Monitoring the reaction:

The CE of the reagents shown previously are compared with the electrophoregrams, obtained at each step of the conjugation at the reducing and non-reducing ends of the polysaccharide to their respective functionalised primers, and the differences in the spectra observed. The different electrophoregrams and their corresponding UV spectra at each step are shown below.

Step 1: β-elimination of HG, for 45 mins, in 100 mM Na-cit buffer (pH 6.0)

In the initial mixture, there is no peak observed in the UV spectrum. After chemical β-elimination, the appearance of a 235 nm peak is seen, in Figure B.13, due to the introduction of the double bond at the non-reducing end. However, the intensity of the 235 nm peak is not high. This is because in every fragment formed, there is only one double bond at each of its terminal residue.

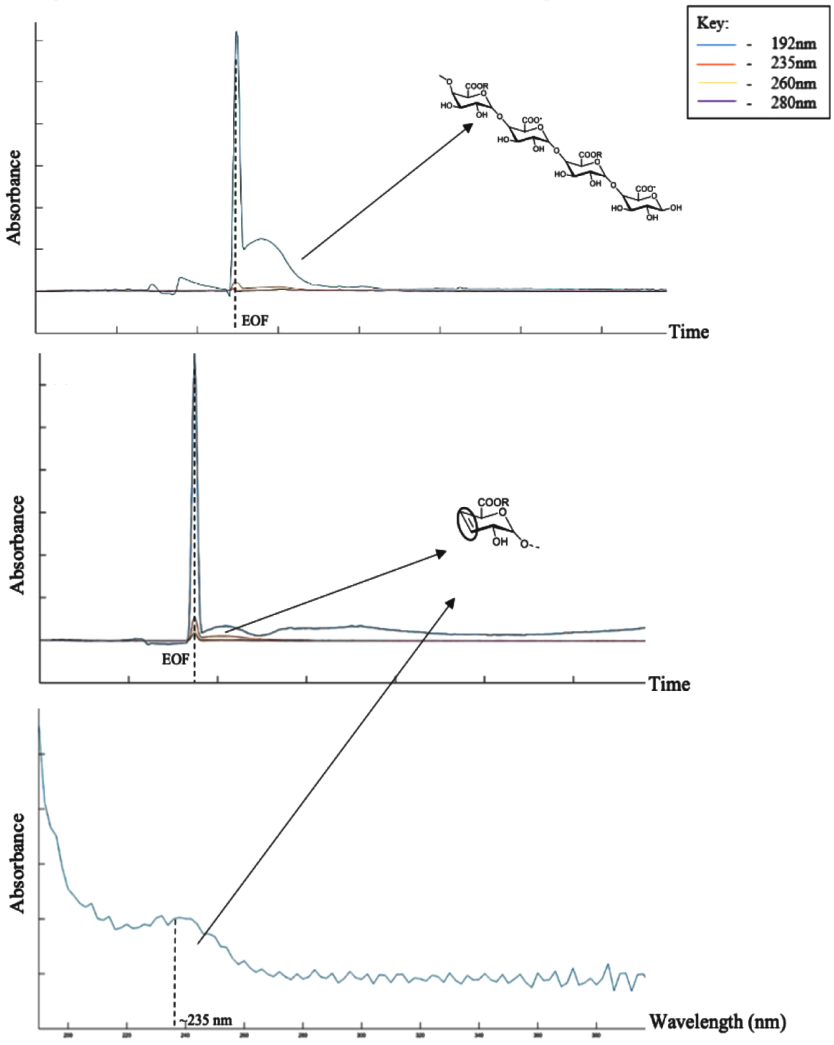

FIGURE B.13: CE spectra before (top) and after (middle) chemical β-elimination of HG, and the corresponding UV spectrum (bottom) of the product after chemical β-elimination.

Step 2: Thiol-ene click (UV) using thiol-PEG-azide linker, for 2 hours, in 100 mM sodium phosphate buffer (pH 6.5)

In the previous step, the unsaturated peak had a characteristic UV absorption at 235 nm as seen from Figure B.13. This peak disappears and a new peak at 250 nm is seen, in Figure B.14, when the unsaturated polysaccharide is subjected to thiol-ene click with the thiol-$(PEG)_{11}$-azide linker. The polysaccharide, now, has an azide group which corresponds to the absorption at 250 nm.

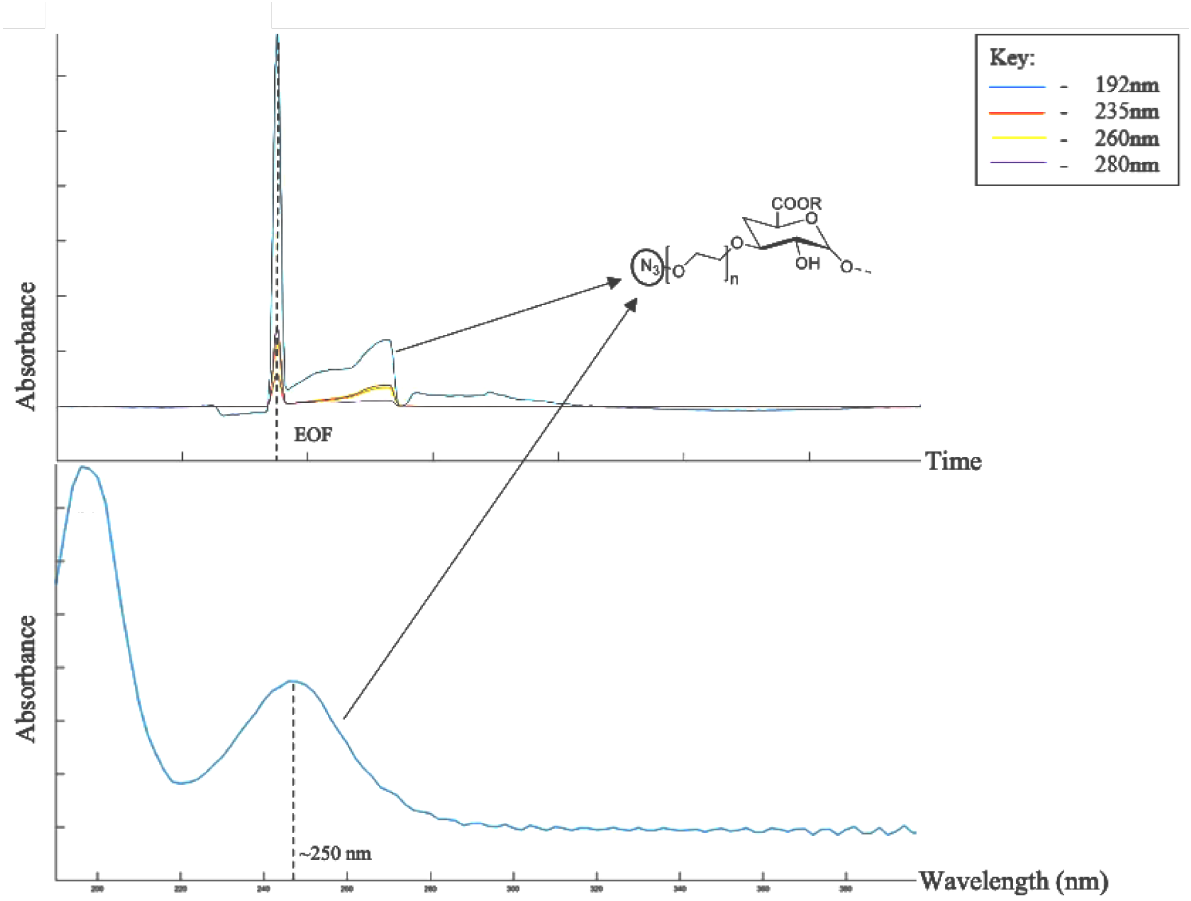

FIGURE B.14: CE spectra after thiol-ene click (top) and the corresponding UV absorption (bottom) of the product forming azide-functionalised HG.

Step 3: Azide-alkyne click of azide-functionalised HG with DBCO primer, for 3 days, in 100 mM TEAA, pH 7.2.

In the next step, a strain-promoted azide-alkyne click takes place between the azide functionalised HG and the alkyne primer, resulting in the formation of a triazole ring, with a conjugated

ring giving a characteristic UV spectrum at 280 nm peak (Figure B.15). This completes the functionalisation at the non-reducing end.

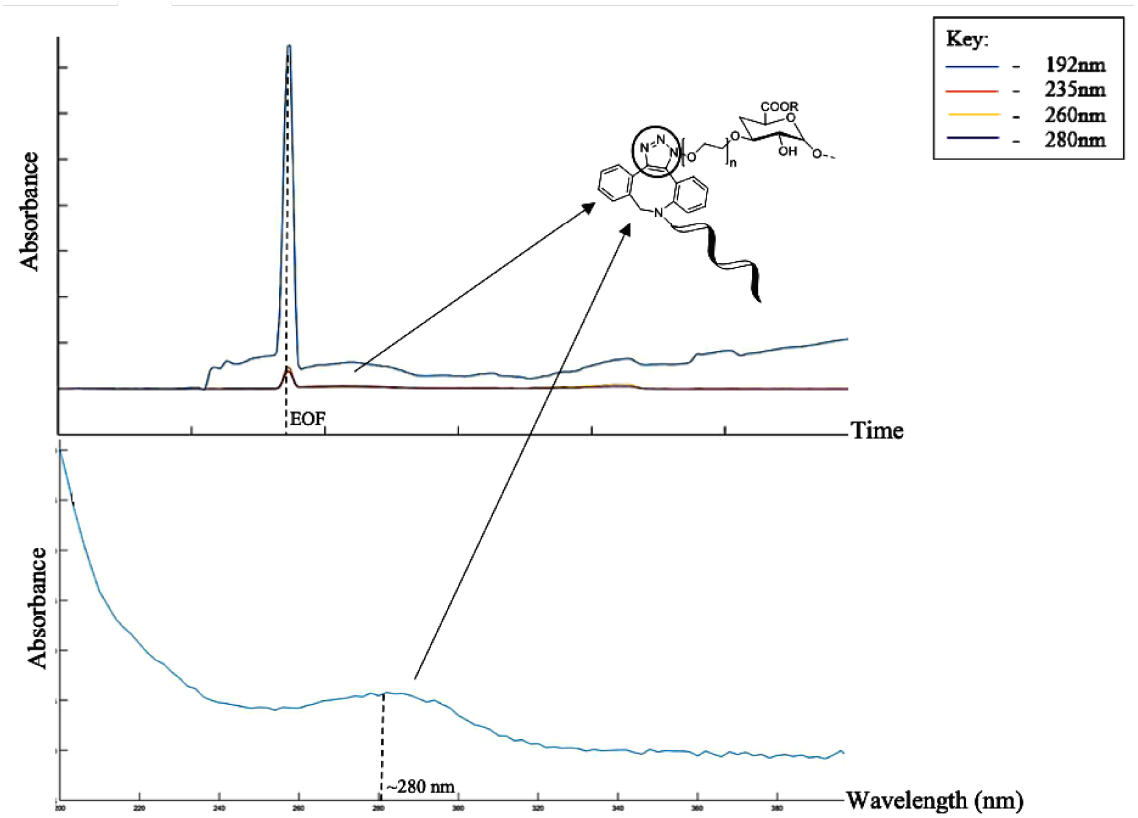

FIGURE B.15: CE spectra after strain-promoted azide-alkyne click (top) forming triazole ring with an adjacent conjugate ring system, and the corresponding UV spectrum (bottom).

Step 4: Aminooxy primer added to the mixture, in 100 mM sodium-phosphate buffer pH 7.0, for 3 days.

In the final step, the reducing end of HG is functionalised via an oxime formation, with an aminooxy primer. On completion of the reaction, there are now two primers attached at both ends of the HG, which is indicated by the presence of a 260 nm peak (as seen in the UV spectra from Figure B.16). On comparison with the unreacted primer, Figure B.16 (middle), the final product peak has shifted towards the region where primers elute. This observed shift is due to the increase in overall negative charge of the products, and the increased mass of the product.

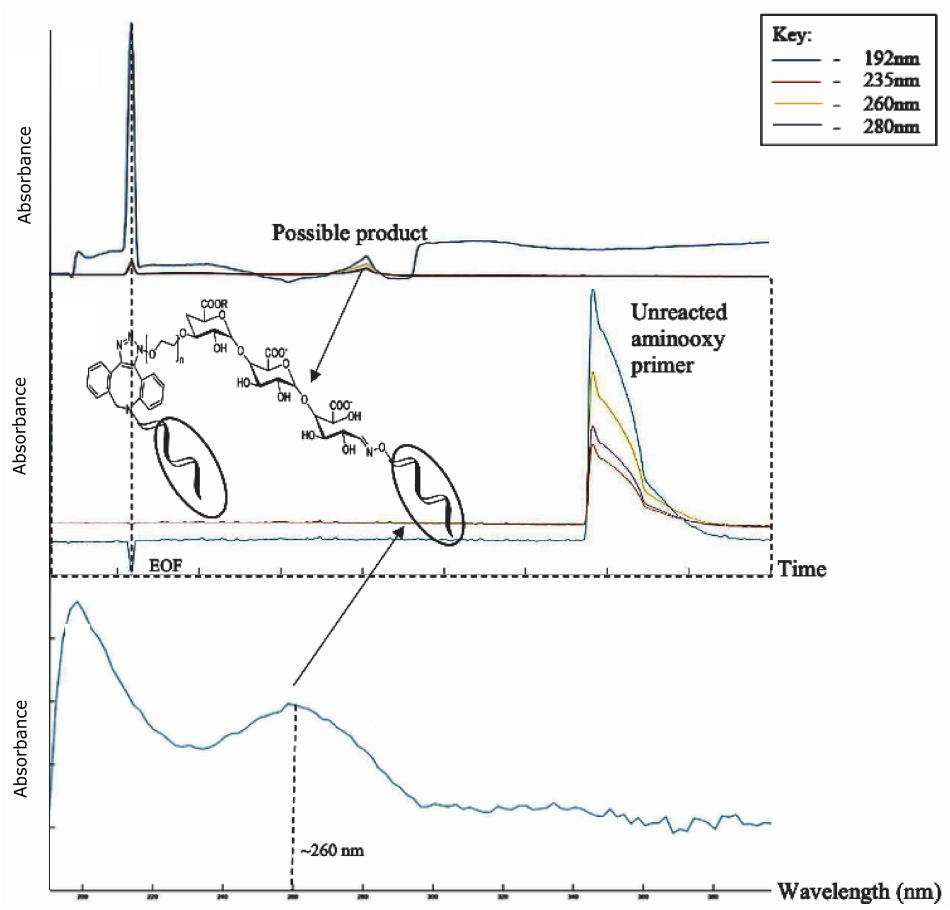

FIGURE B.16: CE spectra of the resulting product peak 3 days after adding the aminooxy primer (top), compared with expected position of unreacted primer (middle), and the corresponding UV spectrum (bottom) of the product.

PCR

From the previous section, the CE results indicated that the primers were attached to the terminals ends of HG, forming a "construct" of primer-HG-primer. The next plan was to then use PCR to extend the primer ends of the construct and form 5 kb DNA strands attached to the polysaccharide ends (Final concentration of primers were all at 0.4 µM). Although, the PCR extension was not successful, the results obtained from the PCR gels provided further evidence regarding the successful formation of the construct. This is explained in the results below.

i) Primer-HG construct with all 4 modified primers involved in the PCR mix

TABLE B.6: The list of primers involved in each PCR tube, and their quantities for primer-HG construct with all 4 modified primers (0 = 10 kb+ ladder).

Tube (#)	Water (µL)	F_BIO (µL)	R_AMO (µL)	F_DBCO (µL)	R_DIG (µL)	Construct (µL)
1	2	1	1			
2	2			1	1	
3		1	1	1	1	
4	2	1			1	
5	1	1			1	1
6	2				1	1
7	2	1				1
8	1	1	1	1		

From the above combinations, the primers that can possibly form longer DNA strands are:

1) F_BIO X R_AMO = BIO-5 kb DNA-AMO
2) F_DBCO X R_DIG = DBCO-5 kb DNA-DIG
3) **F_BIO X R_AMO**-HG-F_DBCO (construct) = **BIO-5 kb DNA**-AMO-HG-F_DBCO
4) R_AMO-HG-**F_DBCO** (construct) X **R_DIG** = R_AMO-HG-DBCO-**5 kb DNA-DIG**

Given the possible PCR products, it can be seen from the gel that mixtures #4 to #7, in Figure B.17, did not result in any band formation of any size. In #4 the biotin and digoxigenin primers do not yield a DNA strand because these primers are 10 kb apart and the DNA polymerase used does not produce such a long-range product. From Figure B.16, the most obvious result is that the PCR mixtures which had the construct present, PCR did not work at all (mixtures #5, #6 and #7). This could possibly be due to the presence of HG in the construct, which hinders the polymerase from attaching to the primer as required for PCR. However, whether it could be due to unreacted HG or an actual construct is still unclear.

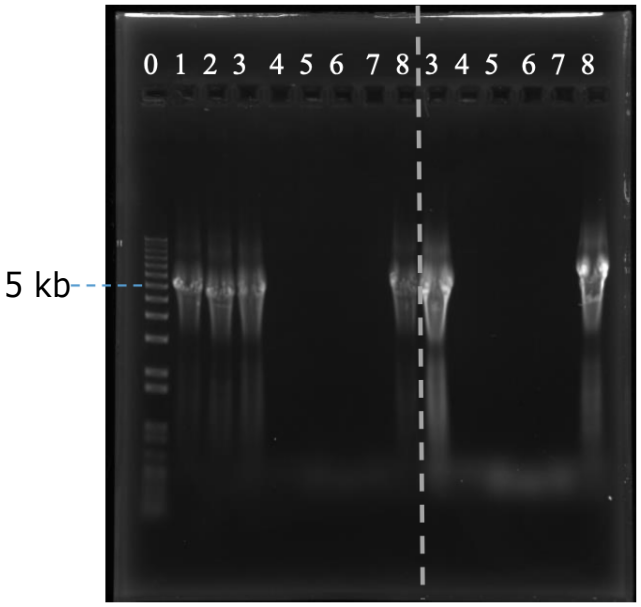

FIGURE B.17: Agarose gel with PCR product of samples containing the construct and 4 modified primers, stained with EtBr, to indicate the presence of 5 kb DNA strands. A larger volume is loaded in the last 6 wells.

ii) Primer-HG construct with 3 modified primers involved in the PCR mix

TABLE B.7: The list of primers involved in each PCR tube, and their quantities for primer-HG construct with 3 modified primers (0 = 10 kb+ ladder).

Tube #	Water (µL)	F_BIO (µL)	R_AMO (µL)	F_DBCO (µL)	R_DIG (µL)	Construct (µL)
1	1	1	1	1		
2		1	1	1		1
3	2	1				1
4		1				3

From Figure B.18, we can see that the presence of the construct in the PCR mixture also hinders the expected PCR product formation, as can be seen when comparing #1 and #2. An excess of construct was added to the PCR mix #4, just to check whether the possibility that the concentration of construct was not sufficient for PCR to occur. However, a 5 kb band is still not seen. It is possible that this could be presence of unreacted HG, compared to the construct, in the reaction mixture that inhibits the reaction.

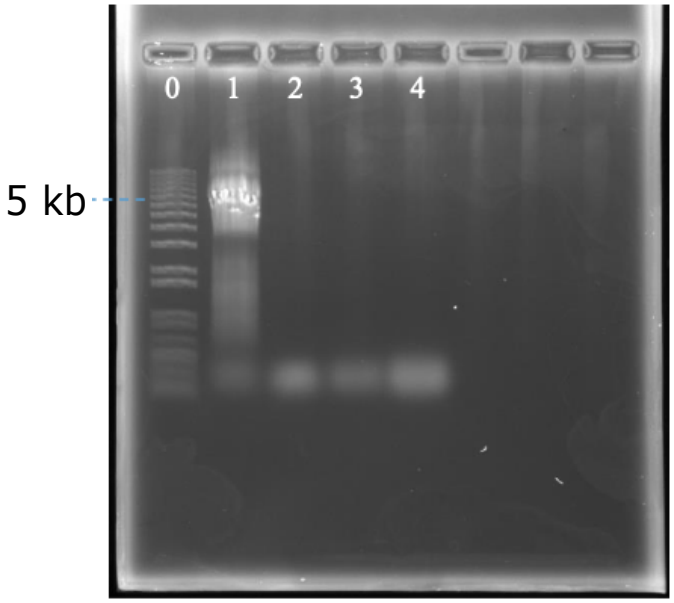

FIGURE B.18: Agarose gel with PCR product of samples containing the construct and 3 modified primers, stained with EtBr, to indicate the presence of 5 kb DNA strands.

iii) Primer-HG construct or HG only with 3 modified primers involved in the PCR mix

TABLE B.8: The list of primers involved in each PCR tube, and their quantities for primer-HG construct with 3 modified primers.

Tube (#)	Water (µL)	F_BIO (µL)	R_AMO (µL)	F_DBCO (µL)	100 mM Sod. Phos. buffer (µL)	1% HG (µL)	Construct (µL)
1	1	1	1	1			
2		1	1	1			1
3	0.9	1	1	1			0.1
4		1	1	1	1		
5		1	1	1		1	

From Figure B.19, we have checked whether the presence of unreacted HG, or the sodium phosphate buffer used, might be responsible for hindering a successful PCR reaction. From the gel results, it can be seen that neither HG nor the buffer hinders with the PCR, and only the presence of the construct, even in small amounts, is able to hinder the PCR.

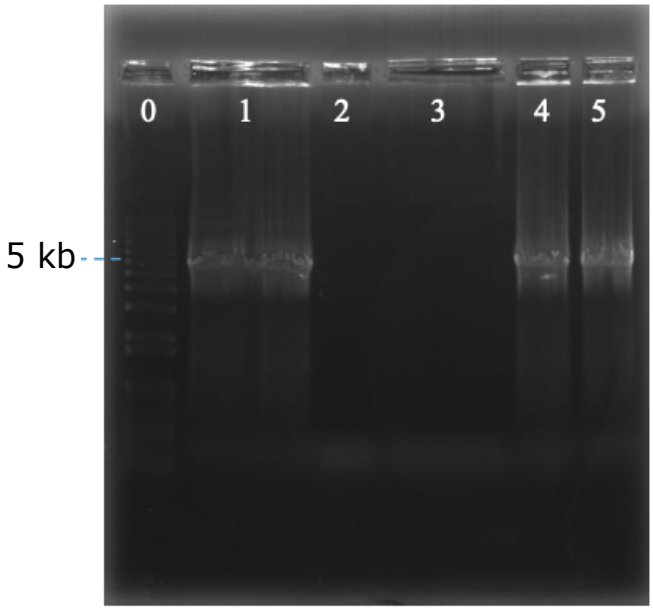

FIGURE B.19: Agarose gel with PCR product of samples containing the construct and 3 modified primers, stained with EtBr, to indicate the presence of 5 kb DNA strands.

iv) Primer-HG half-construct (attachment only at reducing end) with the 2 modified primers, relevant to the reducing end, involved in the PCR mix

TABLE B.9: The list of primers involved in each PCR tube, and their quantities for primer-HG half-construct (attachment only at reducing end) with the 2 modified primers (0 = 10 kb+ ladder).

Tube (#)	Water (µL)	F_BIO (µL)	R_AMO (µL)	Construct (µL)
1	1	1	1	
2		1	1	1
3		1	1	1 ($1/10^{th}$ diluted)
4	1	1		1
5	1	1		1 ($1/10^{th}$ diluted)

From Figure B.20, the construct at $1/10^{th}$ of its dilution is tested with PCR. On comparison of #1, #2 and #3, on $1/10^{th}$ dilution of the construct (#3), PCR can still happen but the intensity of the band is much weaker compared to #1. This suggests that the construct inhibits the polymerase action in a concentration- dependent manner, possibly, either by attaching onto the polymerase or the template DNA.

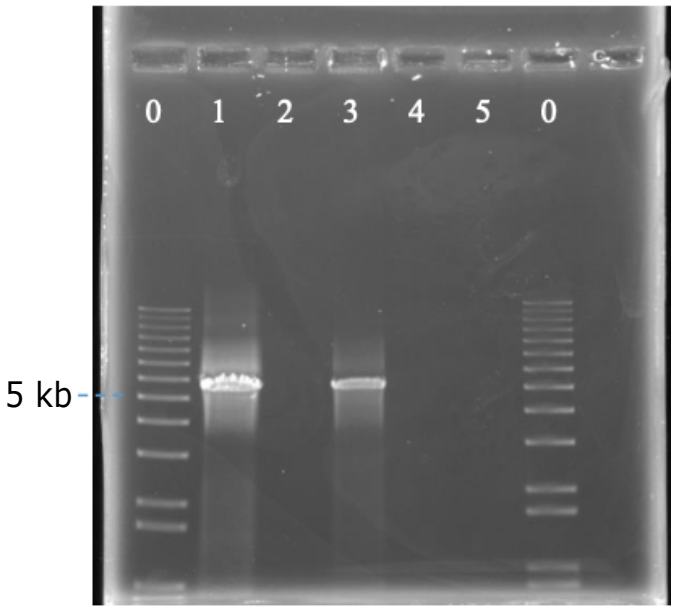

FIGURE B.20: Agarose gel with PCR product of samples containing the construct and 2 modified primers, stained with EtBr, to indicate the presence of 5 kb DNA strands.

PAGE

From the previous techniques, we were only able to focus either the HG or the primer at each time. On the other hand, PAGE was highly useful in analysing the products as the gel can be stained differently to highlight the HG bands (using stains-all) and also, specifically, the primer bands (using ethidium bromide). Due to this characteristic staining, PAGE was used to analyse half-constructs (primer attached to only one terminal end of the polysaccharide) and the full primer construct (primer attached to both terminal ends of the polysaccharide). The following results were obtained.

i. Half-construct (primer attached at reducing end only)

According to the CE, the difference when attaching the primer to HG was seemingly observable by the shifting of the peak (Figure B.16). However, a conclusive time-course was not possible as major differences were not seen in the electrophoregrams. The PAGE gels, for mixtures #2 to #9, in Figure B.21, show a time course change for the attachment of the aminooxy primer to the reducing end of 0.2% and 1% HG solutions. The difference in staining observed depends on the charge of the molecules. Staining is less efficient when the molecule is mostly uncharged as evident from #2 to #5. As the reaction progresses, the methyl ester groups fall off from the chain, making the polysaccharide more charged and improving the staining as seen from #6 to #9.

TABLE B.10: The list of reagents present in each sample for half-construct (attachment at reducing end only).

#	Description
1	(1:25) 10 µM R_AMO primer
2	1% HG + (1:25) 10 µM 5RB primer (negative control) (Day 1)
3	1% HG + (1:25) 10 µM R_AMO primer (Day 1)
4	0.2% HG + (1:25) 10 µM 5RB primer (negative control) (Day 1)
5	0.2% HG + (1:25) 10 µM R_AMO primer (Day 1)
9	1% HG + (1:25) 10 µM 5RB primer (negative control) (Day 5)
7	1% HG + (1:25) 10 µM R_AMO primer (Day 5)
8	0.2% HG + (1:25) 10 µM 5RB primer (negative control) (Day 5)
9	0.2% HG + (1:25) 10 µM R_AMO primer (Day 5)
10	0.5% HG + (1:25) 10 µM 5RB primer (negative control) (2 weeks)
11	0.5% HG + (1:25) 10 µM R_AMO primer (2 weeks)

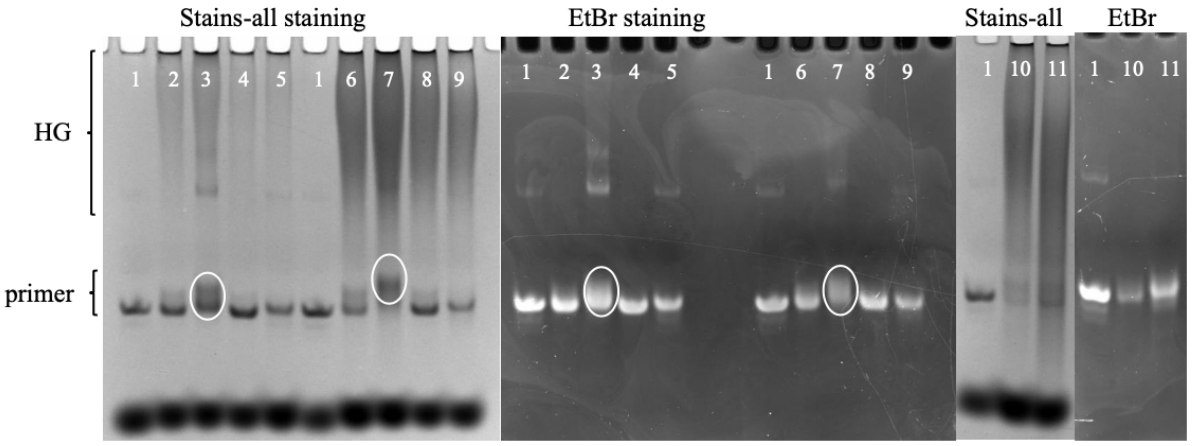

FIGURE B.21: PAGE gels, stained with stains-all and EtBr separately, to indicate presence of HG and EtBr in the samples from D1, D5 and 2 weeks (reducing end).

In all the samples containing the aminooxy primer and HG, the aminooxy primer band smears but the smearing is prominent for 1% HG. This is visible when comparing #3 and #7 where #7 has a much fainter and more smeared band, after 5 days, compared to #3, after one day. Furthermore, from the stains-all, the more prominent band is higher compared to the original position of the primer band. This suggests that the primer has been attached to the polysaccharides, of different sizes, successfully. However, as the shift upwards is smaller than expected, it is possible that the primers have preferentially attached to the smaller pieces of HG present in the solution. The third faint band that appears in all the reactions involving the modified primers could possibly be primer dimer, as it is present in mixtures without the HG and primer alone. This is yet to be further confirmed.

For 0.2% HG solution, there was no observable difference between the unreacted primer and the reaction mixture even after 5 days. This can be seen from comparing #1, #5 and #9. For a 0.5% HG solution, the aminooxy primer band does get fainter after 2 weeks, but the smearing of this band, #11, is less obvious compared to #9. These results suggest that 1% HG solution is favourable for the conjugation of the reducing end of HG to the aminooxy primer.

ii. Half-construct (attachment of primer at non-reducing end only)

From the CE in Figure B.15, the formation of the triazole ring resulting from the click was evident by the UV absorbance peak at 280 nm, after 3 days. Based on this information, the samples for the conjugation at the non-reducing end of HG were analysed on PAGE after 3 days, instead of a detailed time-course (Figure B.22). Contrary to the primer at the reducing end, it appeared that the smearing of the initial primer band was just a consequence of the three-day incubation with

the alkyne primer. This can be seen on comparing #1 and #4, however the smearing is stronger in the presence of HG which does not have an available azide group for the DBCO to attach onto (#5).

TABLE B.11: The list of reagents present in each sample for half-construct (attachment at non-reducing end only).

#	Description
1	(1:25) 10 µM F_DBCO primer
2	1% HG + (1:25) 10 µM 5FA primer (negative control) (Day 3)
3	1% HG + (1:25) 10 µM F_DBCO primer (Day 3)
4	(1:25) 10 µM F_DBCO primer (incubated at 37 °C, 0.1M TEAA, Day 3)
5	1% HG (without linker) + (1:25) 10 µM F_DBCO primer (Day 3)

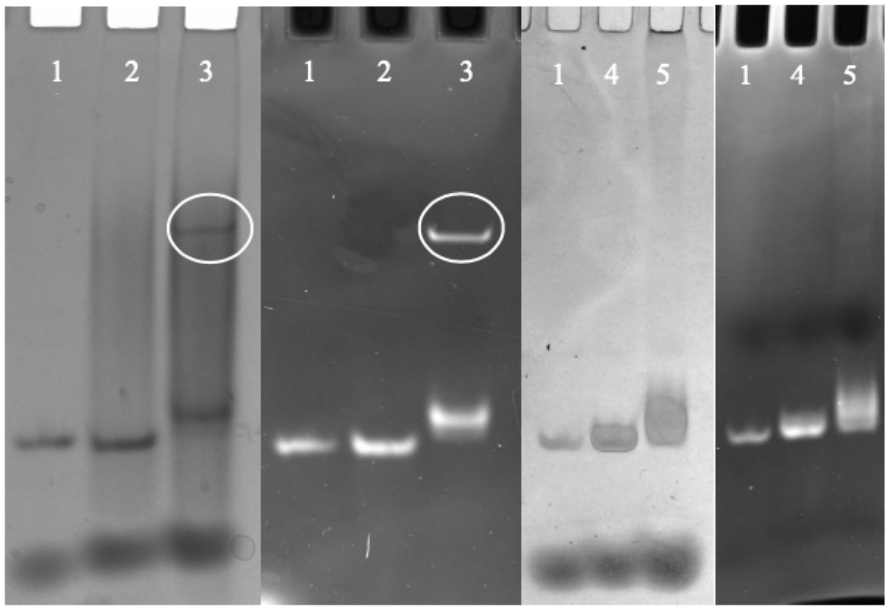

FIGURE B.22: PAGE gels, stained with stains-all and EtBr separately, to indicate presence of HG and DNA in the samples after 3 days (non-reducing end). Lane 3 indicates presence of primer-attached species.

In these gels, the region where HG is present is much lower and brighter compared to the HG band seen in the previous gels as the HG has been chemically chopped to unknown size but smaller fragments, allowing it to form a smear further down in the gel. The staining is also improved as the HG undergoes partial de-methylesterification during the chemical treatment and, also, during the click reaction which is performed at pH 7.2.

In contrast to the PAGE gels discussed in the previously in this chapter, the interesting feature in the gel is the distinct band which appears within the HG region of #3 but is not present in any of the other wells. This feature can very faintly be seen in EtBr staining of #5 but not in stains-all which suggests that the successful attachment of HG to the primer, at the non-reducing end, is responsible for this feature in #3. The mixtures were also run in a denaturing gel to eliminate the possibility of the primer-dimer. If this new distinct band was a primer-dimer, this band would disappear in a denaturing gel as it would be separated into single strands. However, in the denaturing gel it was seen that the band did not disappear, further confirming that this distinct band is, indeed a feature of the half-construct.

iii. Construct (at reducing and non-reducing ends)

Figure B.23 shows a PAGE gel run with samples taken at each step of the construct formation, which have also been simultaneously monitored in the CE. The difference in the samples in each step of the reaction correspond to the changes seen previously in the half-constructs. However, as 0.5% HG was used for the reaction, the changes at the reducing end between #7 and #9 were not observed. This implies that 1% HG is indeed the optimum concentration for attaching the aminooxy primer to the reducing end of the polysaccharide. Another possibility is that the aminooxy primer could also react with the excess unreacted HG more preferentially compared to the half-construct. Hence, a method to separate the unreacted HG from the HG conjugated at the non-reducing end needs to considered for further experiments.

TABLE B.12: The list of reagents present in each sample for construct (at reducing and non-reducing ends).

#	Description
1	(1:25) 10 µM F_DBCO primer
2	0.5% HG (chemically chopped for 45 mins)
3	0.5% HG (UV treated with SH-PEG-N_3 linker for 2 h)
4	0.5% HG + (1:25) 10 µM 5FA primer (negative control) (Day 3)
5	0.5% HG + (1:25) 10 µM F_DBCO primer (Day 3)
6	0.5% HG/(1:25) 10 µM 5FA primer + (1:25) 10 µM 5RB primer (negative control) (Inital)
7	0.5% HG/(1:25) 10 µM F_DBCO primer + (1:25) 10 µM R_AMO primer (Initial)
8	0.5% HG/(1:25) 10 µM 5FA primer + (1:25) 10 µM 5RB primer (negative control) (Day 3)
9	0.5% HG/(1:25) 10 µM F_DBCO primer + (1:25) 10 µM R_AMO primer (Day 3)

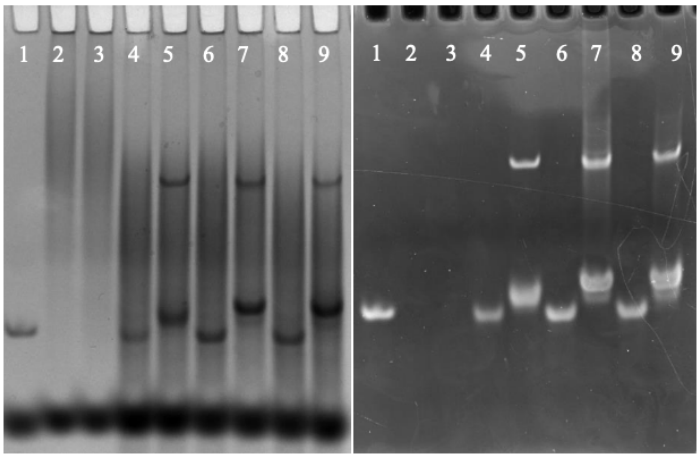

FIGURE B.23: PAGE gels, stained with stains-all and EtBr separately, to indicate presence of HG and EtBr in the samples at each step of the reaction (reducing and non-reducing ends).

B.2.3 Attaching HG in between two functionalised DNA strands

PCR

Once it was established that the terminal ends of HG were successfully attached to functionalised primers, the chemistry was performed again, but using functionalised 5 kb DNA strands instead. The two different 5 kb DNA strands require the desired functional groups on one end of the DNA strand for attachment to the reducing end and non-reducing end of the polysaccharide. In addition, the other end of the DNA strand should have a biotin or digoxigenin end, available for attachment to beads used in optical tweezers. Based on these requirements, AMO-5 kb DNA-biotin and DBCO- 5 kb DNA-digoxigenin strands were synthesised successfully via PCR as shown in Figure B.24.

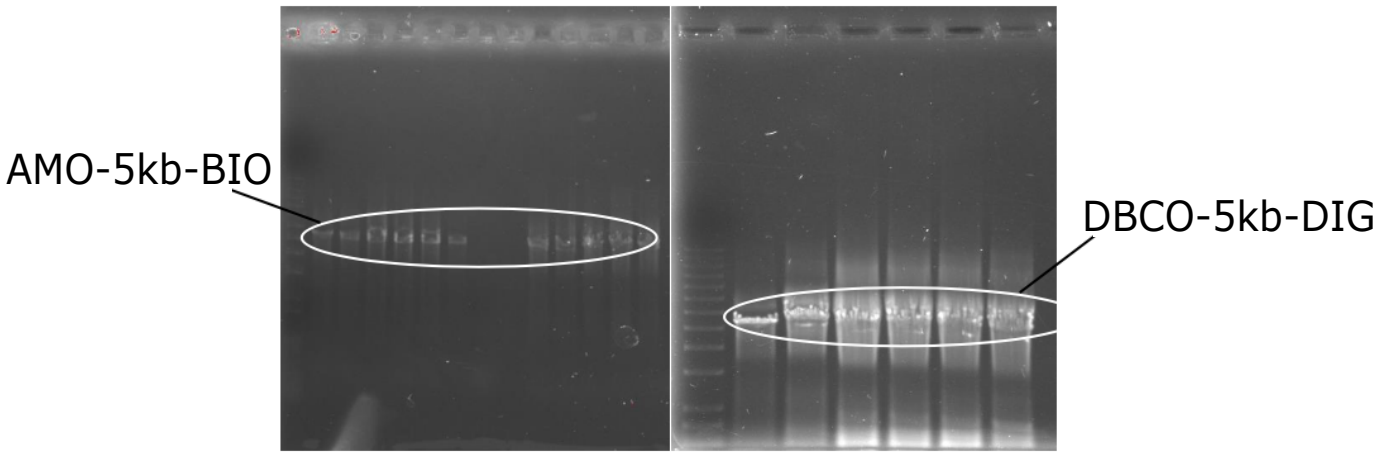

FIGURE B.24: Agarose gels, stained with EtBr, indicating formation of functionalised 5 kb DNA strands.

ELISA

ELISA was performed to test the attachments of the reducing end of HG to AMO-5kb-BIO and non-reducing end of HG to DBCO-5kb-DIG. The same chemistries used for attachment to the corresponding DNA primers was employed. However, all the ELISA results were negative, suggesting that the attachment of HG to the DNA strands at either end, or both ends, were unsuccessful.

Restriction Digest

At the reducing end:

Double restriction digest was performed at the reducing end as the enzymes used can cleave at specific sites in the AMO-5 kb-BIO strand giving a fragment with a size of 223 bp from the aminooxy end. Hence, if a HG strand, of 100 residues, was successfully attached to this fragment, a shift in the band would likely be observed. A double digest is also attempted as it provides a ladder for comparison of the DNA-HG digest.

TABLE B.13: The list of reagents, and their quantities, present in each sample for restriction digestion at reducing end.

#	Description
0	10 kb+ ladder
1	5 kb DNA-biotin (-ve control) – MscI digest
2	5 kb DNA-biotin (-ve control) – PvuI digest
3	5 kb DNA-biotin (-ve control) – MscI + PvuI double digest
4	5 kb DNA-biotin+HG (-ve control) – MscI digest
5	5 kb DNA-biotin+HG (-ve control) – PvuI digest
6	5 kb DNA-biotin+HG (-ve control) – MscI + PvuI double digest
7	AMO-5kb-biotin + HG – MscI digest
8	AMO-5kb-biotin + HG – PvuI digest
9	AMO-5kb-biotin + HG – MscI + PvuI double digest
10	AMO-5kb-biotin + HG (reaction done in 10X PBS)
11	AMO-5kb-biotin + HG (reaction done in 5X PBS)
12	AMO-5kb-biotin (in 5X PBS)
13	AMO-5kb-biotin (in MQ H_2O)

Water (µL)	Enzyme (µL)	suRE cut buffer "NeB" (µL)	Construct ($1/10^{th}$ diluted) (µL)
6.5	0.1	1	2.5

In the restriction digest for the reducing end, single and double digests are tried as shown in Figure B.25. In the first gel, from #1 to #9, there are no observable differences seen in any of the bands, between the negative and positive controls. In the second gel, #10 to #13, the double digest is performed on samples where the reaction is done in higher concentrations of PBS (5X and 10X). However, the high concentration of salt present in the buffer was not ideal for the digestion enzyme to perform, as seen from the absence of bands in #12, and hence digestion was not observed.

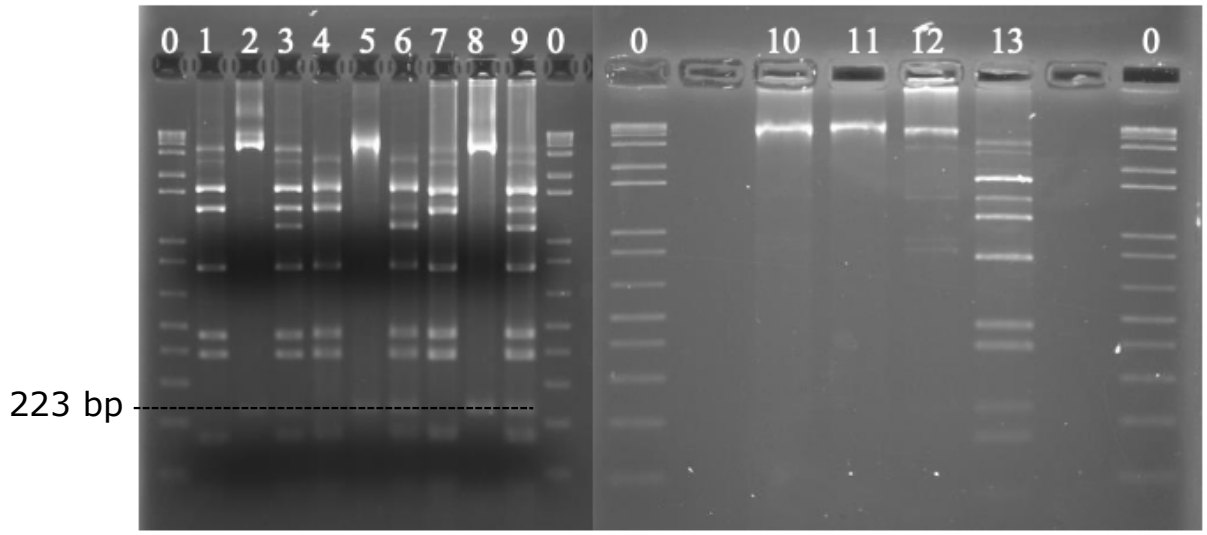

FIGURE B.25: Agarose gels, stained with EtBr, to indicate presence of fragments formed as a result of sample digestion with different restriction enzymes, MscI and PvuI (reducing end).

At the non-reducing end:

A single digestion is done with EcoRV it was the only enzyme we had currently available to cleave at a site nearer to the DBCO group in the DBCO-5kb-DIG. However, the cleavage site is too far away from the DBCO functional group and, hence, an observable shift in the band when attached to a chopped piece of HG might not be apparent. The digestion was still given a try and the following gel was obtained.

TABLE B.14: The list of reagents present in each sample for restriction digestion at non-reducing end.

#	Description
0	10 kb+ ladder
1	DBCO-5kb-DIG
2	0.5% HG + DBCO-5kb-DIG

In the restriction digest for the non-reducing end, a single digest was performed, and the gel shown in Figure B.25 was obtained. As expected, there was no observable differences between the DNA and DNA/HG sample. However, this result is inconclusive as the cleavage site for the enzyme used gives a large fragment of 940 bp, to which addition of a HG strand (25-50 residues) does not necessarily result in a visible shift in the fragment band.

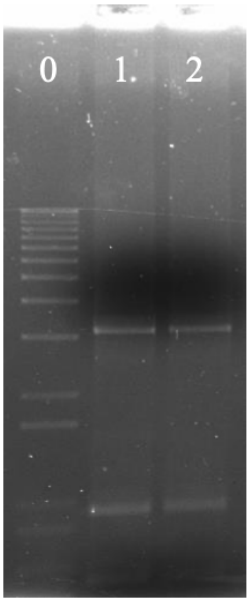

FIGURE B.26: Agarose gel stained with EtBr, to indicate presence of fragments formed as a result of sample digestion with EcoRV restriction enzyme (non-reducing end).

B.3 Preliminary Conclusion

This project aims to facilitate a methodology that allows for single molecule studies, for example using optical tweezers, on short or long polysaccharides. In this study, we have chosen homogalacturonan, a short polysaccharide, as the subject of interest. We have tried three different possible approaches where the terminal ends of the polysaccharide can be 1) directly attached to 'sticky" biotin or digoxigenin ends, 2) attached to suitably functionalised primers and, 3) attached to suitably functionalised 5 kb long DNA strands. From these approaches mentioned, the former two methods have worked successfully. We have used different analytical techniques to monitor our reaction and analyse the results, namely ELISA, CE, PCR and PAGE. For the direct attachment of HG, the samples were tested with ELISA and positive results were attained for the conjugation of the polysaccharide at the reducing and non-reducing end. On the other hand for the attachment of HG in between two different primers, CE, PCR and PAGE were employed to monitor the reactions. The results from all the techniques provided evidence that primers were, indeed, successfully attached to the terminals ends of HG. The attachment of HG to DNA strands was analysed using ELISA and restriction digestion. However, the results from both methods indicated that this attachment was unsuccessful.

Appendix C

Statement of Contribution and DRC16 Forms

- All the CE experiments and analysis in the entire thesis were performed by myself and Lisa Kent.
- I was an active participant in the CE collection and analysis of the formation and application of divalent streptavidin linkers. Gels and separation of divalent streptavidin were carried out by Lisa Kent. Optical Tweezers experiments and analysis were carried out by Allan Raudsepp. (Chapter 3)
- I was an active participant in the terminal ends' modification of the saccharides and in their CE and ELISA analysis. NMR analysis was carried out by Pat Edwards. (Chapter 4)

DRC 16

MASSEY UNIVERSITY TE KUNENGA KI PŪREHUROA UNIVERSITY OF NEW ZEALAND | GRADUATE RESEARCH SCHOOL

STATEMENT OF CONTRIBUTION
DOCTORATE WITH PUBLICATIONS/MANUSCRIPTS

We, the candidate and the candidate's Primary Supervisor, certify that all co-authors have consented to their work being included in the thesis and they have accepted the candidate's contribution as indicated below in the *Statement of Originality*.

Name of candidate:	Nimisha Mohandas
Name/title of Primary Supervisor:	M.A.K. Williams
In which chapter is the manuscript /published work:	3

Please select one of the following three options:

(●) The manuscript/published work is published or in press

- Please provide the full reference of the Research Output:

IN PRESS Journal: ACS Omega; Title: "Progress towards plug-and-play polymer strings for optical tweezers experiments: Concatenation of DNA using Streptavidin-Linkers"
Author(s): Mohandas, Nimisha; Kent, Lisa; Raudsepp, Allan; Jameson, Geoffrey; Williams, Martin

( ) The manuscript is currently under review for publication – please indicate:

- The name of the journal:

- The percentage of the manuscript/published work that was contributed by the candidate: 75.00

- Describe the contribution that the candidate has made to the manuscript/published work:

Nimisha carried out the lion's share of the experimental work and contributed to the design, analysis and writing of the study.

( ) It is intended that the manuscript will be published, but it has not yet been submitted to a journal

Candidate's Signature:	
Date:	01-Feb-2022
Primary Supervisor's Signature:	ExpressVPN Client — Digitally signed by ExpressVPN Client Date: 2022.02.02 13:34:26 +13'00'
Date:	2-Feb-2022

This form should appear at the end of each thesis chapter/section/appendix submitted as a manuscript/ publication or collected as an appendix at the end of the thesis.

DRC 16

MASSEY UNIVERSITY TE KUNENGA KI PŪREHUROA UNIVERSITY OF NEW ZEALAND | GRADUATE RESEARCH SCHOOL

STATEMENT OF CONTRIBUTION
DOCTORATE WITH PUBLICATIONS/MANUSCRIPTS

We, the candidate and the candidate's Primary Supervisor, certify that all co-authors have consented to their work being included in the thesis and they have accepted the candidate's contribution as indicated below in the *Statement of Originality*.

Name of candidate:	Nimisha Mohandas
Name/title of Primary Supervisor:	M.A.K. Williams
In which chapter is the manuscript /published work:	4

Please select one of the following three options:

○ The manuscript/published work is published or in press

- Please provide the full reference of the Research Output:

○ The manuscript is currently under review for publication – please indicate:

- The name of the journal:
- The percentage of the manuscript/published work that was contributed by the candidate:
- Describe the contribution that the candidate has made to the manuscript/published work:

◉ It is intended that the manuscript will be published, but it has not yet been submitted to a journal

Candidate's Signature:	
Date:	01-Feb-2022
Primary Supervisor's Signature:	ExpressVPN Client Digitally signed by ExpressVPN Client Date: 2022.02.02 13:36:57 +13'00'
Date:	2-Feb-2022

This form should appear at the end of each thesis chapter/section/appendix submitted as a manuscript/ publication or collected as an appendix at the end of the thesis.

Bibliography

(1) Fry, S. C., *"The growing plant cell wall: chemical and metabolic analysis"*; Longman Group Limited: 2000; Vol. 3.

(2) Costa, G.; Plazanet, I. "Plant cell wall, a challenge for its characterisation". *Advances in Biological Chemistry* **2016**, *6*, 70–105, DOI: 10.4236/abc.2016.63008.

(3) Zablackis, E.; Huang, J.; Muller, B.; Darvill, A. G.; Albersheim, P. "Characterization of the cell-wall polysaccharides of Arabidopsis thaliana leaves". *Plant Physiology* **1995**, *107*, 1129–1138, DOI: 10.1104/pp.107.4.1129.

(4) Wang, D.; Yeats, T. H.; Uluisik, S.; Rose, J. K.; Seymour, G. B. "Fruit softening: revisiting the role of pectin". *Trends in Plant Science* **2018**, *23*, 302–310, DOI: 10.1016/j.tplants.2018.01.006.

(5) Redgwell, R. J.; MacRae, E.; Hallett, I.; Fischer, M.; Perry, J.; Harker, R. "In vivo and in vitro swelling of cell walls during fruit ripening". *Planta* **1997**, *203*, 162–173, DOI: 10.1007/s004250050178.

(6) Paniagua, C.; Posé, S.; Morris, V. J.; Kirby, A. R.; Quesada, M. A.; Mercado, J. A. "Fruit softening and pectin disassembly: an overview of nanostructural pectin modifications assessed by atomic force microscopy". *Annals of Botany* **2014**, *114*, 1375–1383, DOI: 10.1093/aob/mcu149.

(7) Haas, K. T.; Wightman, R.; Peaucelle, A.; Höfte, H. "The role of pectin phase separation in plant cell wall assembly and growth". *The Cell Surface* **2021**, 100054, DOI: 10.1016/j.tcsw.2021.100054.

(8) Ridley, B. L.; O'Neill, M. A.; Mohnen, D. "Pectins: structure, biosynthesis, and oligogalacturonide-related signaling". *Phytochemistry* **2001**, *57*, 929–967, DOI: 10.1016/S0031-9422(01)00113-3.

(9) Caffall, K. H.; Mohnen, D. "The structure, function, and biosynthesis of plant cell wall pectic polysaccharides". *Carbohydrate Research* **2009**, *344*, 1879–1900, DOI: 10.1016/j.carres.2009.05.021.

(10) Leclere, L.; Van Cutsem, P.; Michiels, C. "Anti-cancer activities of pH-or heat-modified pectin". *Frontiers in Pharmacology* **2013**, *4*, 128, DOI: 10.3389/fphar.2013.00128.

(11) Thibault, J.-F.; Renard, C. M.; Axelos, M. A.; Roger, P.; Crépeau, M.-J. "Studies of the length of homogalacturonic regions in pectins by acid hydrolysis". *Carbohydrate Research* **1993**, *238*, 271–286, DOI: 10.1016/0008-6215(93)87019-O.

(12) Ralet, M.-C.; Crépeau, M.-J.; Lefèbvre, J.; Mouille, G.; Höfte, H.; Thibault, J.-F. "Reduced number of homogalacturonan domains in pectins of an Arabidopsis mutant enhances the flexibility of the polymer". *Biomacromolecules* **2008**, *9*, 1454–1460, DOI: 10.1021/bm701321g.

(13) De Vries, J.; Den Uijl, C.; Voragen, A.; Rombouts, F.; Pilnik, W "Structural features of the neutral sugar side chains of apple pectic substances". *Carbohydrate Polymers* **1983**, *3*, 193–205, DOI: 10.1016/0144-8617(83)90018-8.

(14) Mohnen, D. "Pectin structure and biosynthesis". *Current Opinion in Plant Biology* **2008**, *11*, 266–277, DOI: 10.1016/j.pbi.2008.03.006.

(15) Carpita, N. C.; Gibeaut, D. M. "Structural models of primary cell walls in flowering plants: consistency of molecular structure with the physical properties of the walls during growth". *The Plant Journal* **1993**, *3*, 1–30, DOI: 10.1111/j.1365-313x.1993.tb00007.x.

(16) Komalavilas, P.; Mort, A. J. "The acetylation of O-3 of galacturonic acid in the rhamnose-rich portion of pectins". *Carbohydrate Research* **1989**, *189*, 261–272.

(17) Schols, H. A.; Posthumus, M. A.; Voragen, A. G. "Structural features of hairy regions of pectins isolated from apple juice produced by the liquefaction process". *Carbohydrate Research* **1990**, *206*, 117–129, DOI: 10.1016/0008-6215(90)84011-I.

(18) Schols, H. A.; Voragen, A. G. "Occurrence of pectic hairy regions in various plant cell wall materials and their degradability by rhamnogalacturonase". *Carbohydrate Research* **1994**, *256*, 83–95, DOI: 10.1016/0008-6215(94)84229-9.

(19) Srivastava, P.; Malviya, R. "Sources of pectin, extraction and its applications in pharmaceutical industry- An overview". *Indian Journal of Natural Products and Resources* **2011**, *2*, 10–18.

(20) Vauquelin, M. "Analyse du tamarim". *Annales de chimie* **1790**; Vol. 5, pp 92–106.

(21) Braconnot, H. "Recherches sur un novel acide universellement repand dans tous les vegetaux". *Annales de Chimie et de Physique* **1825**; Vol. 28, pp 173–178.

(22) Stratford, R. K. "An investigation of the effects of sugar, acid and pectin on the quality of gels". [Thesis] **1921**. University of Massachusetts.

(23) Minzanova, S. T.; Mironov, V. F.; Arkhipova, D. M.; Khabibullina, A. V.; Mironova, L. G.; Zakirova, Y. M.; Milyukov, V. A. "Biological activity and pharmacological application of pectic polysaccharides: A review". *Polymers* **2018**, *10*, 1407, DOI: 10.3390/polym10121407.

(24) Lupi, F. R.; Gabriele, D.; Seta, L.; Baldino, N.; de Cindio, B.; Marino, R. "Rheological investigation of pectin-based emulsion gels for pharmaceutical and cosmetic uses". *Rheologica Acta* **2015**, *54*, 41–52, DOI: 10.1007/s00397-014-0809-8.

(25) Sato, A. C.; Oliveira, P. R.; Cunha, R. L. "Rheology of mixed pectin solutions". *Food Biophysics* **2008**, *3*, 100–109, DOI: 10.1007/s11483-008-9058-7.

(26) Chan, S. Y.; Choo, W. S.; Young, D. J.; Loh, X. J. "Pectin as a rheology modifier: Origin, structure, commercial production and rheology". *Carbohydrate Polymers* **2017**, *161*, 118–139, DOI: 10.1016/j.carbpol.2016.12.033.

(27) Fraeye, I.; Duvetter, T.; Doungla, E.; Van Loey, A.; Hendrickx, M. "Fine-tuning the properties of pectin-calcium gels by control of pectin fine structure, gel composition and environmental conditions". *Trends in Food Science & Technology* **2010**, *21*, 219–228, DOI: 10.1016/j.tifs.2010.02.001.

(28) Fu, J.; Rao, M. "Rheology and structure development during gelation of low-methoxyl pectin gels: the effect of sucrose". *Food Hydrocolloids* **2001**, *15*, 93–100, DOI: doi.org/10.1016/S0268-005X(00)00056-4.

(29) Kastner, H.; Einhorn-Stoll, U.; Senge, B. Structure formation in sugar containing pectin gels-Influence of Ca2+ on the gelation of low-methoxylated pectin at acidic pH. *Food Hydrocolloids* **2012**, *27*, 42–49.

(30) Axelos, M.; Thibault, J. The chemistry and technology of pectin. *Academic Press, California* **1991**, 109.

(31) Voragen, F.; Schols, H.; Visser, R. G., *"Advances in pectin and pectinase research"*; Springer: 2013.

(32) Willats, W. G.; Knox, J. P.; Mikkelsen, J. D. Pectin: new insights into an old polymer are starting to gel. *Trends in Food Science & Technology* **2006**, *17*, 97–104.

(33) Naseri, A. T.; Thibault, J.-F.; Ralet-Renard, M.-C. "Citrus pectin: structure and application in acid dairy drinks", *Global Science Books* **2008**, *1*, 60-70.

(34) Maroziene, A; De Kruif, C. "Interaction of pectin and casein micelles". *Food Hydrocolloids* **2000**, *14*, 391–394, DOI: 10.1016/S0268-005X(00)00019-9.

(35) Tuinier, R; Rolin, C; De Kruif, C. "Electrosorption of pectin onto casein micelles". *Biomacromolecules* **2002**, *3*, 632–638, DOI: 10.1021/bm025530x.

(36) Liang, L.; Luo, Y., et al. "Casein and pectin: Structures, interactions, and applications". *Trends in Food Science & Technology* **2020**, *97*, 391–403, DOI: 10.1016/j.tifs.2020.01.027.

(37)Kohli, P.; Gupta, R. "Alkaline pectinases: a review". *Biocatalysis and Agricultural Biotechnology* **2015**, *4*, 279–285, DOI: 10.1016/j.bcab.2015.07.001.

(38) Micheli, F. "Pectin methylesterases: cell wall enzymes with important roles in plant physiology". *Trends in Plant Science* **2001**, *6*, 414–419, DOI: 10.1016/s1360-1385(01)02045-3.

(39) Wolf, S.; Mouille, G.; Pelloux, J. "Homogalacturonan methyl-esterification and plant development". *Molecular Plant* **2009**, *2*, 851–860, DOI: 10.1093/mp/ssp066.

(40) Hocq, L.; Pelloux, J.; Lefebvre, V. "Connecting homogalacturonan-type pectin remodeling to acid growth". *Trends in Plant Science* **2017**, *22*, 20–29, DOI: 10.1016/j.tplants.2016.10.009.

(41) Osorio, S.; Castillejo, C.; Quesada, M. A.; Medina-Escobar, N.; Brownsey, G. J.; Suau, R.; Heredia, A.; Botella, M. A.; Valpuesta, V. "Partial demethylation of oligogalacturonides by pectin methyl esterase 1 is required for eliciting defence responses in wild strawberry (Fragaria vesca)". *The Plant Journal* **2008**, *54*, 43–55, DOI: 10.1111/j.1365-313X.2007.03398.x.

(42) Ralet, M.-C.; Thibault, J.-F. "Interchain heterogeneity of enzymatically deesterified lime pectins". *Biomacromolecules* **2002**, *3*, 917–925, DOI: 10.1021/bm020055o.

(43) Kent, L. M.; Loo, T. S.; Melton, L. D.; Mercadante, D.; Williams, M. A.; Jameson, G. B. "Structure and properties of a non-processive, salt-requiring, and acidophilic pectin methylesterase from Aspergillus niger provide insights into the key determinants of processivity control". *Journal of Biological Chemistry* **2016**, *291*, 1289–1306, DOI: 10.1074/jbc.M115.673152.

(44) Denès, J.-M.; Baron, A.; Renard, C. M.; Péan, C.; Drilleau, J.-F. "Different action patterns for apple pectin methylesterase at pH 7.0 and 4.5". *Carbohydrate Research* **2000**, *327*, 385–393, DOI: 10.1016/s0008-6215(00)00070-7.

(45) Cameron, R. G.; Luzio, G. A.; Goodner, K.; Williams, M. A. "Demethylation of a model homogalacturonan with a salt-independent pectin methylesterase from citrus: I. Effect of pH on demethylated block size, block number and enzyme mode of action". *Carbohydrate Polymers* **2008**, *71*, 287–299, DOI: 10.1016/j.carbpol.2007.07.007.

(46) Saharan, R.; Sharma, K. P. "Production, purification and characterization of pectin lyase from Bacillus subtilis isolated from moong beans leaves (Vigna radiata)". *Biocatalysis and Agricultural Biotechnology* **2019**, *21*, 101306, DOI: 10.1016/j.bcab.2019.101306.

(47) Sassi, A. H.; Trigui-Lahiani, H.; Abdeljalil, S.; Gargouri, A. "Enhancement of solubility, purification and inclusion-bodies-refolding of an active pectin lyase from Penicillium occitanis expressed in Escherichia coli". *International Journal of Biological Macromolecules* **2017**, *95*, 256–262, DOI: 10.1016/j.ijbiomac.2016.11.036.

(48) Alahuhta, M.; Taylor, L. E.; Brunecky, R.; Sammond, D. W.; Michener, W.; Adams, M. W.; Himmel, M. E.; Bomble, Y. J.; Lunin, V. "The catalytic mechanism and unique low pH optimum of Caldicellulosiruptor bescii family 3 pectate lyase". *Acta Crystallographica Section D: Biological Crystallography* **2015**, *71*, 1946–1954, DOI: 10.1107/S1399004715013760.

(49) Yadav, S.; Yadav, P. K.; Yadav, D.; Yadav, K. D. S. "Pectin lyase: a review". *Process Biochemistry* **2009**, *44*, 1–10, DOI: 10.1016/j.procbio.2008.09.012.

(50) Biz, A.; Farias, F. C.; Motter, F. A.; de Paula, D. H.; Richard, P.; Krieger, N.; Mitchell, D. A. "Pectinase activity determination: an early deceleration in the release of reducing sugars throws a spanner in the works!" *PLoS One* **2014**, *9*, e109529, DOI: 10.1371/journal.pone.0109529.

(51) Zheng, L.; Xu, Y.; Li, Q.; Zhu, B. "Pectinolytic lyases: a comprehensive review of sources, category, property, structure, and catalytic mechanism of pectate lyases and pectin lyases". *Bioresources and Bioprocessing* **2021**, *8*, 1–13, DOI: 10.1186/s40643-021-00432-z.

(52) Wu, P.; Yang, S.; Zhan, Z.; Zhang, G. "Origins and features of pectate lyases and their applications in industry". *Applied Microbiology and Biotechnology* **2020**, 1–14, DOI: 10.1007/s00253-020-10769-8.

(53) Markovič, O.; Janeček, Š. "Pectin degrading glycoside hydrolases of family 28: sequence-structural features, specificities and evolution". *Protein Engineering* **2001**, *14*, 615–631, DOI: 10.1093/protein/14.9.615.

(54) Protsenko, M.; Buza, N.; Krinitsyna, A.; Bulantseva, E.; Korableva, N. "Polygalacturonase-inhibiting protein is a structural component of plant cell wall". *Biochemistry (Moscow)* **2008**, *73*, 1053–1062, DOI: 10.1134/s0006297908100015.

(55) Hunt, J.; Cameron, R.; Williams, M. A. "On the simulation of enzymatic digest patterns: The fragmentation of oligomeric and polymeric galacturonides by endo-polygalacturonase II". *Biochimica et Biophysica Acta* **2006**, *1760*, 1696–1703, DOI: 10.1016/j.bbagen.2006.08.022.

(56) Abbott, D. W.; Boraston, A. B. "The structural basis for exopolygalacturonase activity in a family 28 glycoside hydrolase". *Journal of Molecular Biology* **2007**, *368*, 1215–1222, DOI: 10.1016/j.jmb.2007.02.083.

(57) Chen, J.; Liu, W.; Liu, C.-M.; Li, T.; Liang, R.-H.; Luo, S.-J. "Pectin modifications: a review". *Critical Reviews in Food Science and Nutrition* **2015**, *55*, 1684–1698, DOI: 10.1080/10408398.2012.718722.

(58) Keijbets, M. J.; Pilnik, W. "β-elimination of pectin in the presence of anions and cations". *Carbohydrate Research* **1974**, *33*, 359–362, DOI: 10.1016/s0008-6215(00)82815-3.

(59) Einhorn-Stoll, U.; Kastner, H.; Urbisch, A.; Kroh, L. W.; Drusch, S. "Thermal degradation of citrus pectin in low-moisture environment-Influence of acidic and alkaline pre-treatment". *Food Hydrocolloids* **2019**, *86*, 104–115, DOI: 10.1016/j.foodhyd.2018.02.030.

(60) Diaz, J. V.; Anthon, G. E.; Barrett, D. M. "Nonenzymatic degradation of citrus pectin and pectate during prolonged heating: effects of pH, temperature, and degree of methyl esterification". *Journal of Agricultural and Food Chemistry* **2007**, *55*, 5131–5136, DOI: 10.1021/jf0701483.

(61) Muñoz-Almagro, N.; Montilla, A.; Moreno, F. J.; Villamiel, M. "Modification of citrus and apple pectin by power ultrasound: Effects of acid and enzymatic treatment". *Ultrasonics Sonochemistry* **2017**, *38*, 807–819, DOI: 10.1016/j.ultsonch.2016.11.039.

(62) Burana-osot, J.; Soonthornchareonnon, N.; Hosoyama, S.; Linhardt, R. J.; Toida, T. "Partial depolymerization of pectin by a photochemical reaction". *Carbohydrate Research* **2010**, *345*, 1205–1210, DOI: 10.1016/j.carres.2010.04.007.

(63) Sila, D. N.; Smout, C.; Elliot, F.; Loey, A. V.; Hendrickx, M. "Non-enzymatic depolymerization of carrot pectin: toward a better understanding of carrot texture during thermal

processing". *Journal of Food Science* **2006**, *71*, E1–E9, DOI: 10.1111/j.1365-2621.2006.tb12391.x.

(64) Polesca, C. M.; Coimbra, J. S. R.; Souza, V. G. L.; Sousa, R. C. S. "Structure and Applications of Pectin in Food, Biomedical, and Pharmaceutical Industry: A Review". *Coatings* **2021**, *11*, 922, DOI: 10.3390/coatings11080922.

(65) Agten, S. M.; Suylen, D.; Ippel, H.; Kokozidou, M.; Tans, G.; van de Vijver, P.; Koenen, R. R.; Hackeng, T. M. "Chemoselective oxime reactions in proteins and peptides by using an optimized oxime strategy: the demise of levulinic acid". *ChemBioChem* **2013**, *14*, 2431–2434, DOI: 10.1002/cbic.201300598.

(66) Wang, S.; Nawale, G. N.; Kadekar, S.; Oommen, O. P.; Jena, N. K.; Chakraborty, S.; Hilborn, J.; Varghese, O. P. "Saline Accelerates Oxime Reaction with Aldehyde and Keto Substrates at Physiological pH". *Scientific Reports* **2018**, *8*, 1–7, DOI: 10.1038/s41598-018-20735-0.

(67) McReynolds, K. D.; Dimas, D.; Le, H. "Synthesis of hydrophilic aminooxy linkers and multivalent cores for chemoselective aldehyde/ketone conjugation". *Tetrahedron Letters* **2014**, *55*, 2270–2273, DOI: 10.1016/j.tetlet.2014.02.085.

(68) Pedrolli, D. B.; Carmona, E. C. "Purification and characterization of a unique pectin lyase from Aspergillus giganteus able to release unsaturated monogalacturonate during pectin degradation". *Enzyme Research* **2014**, *3*, 2931–353915, DOI: 10.1155/2014/353915.

(69) Jayani, R. S.; Saxena, S.; Gupta, R. "Microbial pectinolytic enzymes: a review". *Process Biochemistry* **2005**, *40*, 2931–2944, DOI: 10.1016/j.procbio.2005.03.026.

(70) Michael Green, N. "Avidin and streptavidin". *Methods in Enzymology*, Wilchek, M., Bayer, E. A., Eds.; AcademicPress **1990**, *184*, 51–67, DOI: 10.1016/0076-6879(90)84259-J.

(71) Weber, P. C.; Ohlendorf, D. H.; Wendoloski, J.; Salemme, F. "Structural origins of high-affinity biotin binding to streptavidin". *Science* **1989**, *243*, 85–88, DOI: 10.1126/science.2911722.

(72) Hendrickson, W. A.; Pähler, A.; Smith, J. L.; Satow, Y.; Merritt, E. A.; Phizackerley, R. P. "Crystal structure of core streptavidin determined from multiwavelength anomalous diffraction of synchrotron radiation". *Proceedings of the National Academy of Sciences* **1989**, *86*, 2190–2194, DOI: 10.1073/pnas.86.7.2190.

(73) Pähler, A; Hendrickson, W. A.; Kolks, M.; Argarana, C.; Cantor, C. R. "Characterization and crystallization of core streptavidin". *Journal of Biological Chemistry* **1987**, *262*, 13933–13937, DOI: 10.1016/S0021-9258(18)47884-2.

(74) Jones, M. L.; Kurzban, G. P. "Noncooperativity of biotin binding to tetrameric streptavidin". *Biochemistry* **1995**, *34*, 11750–11756, DOI: 10.1021/bi00037a012.

(75) Sano, T.; Vajda, S.; Reznik, G. O.; Smith, C. L.; Cantor, C. R. "Molecular Engineering of Streptavidin". *Annals of the New York Academy of Sciences* **1996**, *799*, 383–390, DOI: 10.1111/j.1749-6632.1996.tb33229.x.

(76) González, M.; Bagatolli, L. A.; Echabe, I.; Arrondo, J. L. R.; Argaraña, C. E.; Cantor, C. R.; Fidelio, G. D. "Interaction of biotin with streptavidin". *Journal of Biological Chemistry* **1997**, *272*, 11288–11294, DOI: 10.1074/jbc.272.17.11288.

(77) Howarth, M.; Chinnapen, D. J.; Gerrow, K.; Dorrestein, P. C.; Grandy, M. R.; Kelleher, N. L.; El-Husseini, A.; Ting, A. Y. "A monovalent streptavidin with a single femtomolar biotin binding site". *Nature Methods* **2006**, *3*, 267–273, DOI: 10.1038/nmeth861.

(78) Lemercier, G.; Johnsson, K. "Chimeric streptavidins with reduced valencies". *Nature Methods* **2006**, *3*, 247–248, DOI: 10.1038/nmeth0406-247.

(79) Aslan, F.; Yu, Y.; Vajda, S.; Mohr, S.; Cantor, C. "Engineering a novel, stable dimeric streptavidin with lower isoelectric point". *Journal of Biotechnology* **2007**, *128*, 213–225, DOI: 10.1016/j.jbiotec.2006.08.014.

(80) Demonte, D.; Dundas, C. M.; Park, S. "Expression and purification of soluble monomeric streptavidin in Escherichia coli". *Applied Microbiology and Biotechnology* **2014**, *98*, 6285–6295, DOI: 10.1007/s00253-014-5682-y.

(81) Qureshi, M. H.; Yeung, J. C.; Wu, S.-C.; Wong, S.-L. "Development and characterization of a series of soluble tetrameric and monomeric streptavidin muteins with differential biotin binding affinities". *Journal of Biological Chemistry* **2001**, *276*, 46422–46428, DOI: 10 . 1074 / jbc.M107398200.

(82) Aslan, F. M.; Yu, Y.; Mohr, S. C.; Cantor, C. R. "Engineered single-chain dimeric streptavidins with an unexpected strong preference for biotin-4-fluorescein". *Proceedings of the National Academy of Sciences* **2005**, *102*, 8507–8512, DOI: 10.1073/pnas.0503112102.

(83) Sun, X.; Montiel, D.; Li, H.; Yang, H. ""Plug-and-Go" Strategy To Manipulate Streptavidin Valencies". *Bioconjugate Chemistry* **2014**, *25*, 1375–1380, DOI: 10.1021/bc500296p.

(84) Xu, D.; Wegner, S. V. "Multifunctional streptavidin-biotin conjugates with precise stoichiometries". *Chemical Science* **2020**, *11*, 4422–4429, DOI: 10.1039/D0SC01589J.

(85) Katz, B. A. Binding of biotin to streptavidin stabilizes intersubunit salt bridges between Asp61 and His87 at low pH. *Journal of molecular biology* **1997**, *274*, 776–800.

(86) Bustamante, C. J.; Chemla, Y. R.; Liu, S.; Wang, M. D. "Optical tweezers in single-molecule biophysics". *Nature Reviews Methods Primers* **2021**, *1*, 1–29, DOI: 10.1038/s43586-021-00021-6.

(87) Ashkin, A. "History of optical trapping and manipulation of small-neutral particle, atoms, and molecules". *IEEE Journal of Selected Topics in Quantum Electronics* **2000**, *6*, 841–856, DOI:10.1109/2944.902132.

(88) Ashkin, A. "Acceleration and trapping of particles by radiation pressure". *Physical Review Letters*, *24*, 156, DOI: 10.1103/PhysRevLett.24.156.

(89) Frieda, K. L.; Block, S. M. "Direct observation of cotranscriptional folding in an adenine riboswitch". *Science* **2012**, *338*, 397–400, DOI: 10.1126/science.1225722.

(90) Smith, S. B.; Finzi, L.; Bustamante, C. "Direct mechanical measurements of the elasticity of single DNA molecules by using magnetic beads". *Science* **1992**, *258*, 1122–1126, DOI: 10.1126/science.1439819.

(91) Wang, M. D.; Yin, H.; Landick, R.; Gelles, J.; Block, S. M. "Stretching DNA with optical tweezers". *Biophysical Journal* **1997**, *72*, 1335–1346, DOI: 10.1016/S0006-3495(97)78780-0.

(92) Raudsepp, A.; Kent, L. M.; Hall, S. B.; Williams, M. A. "Overstretching partially alkyne functionalized dsDNA using near infrared optical tweezers". *Biochemical and Biophysical Research Communications* **2018**, *496*, 975–980, DOI: 10.1016/j.bbrc.2018.01.087.

(93) Synakewicz, M.; Bauer, D.; Rief, M.; Itzhaki, L. S. "Bioorthogonal protein-DNA conjugation methods for force spectroscopy". *Scientific Reports* **2019**, *9*, 13820, DOI: 10.1038/s41598-019-49843-1.

(94) Jadhav, V. S.; Brüggemann, D.; Wruck, F.; Hegner, M. "Single-molecule mechanics of protein-labelled DNA handles". *Beilstein Journal of Nanotechnology* **2016**, *7*, 138–148, DOI: 10.3762/bjnano.7.16.

(95) Cecconi, C.; Shank, E. A.; Marqusee, S.; Bustamante, C. "DNA molecular handles for single-molecule protein-folding studies by optical tweezers". *Methods in Molecular Biology* **2011**, *749*, 255–271, DOI: 10.1007/978-1-61779-142-0_18.

(96) Cecconi, C.; Shank, E. A.; Dahlquist, F. W.; Marqusee, S.; Bustamante, C. "Protein-DNA chimeras for single molecule mechanical folding studies with the optical tweezers". *European Biophysics Journal* **2008**, *37*, 729–738, DOI: 10.1007/s00249-007-0247-y.

(97) Hao, Y.; Canavan, C.; Taylor, S. S.; Maillard, R. A. "Integrated method to attach DNA handles and functionally select proteins to study folding and protein-ligand interactions with optical tweezers". *Scientific Reports* **2017**, *7*, 1–8, DOI: 10.1038/s41598-017-11214-z.

(98) Tagliaro, F; Turrina, S; Smith, F. "Capillary electrophoresis: principles and applications in illicit drug analysis". *Forensic Science International* **1996**, *77*, 211–229, DOI: 10.1016/0379-0738(95)01863-8.

(99) Ewing, A. G.; Wallingford, R. A.; Olefirowicz, T. M. "CAPILLARY ELECTROPHORESIS". *Analytical Chemistry* **1989**, *61*, 292A–303A, DOI: 10.1021/ac00179a002.

(100) St. Claire, R. L. "Capillary electrophoresis". *Analytical Chemistry* **1996**, *68*, 569–586.

(101) Choudhary, G.; Horváth, C. "Dynamics of capillary electrochromatography experimental study on the electrosmotic flow and conductance in open and packed capillaries". *Journal of Chromatography A* **1997**, *781*, 161–183, DOI: 10.1016/s0021-9673(97)00626-2.

(102) Henskens, Y.; van Dieijen-Visser, M. "Capillary zone electrophoresis as a tool to detect proteins in body fluids: Reproducibility, comparison with conventional methods and a review of the literature". *Nederlands Tijdschrift voor Klinische Chemie* **2000**, *25*, 219–228.

(103) Williams, M. A.; Foster, T. J.; Schols, H. A. "Elucidation of pectin methylester distributions by capillary electrophoresis". *Journal of Agricultural and Food Chemistry* **2003**, *51*, 1777–1781,DOI: 10.1021/jf0259112.

(104) Weinberger, R., *Practical capillary electrophoresis*; Elsevier: **2000**.

(105) Zhong, H.-J.; Williams, M. A.; Goodall, D. M.; Hansen, M. E. "Capillary electrophoresis studies of pectins". *Carbohydrate Research* **1998**, *308*, 1–8, DOI: 10.1016/S0008-6215(97)10105-7.

(106) Engvall, E.; Perlmann, P. "Enzyme-linked immunosorbent assay (ELISA) quantitative assay of immunoglobulin G". *Immunochemistry* **1971**, *8*, 871–874, DOI: 10.1016/0019-2791(71)90454-x.

(107) Van Weemen, B.; Schuurs, A. "Immunoassay using antigen—enzyme conjugates". *FEBS Letters* **1971**, *15*, 232–236, DOI: 10.1016/0014-5793(71)80319-8.

(108) Gao, Z.; Xu, M.; Hou, L.; Chen, G.; Tang, D. "Magnetic bead-based reverse colorimetric immunoassay strategy for sensing biomolecules". *Analytical Chemistry* **2013**, *85*, 6945–6952, DOI: 10.1021/ac401433p.

(109) Lin, H.; Liu, Y.; Huo, J.; Zhang, A.; Pan, Y.; Bai, H.; Jiao, Z.; Fang, T.; Wang, X.; Cai, Y., et al. "Modified enzyme-linked immunosorbent assay strategy using graphene oxide sheets and gold nanoparticles functionalized with different antibody types". *Analytical Chemistry* **2013**, *85*, 6228–6232, DOI: 10.1021/ac401075u.

(110) Heiat, M.; Ranjbar, R.; Alavian, S. M. "Classical and modern approaches used for viral hepatitis diagnosis". *Hepatitis Monthly* **2014**, *14*, DOI: 10.5812/hepatmon.17632.

(111) Kohl, T. O.; Ascoli, C. A. "Direct competitive enzyme-linked immunosorbent assay (ELISA)". *Cold Spring Harbor Protocols* **2017**, *7*, pdb–prot093740, DOI: 10.1101/pdb.prot093740.

(112) Kohl, T. O.; Ascoli, C. A. "Indirect immunometric ELISA". *Cold Spring Harbor Protocols* **2017**, *7*, pdb–prot093708, DOI: 10.1101/pdb.prot093708.

(113) Kohl, T. O.; Ascoli, C. A. "Immunometric double-antibody sandwich enzyme-linked immunosorbent assay". *Cold Spring Harbor Protocols* **2017**, *7*, pdb–prot093724, DOI: 10.1101/pdb.prot093724.

(114) Gan, S. D.; Patel, K. R., et al. "Enzyme immunoassay and enzyme-linked immunosorbent assay". *The Journal of Investigative Dermatology* **2013**, *133*, e12, DOI: 10.1038/jid.2013.287.

(115) Moises, S. S.; Schäferling, M. "Toxin immunosensors and sensor arrays for food quality control". *Bioanalytical Reviews* **2009**, *1*, 73–104, DOI: 10.1007/s12566-009-0006-x.

(116) Shah, K.; Maghsoudlou, P. "Enzyme-linked immunosorbent assay (ELISA): the basics". *British Journal of Hospital Medicine*, *77*, C98–C101, DOI: 10.12968/hmed.2016.77.7.C98.

(117) Engvall, E. "The ELISA, enzyme-linked immunosorbent assay". *Clinical Chemistry* **2010**, *56*, 319–320, DOI: 10.1373/clinchem.2009.127803.

(118) Hartland, C. L.; Youngsaye, W.; Morgan, B.; Ting, A.; Nag, P.; Buhrlage, S.; Johnston, S.; Bittker, J.; Vincent, B.; Whitesell, L., et al. "Identification of small molecules that selectively inhibit fluconazole-resistant Candida albicans in the presence of fluconazole but not in its absence-Probe 3". *Probe Reports from the NIH Molecular Libraries Program [Internet]* **2011**.

(119) Alam, T. M.; Jenkins, J. E. "HR-MAS NMR spectroscopy in material science". *Advanced Aspects of Spectroscopy* **2012**, *10*, 279, DOI: 10.5772/48340.

(120) In *Solving Problems with NMR Spectroscopy (Second Edition)*, ur Rahman, A., Choudhary, M. I., tul Wahab, A., Eds., Second Edition; Academic Press: Boston, **2016**, 265–386.

(121) McAlpine, J. B.; Chen, S.-N.; Kutateladze, A.; MacMillan, J. B.; Appendino, G.; Barison, A.; Beniddir, M. A.; Biavatti, M. W.; Bluml, S.; Boufridi, A., et al. "The value of universally available raw NMR data for transparency, reproducibility, and integrity in natural product research". *Natural Product Reports* **2019**, *36*, 35–107, DOI: 10.1039/C7NP00064B.

(122) Garibyan L., A. N. "Polymerase chain reaction". *Journal of Investigative Dermatology* **2013**, *133*, DOI: 10.1038/jid.2013.1.

(123) Kavya, S. "PCR Technique with its application. research and reviews". *Journal of Microbiology and Biotechnology* **2015**, *4*, 1–12.

(124) Nowakowski, A. B.; Wobig, W. J.; Petering, D. H. "Native SDS-PAGE: high resolution electrophoretic separation of proteins with retention of native properties including bound metal ions". *Metallomics* **2014**, *6*, 1068–1078, DOI: 10.1039/c4mt00033a.

(125) Mardali, M.; Sarraf-Mamoory, R.; Sadeghi, B.; Safarbali, B. "Acrylamide route for the co-synthesis of tungsten carbide-cobalt nanopowders with additives". *Ceramics International* **2016**, *42*, 9382–9386, DOI: 10.1016/j.ceramint.2016.02.152.

(126) Walker, J. M. "SDS Polyacrylamide gel electrophoresis of proteins". *"The Protein Protocols Handbook*; Springer: **2009**, 177–185, DOI: 10.1007/978-1-60327-259-9_11.

(127) Hartfelder, K.; Bitondi, M. M.; Brent, C. S.; Guidugli-Lazzarini, K. R.; Simões, Z. L.; Stabentheiner, A.; Tanaka, É. D.; Wang, Y. "Standard methods for physiology and biochemistry research in Apis mellifera". *Journal of Apicultural Research* **2013**, *52*, 1–48, DOI: 10.3896/IBRA.1.52.1.06.

(128) Stellwagen, N. C. "Electrophoresis of DNA in agarose gels, polyacrylamide gels and in free solution". *Electrophoresis* **2009**, *30*, S188–S195, DOI: 10.1002/elps.200900052.

(129) Sano, T.; Cantor, C. R. "Streptavidin-containing chimeric proteins: design and production". *Methods in Enzymology* **2000**, *326*, 305–311, DOI: 10.1016/s0076-6879(00)26061-8.

(130) Fuller, D. N.; Gemmen, G. J.; Rickgauer, J. P.; Dupont, A.; Millin, R.; Recouvreux, P.; Smith, D. E. "A general method for manipulating DNA sequences from any organism with optical tweezers". *Nucleic Acids Research* **2006**, *34*, e15–e15, DOI: 10.1093/nar/gnj016.

(131) Fairhead, M.; Krndija, D.; Lowe, E. D.; Howarth, M. "Plug-and-play pairing via defined divalent streptavidins". *Journal of Molecular Biology* **2014**, *426*, 199–214, DOI: 10.1016/j.jmb.2013.09.016.

(132) Dittmer, J.; Dittmer, A.; Bruna, R. D.; Kasche, V. "A native, affinity-based protein blot for the analysis of streptavidin heterogeneity: Consequences for the specificity of streptavidin mediated binding assays". *Electrophoresis* **1989**, *10*, 762–765, DOI: 10.1002/elps.1150101106.

(133) Russell, D. W.; Sambrook, J., *"Molecular cloning: a laboratory manual"*; Cold Spring Harbor Laboratory Cold Spring Harbor, NY: 2001; Vol. 1.

(134) Wilfinger, W.; Mackey, K; Chomczynski, P "DNA sequencing II optimizing preparation and cleanup". *Assessing the Quantity, Purity and Integrity of RNA and DNA Following Nucleic Acid Purification* **2006**, 291–312.

(135) Gratzer, W. "Spectrophotometric determination of protein concentration in the short wavelength ultraviolet". *Handbook of Biochemistry and Molecular Biology* **1976**, *2*, 197.

(136) Scopes, R. "Measurement of protein by spectrophotometry at 205 nm". *Analytical Biochemistry* **1974**, *59*, 277–282, DOI: 10.1016/0003-2697(74)90034-7.

(137) Neish, C. S.; Martin, I. L.; Henderson, R. M.; Edwardson, J. M. "Direct visualization of ligand-protein interactions using atomic force microscopy". *British Journal of Pharmacology* **2002**, *135*, 1943–1950, DOI: 10.1038/sj.bjp.0704660.

(138) Suei, S.; Raudsepp, A.; Kent, L. M.; Keen, S. A.; Filichev, V. V.; Williams, M. A. "DNA visualization in single molecule studies carried out with optical tweezers: Covalent versus non-covalent attachment of fluorophores". *Biochemical and Biophysical Research Communications* **2015**, *466*, 226–231, DOI: 10.1016/j.bbrc.2015.09.013.

(139) Prasher, P.; Sharma, M.; Mehta, M.; Satija, S.; Aljabali, A. A.; Tambuwala, M. M.; Anand, K.; Sharma, N.; Dureja, H.; Jha, N. K., et al. "Current-status and applications of polysaccharides in drug delivery systems". *Colloid and Interface Science Communications* **2021**, *42*, 100418.

(140) Srivastava, R. K.; Sushant, P; Sathvik, A.; Kolluru, V. C.; Ahamad, M. I.; Alharthi, M. A.; Luqman, M. In *Food, Medical, and Environmental Applications of Polysaccharides*; Elsevier: 2021, 511–530, DOI: 10.1016/j.colcom.2021.100418.

(141) Stephen, A. M.; Phillips, G. O., *"Food polysaccharides and their applications"*; CRC press: **2016**.

(142) Hellín, P.; Ralet, M.-C.; Bonnin, E.; Thibault, J.-F. "Homogalacturonans from lime pectins exhibit homogeneous charge density and molar mass distributions". *Carbohydrate Polymers* **2005**, *60*, 307–317, DOI: 10.1016/j.carbpol.2005.01.017.

(143) Yapo, B. M.; Lerouge, P.; Thibault, J.-F.; Ralet, M.-C. "Pectins from citrus peel cell walls contain homogalacturonans homogenous with respect to molar mass, rhamnogalacturonan I and rhamnogalacturonan II". *Carbohydrate Polymers* **2007**, *69*, 426–435, DOI: 10.1016/j.carbpol.2006.12.024.

(144) Tanhatan-Nasseri, A.; Crépeau, M.-J.; Thibault, J.-F.; Ralet, M.-C. "Isolation and characterization of model homogalacturonans of tailored methylesterification patterns". *Carbohydrate Polymers* **2011**, *86*, 1236–1243, DOI: 10.1016/j.carbpol.2011.06.019.

(145) Mohandas, N.; Kent, L. M.; Raudsepp, A.; Jameson, G. B.; Williams, M. A. K. "Progress toward Plug-and-Play Polymer Strings for Optical Tweezers Experiments: Concatenation of DNA Using Streptavidin Linkers". *ACS Omega* **2022**, *7(7)*, 6427-6435, DOI: 10.1021/acsomega.2c00198.

(146) Schatz, C.; Lecommandoux, S. "Polysaccharide-containing block copolymers: synthesis, properties and applications of an emerging family of glycoconjugates". *Macromolecular Rapid Communications* **2010**, *31*, 1664–1684, DOI: 10.1002/marc.201000267.

(147) Borch, R. F. "Reductive amination with sodium cyanoborohydride: N, N-Dimethylcyclohexylamine". *Organic Syntheses* **1972**, *52*, 124, DOI: 10.15227/orgsyn.052.0124.

(148) Pedrolli, D. B.; Monteiro, A. C.; Gomes, E.; Carmona, E. C. "Pectin and pectinases: production, characterization and industrial application of microbial pectinolytic enzymes". *Open Biotechnology Journal* **2009**, *3*, 9–18, DOI: 10.2174/1874070700903010009.

(149) Kalia, J.; Raines, R. T. "Hydrolytic stability of hydrazones and oximes". *Angewandte Chemie International Edition* **2008**, *47*, 7523–7526, DOI: 10.1002/anie.200802651.

(150) Fuchs, A "The trans-eliminative breakdown of Na-polygalacturonate by Pseudomonas fluorescens". *Antonie van Leeuwenhoek* **1965**, *31*, 323–340, DOI: 10.1007/BF02045912.

(151) Marín-Rodríguez, M. C.; Orchard, J.; Seymour, G. B. "Pectate lyases, cell wall degradation and fruit softening". *Journal of Experimental Botany* **2002**, *53*, 2115–2119, DOI: 10.1093/jxb/erf089.

(152) Hermanson, G. T. "Avidin-biotin systems". *Bioconjugate Techniques* **2013**, *2*, 465–505, DOI: B978-0-12-382239-0.00011-X.

(153) Hermanson, G. T. "Avidin-biotin systems". *Bioconjugate Techniques* **2013**, *2*, 229–258, DOI: B10.1016/B978-0-12-382239-0.00003-0.

(154) Fischer, M. J. "Amine coupling through EDC/NHS: a practical approach". *Surface plasmon resonance*; Springer: **2010**, 55–73.

(155) Ahmed, E. M. "Hydrogel: Preparation, characterization, and applications: A review". *Journal of advanced research* **2015**, *6*, 105–121, DOI: 10.1016/j.jare.2013.07.006.

(156) Sawicki, L. A.; Kloxin, A. M. "Design of thiol-ene photoclick hydrogels using facile techniques for cell culture applications". *Biomaterials Science* **2014**, *2*, 1612–1626, DOI: 10.1039/c4bm00187g.

(157) Hachet, E.; Sereni, N.; Pignot-Paintrand, I.; Ravaine, V.; Szarpak-Jankowska, A.; Auzély-Velty, R. Thiol-ene clickable hyaluronans: From macro-to nanogels. *Journal of colloid and interface science* **2014**, *419*, 52–55.

(158) Renard, C.; Jarvis, M. "Acetylation and methylation of homogalacturonans 2: effect on ion-binding properties and conformations". *Carbohydrate Polymers* **1999**, *39*, 209–216, DOI: 10.1016/S0144-8617(99)00015-6.

(159) Williams, M. A.; Cucheval, A.; Ström, A.; Ralet, M.-C. "Electrophoretic behavior of copolymeric galacturonans including comments on the information content of the intermolecular charge distribution". *Biomacromolecules* **2009**, *10*, 1523–1531, DOI: https://pubmed.ncbi.nlm.nih.gov/19385647/.

(160) Williams, M. A.; Cucheval, A.; Nasseri, A. T.; Ralet, M.-C. "Extracting intramolecular sequence information from intermolecular distributions: highly nonrandom methylester substitution patterns in homogalacturonans generated by pectinmethylesterase". *Biomacromolecules* **2010**, *11*, 1667–1675, DOI: 10.1021/bm1003527.

(161) Lin, F.; Yu, J.; Tang, W.; Zheng, J.; Defante, A.; Guo, K.; Wesdemiotis, C.; Becker, M. L. "Peptide-functionalized oxime hydrogels with tunable mechanical properties and gelation behavior". *Biomacromolecules* **2013**, *14*, 3749–3758, DOI: 10.1021/bm401133r.

(162) Sestak, J.; Mullins, M.; Northrup, L.; Thati, S.; Forrest, M. L.; Siahaan, T. J.; Berkland, C. "Single-step grafting of aminooxy-peptides to hyaluronan: a simple approach to multifunctional therapeutics for experimental autoimmune encephalomyelitis". *Journal of Controlled Release* **2013**, *168*, 334–340, DOI: 10.1016/j.jconrel.2013.03.015.

(163) Solbak, A. I.; Richardson, T. H.; McCann, R. T.; Kline, K. A.; Bartnek, F.; Tomlinson, G.; Tan, X.; Parra-Gessert, L.; Frey, G. J.; Podar, M., et al. "Discovery of pectin-degrading enzymes and directed evolution of a novel pectate lyase for processing cotton fabric". *Journal of Biological Chemistry* **2005**, *280*, 9431–9438, DOI: 10.1074/jbc.M411838200.

(164) Zhao, Y.; Yuan, Y.; Zhang, X.; Li, Y.; Li, Q.; Zhou, Y.; Gao, J. "Screening of a novel polysaccharide lyase family 10 pectate lyase from Paenibacillus polymyxa KF-1: cloning, expression and characterization". *Molecules* **2018**, *23*, 2774, DOI: 10.3390/molecules23112774.

(165) Kravtchenko, T. Studies on the structure of industrial high methoxyl pectins, WU thesis 1538 Proefschrift Wageningen, Ph.D. Thesis, **1992**.

(166) Sila, D.; Van Buggenhout, S.; Duvetter, T.; Fraeye, I.; De Roeck, A.; Van Loey, A.; Hendrickx, M. "Pectins in processed fruits and vegetables: Part II—Structure–function relationships". *Comprehensive Reviews in Food Science and Food Safety* **2009**, *8*, 86–104, DOI: 10.1111/j.1541-4337.2009.00071.x.

(167) Cornuault, V.; Knox, J. P. "Sandwich enzyme-linked immunosorbent assay (ELISA) analysis of plant cell wall glycan connections". *Bio-protocol* **2014**, *4*, e1106–e1106, DOI: 10.21769/BioProtoc.1106.

(168) Clausen, M. H.; Willats, W. G.; Knox, J. P. "Synthetic methyl hexagalacturonate hapten inhibitors of anti-homogalacturonan monoclonal antibodies LM7, JIM5 and JIM7". *Carbohydrate Research* **2003**, *338*, 1797–1800, DOI: 10.1016/s0008-6215(03)00272-6.

(169) Zhu, L.; He, J.; Cao, X.; Huang, K.; Luo, Y.; Xu, W. "Development of a double-antibody sandwich ELISA for rapid detection of Bacillus Cereus in food". *Scientific Reports* **2016**, *6*, 1–10, DOI: 10.1038/srep16092.

(170) Baláž, M.; Kudličková, Z.; Vilková, M.; Imrich, J.; Balážová, L.; Daneu, N. "Mechanochemical synthesis and isomerization of N-substituted indole-3-carboxaldehyde oximes". *Molecules* **2019**, *24*, 3347, DOI: 10.3390/molecules24183347.

(171) Taşdemir, H. U.; Sevgi, F.; TÜRKKAN, E. "Determination of 1H and 13C Nuclear Magnetic Resonance Chemical Shift Values of Glyoxime Molecule with Experimental and Theoretical Methods". *Adıyaman University Journal of Science* **2019**, *9*, 99–112.

(172) Bayer, E. A.; Ehrlich-Rogozinski, S.; Wilchek, M. "Sodium dodecyl sulfate-polyacrylamide gel electrophoretic method for assessing the quaternary state and comparative thermostability of avidin and streptavidin". *Electrophoresis* **1996**, *17*, 1319–1324, DOI: 10.1002/elps.1150170808.

(173) Owen, J.; Kent, L.; Ralet, M.-C.; Cameron, R.; Williams, M. "A tale of two pectins: Diverse fine structures can result from identical processive PME treatments on similar high DM substrates". *Carbohydrate Polymers* **2017**, *168*, 365–373, DOI: 10.1016/j.carbpol.2017.03.039.